Université catholique de Louvain
Louvain Drug Research Institute

DEVELOPMENT OF A LONG-ACTING VERSION OF ALPHA1 ANTITRYPSIN FOR AUGMENTATION THERAPY IN ALPHA1 ANTITRYPSIN DEFICIENCY

Xiao Liu

Thèse présentée en vue de l'obtention du grade de docteur en Sciences biomédicales et pharmaceutiques

Director : Rita Vanbever

2022

ACKNOWLEDGEMENTS

At the end of this special journey in Belgium, I would like to express my sincere gratitude to many people who have come to my aid in various ways. First, I would like to thank my supervisor Prof. Rita Vanbever, who has always been available, patient and supportive during my entire PhD program. Without your guidance, I would be unable to complete this project.

I would like to acknowledge my family members, particularly my mother Huifang, who has a fairly open mind and is always willing to talk and listen to me.

Thank you in particular to my dearest friend Sheng-ju, who has already begun a new adventure in Taiwan. Despite this, there is no doubt that our friendship will last a lifetime. You introduced me to the wonderful Belgian beers. Thank you for sharing so much delicious food and for being such a fantastic friend. I would like to express my sincere gratitude to my Manderin-speaking friends: Mengnan, Yuan D, Mingchao, Chim-Kei, Yuan W, Sissi, and Juan. Together, we feel that we are not so far away from our hometowns.

In addition, I would like to thank my greatest colleagues and friends at ADDB. Sohaib, I would like to thank you for sharing your wisdom with me and I truly appreciated our time together. Nikos, I appreciate you always being unconditionally supportive, and if there is another opportunity in the future I would like to be your desk-mate once more. Elia and Cecilia, I absolutely enjoyed every moment we were together, eating, drinking, gaming and laughing. Mathilde, who has the most beautiful heart in the world, thank you for being such a good listener and a great friend. Alessio and Yasmine, thank you for your company when I hit the "blue" period of my life. Tobias, thank you for all the discussions about either science or life, which are always inspiring. Thank you to Ariane, Viridiane, Alessandra, Jessica, Aurélie, Jérôme, Silvia and many more for the enjoyable time we spent together. Especially, I would like to thank Wilfried, whose presence made a highlight of my PhD years. Last but not least, thank you to Murielle, Bernard and Kevin, who take care of us and are supportive as always.

I would like to thank Bertrand, who offered me comforting company and strengths when I was stressed or upset. François, thank you for teaching me how to dance and for being such a good friend. Finally, I would like to thank my cat Sheriff for bringing me so much joy.

To all of you

Thank you!

TABLE OF CONTENTS

ABBREVIATION LIST

AAT	Alpha1 antitrypsin
AATD	Alpha1 antitrypsin deficiency
AAV	Adeno-associated virus
AB	Antibody
ACN	Acetonitrile
AEC	Anion exchange chromatography
AMP	Antimicrobial peptide
ANS	8-anilino-1-naphtalene-sulfonic acid
ATS	American Thoracic Society
AUC	Area under the curve
BAL	Bronchoalveolar lavage
BCA	Bicinchoninic acid
BDNF	Brain-derived neurotrophic factor
BSA	Bovine serum albumin
CF	Cystic fibrosis
CFTR	CF transmembrane conductance regulator
COPD	Chronic obstructive pulmonary disease
COVID	Coronavirus disease
CRISPR	Clustered regularly interspaced short palindromic repeats
CT	Computed tomography
DLS	Dynamic light scattering
DNA	Deoxyribonucleic acid
DPBS	Dulbecco's phosphate-buffered saline
EGFR	epidermal growth factor receptor
ELISA	Enzyme-linked immunoassay
EMA	European Medicines Agency
EPI	Epirubicin
ESI-Q-TOF	Electrospray-ionization quadrupole time-of-flight mass spectrometry
EU	European Union
FBS	Fetal bovine serum
FDA	Food and Drug Administration
FEV	Forced expiratory volume
FPLC	Fast protein liquid chromatography
GCSF	Granulocyte colony stimulating factor
GHA	Growth hormone antagonist
HBSS	Hanks' Balanced Salt Solution
hCAP-18	Human cathelicidin antimicrobial peptide 18
hNE	Human neutrophil elastase
HRP	Horseradish peroxidase
IEF	Isoelectric focusing
IFN-α	Interferon α

IL-1β	Interleukin 1 beta
IL-6	Interleukin 6
IT	Intratracheal instillation
IV	Intravenous
LDH	Lactate dehydrogenase
LPS	Lipopolysaccharides
MHS	Murine alveolar macrophages
MIP-2	Macrophage inflammatory protein 2
MMP	Matrix metalloproteinase
MS	Mass Spectrometry
MTT	3-(4,5-dimethylthiazol-2-yl)-2,5-diphenyl-2H-tetrazolium bromide
MW	Molecular weight
NAL	Nasal lavage
NHS	N-Hydroxysuccinimide
OD	Optical density
OPSS	Orthopyridyl disulfide
PAGE	Polyacrylamide gel electrophoresis
PAS	Periodic acid–Schiff
PBS	Phosphate-buffered saline
PDI	Polydispersity index
PEG	Polyethylene glycol
PEGald	PEG-aldehyde
PEGmal	PEG-maleimide
PK	Pharmacokinetics
PMT	Photomultiplicator
PNGase F	N-glycosidase F
PPE	Porcine elastase
PVDF	Polyvinylidene fluoride
RAPID	Randomized, Placebo-controlled Trial of Augmentation Therapy in Alpha 1 Proteinase Inhibitor Deficiency
RCL	Reactive central loop
RNA	Ribonucleic acid
ROS	Reactive oxygen species
RPMI	Roswell Park Memorial Institute
SARS	Severe acute respiratory syndrome
SDS	Sodium dodecyl-sulfate
SEC	Size exclusion chromatography
SEM	Standard error of the mean
TACE	Metalloprotease tumor necrosis factor-α-converting enzyme
TCEP	tris(2-carboxyethyl)phosphine
TEAB	Triethylammonium bicarbonate
TNF-α	Tumor necrosis factor α
TRAIL	Tumor necrosis factor (TNF)-related apoptosis-inducing ligand
VEGF	Vascular endothelial growth factor
WB	Western blot

CHAPTER I

INTRODUCTION

TABLE OF CONTENTS

I. ALPHA1 ANTITRYPSIN DEFICIENCY AND THERAPIES

Alpha1 antitrypsin (AAT) deficiency is a genetic disorder described by low AAT circulating levels (< 11 μM) [1]. The decreased level of AAT expression is fundamentally due to the mutations in the SERPINA1 gene [2]. The low level of AAT in the circulation predisposes to liver, lung or rarely skin manifestations [3]. In Europe, the frequency of homozygous AAT deficiency is estimated to be at 0.01–0.02 % [4]. However, the mutation affects 1 in 2000 people in Caucasian population [5], which makes AAT deficiency one of the most recognized hereditary diseases in Europe.

I.1. ALPHA1 ANTITRYPSIN: STRUCTURE, ACTIVITY AND FUNCTIONS

Alpha1 antitrypsin (AAT) is a 52 kDa glycosylated protein consisting of 394 amino acids. AAT is produced for the most part by hepatocytes in the liver, providing an antiprotease protective screen throughout the body, particularly in the lungs [6, 7]. Monocytes, neutrophils and airway epithelial cells also produce AAT, nonetheless, the production is much lower than that in hepatocytes [8].

AAT contains three β-sheets and nine α-helices [9]. Three internal salt bridges are implicated in folding and polymerization. Plasma-derived AAT contains one single cysteine residue (position 232), which is conjugated with another free cysteine [10]. This structure is referred to the "cysteine cap". Among all the commercial human AAT products, only Respreeza® shows completely uncysteinylated Cys232, which results from a reduction step performed during production [11]. Rapidly after the IV infusion, the exposed Cys232 will be oxidized to the normal cysteinylated form. Uncysteinylated AAT presents the same biological activity as cysteinylated AAT [10]. Substitution or modification of the Cys232 residue does not alter the anti-elastase activity of AAT [12–14].

Three N-glycosylated oligosaccharides are attached to the three asparagine residues of completely processed mature AAT (46, 83, 247) (Figure 1). These carbohydrate groups represent approximately 12−16% of the weight of AAT [15]. *N*-glycans of native AAT proteins consist of sialic acids, galactose, N-acetylglucosamine, and mannose, and are found as di-, tri-, or tetra-antennary structures [15]. Un-, mono-, di- and tri-glycosylated forms of AAT are identified in the plasma in some population [16]. According to Yu et al, glycosylation of AAT retarded unfolding without significantly affecting refolding, suggesting that the stability increase is due to stabilizing the native state rather than decreasing the frequency of the unfolded state [17]. Pain et al demonstrated that the lack of glycosylation in recombinant AAT led to a tendency to aggregation upon refolding, especially after extended denaturation times [18]. The glycosylation of AAT, moreover, increases flexibility in its dynamic state [19]. The glycosylation protects AAT from proteolysis, thus prolongs its half-life and also protects it from aggregation. It has been proved that

an additional N-glycosylation in the flexible N-terminal region of recombinant AAT increased the half-life of recombinant AAT in vivo without changing its protease inhibitory activity [20]. N-glycosylation of AAT is also important for the elastase inhibitory activity and immune modulatory properties of AAT [21]. Martin et al demonstrated that recombinant AAT, which lacks glycosylation compared to plasma-derived AAT, exhibited limited efficacy in reducing the hNE activity and other inflammation markers [22]. On the contrary, plasma-derived AAT was proved to be effective in decreasing inflammation markers in cystic fibrosis patients [23, 24].

Native AAT exists in a meta-stable state, which transforms to a more stable state during its inhibition of NE [25, 26]. The inhibition of serine proteases by AAT involves the cleavage of the reactive center loop (RCL) in AAT, which results in the formation of a protease-AAT complex. During this process, the RCL inserts into the β-sheet A, forming a fourth strand; while the protease is distorted and catalytically inactivated and then flips to the opposite end of AAT [27]. Upon complexation with a protease, AAT undergoes a conformational change that results in the appearance of new binding sites that are recognized by surface receptors such as serpin-enzyme complexes or by receptors for low- and very low-density lipoproteins [28, 29].

Another factor involved in AAT's inhibitory mechanism is its methionine residues, which can be easily oxidized [30]. Oxidation of Met358 and Met351 leads to a marked loss of affinity of AAT for neutrophil elastase and cathepsin G [31]. Cigarette smoke contains hydrogen peroxide, which oxidizes and inactivates AAT, as can N-Chloroamines and hypochlorous acid in neutrophils [11, 32]. Other lung diseases such as cystic fibrosis, adult respiratory distress syndrome, and bronchiectasis have also been linked to oxidant-mediated inactivation of AAT [33, 34]. Ueda et al demonstrated that oxidized AAT was found in higher concentrations in sera from patients with inflammatory and rheumatoid diseases than in healthy subjects [35].

AAT is a serine protease inhibitor, which inhibits serine proteases such as neutrophil elastase (NE), protease 3 (PR-3) [36], and so forth. AAT was also reported to inhibit non-serine proteases, for instance, cysteine protease caspase-3 [37] and the metalloprotease tumor necrosis factor-α-converting enzyme (TACE) [38]. The predominant proteinase inhibited by AAT is neutrophil elastase. NE is inhibited by AAT with a stoichiometric ratio of 1, but PR3 and Cathepsin G result in a higher inhibitor/enzyme ratio because of partial proteolytic inactivation of some inhibitor molecules during the process of interaction. The second-order constants of association of AAT with NE, PR3, and Cathepsin G are 6.5×10^7, 8.1×10^6, and 4.1×10^5 $M^{-1} \cdot s^{-1}$, respectively [39]. A comparison of the association rate constant for other serine proteinases demonstrates a decreasing order with NE > chymotrypsin > anionic trypsin > cationic trypsin > plasmin > thrombin [40].

Other than its broad anti-protease activity, AAT has been demonstrated to have anti-inflammatory, anti-apoptotic and immunomodulatory activities. AAT activates and modulates multiple immune cell types, including neutrophils, macrophages and T cells [41, 42]. Studies have also shown that AAT inhibits the inflammation cytokines production in vitro [43] or in vivo [44]. The mechanism behind the anti-inflammation and immunomodulatory is not fully investigated yet. It is believed that these effects relate to the anti-protease property of AAT. However, in some cases, the anti-inflammatory effect of AAT was independent from its protease inhibition activity [45]. Jonigk et al demonstrated that a recombinant AAT without elastase inhibition capacity exhibited anti-inflammatory effect in isolated human blood neutrophils and in LPS-challenged mice [46]. Although the anti-protease activity may not be essential for the anti-inflammatory and immunomodulatory properties of AAT, the proper glycosylation seems to be important, independent from the integrity of AAT [21]. Recombinant AAT lacking glycosylation cannot bind and modulate IL-8 and lacks other associated anti-inflammatory effects [15]. Reeves et al demonstrated that truncated AAT derived from AAT patient's plasma, whose molecular weight was 49 kDa, lacking 22 residues at its C-terminus, was able to bind IL-8 and leukotriene B4, thus exhibiting anti-inflammatory properties [47]. It has been reported that AAT inhibits NF$\varkappa$B activation [48, 49] and also increases cAMP synthesis [50], which are both essential in modulating cytokine production in mononuclear cells. A hypothesis is that some of the immunomodulatory effects of the AAT could also be mediated via non-protease interactions. However, the exact structures of the AAT binding domains that interact with these non-protease molecules remain unclear [51].

Recently, researchers have found the anti-viral activity of AAT, especially against severe acute respiratory syndrome coronavirus 2 (SARS-CoV-2) [52, 53]. Combined with its anti-inflammatory property, AAT might be valuable in the treatment of COVID-19 patients with acute respiratory distress syndrome [54]. Since 2020, several clinical trials (as shown in Table 1) were conducted to explore whether COVID19 patients could benefit from AAT supplementary therapy [55]. However, the results of those studies have not yet been published.

The anti-inflammatory and immunomodulatory effects of AAT also make it potentially useful to treat diabetes. AAT activities are significantly lower in the plasma of Type 1 Diabetes Mellitus (T1DM) patients [56], and successively decrease during the progression of diabetes. Augmentation therapy of human AAT in the patients prevents T1DM development, prolongs islet allograft survival [57], increases insulin release capacity [58], and inhibits pancreatic B-cell apoptosis [59]. Despite the fact that there are less evidence of the role of AAT in Type 2 Diabetes Mellitus (T2DM), it has been reported that the level of degraded AAT in the urine of T2DM patients with diabetic

kidney disease was significantly higher [60]. In view of the potential benefits of AAT augmentation in ameliorating T1DM-associated inflammation and improving β-cell function, several clinical trials were carried out to evaluate the potency of AAT therapy to treat T1DM (as shown in Table 2). Although the safety and tolerance of AAT therapy on T1DM patients have been demonstrated [61], considering the small samples sizes in each clinical trials, the benefits of the therapy was still not certain for all the patients involved. More studies are required to characterize the actual necessity and benefit of AAT therapy in T1DM, before it will be approved in treating this condition.

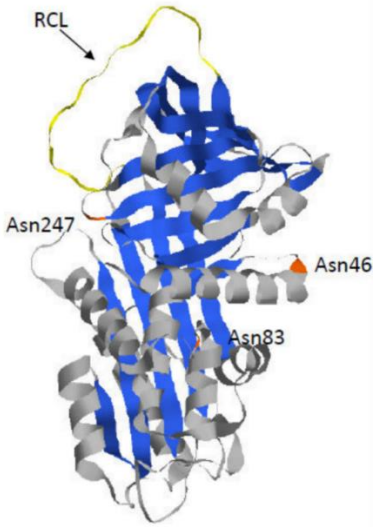

Figure 1. Structure of Alpha 1-Antitrypsin (AAT) (pdb 6I7U). The three asparagine (46, 83, 247) are shown in orange, which are the glycosylation sites. The three β-sheets are in blue and the nine α-helices are in grey. RCL is shown in yellow. This figure was adapted from Karatas et al [9].

Table 1. Clinical trials on the impact of AAT treatment in COVID-19 cases.

Study title	NCT number	Interventions	Phase	Start date	Complete date	Country
Study to Evaluate the Safety and Efficacy of Liquid Alpha1-Proteinase Inhibitor (Human) in Hospitalized Participants With COVID-19	NCT04495101	Biological: Prolastin (Intravenous infusion 120 mg/kg); Drug: Standard Medical Treatment.	Phase II	29-Jul-20	10-Jun-21	Spain
Study to Evaluate the Safety and Efficacy of Liquid Alpha1-Proteinase Inhibitor (Human) in Hospitalized Participants with Coronavirus Disease (COVID-19)	NCT04547140	Biological: Liquid human alpha1 antitrypsin (Intravenous infusion 120 mg/kg); Drug: Standard Medical Treatment.	Phase II	29-Jan-21	Ongoing	United States
Trial of Alpha One Antitrypsin Inhalation in Treating Patient with Severe Acute Respiratory Syndrome Coronavirus 2 (SARS-CoV-2)	NCT04385836	Drug: Glassia (Inhalation, every 12 h for 5 d).	Early Phase I	1-Jun-20	Ongoing	Saudi Arabia

Table 2. Clinical trials of AAT in Type 1 diabetes mellitus. Adapted from U.S. National Library of Medicine and Park et al [59].

Study title	NCT number	Interventions	Phase	Country	Main Outcomes
The Effects of Alpha-1 Antitrypsin (AAT) on the Progression of Type 1 Diabetes	NCT01319331	8 consecutive weekly infusions of 80 mg/kg of AAT (Aralast; Baxter Inc) were given.	Phase I	United States	No significant adverse effects were detected. Decreased total content of TLR4-induced cellular IL-1β. Improved β-cell function correlated with lower IL-1β production.
Study of the Safety and Efficacy of Intravenous Alpha-1 Antitrypsin in Type 1 Diabetes Mellitus	NCT01304537	18 infusions of 40, 60, or 80 mg/kg/dose high-purity, liquid, ready to use AAT (Glassia®; Kamada Ltd.) over 28 weeks. 12 weeks: weekly. 12–20 weeks: once every 2 weeks, 20–28 weeks: once every 4 weeks.	Phase I/II	Israel	No serious adverse events were reported. Glycemic control parameters improved during the study in all groups, independent of dosage. Eight subjects (33.3%) that were considered possible responders had a shorter duration of T1DM) and a greater decrease in their HbA1c
A Research Trial of Aralast in New Onset Diabetes (RETAIN) (RETAIN)	NCT01183468	12 infusions of AAT (Aralast NP; Baxter Inc): a low dose of 45 mg/kg weekly for 6 weeks, followed by a higher dose of 90 mg/kg for 6 weeks.	Phase II	srael	C-peptide secretion during a mixed meal remained relatively stable during the treatment period in adults and decreased in children. HbA1c and Insulin usage remained relatively stable during the treatment period on both groups but gradually increased afterward. AAT suppressed expression of genes involved in NF-ϰB activation and apoptosis pathways.

Study title	NCT number	Interventions	Phase	Country	Main Outcomes
Phase II Study to Evaluate the Efficacy and Safety of Glassia® in Type-1 Diabetes	NCT02005848	22 infusions of AAT (Glassia®; Kamada Ltd.) (60 or 120 mg/kg) or placebo.	Phase II	Israel	AAT was tolerated well, with a similar safety profile between groups. C-peptide, glycated hemoglobin (HbA1c), and the total insulin dose (U/kg) were similar across groups. C-peptide AUC levels in the AAT-120 mg/kg adolescent group remained relatively stable in contrast to the decline observed in the placebo and AAT-60 mg/kg groups. The frequency of responders with at least 95% β-cell function reserve was 29% in the AAT-120 group and nil in the placebo.

I.2. HISTORY AND DISCOVERY OF AAT AND AAT DEFICIENCY

The protease inhibitory activity of human plasma was first discovered in 1894. However, due to limited laboratory techniques at that time, it was not before 1955 that AAT was eventually isolated and identified by Schultze [62]. It was named alpha1 antitrypsin because of its location in the α1 band of globulins and its ability to inhibit trypsin [63]. In 1963, Laurell and Eriksson discovered that serum protein electrophoreses of several patients with severe obstructive lung disease of early onset lacked a band for α1 globulin [64]. A few years after linking AAT deficiency to lung diseases, Sharp et al described an association between AAT deficiency and liver cirrhosis [65]. With the improvement of laboratory diagnostic techniques and the invention of isoelectric focusing (IEF), AAT phenotypes were classified and the deficiency states of AAT deficiency were identified [66]. In the 1980s, the structure of human AAT was revealed, its gene was also cloned and sequenced [67]. Nowadays, AAT deficiency is defined by low AAT serum levels (< 11 μM) [68]. In 1987, the US Food and Drug Administration (FDA) had approved the marketing of Prolastin (AAT purified from healthy blood donors' plasma) for augmentation therapy in adults with severe AAT deficiency-related emphysema.

I.3. GENE, GENETIC HERITAGE AND EPIDEMIOLOGY OF AAT DEFICIENCY

The gene for AAT called SERPINA1 is located on the long arm (q) of the 14th chromosome [69]. SERPINA1 gene has two alleles, which are transmitted from parents to children by autosomal codominant Mendelian inheritance [70, 71]. This means that a child inherits one of each parent's two SERPINA1 alleles. SERPINA1 alleles encoding AAT have co-dominant expression, which means that in heterozygotes with AAT deficiency, half of the AAT produced is normal, while the other half is abnormal according to the genetic variant. In consequence, the risks to an offspring of a patient are determined by the genetic status of both parents. A healthy individual has the two normal alleles called MM genotype. The most common deficient alleles are named S and Z (Table 3), which are more found in the Caucasian populations [72–74]. Both mutations result in single amino acid substitutions: valine for glutamate 264 (Glu264Val) in the case of S variants and lysine for glutamate 342 (Glu342Lys) for Z variants (Figure 2). The Z allele is present in 1 in 25 persons of European descent and S allele is found in 1 in 4 persons in the Iberian peninsula [75]. In addition to the most common AAT deficiency alleles S and Z, many other alleles have been described that have variable effects. However, among the AAT-deficient patients in clinical practice, 95 % of them exhibit Pi*ZZ genotypes, and 5 % combinations of Z and other mutated alleles [75]. Asians, Africans and middle easterners are less likely to suffer from AAT deficiency [76, 77].

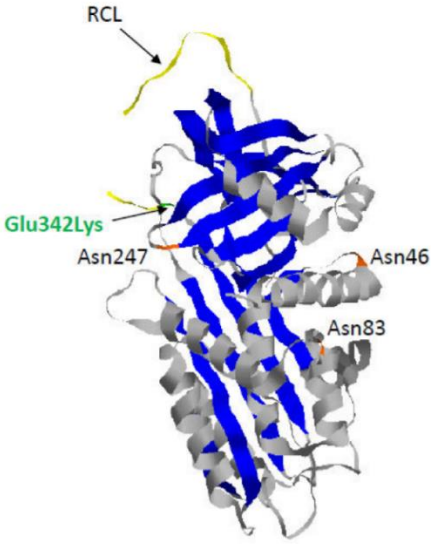

Figure 2. Crystal structure of recombinant human Z-AAT (pdb 5IO1) [9]. Z-AAT protein results from the substitution of glutamic acid by lysine at position 342 (Glu342Lys) (in green).

I.4. A COMPARISON OF THE MURINE AND HUMAN AAT

It is striking that, in the human genome, AAT is represented by a single gene, while in guinea pigs and rabbits, four gene members are present, and mouse species have more isoforms [78]. In the mouse, the SERPINA1 gene includes six members a to f [79]. Murine AAT amino acid sequence is homologous to the human sequence. There is 65% identity (268 out of 412 residues) between the two sequences, and many of the amino acid substitutions are conserved [80]. AAT sequences from mice and humans show homology with the signal peptide of human sequences that is responsible for insertion of the protein into the rough endoplasmic reticulum lumens [81].

An examination of the latent mouse AAT in comparison with the human AAT has been carried out by Dewilde et al [82]. A differential positioning of helix A was demonstrated, as well as differences in the gate region and changes in the position of the reactive loop center. However, despite the subtle difference in structure between human and murine AAT, human AAT is able to inhibit murine elastase and PR3 [83]. Thus, human AAT can be used to examine NE suppression in mouse models.

Table 3. Key Alleles Associated with Alpha1-Antitrypsin (AAT) Deficiency. Adapted from Strnad et al [84].

Variant	Mutation	Molecular Basis of Disease	Clinical Features	Epidemiology
Deficiency alleles				
S	Glu264Val	Protein misfolding and reduced secretion; can form heteropolymers with Z AAT	Emphysema seen in SZ heterozygotes but less severe than in ZZ; cirrhosis reported in SZ heterozygotes	Most common deficiency variant; carrier frequency: 1 in 5 persons in southern Europe, 1 in 30 in the United States, 1 in 23 among persons of European descent in Australia, 1 in 26 among those of European descent in New Zealand; rare or nonexistent in Asia, Africa, and Aboriginal Australians
Z	Glu342Lys	Intracellular degradation and polymerization; low serum level	In homozygotes, well-established association with liver disease and emphysema; MZ heterozygotes may be more susceptible to airflow obstruction and chronic liver disease	Most common severe deficiency variant; carrier frequency: 1 in 27 persons in northern Europe, 1 in 83 in the United States, 1 in 75 persons of European descent in Australia, 1 in 46 persons of European descent in New Zealand; not seen in China, Japan, Korea, Malaysia, or northern and western Africa
M_{malton}	Δ52Phe (M2 variant)	Intracellular degradation and polymerization; low serum level	Well-established association with liver dis ease and emphysema in homozygotes	Most common rare deficiency allele in Sardinia; seen sporadically in the United Kingdom and Canada
S_{iiyama}	Ser53Phe	Intracellular degradation and polymerization; low serum level	Liver disease and emphysema in homo zygotes	Rare, but most common deficiency allele in Japan

Variant	Mutation	Molecular Basis of Disease	Clinical Features	Epidemiology
Null (QO) alleles	Various from cases	No detectable AAT mRNA; Truncated protein; intracellular degradation and no secreted protein	High risk of emphysema in homozygotes and compound heterozygotes	Case report

I.5. RESPIRATORY MANIFESTATION

The major clinical features of AAT deficiency include respiratory and hepatic diseases. Misfolded AAT (Z-AAT) forms polymers which accumulate as hepatocyte inclusions [85]. This misfolded protein causes proteotoxic stress and a liver disease implying loss of function [86]. AAT deficiency also predisposes to skin (panniculitis) disease and to vasculitis [87]. Here, we primarily discuss the respiratory manifestation related to AAT deficiency.

I.5.1. Chronic obstructive pulmonary diseases and emphysema related to AAT deficiency

Chronic obstructive pulmonary disease (COPD) in general, more specifically panacinar type pulmonary emphysema, is the most prevalent clinical pulmonary manifestation of AAT deficiency and the major cause of disability and death among AAT deficiency subjects [88]. Approximately 3.7 % of patients with COPD are found to be Pi*ZZ genotype, while 1.7 % for the Pi*SZ genotype [89–91]. Neither Pi*MZ heterozygotes nor Pi*SZ are not considered at high risk for emphysema, however, the former is more susceptible to develop airflow obstruction than MM individuals [92], and the latter will be at high risk with the combination of smoking and other unhealthy lifestyle [90]. The major cause for the emphysematous lung disease in AAT-deficient patients is the imbalance of protease and inhibitor in the lungs. There is insufficient AAT to protect the alveoli from NE, resulting in progressive alveolar destruction and eventually emphysema. This protease-inhibitor imbalance can be aggravated by smoking and lung infection [93]. The symptoms of AAT-deficiency related emphysema are similar to COPD caused by any etiology. Dyspnea is the most common symptom, which is present in 80%–90% of the patients. Chronic cough and wheeze are also reported in 65 – 75 % of the patients [94]. Occupational and environmental exposures such as smoke and dust need to be considered when diagnosing patients with AAT-deficiency-associated COPD. Pulmonary function tests, such as spirometry, lung volumes, and carbon monoxide diffusing capacity, are helpful in determining the severity of COPD [95]. Early disease stages can result in normal chest radiography, making computed tomography (CT) scans useful for detecting the disease earlier [96].

I.5.2. Bronchiectasis related to AAT deficiency

Bronchiectasis is a chronic condition that causes coughing up of mucus. In this condition, the walls of the bronchi are thickened from inflammation and infection [97]. Two of the first 5 patients diagnosed for AAT deficiency by Laurell and Eriksson in the early 1960s had bronchiectasis [98]. Bronchiectasis usually occurs in patients with COPD but can also manifest in AAT deficiency

related conditions. It can be associated with or without concomitant emphysema [99]. A recent study demonstrated that, similar to COPD patients, bronchiectasis patients exhibit higher frequency of AAT deficiency genotypes [100]. The available data, however, is still insufficient to draw any concrete conclusions about the association between AAT deficiency and bronchiectasis.

I.5.3. Asthma related to AAT deficiency

AAT deficiency has been reported to cause asthma-like symptoms in some patients [101]. Furthermore, individuals with AAT deficiency showed a high rate (22 %) of asthmatic symptom markers such us wheezing, atopy, elevated serum IgE, et cetera., compared to those with COPD but not AAT deficiency [94]. Other studies have shown an increased prevalence of asthma in the alpha1-antitrypsin-deficient population over time (4–38%) [102]. The biological mechanism behind this has not yet been well investigated. The main hypothesis is that the link between asthma and AAT deficiency might be due to the protease-inhibitor imbalance and the pro-inflammatory effect caused by misfolded or degraded AAT. Research is needed to better understand the molecular mechanisms that underlie AAT deficiency and asthma. It is also recommended to screen for AAT deficiency in late-onset asthma patients.

I.5.4. Other respiratory manifestations that can benefit from AAT therapy

Cystic fibrosis (CF) is a hereditary disorder caused by mutations on the CF transmembrane conductance regulator (CFTR) gene, a 27-exon, 250-kb segment of chromosome 7 [103]. The most common cause of morbidity and mortality in CF is lung disease, which begins in childhood with thick mucus, chronic airway infection, and inflammation, resulting in progressive impairment of lung function and early death [104, 105]. AATD and CF have some significant characteristics in common. The chronic conditions are both hereditary, occurring mainly in white people, with most of their symptoms affecting the lungs. The neutrophil is the principal inflammatory cell in both conditions, and NE plays an integral role in their pathogenesis [32, 106]. CF has a high neutrophil burden with a predominantly bronchial distribution, suggesting that it is an ideal situation for aerosol delivery of AAT [24].

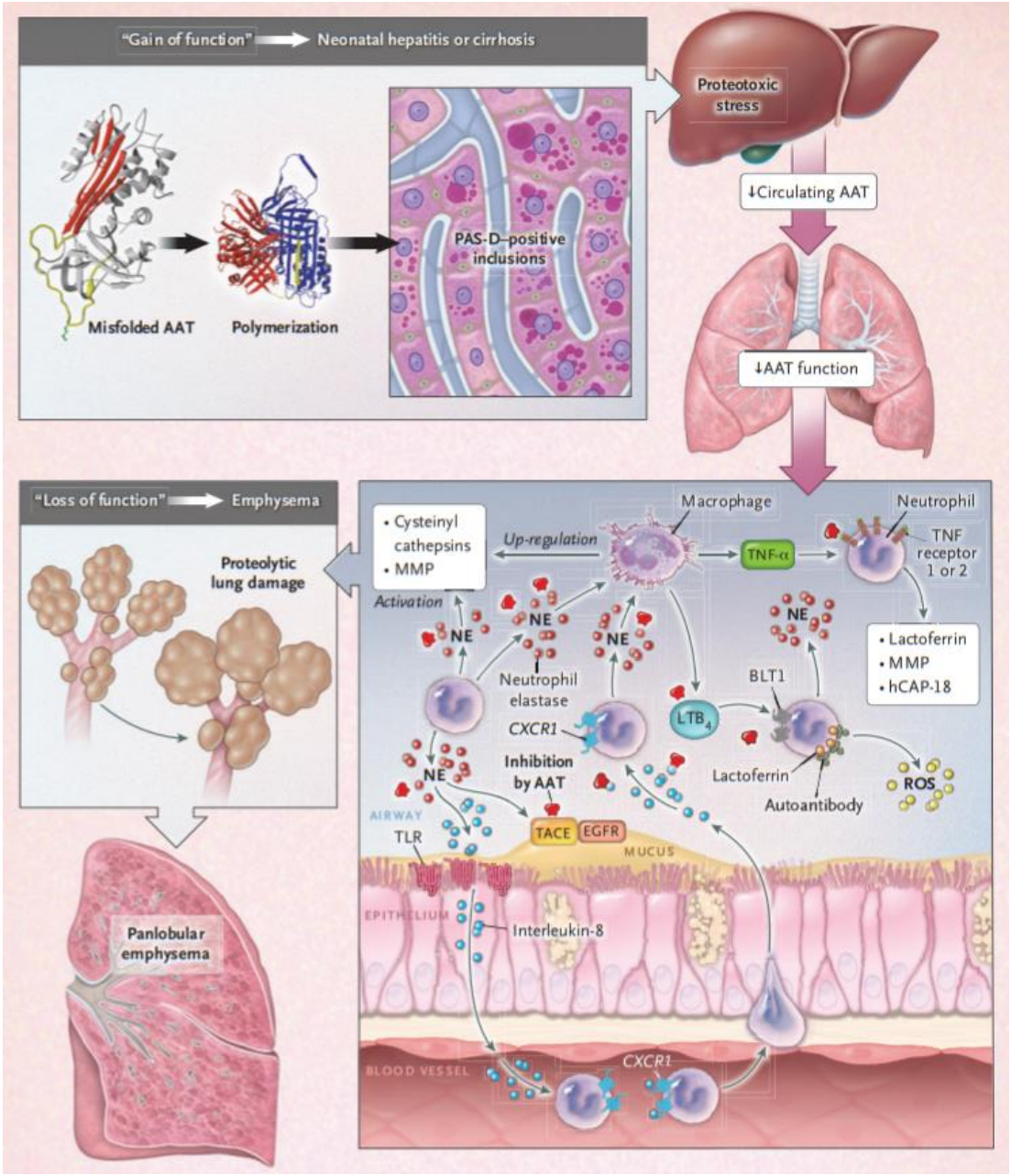

Figure 3. Pathophysiology of AAT deficiency [84]. Misfolded AAT forms polymers that accumulate as hepatocyte inclusions, which are positive on periodic acid–Schiff staining with diastase digestion (PAS-D). The misfolded AAT causes proteotoxic stress and a gain-of-function liver disease. AAT deficiency results in an excess of NE, which leads to mucin production and secretion and increases expression of other proteases and inflammatory cytokines. AAT is also a potent anti-inflammatory agent, regulating neutrophil chemotaxis, degranulation, autoimmunity, and apoptosis through interactions with interleukin-8, leukotriene B4 (LTB4), and tumor necrosis factor α (TNF-α). AAT is inactivated by oxidation, proteolytic cleavage, and polymerization. Thus, with a deficiency of AAT, neutrophils are increased, and protease activity is unopposed. Structural damage and susceptibility to infection occur, leading to tissue damage and emphysema. Abbreviations: BLT1, denotes LTB4 receptor 1; CXCR1, C-X-C motif chemokine receptor 1; EGFR, epidermal growth factor receptor; hCAP-18, human cathelicidin antimicrobial peptide 18; MMP, matrix metalloproteinase; ROS, reactive oxygen species; TACE, TNF-α converting enzyme; TLR, toll-like receptor.

I.6. DEVELOPMENT OF THERAPIES

I.6.1. Intravenous augmentation

Patients with AAT-deficiency-associated respiratory disease can currently receive weekly IV infusions of plasma-derived AAT, which are intended to slow the progression of emphysema, reduce exacerbations, and improve quality of life. There are several approved products available in the US and EU, as listed in Table 4. Different products exhibit different purities and activities. According to the author of a study comparing four plasma-derived AATs commercially available in EU, Respreeza® has the highest level of purity and most specific activity [11]. The augmentation therapy was approved by the US Food and Drug Administration (FDA) in 1987. Clinical trials examining the efficacy of AAT augmentation therapy have been conducted later, in randomized, controlled studies. A summary of those studies is provided in Table 5. Among the studies listed, five showed lower forced expiratory volume (FEV) decline in the treatment group, and five showed lower CT lung density decline in the treatment group. In some cases, the two efficacy effects were combined, while in some cases, only one readout was reached. Additionally, IV infusion of AAT reduced the exacerbation frequency and mortality rate. Different trials show a wide variety of results, perhaps due to the different products used, doses, study designs, target populations, et cetera.

The augmentation therapy is recommended for 60 mg/kg weekly infusions by the European Respiratory Society (ERS)/American Thoracic Society (ATS), which has been proved to maintain serum levels of AAT above the protective threshold (11 μM) [107]. The therapy was approved based on the pharmacokinetics of AAT without the evaluation of its efficacy. Conclusive evidence for the clinical efficacy of AAT therapy was first demonstrated by the Randomized, Placebo-controlled Trial of Augmentation Therapy in Alpha 1 Proteinase Inhibitor Deficiency (RAPID) program, which highlighted the importance of early AAT deficiency detection and treatment to preserve functional lung tissue and reduce the severity and frequency of lung infections. Besides 60 mg/kg weekly administration, higher dose (120 mg/kg every 2 weeks) is indicated in the Spanish guidelines. Studies have also been conducted at higher doses and longer intervals (150/180 mg/kg every 3 weeks, 250 mg/kg every 4 weeks), but these doses failed to maintain serum concentrations of AAT within the dose window [108]. Due to the inconvenience of weekly IV infusions over a lifetime, alternative methods of administration were explored, such as self-administration or at-home administration. Respreeza® is the only approved IV AAT therapy licensed for self-administration in Europe. With proper trainings, patients can be able to perform self-administration. By utilizing self-administration rather than traditional healthcare professional

procedures (in a hospital or clinic), patients are able to take care of their disease in their own environment, saving work time, hospital visits, travel time, and reducing the chance of contracting COVID19 under pandemic conditions [109].

Unfortunately, the access to IV infusions of human AAT for augmentation therapy is rather limited for patients. To begin with, AAT therapy has not yet been approved in all countries. This therapy is available in the US, Canada, Germany, Austria, Poland, Spain, Italy, Ireland, France, Belgium, Switzerland, The Netherlands, Denmark, Sweden, Norway, Finland, Greece, Portugal, Argentina, Brazil, Chile, Colombia, and Mexico [110]. A second problem is that the therapy involves high expenses, which can be financially draining for patients. Taking into account other costs, such as doctor visits, hospital stays, and prescription drug costs, the therapy costs approximately $82,000 per patient per year in the United States [111]. Furthermore, not all the patients who present symptoms can benefit from the augmentation therapy. The therapy is usually recommended to treat the most severe forms of AAT deficiency (patients with PI*ZZ and PI*Null genotypes) [112]. There is no specific data supporting AAT therapy in PI*SZ and PI*MZ individuals [113], and it remains unclear whether AAT therapy is beneficial in these patients [114]. AAT therapy that involves weekly IV infusions over the course of a lifetime still poses an inconvenience to patients. Due to the COVID19 pandemic since 2020, it has become more difficult and riskier for patients to receive continuous augmentation treatment. Hence, it is imperative to seek new, cost-effective, more affordable, and convenient approaches to treat AATD related diseases.

I.6.2. Inhaled AAT

I.6.2.1. Inhaled AAT in treating COPD related emphysema

Besides the IV infusion of AAT, inhaled AAT was considered as a possible alternative administration route [115]. One of the biggest advantages of inhaled AAT over IV infusion is that it does not require intravenous access. Additionally, it provides direct delivery to the lung injury site. The first attempt of using inhaled AAT was by Hubbard et al in 1989 [116]. In this approach, approximately 100 mg of human plasma derived AAT was administered by aerosol every 12 hours for seven days. In this short-term aerosol administration of human plasma AAT to patients suffering from AAT deficiency, the anti-neutrophil-elastase defenses found in the lower respiratory tract returned to normal.

Stolk et al. reported the first randomized placebo-controlled clinical trial evaluating the efficacy of nebulized inhaled AAT [117]. The recent trial targeted 168 COPD patients with AAT deficiency-ZZ with a high risk for exacerbations, who received twice-daily inhalations of 80 mg AAT solution

or placebo for 50 weeks. Inhalation of AAT did not prolong the time to the first event-based exacerbation after randomization, but it did reduce significantly the symptomatic Anthonisen type I exacerbations after randomization. For instance, 18.8% of AAT-treated patients showed the worsening of three symptoms (dyspnoea, sputum volumes and color), while the percentage of the placebo group was 31.3%.

Study conducted by Stolk et al. encountered some issues that could have hindered the efficacy of therapy. During the study, nebulizer device and medication dispensing were improved based on feedback from patients. The rate of adverse events was significantly reduced in the AAT group following optimization. It is possible that a selection of exacerbations as the primary outcome would pose some limitations. As emphysematous patients may experience pauci-inflammatory episodes, it is unclear whether the anti-NE effect can contribute to the prevention of exacerbations of AATD [118, 119]. The majority of patients, ~85 %, experienced at least one exacerbation during the trial, however, one half of the patients only experienced a type III exacerbation that presented with only one symptom. As a single symptom, dyspnoea was most reported by these patients. It was difficult to estimate the impact of the anti-NE treatment on exacerbations defined solely by an increase in dyspnea recorded in a diary. Moreover, participants were included in the study if they had experienced at least two moderate or severe exacerbations during the previous 18 months, one of which occurred within the last year. Patients did not necessarily suffer from frequent exacerbations based on this definition, and in fact 25% of patients did not meet the standard definition of a frequent exacerbator, which may have limited the potential for improvement.

In this trial, it was demonstrated that inhaled AAT was safe and feasible, and that the inhalation device and technique could be improved over treatment. The results obtained were not as positive as anticipated, which did not support the use of inhaled AAT for most patients with AAT-deficiency associated emphysema. It is possible, however, that patients with frequent exacerbations of infective diseases and increased sputum volume/purulence may benefit more from inhalation of AAT.

I.6.2.2. Inhaled AAT in treating cystic fibrosis

Inhaled AAT has also been studied to treat CF [120]. The major causes of morbidity and mortality in CF are related to lung disease, which starts in childhood with the occurrence of thick mucus, chronic airway infection and inflammation [106]. CF represents one of the most striking examples of a neutrophil-dominated lung inflammation. CF lung neutrophils constitute more than 70 % of the inflammatory cell population in the epithelial lining fluid (ELF), while in a healthy lung, this figure is only 1 % [121]. Individuals with CF have significantly higher levels of NE in BAL than

those with non-CF bronchiectasis and AATD [23, 122]. Although the levels of AAT and anti-NE molecules, such as secretory leukoprotease inhibitor (SLPI) and elafin are actually increased in the CF lung, given the increased oxidant burden and decreased antioxidant level found in the CF lung, these anti-NE molecules are however oxidized by oxidants released by neutrophils, or are rendered inactive by the cleavage by excess NE and other proteases. This excess burden of NE in the CF lung, with its obvious deleterious effects, led to the evaluation of AAT treatment in CF.

McElvaney and colleagues made the first attempt to evaluate the efficacy of inhaled AAT in CF patients in 1991 [23]. In this study, 1.5 – 3 mg/kg AAT was given twice daily for 1 week by aerosol. The inhibition of NE and re-establishment of anti-NE capacity on the respiratory epithelial surface was achieved when AAT level was above 8 μM in ELF. In addition, the treatment also reversed the inhibitory effect of CF ELF on Pseudomonas killing by neutrophils. In 1995, Berger et al carried out a phase I study of aerosolized Prolastin to evaluate its efficacy in CF airways, with the dose of 100, 200 and 350 mg AAT delivered to 26 patients for 4 weeks [123]. The inhibition of NE in ELF was demonstrated to be dose dependent. However, AAT did not reduce IL-8 levels or neutrophil counts. In 2007, Griese et al examined the effect of 4 weeks of AAT inhalation on lung function, protease–antiprotease balance and airway inflammation in CF patients [24]. In this prospective randomized study, 52 CF patients received a daily inhalation of 25 mg AAT for 4 weeks. The treatment increased AAT levels and decreased the levels of elastase activity, neutrophils, pro-inflammatory cytokines, and the numbers of *P. aeruginosa* in the induced sputum. A significant effect was however not observed on lung function. Another randomized, double-blind, placebo-controlled study to evaluate the safety of a new aerosolized AAT formulation in CF patients was performed in 2016 by Gaggar et al [32]. AAT was inhaled once daily for 3 weeks with a placebo, 100 mg, or 200 mg of AAT in thirty CF patients. An increase in the level of AAT in sputum was confirmed to be dose dependent. Study results concluded that inhaled AAT was safe and well tolerated by patients with CF.

I.6.2.3. Inhalation device used in aerosol AAT delivery

In the early study of inhaled AAT, an Ultravent nebulizer was used to deliver AAT to the lung [116]. Brand et al. subsequently compared the deposition of AAT using four commercial inhalation devices [124]. Six patients with mild-to-severe COPD received inhaled AAT by either PARI-LC Star, HaloLite, or AKITA system in combination with LC Star and Sidestream. The highest peripheral deposition and the shortest inhalation times could be obtained by an optimized breathing pattern, which could be controlled by AKITA. By utilizing the AKITA device, the inhaled volume could be programmable according to the individual lung function of the patient

and allowed for the patient to inhale the maximum volume possible. The HaloLite device also provided control over the volume of inhalation. It is passively controlled however by adapting the nebulization process to the patient's breathing pattern. The patients were free to inhale whatever slowly or fast, shallow or deep. The HaloLite device therefore needed more time to deliver the same amount of drug in the lung than the AKITA device. When using a conventional procedure without controlling the breathing pattern, the distribution of the drug in the lungs was generally heterogeneous.

In the clinical trial of inhaled AAT in patients with severe AAT deficiency and frequent exacerbations of COPD, an eFlow® inhalation device was used. AAT-treated individuals experienced significantly fewer safety events due to improved handling of the nebulizer and drug [117]. It revealed that not only could an inhalation device be optimized for better pulmonary delivery, but also to minimize adverse effects.

I.6.3. Other therapies

Some other alternative approaches are also being developed and tested in pre- and/or clinical studies for AAT deficiency treatment, such as orally bioavailable neutrophil elastase inhibitors [125], liver-directed therapies that include gene-silencing molecules [126], protein-folding and chaperone modifiers [127], autophagy enhancers and polymerization blockers [128], et cetera. Clinical trials have been conducted with some of these products, but none have yet been approved for clinical application.

Recent developments in clustered regularly interspaced short palindromic repeats (CRISPR) have led researchers to explore the potential use of this novel gene editing technique in the correction of the gene mutation responsible for AAT deficiency [129]. To correct the Z mutation and increase the serum level of M-AAT, one common approach is to inject an adeno-associated virus (AAV) vector that encodes an AAT guide RNA and homology-directed repair template [130, 131]. Another strategy that could be used in combination with the above approach would be to decrease liver aggregates, as done by Shen et al [132]. The single or combined approaches resulted in everting the AATD pathology [131] and the genomic analysis confirmed significant disruption to the gene [130, 131]. It also completely [132] or at least partially [130] restored the serum level of M-AAT. It is an important milestone that may lead to a cure for AAT deficiency, but it must be further evaluated, and more research and trials should be conducted before it is applied clinically.

Table 4. Approved AAT therapy preparations. Adapted from Parr et al [133] and Rahaghi [134].

Trade name	Company	Availability	Specific activity and concentration
Aralast-NP[a]	Baxter	US	⩾0.55mg of AAT per mg of total protein; 20mg/ml after reconstitution in provided diluent
Glassia®	Kamada	US, Canada, Australia, New Zealand	⩾0.7mg of AAT per mg of total protein; provided in solution at 20mg/ml
Prolastin®-C[b]	Grifols	US, Argentina, Colombia	⩾0.7mg of AAT per mg of total protein; provided in solution at 50mg/ml
Zemaira®[c]	CSL Behring	US	⩾0.7mg of AAT per mg of total protein; 50mg/ml after reconstitution in provided diluent
Alfalastin®	LFB	France	0.67mg of AAT per mg of total protein; 33.33mg/ml after reconstitution in provided diluent
Prolastin®[d]	Grifols	National licenses in EU with mutual recognition procedure	⩾0.35mg of AAT per mg of total protein; 25mg/ml after reconstitution in provided diluent
Respreeza®	CSL Behring	Countries within the EU	⩾0.7mg of AAT per mg of total protein; 50mg/ml after reconstitution in provided diluent

[a] Aralast-NP is a newer preparation of a previously approved product, Aralast™.

[b] Prolastin®-C is a newer preparation of a previously approved product, Prolastin®.

[c] Zemaira® is marketed as Respreeza® in Europe.

[d] Prolastin® is licensed in the member states of European Economic Area in Austria, Ireland, Italy, Germany, Greece, Poland, Portugal, and The Netherlands. Prolastin® is also marketed as Prolastina® in Denmark, Finland, Norway, Spain, and Sweden, and marketed as Pulmolast® in Belgium.

AAT, alpha1 antitrypsin ; EU, European Union; LFB, Laboratoire français de Fractionnement et de Biotechnologies ; US, United States.

Table 5. Studies to assess efficacy of AAT augmentation therapy. Adapted from Parr et al [133].

Authors	Dose	Study design	Primary outcome	Principal results
Seersholm et al, 1997 [135]	60 mg/kg weekly	Observational with control group (n=295)	FEV1 decline	Lower FEV1 decline in treatment group (56 vs 75 mL/ year; P=0.02); treatment of apparent benefit in patients with FEV1 31%–65% predicted
American AAT Deficiency Registry Study Group, 1998 [136]	60 mg/kg, weekly for 33% of the patients, fortnightly for 43% and monthly for 24%	Observational with control group (n=1,129)	FEV1 decline, mortality	Mortality reduction (OR 0.64; P=0.02); lower FEV1 decline in patients receiving IV AAT treatment and FEV1 35%–49% predicted (66 vs 93 mL/year; P=0.03)
Dirksen et al, 1999[137]	250 mg/kg/28 days	Randomized, double-blind, placebo controlled	FEV1 decline, CT lung density decline	Lower CT lung density decline (2.6 g/L/year vs 1.5 g/L/year, P=0.07).
Lieberman, 2000 [138]	60 mg/kg weekly for 55% of the patients, fortnightly for 37%, monthly for 8%	Observational (on-line questionnaire) (n=89)	Exacerbation frequency	Reduction in exacerbation frequency (3–5 exacerbations/year vs 0–1/year during AAT IV treatment)
Wencker et al, 2001 [139]	60 mg/kg weekly	Observational cohort without control group (n=96)	FEV1 decline	Lower FEV1 decline rate during treatment (49.2 vs 34.2 mL/year, P=0.019); patients with FEV1 .65% (256 vs 53 mL/year, P=0.001)
Stockley et al, 2002 [140]	60 mg/kg weekly	Descriptive/mechanistic (n=12)	inflammatory markers (sputum)	Significant reduction in sputum LTB4

Authors	Dose	Study design	Primary outcome	Principal results
Tonelli et al, 2009 [141]	60 mg/kg weekly	Observational with control group (n=164)	FEV1 decline, mortality	Increase in FEV1 (10.6±21.4 mL/year) vs decline (36.96±12.1 mL/year; P=0.05); no difference in mortality
Dirksen et al, 2009 [142]	60 mg/kg weekly	Double–blind, randomized, placebo-controlled study (FEV1 =25%–80% predicted) (n=77)	Lung function, quality of life, exacerbations and lung density measured by CT	Reduced rate of CT lung density decline in treated individuals (P=0.049); no difference in FEV1 and DLCO; no difference in exacerbation rate but less severe in patients on active treatment
Chapman et al, 2009 [143]	60 mg/kg weekly	Meta-analysis of studies including patients treated with IV AAT compared with controls from Canadian Registry (n=1,509)	FEV1 decline	Reduction in FEV1 decline in patients with AAT IV treatment in 26% (17.9 mL/year); limited to subjects with FEV1 30%–65% predicted
Cochrane review Gøtzsche and Johansen, 2010 [144]	60 mg/kg weekly	Meta-analysis of 2 randomized studies, controlled with placebo (n=140)	FEV1 decline, DLCO decline, lung density (CT), exacerbations	Lung density decrease is lower in patients under IV treatment (P=0.03); no differences in lung function; no differences in exacerbations; augmentation therapy not recommended
Stockley et al, 2010 [145]	60 mg/kg weekly	Integrated analysis of lung density (n=119)	Density decline, FEV1 decline	Lower lung density decline in treated patients (1.73 vs 2.74 g/L, P=0.006); no differences in FEV1 decline
Barros-Tizón et al, 2012 [146]	180 mg/kg/21 days	Retrospective study (pre–post AAT IV treatment) (n=127)	Frequency and severity of exacerbations and hospitalization costs	Decrease in number and severity of exacerbations and costs related with hospitalizations

Authors	Dose	Study design	Primary outcome	Principal results
Ma et al, 2013 [147]	60 mg/kg weekly	Observational cohort with control group (n=100)	Plasmatic desmosine and isodesmosine	Significant decrease in desmosine and isodesmosine levels in the treated cohort against non-treated cohort (P,0.0001), with similar values to normal population
Chapman et al, 2015 [148]	60 mg/kg weekly	Multicenter study, double-blind, randomized, control with placebo (Pi*ZZ, null or rare genotype with AAT ,11 μM, emphysema confirmed by CT and FEV1 35%–70% predicted) (n=180)	Lung function, quality of life, exacerbations, pulmonary density by CT	Reduction in decrease of lung density in treated patients (P=0.03); no differences in FEV1 or DLCO; no differences in exacerbations; no differences in quality of life; AAT IV treatment is safe
McElvaney et al, 2017[149]	60 mg/kg weekly	Open label extension for RAPID patients who had received active (early start group) or placebo (delayed start group)	CT lung density decline, FEV1 decline, DLCO decline	Reduced and comparable lung density decline for both groups on active treatment No difference in FEV1 or DLCO decline

AAT, alpha1 antitrypsin; OR, odds ratio; IV, intravenous; CT, computed tomography; FEV1, forced expiratory volume in 1 second; DLCO, carbon monoxide diffusion capacity.

II. PEGYLATION OF PROTEIN THERAPEUTICS

Polyethylene glycol (PEG) is a biocompatible, non-immunogenic compound composed of ethylene glycol repeats [150]. Synthetic, highly water-soluble, and available in a wide range of molecular weights [151], PEGs have been used for decades as an excipient in cosmetics, consumer products, and also in pharmaceutical technology [152]. PEGylation is a process of conjugating PEG molecules, either covalently or noncovalently, to small molecules or macromolecules such as proteins, macromolecular carriers, oligonucleotides, et cetera. to improve their pharmaceutical properties [153]. PEGylation may prolong circulation time of a macromolecule, enhance solubility of drug substances, protect against proteolysis breakdown in vivo, and reduce immunogenicity of some biopharmaceuticals [154]. To date, dozens of PEGylated protein therapeutics have been approved for clinical use, the majority of which are macromolecules and a few of which are small molecules or nanoparticles (Table 6). Others are currently undergoing clinical trials against a variety of diseases, such as COVID19, HIV, and cancer (available at:

https://clinicaltrials.gov/ct2/results?term=Pegylated&Search=Apply&recrs=d&age_v=&gndr=&type=&rslt=).

PEGylation was initially introduced by Davis and Abuchowski in 1970 for albumin and catalase alteration [155]. Since then, PEGylation strategies have been improved and have experienced substantial improvements [156, 157]. First generation PEGylation involved random PEG conjugation to the macromolecule, which resulted in multiple isoforms of products with various physicochemical and pharmaceutical properties [158]. The second generation of PEGylation benefited from PEG derivatives, including polymers with higher molecular weights and branched PEG structures [159]. The usage of large activated PEG enabled site-specific PEGylation, which significantly improved the purity of the synthesized PEGylated products [160]. Branched PEG was better at decreasing immunogenicity and increasing serum half-life compared to linear PEG, but it sometimes decreased the activity of biomolecules [161]. The third generation of PEGylation is intended to rationalize the PEGylation chemistry and preserve the bioactivity of the biomolecule [162–164].

Here, we will discuss the mainstream PEGylation chemistries, the effects of PEGylation on protein therapeutics, the advantages, and concerns of PEGylation, and some cases of PEGylated AAT.

Table 6. FDA Approved PEGylated Drugs on the market. Available online: https://www.biochempeg.com/article/58.html

Drug	Company	PEGylated entity	Indications	Average MW of PEGs	Approved Year
Macromolecular Drugs					
Besremi	PharmaEssentia Corp	Interferon	polycythemia vera	40 kDa	2021
Skytrofa	Ascendis	Human growth hormone	Growth hormone deficiency	4 x 10 kDa	2021
Empaveli	Apellis	Pentadecapeptide	Paroxysmal nocturnal hemoglobinuria (PNH)	40 kDa	2021
Nyvepria	Pfizer Inc.	G-CSF	Neutropenia Associated with Chemotherapy	20 kDa	2020
Esperoct	Novo Nordisk	Recombinant antihemophilic factor	hemophilia A	40 kDa	2019
Ziextenzo	Sandoz	G-CSF	infection during chemotherapy	20 kDa	2019
Udenyca	Coherus Biosciences	G-CSF	infection during chemotherapy	20 kDa	2018
Palynziq	BioMarin Pharmaceutical	Recombinant Phenylalanine ammonia lyase	phenylketonuria	~ 9 X 20 kDa	2018
Revcovi	Leadiant Bioscience	Recombinant adenosine deaminase	ADA-SCID	80 kDa	2018
Fulphila	Mylan GmbH	G-CSF	infection during chemotherapy	20 kDa	2018
Asparlas	Servier Pharma	L-asparaginase	leukemia	31-39 x 5 kDa	2018

Jivi	Bayer Healthcare	Recombinant antihemophilic factor	hemophilia A	2 X 30 kDa	2017
Rebinyn	Novo Nordisk	Recombinant coagulation factor lX	hemophilia B	40 kDa	2017
Adynovate	Baxalta	Recombinant antihemophilic factor	hemophilia A	≥1 X 20 kDa	2015
Plegridy	Biogen	Peginterferon β-1a	multiple sclerosis	20 kDa	2014
Omontys	Takeda	Erythropoietin	anemia	2 X 20 kDa	2012
Sylatron	Merck	Peginterferon-alfa-2b	melanoma	12 kDa	2011
Krystexxa	Horizon Pharma	Recombinant uricase protein	gout	40 X 10 kDa	2010
Cimzia	UCB	Antitumor necrosis factor	rheumatoid arthritis	40 kDa	2008
Mircera	Roche	Erythropoietin	anemia	30 kDa	2007
Macugen	Pfizer	Aptamer	macular degeneration	2 X 20 kDa	2004
Somavert	Pfizer	Human growth hormone	acromegaly	4-6 X 5 kDa	2003
Neulasta	Amgen	G-CSF	infection during chemotherapy	20 kDa	2002
Pegasys	Roche	Peginterferon-alfa-2a	hepatitis B and C	40 kDa	2002
Pegintron	Schering	Peginterferon-alfa-2b	hepatitis C, melanoma	12 kDa	2001
Oncaspar	Enzon	Asparaginase	leukemia	69-82 X 5 kDa	1994

Adagen	Enzon	Adenosine deaminase	ADA-SCIO	11-17 X 5 kDa	1990
Small Molecular Drugs					
Movantik	AstraZeneca	Naloxone	constipation	339 Da	2014
Asclera	Chemische Fabrik Kreussler	Dodecyl alcohol	varicose veins	400 Da	2010

List of drugs containing peg is indicated (number of units) x (MW of each PEG unit). G-CSF: growth colony-stimulating factor.

II.1. PROTEIN PEGYLATION CHEMISTRY

II.1.1. First generation: random PEGylation

In the early days of PEGylation, the reaction primarily targeted the amine groups of macromolecules, mostly the alpha and epsilon amino groups of lysine [150]. Random PEGylation reactions were successfully used in some approved PEGylated products (Table 6). For instance, Adagen® and Oncaspar®, are both complex mixtures of various PEGylated conjugates (higher polydispersity) at lysine and N-terminal residues. Similarly, SynlatronTM, PEGASYS®, and Mircera® are also randomly PEGylated drugs, however they are mixtures of mono-PEGylated positional isomers with prolonged half-lives [165]. First generation of PEGylation typically involves small PEG derivatives, including: PEG dichlorotrizaine, PEG tresylate, PEG succinimidyl carbonate, PEG benzotriazole carbonate, PEG p-nitrophenyl carbonate, PEG trichlorophenyl carbonate, PEG carbonylimidazole and PEG succinimidyl succinate [159].

Cyanuric chloride (2, 4, 6-trichloro-s-triazine) was used in the initial work of Davis et al to prepare activated PEG for protein conjugation [155]. In addition to lysine, PEG dichlorotriazine also reacts with serine, tyrosine, cysteine and histidine. Despite less reactivity with nucleophilic residues, the remaining chloride is sufficient to crosslink proteins that contain additional nucleophilic residues. Ultimately, due to the lack of specificity and toxicity of cyanuric chloride derivatives, they are not suitable for use in commercial products [156].

PEG tresylate is more specific for lysine conjugation than PEG dichlorotriazine. PEGylation chemistry for this conjugation, however, is not well understood. Upon reaction with small molecules amines, a sulfamate-linked product was formed, which would result in a complex heterogeneous mixture [166].

Due to the limitations in the early reactions of PEGylation, such as impurities, low molecular weight products, unstable linkages, and lack of selectivity, acylation of amino groups has been explored through urethane linkages, in which PEG p-nitrophenyl carbonate, PEG trichlorophenyl carbonate, and PEG carbonylimidazole have been employed for polypeptide modification. PEG succinimidyl succinate (PEG-SS) is another first-generation PEG-reagent that has been used for protein PEGylation. The linkage is, however, susceptible to hydrolysis after PEGylation and has hydrolysis and immunogenic issues [167].

Several drawbacks of the first-generation PEG reagents, including lack of specificity, degradability, decreased conjugate activity, hydrolysis, and heterogeneity of conjugates, led to the development of a second generation of PEGylation, also using higher molecular weight PEG.

II.1.2. Second generation: site-specific PEGylation

The second-generation PEGylation has been developed in order to address the shortcomings of the first generation. Site-selective PEGylation can be very useful to introduce PEG at specific amino acid sites in various proteins. A successful example of site-selective PEGylation is Neulasta®, which is a N-terminal mono-PEGylated granulocyte colony-stimulating factor bearing a 20-kDa PEG [168]. The improved pharmacokinetic behavior of this biopharmaceutical significantly reduced the administration frequency from once per day, to only once per chemotherapy cycle compared to the unconjugated form, Neupogen® [169].

Other site specific PEGylation strategies include i) amino acid targeting such as cysteine, serine, threonine, tyrosine and tryptophan, ii) C-terminal PEGylation, iii) enzymatic PEGylation [170]. PEGylation yield can be dramatically increased by enzyme selectivity, particularly when targeting certain sites which cannot be reached by chemical methods. The focus of this section will be on N-terminal PEGylation and thiol PEGylation, as these two types of PEGylation have been primarily used in this thesis.

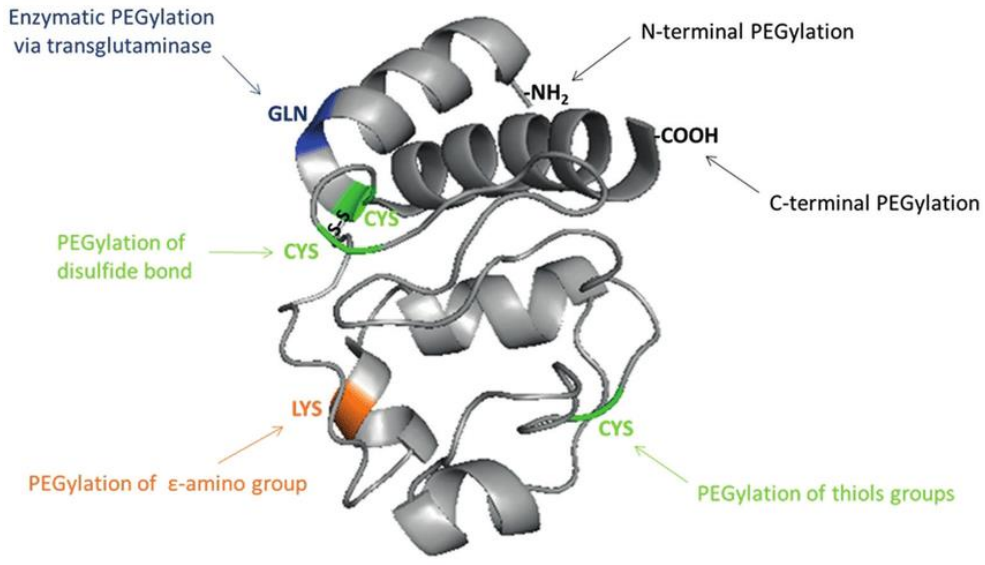

Figure 4. Potential sites of PEGylation in proteins. Adapted from [158].

N-terminal PEGylation takes advantages of the difference in *pK*a values between the amino group of the N-terminal amino acid residue, about 7.6 – 8, and the amino group in the side chains of lysine (~10.5). This difference allows the selectivity at the N-terminus of proteins at mildly acidic conditions (pH 4.5 – 6.5), with the use of reductive agents like sodium cyanoborohydride. PEG

aldehydes were commonly used in N-terminal PEGylation. The reaction proceeds through an intermediate Schiff base reduced in situ to obtain a stable secondary amine (Figure 5). Despite the increase in selectivity with lower pH, subsequent purification steps cannot be omitted. In the case of AAT, as a result of the unique cysteine cap in the molecule, the disulfide bond between Cys232 and the free cysteine cap protects the thiol group. Thus, a free carboxyl group and amine group are exposed in cysteine cap. However, the stabilized thiolate led to the raise of the pKa of the cysteine cap [171], which is similar to that of lysine. Thus, it is also possible that PEG-aldehyde is conjugated to lysine or the cysteine cap in AAT.

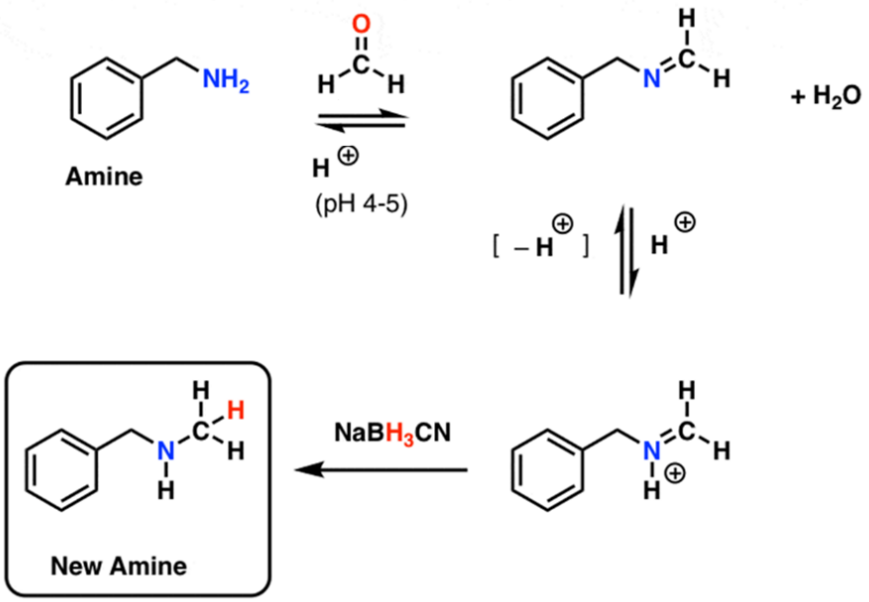

Figure 5. The chemical mechanism of reductive alkylation. An intermediate Schiff base is formed under acidic condition with the presence of formaldehyde, which is further reduced by a reducing agent.

Aside from the traditional N-terminal PEGylation, some other strategies have also been investigated to attain the N-terminal selectivity, as shown in Figure 4. Schoffelen et al demonstrated that the use of imidazole-1-sulfonyl azide can efficiently convert protein amines to azides [172]. Chan et al introduced a N-terminal PEGylation strategy with an alkyne group by reacting with a ketene at pH 6.3 – 9.2 [173]. Obermeyer et al demonstrated an oxidative strategy for the efficient modification of N-terminal residues on peptides and N-terminal proline residues on proteins. The strategy uses o-aminophenols or o-catechols that are oxidized to active coupling species in situ using potassium ferricyanide [174]. Song et al discovered the selectivity on N-terminal alpha-amine over the epsilon-amine of lysine, from catechol, which has been extensively utilized as an adhesive molecule for material-independent surface chemistry and as a crosslinker in hydrogel preparation [175].

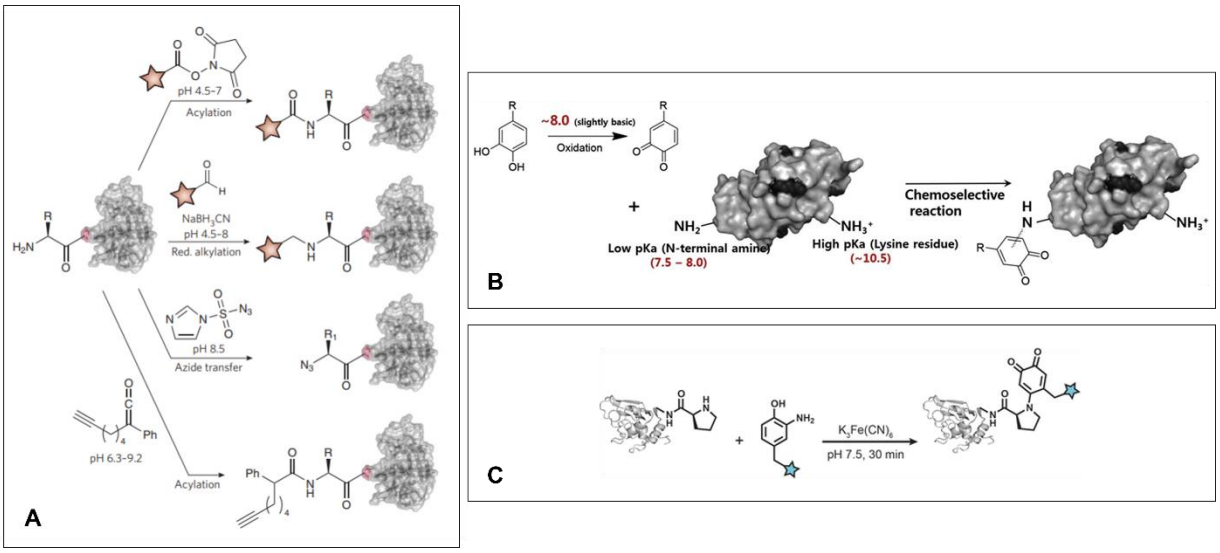

Figure 6. N-terminal PEGylation strategies, adapted from [173–176].

It is uncommon to find a single free cysteine in the amino acid sequence of a protein because the -SH group has a high degree of activity, forming disulfide bonds with a second cysteine. However, when a protein possesses, or is engineered to possess, a single cysteine, high selectivity can be obtained. Alpha1 antitrypsin is one of the proteins which presents a single cysteine in its sequence. The thiol PEGylation of AAT will be discussed later in this section. PEG maleimide is the most commonly used active PEG for thiol PEGylation [177]. A thioether bond is formed by Michael's addition between the double bond of the maleimide ring and the thiol group [178]. Thiol PEGylation was also accomplished using orthopyridyl disulfide (PEG-OPSS). In this case, the resulting linkage is a disulfide bridge formed with the thiol group on the protein [177]. The cysteine residue is sometimes enclosed in hydrophobic patches, which makes it difficult to achieve for thiol PEGylation. Partially unfolded proteins might expose otherwise inaccessible sites, leading to increased reactivities. To overcome this obstacle, Tayar carried out a two-step reaction for PEGylation of the hidden Cys17 on interferon α (IFN- α), which is generally inaccessible to high molecular weight PEG. A small bi-functionalized PEG–OPSS was firstly introduced to the Cys17 and then further PEGylated through the remaining OPSS group [177].

Disulfide bridge opening and protein engineering strategy were used to overcome the scarcity of the free unpaired cysteine in proteins [179]. Cysteine was frequently introduced at the N- or C-terminus of proteins in order to enhance accessibility and prevent structural changes [180, 181]. A critical disadvantage of opening disulfide bridges is the modification of the secondary structure, which can lead to complete inactivation of the protein. Consequently, any modification at this level should preserve the distance between the two sulfur atoms [177].

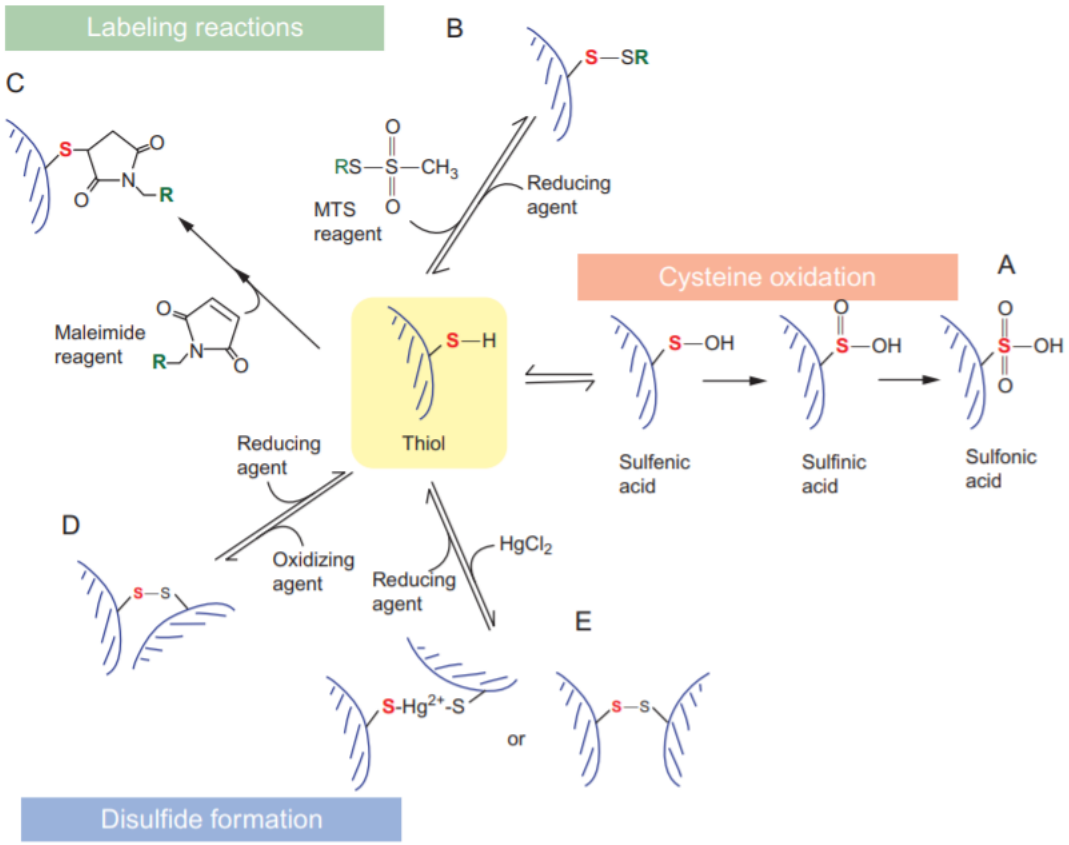

Figure 7. The thiol group of cysteine can be modified by several reactive agents. Adapted from [182]. Cysteinyl thiol (yellow box) reacts with several different reactive groups, including A) MTS reagents to form a mixed disulfide, B) maleimide reagents to form a bulky thioester bond, C) Hg2+ ion to form either a disulfide or a Hg2+ coordinated cross-link, D) oxidizing agents such as CuPhen that catalyze disulfide bond formation with adjacent cysteinyl thiols, and E) ambient oxygen to form higher oxidation states. The red, emboldened "S" signifies the cysteinyl sulfur group in the cysteine reactant. The green emboldened "R" signifies functional groups to be attached to the thiol. B and C are used in thiol PEGylation.

II.1.3. Third generation: customized PEGylation

Third-generation PEGylation looks to minimize the current trade-off between potency and circulation half-life for longer-lasting drugs [161]. A prodrug approach employing releasable PEG conjugates has been proposed as one method. Proteins are attached to PEG derivatives through cleavable linkages, which release the protein in vivo at a predetermined kinetic rate [150]. Releasable PEGylation presents the challenge of customizing the coupling chemistry that allows control of the release rate of the protein from the polymer [183]. As a general rule, the release mechanism should leave the protein completely unmodified (traceless) or minimally modified (nontraceless). Gong et al. presented substituted phenylglyoxal mPEGs that selectively phosphorylated arginine in antimicrobial peptides (AMPs), protected them from serum proteases, and released them in a traceless manner with full bioactivity at a rate influenced by the substituent [184]. Various

extensions of circulation time could be achieved by varying the identity, biodistribution, and dose of PEGylated AMPs, between 10 minutes and 1 to 2 days. Other reversible PEGylation reactions involve bicine linkers, histidine PEGylations, glucose, and other ligands that are cleaved by serum proteases and other enzymes, especially via β-elimination reaction [185, 186].

To preserve the bioactivity of the therapeutic protein, another approach is to create customizable PEGylation sites in order to decrease the steric hindrance caused by the conjugated PEG. It may also be possible to reduce steric hindrance in proteins by defining the PEG shapes and hydrodynamic radii. Molecular dynamics (MD) simulations can be a powerful tool in explaining and predicting experimental results and are efficient in providing an atomic-level insight into the interactions between PEG molecules and other compounds [187], which may greatly help with the design and screen for customized PEGylation. Ramezanghorbani et al achieved the accurate prediction of the interactions between PEG and proteins [188]. They simulated PEGylated chymotrypsin and found that PEG chains could stabilize partially unfolded intermediates and even assist in their refolding, depending on pH. The MD simulation confirmed the experimental results regarding the effect of PEG on protein folding and can assist in rational polymer design for protein-polymer conjugates.

Although MD simulation could be a powerful tool for predicting or anticipating a customized PEGylation in therapeutic proteins, there are some challenges that must still be addressed. First, biological complexes, reaction kinetics and mass transport conditions of experiments and simulations differ, which precludes any quantitative comparison between simulations and experiments [187]. Second, more accurate PEG force fields (FFs) need to be developed to predict the interactions between PEG and other molecules such as nucleotides and amino acids [189]. Last, large complexes of PEGylated drugs interacting with other molecules should be considered.

II.2. THE IMPACT OF PEGYLATION ON PROTEIN PHARMACEUTICS

In the late 1970s, Davis et al introduced PEGylation to decrease the immunogenicity of a protein [190]. Subsequently, PEGylation was also found to extend serum half-life, to reduce protein aggregation and proteolysis, and to increase protein shelf-life [191, 192]. The PEGylation of therapeutic proteins is one of the most widely used methods to enhance their pharmacokinetic properties.

The extended serum half-life of PEGylated proteins derives from the large hydrodynamic radius of PEG, which decreases renal clearance by preventing large PEG-protein conjugates (for PEG ≥ 20 kDa) from being filtered through the pores of the glomerular wall [170]. Large PEG also offers

a protection shield to the protein against proteases and antibodies via simple steric occlusion. PEG-protein conjugate is often less active than its non-PEGylated counterpart in vitro, presumably due to the limited access of substrates or binding partners to the protein surface/active site caused by the shielding effect from the PEG [193]. However, PEG-protein conjugates are also frequently found to be more effective in vivo, as the extended serum half-life compensates the loss of activity, which allows the therapeutic protein to be administrated less frequently.

Neulasta® is the PEGylated form of granulocyte colony-stimulating factor (G-CSF), which is produced by conjugating a 20 kDa PEG molecule to the N-terminus of the protein [194]. Its unconjugated counterpart, recombinant G-CSF, requires multiple daily doses due to its short half-life (3.5 – 3.8 h). In vitro biological activity of recombinant G-CSF was reduced following PEGylation. In contrast, PEGylated G-CSF, which showed prolonged serum half-life, demonstrated an overall better therapeutic value in vivo [168].

Interferons combined with ribavirin are commonly used to treat viral infections and cell-proliferative disorders [195]. Due to their short half-lives (4 - 5 hours), interferons must be administered three times per week by subcutaneous injection. Pegasys®, a PEGylated interferon-α-2a (IFNα-2a), was produced by conjugating a branched 40 kDa PEG to the lysine residues. The product is a mixture of mono-PEGylated IFNα-2a at either Lys31, 121, 131 or 134 [196]. The in vitro activity of PEGylated IFNα-2a is only 7 % of that of unconjugated IFNα-2a. In vivo, however, the prolonged pharmacokinetics of the drug compensated for its reduced in vitro potency. The frequency of administration was reduced to once per week, which still offered a higher rate of viral eradication.

Following the inhalation of therapeutic proteins, PEGylation has also been shown to enhance their retention in the lungs. Cantin et al. reported that a PEGylated version of recombinant non-glycosylated human AAT (to 20 kDa PEG) led to the persistence of the conjugates in the bronchoalveolar lavage after intranasal instillation in mice for at least 48 h, while its unconjugated counterpart was cleared within 24 h [14]. Koussoroplis et al demonstrated that mono-PEGylation of anti-IL17A F(ab')2 and anti-IL13 Fab' with two-armed 40 kDa PEG significantly sustained the presence of these antibody fragments in the murine lungs following intranasal administration. Moreover, IL17A F(ab')2 conjugated to 40 kDa PEG exhibited an improved therapeutic efficacy in reducing cellular infiltration and inflammation markers in a murine model of house dust mite-induced lung [197]. According to Guichard et al., conjugation of linear 30 kDa PEG or 2-armed 40 kDa PEG preserved the presence of the recombinant human deoxyribonulease I (rhDNase) in murine lungs for 15 days. [198]. The PEGylated RhDNase also provided similar therapeutic benefit in reducing DNA levels in the lungs of β-ENaC mice, a model of CF lung disease, as five consecutive daily doses of unconjugated rhDNase.

II.3. CONCERNS ABOUT PEGYLATION

PEGs are excipients approved by FDA and EMA, used extensively in intravascular, topical and oral formulations [199]. PEG molecules below 20 kDa are cleared through renal filtration, while larger PEG molecules are eliminated primarily through liver sequestration followed by biliary excretion [200, 201]. The toxicity of PEG at a wide range of doses is negligible. It only generates toxicity in the case of parenteral route at a high dose. The World Health Organization recommended that an oral daily intake of PEG up to 10 mg/kg is acceptable.

PEG has been evaluated for toxicity in a variety of animal species. Some toxicity studies in rabbits showed that high dose (350 mg/kg/day) resulted in chronic toxicities including renal tubular swelling, hepatic parenchyma. Higher dose (up to 10 000 mg/kg) could cause acute toxicity and death in rabbits [202]. Nevertheless, the levels of PEG used for drug delivery are far below its toxicity level, thus PEG is generally considered non-toxic in pharmaceutical studies.

It has been reported that, despite the widespread use of PEGylated proteins in clinical settings, there is some controversy regarding the effects of PEG accumulation and immunotoxicity [203–205]. The majority of PEG conjugates are cleared by kidney and liver, sometimes by proteolysis with concomitant renal clearance. In the case of high PEG concentrations, accumulation of PEGylated drugs has been observed in Kuppfer cells of the liver, resulting in hepatic cellular vacuolization [206–208]. It should be noted, however, that vacuoles often disappear following cessation of the treatment, and there have not been any reported effects of PEG related to vacuolization in humans [209, 210]. In the animal toxicity study, much higher bolus and cumulative doses are administered compared to those administered in humans. In humans, PEG doses are typically 1mg/kg, which is much less than the amount required to cause PEG toxicity in animals The accumulation of PEG over 30 kDa is more likely to occur [211]. For better improvement in circulation time, branched PEG derived from precursors of 20 kDa PEG could be utilized.

Recently, increasing numbers of reports have raised concerns about the presence of anti-PEG antibodies following repeated injections of PEGylated proteins [212–214]. Soluble free PEG exhibits no/weak immunogenicity, even in the presence of Freund's adjuvant [215, 216]. It becomes immunogenic, however, when conjugated with macromolecules. The generation of anti-PEG antibodies has been associated with the immunogenic character of the protein moiety. The development of anti-PEG antibodies to mono-PEGylated proteins is not as prevalent as with hyper-PEGylated proteins [217]. For instance, Adagen, Oncaspar and Krystexxa are reported to be immunogenic. In the above three products, the PEGylated entities are not human-sourced (Table 7). PEGylation of those target proteins was intended to reduce their immunogenicity, since

otherwise they would be of little clinical benefit. In the case of Krystexxa, anti-PEG antibodies were observed in the majority of patients receiving the treatment [161]. The immunogenicity of PEGylated proteins was also compounded by the presence of pre-existing PEG antibodies in ~25 % of the population [203]. The occurrence of anti-PEG antibodies in individuals who did not receive PEGylated therapeutics can be explained by the wide usage of PEG in cosmetics and household products.

Table 7. Composition and protein origin of three marketed PEGylated protein pharmaceutics that are reported to be immunogenic.

Drug	Company	PEGylated entity	Protein Origin
Adagen	Enzon	adenosine deaminase	Bovine
Oncaspar	Enzon	asparaginase	Escherichia coli
Krystexxa	Horizon Pharma	recombinant uricase protein	Escherichia coli

Although anti-PEG antibodies do exist in some populations, their neutralizing properties have not been demonstrated. Since PEG is highly flexible, it has relatively low affinity to anti-PEG antibodies, especially for mono-PEGylated proteins. As a matter of fact, most of the clinically toxicological or immunological effects of PEGylated proteins are directly related to the protein [151, 218, 219]. A PEGylated conjugate is expected to be safe if the host protein is clinically safe and non-immunogenic, especially for mono-PEGylation [220].

In the study by Lubich et al [221], they established robust antibody analytics and screened two cohorts of healthy individuals (>1000 healthy donors) and one cohort of hemophilia patients (110 patients) for the expression of anti-PEG antibodies. Hemophilia patients were chosen because i) recombinant coagulation factors VIII and IX used for treatment or prophylaxis are frequently formulated with excipients containing PEGs, and ii) recombinant coagulation factors derived from human plasma may contain small amounts of PEGs used in the manufacturing process. The results showed that IgM and/or IgG anti-PEG antibodies are expressed by some healthy individuals and by some patients with hemophilia who have not received PEGylated biotherapeutics. These antibodies can be either transient or persistent and are able to recognize PEGs of different sizes with or without terminal methoxy groups. Furthermore, the authors found that even high-affinity anti-PEG antibodies had no cross-reactivity with human tissue when tested against a standard panel of different types of human tissue. Even when anti-PEG responses were persistent, none of these antibodies had a pathogenic character, supporting the harmless nature of the antibodies.

II.4. PEGYLATED ALPHA1-ANTITRYPSIN

PEGylation of AAT and its potential use in pulmonary delivery was firstly explored by Cantin et al [14]. The authors demonstrated that the site-specific conjugation with either 20 or 40 kDa PEG-maleimide at Cys232 of nonglycosylated recombinant human AAT (rhAAT) preserved the elastase inhibition capacity of AAT, as well as its ability to form the covalent complex with elastase in vitro. PEGylation extended the half-life rhAAT in plasma and lung as compared with the unconjugated rhAAT. The authors further demonstrate that PEGylated rhAAT provides an extended protection against lung injury induced by intratracheal administration of human neutrophil elastase when compared to unconjugated rhAAT. Specifically, 72 hours after airway instillation, PEGylated rhAAT offered significantly better protection in the lung against elastase mediated lung hemorrhage.

Cantin et al. 's work had great significance because i) it confirmed that PEGylation can extend the half-life of rhAAT, which implies that human AAT can also benefit from this procedure. AAT derived from human plasma, which is already being used to treat individuals with AAT deficiency, can be prolonged in half-life, which may contribute to extending the dosage interval, thereby extending the limited supply available worldwide; ii) it may provide an additional source of AAT for intravenous delivery; and iii) it offered an experimental template for the delivery of other PEGylated recombinant proteins to the lungs.

Later, PEGylation of rhAAT was again investigated by Zhu et al in 2018 [222]. In this study, rhAAT was expressed in Escherichia coli and mutant forms of AAT were engineered to achieve enhanced thermostability and resistance to oxidation. A novel triple-mutant form of AAT (F51L/M351V/M358V) with enhanced thermal stability and oxidation resistance was characterized, which also presented unmodified biological activity. Most importantly, a PEGylated version of wild type rhAAT was developed. By thiol PEGylation, 20 kDa PEG-maleimide was conjugated to Cys232. The PEGylated RhAAT displayed the same efficacy in inhibiting elastase as the unconjugated form, which is in agreement with Cantin's findings. There was, however, no in vivo characterization of PEGylated rhAAT. There has been no comparison between rhAAT and PEGylated AAT regarding in vivo PK profiles or efficacy.

PEGylation of AAT was also used to investigate its folding process. Krishnan et al produced a series of single cysteine mutants of AAT by conjugating the mutant to PEG-maleimide, among which, seventeen variants passed the qualitative activity screen, showing similar anti-trypsin activity [223]. It has been demonstrated that the less reactive positions are also the most hydrophobic and unfolding resistant.

Despite almost 20 years passing since Cantin and colleagues first investigated the PEGylation of AAT, to the best of our knowledge, no study has ever been conducted on PEGylated human AAT or rhAAT for its possible clinical application. Cantin's study contained several noteworthy features as described previously, however, it still exhibited a number of limitations. First of all, the author did not investigate whether rhAAT and its PEGylated version differ in immunogenicity. Secondly, the tissue distribution of rhAAT and PEG-rhAAT was not evaluated. Finally, the murine lung injury model was acute, which might not accurately reflect the clinical manifestation of AAT deficiency related respiratory diseases.

III. CONCLUSION

Alpha-1 antitrypsin is an endogenous inhibitor of serine proteases which, in physiological conditions, neutralizes the excess of neutrophil elastase and other serine proteases in tissues and especially the lungs. In addition to its anti-protease properties, AAT has proved to have anti-inflammatory, anti-apoptotic effect and immunomodulatory activities.

AAT deficiency is characterized by low serum level of AAT (<11 μM), which can lead to respiratory and hepatic diseases. The only approved therapy for patients with AAT deficiency associated with respiratory disease is weekly intravenous administration of plasma-purified human AAT. However, only 2 % of the AAT dose reach the lungs after intravenous infusion. Hence, inhalation of AAT could serve as an alternative route of administration. The rapid clearance of AAT from the respiratory tract, however, results in high and frequent doses of AAT and a limited efficacy. Other therapies for AAT deficiency include gene-silencing molecules, protein-folding and chaperone modifiers, autophagy enhancers and polymerization blockers and CRISPR genome editing. Some of these products have advanced to clinical trials, but none have been approved for clinical use yet.

PEGylation of therapeutic proteins is considered to be one of the most promising approaches among the various protein conjugation options, due to the fact that it extends the half-life of the protein, thus reducing the dose and frequency of administration. Since the development of different PEGylation chemistries, as well as the growing technology of molecular simulation, the goal of PEGylation has moved from reducing immunogenicity of a protein by random or multiple PEGylation, with a consequent decrease in protein activity, to rationally choosing the PEGylation site and chemical, in order to create a mono-PEGylated, homogenous product, preserving its biological activity.

Numerous researchers have demonstrated the benefits of PEGylation, in particular prolonging the half-life of therapeutic proteins. Years of application of PEGylated proteins in the market proved the safety and effectiveness of PEGylation. While some concerns have been raised regarding the immunogenicity of PEG, the presence of anti-PEG antibodies has been associated with the host protein rather than the PEG moiety. Moreover, the neutralizing character and clinical consequence of anti-PEG antibodies have only been demonstrated for PEGylated endogenous protein therapeutics. In terms of soluble polymers used in protein conjugation, PEG has been studied the most and has been shown to significantly impede exogenous protein immunogenicity, as well as producing weak anti-polymer antibody responses [212].

IV. OBJECTIVES

Through the process of PEGylation of the protein, this thesis aimed to prepare an AAT derivative that would remain in intact form within the lungs after intravenous or pulmonary administration. In our hypothesis, the PEGylation of AAT would prolong its residence in intact form within the body, increasing its local potency.

Objective 1: Production and purification of mono-PEGylated AAT

The N-terminal and thiol PEGylation reactions of plasma-purified human AAT were optimized. A series of factors were evaluated including the PEG: AAT molar ratio, the reaction time, the AAT concentration and, in case of N-terminal PEGylation, the reaction pH. Large linear and branched PEG were used as they were reported to prolong more the body residency of protein therapeutics. The sizes and architectures of PEG used included linear 30kDa PEG, linear 40kDa PEG and two-armed 40kDa PEG. Six different mono-PEGylated AAT were produced and purified.

Objective 2: Characterization of mono-PEGylated AAT

The biological activity of the PEG-AAT conjugates produced under the optimized reaction conditions was assessed by measurement of their elastase inhibitory capacity. Circular dichroism and fluorescence spectroscopy were used to analyze the possible changes in secondary and tertiary structure of AAT following PEGylation. The PEG-AAT conjugates were analyzed using mass spectrometry and peptide mapping to determine their level of PEGylation and their site of PEGylation. In order to assess the effects of PEGylation on the physicochemical stability and biological stability of AAT, we exposed the PEG-AAT conjugates as well as their unconjugated counterpart to various stresses (high temperature, chemical denaturation, freezing and thawing, aerosolization by jets nebulizers, proteolytic exposure). Protein denaturation due to high temperature and denaturant agent (guanidinium chloride) was analyzed by circular dichroism and fluorescence spectroscopy. A UV spectroscopy at 350 nm and size exclusion chromatography were used to determine the formation of protein aggregates during freeze/thawing or aerosolization. The activity of PEGylated AAT and unconjugated AAT after exposing to freeze/thawing or aerosolization was evaluated by elastase inhibition assay. Finally, AAT inactivation by proteolysis was assessed by measurement of AAT elastase inhibitory capacity. As a result of this step, the most appropriate PEGylation chemistry as well as the ideal PEG size and architecture for optimal stability of PEG-AAT were determined. The selected PEG-AAT conjugate would be used for the in vivo evaluation.

Objective 3: Disposition and therapeutic efficacy of mono-PEGylated AAT in vivo

The fate of the selected PEG-AAT conjugate and of the native glycoprotein in the respiratory tract and plasma of healthy Swiss mice following either intratracheal instillation or intranasal instillation was determined. The content of AAT and PEG-AAT conjugates was quantified in bronchoalveolar lavage (supernatant and cell pellet), lung tissue (after crushing) and blood at different times after intratracheal instillation of a 1.35 mg/kg dose, or after intravenous injection of a 60 mg/kg dose, which are similar to the human dose. The total protein content in the bronchoalveolar lavage at selected time point were determined and compared with the basal content quantified in the BAL of healthy Swiss mice which did not receive any protein instillation.

The therapeutic efficacy of the PEG-AAT conjugate versus the non-conjugated AAT following pulmonary delivery and intravenous injection in a murine COPD model was evaluated. The COPD murine model was established by the intranasal instillation of 1.2 U PPE on day 1 of each week and 7 μg LPS on day 4 of each week for 4 consecutive weeks. The treatment groups received AAT or PEG-AAT 2 h prior to the PPE or LPS challenge. The control groups received the corresponding buffer (for AAT, PEG-AAT, LPS and PPE) instead.

In the first experiment, native AAT (doses ranging from 12 to 120 μg/mouse) was administered by intranasal instillation to the mice. Seven days after the final dose, mice were sacrificed by cervical dislocation. A bronchoalveolar lavage was performed, centrifuged and the cell pellet used for counting of total cells and differential cells. The bronchoalveolar lavage supernatant was used for biochemical measurements: lactate dehydrogenase activity, concentration of total proteins, albumin, concentration of cytokine markers. A dose of AAT presenting a sub-optimal efficacy was selected and used for the next experiment which compared PEGylated AAT and unconjugated AAT.

In the second experiment, native AAT or mono-PEGylated AAT was administered at the selected dose by intranasal instillation, or by intravenous injection at a dose of 60 mg/kg, to the mice. PEG was not counted in the mass of PEG-AAT delivered. Seven days after the last dose, mice were sacrificed and a bronchoalveolar lavage was performed and analyzed for biochemical and cellular markers of inflammation as in the first experiment. Histopathology of the lung tissue was also performed. The AAT concentrations were measured in the supernatant and cell pellet of bronchoalveolar lavage, supernatant of the remaining lung lobes (after crushing) and in blood. The level of anti-AAT, anti-elastase and anti-PEG antibodies in the plasma was evaluated by ELISA.

V. REFERENCES

[1] Chapman KR, Chorostowska-Wynimko J, Koczulla AR, Ferrarotti I, McElvaney NG. Alpha 1 antitrypsin to treat lung disease in alpha 1 antitrypsin deficiency: recent developments and clinical implications. International journal of chronic obstructive pulmonary disease 2018;13:419–32.

[2] Foil KE. Variants of SERPINA1 and the increasing complexity of testing for alpha-1 antitrypsin deficiency. Therapeutic advances in chronic disease 2021;12_suppl:20406223211015954.

[3] Serres F de, Blanco I. Role of alpha-1 antitrypsin in human health and disease. Journal of internal medicine 2014;276(4):311–35.

[4] Greulich T, Nell C, Hohmann D, et al. The prevalence of diagnosed α1-antitrypsin deficiency and its comorbidities: results from a large population-based database. The European respiratory journal 2017;49(1).

[5] Miravitlles M, Dirksen A, Ferrarotti I, et al. European Respiratory Society statement: diagnosis and treatment of pulmonary disease in α1-antitrypsin deficiency. The European respiratory journal 2017;50(5).

[6] Torres-Durán M, Lopez-Campos JL, Barrecheguren M, et al. Alpha-1 antitrypsin deficiency: outstanding questions and future directions. Orphanet journal of rare diseases 2018;13(1):114.

[7] Greene CM, McElvaney NG. Z α-1 antitrypsin deficiency and the endoplasmic reticulum stress response. World journal of gastrointestinal pharmacology and therapeutics 2010;1(5):94–101.

[8] Dunlea DM, Fee LT, McEnery T, McElvaney NG, Reeves EP. The impact of alpha-1 antitrypsin augmentation therapy on neutrophil-driven respiratory disease in deficient individuals. Journal of inflammation research 2018;11:123–34.

[9] Karatas E, Bouchecareilh M. Alpha 1-Antitrypsin Deficiency: A Disorder of Proteostasis-Mediated Protein Folding and Trafficking Pathways. International journal of molecular sciences 2020;21(4).

[10] Kolarich D, Turecek PL, Weber A, et al. Biochemical, molecular characterization, and glycoproteomic analyses of alpha(1)-proteinase inhibitor products used for replacement therapy. Transfusion 2006;46(11):1959–77.

[11] Boerema DJ, An B, Gandhi RP, et al. Biochemical comparison of four commercially available human α1-proteinase inhibitors for treatment of α1-antitrypsin deficiency. Biologicals journal of the International Association of Biological Standardization 2017;50:63–72.

[12] Miyamoto Y, Akaike T, Maeda H. S-Nitrosylated human α1-protease inhibitor. Biochimica et Biophysica Acta (BBA) - Protein Structure and Molecular Enzymology 2000;1477(1-2):90–7.

[13] Tyagi SC, Simon SR. Role of disulfide exchange in alpha 1-protease inhibitor. Biochemistry 1992;31(43):10584–90.

[14] Cantin AM, Woods DE, Cloutier D, Dufour EK, Leduc R. Polyethylene glycol conjugation at Cys232 prolongs the half-life of alpha1 proteinase inhibitor. American journal of respiratory cell and molecular biology 2002;27(6):659–65.

[15] McCarthy C, Saldova R, Wormald MR, Rudd PM, McElvaney NG, Reeves EP. The role and importance of glycosylation of acute phase proteins with focus on alpha-1 antitrypsin in acute and chronic inflammatory conditions. Journal of proteome research 2014;13(7):3131–43.

[16] Mills K, Mills PB, Clayton PT, Mian N, Johnson AW, Winchester BG. The underglycosylation of plasma alpha 1-antitrypsin in congenital disorders of glycosylation type I is not random. Glycobiology 2003;13(2):73–85.

[17] Kwon K-S, Yu M-H. Effect of glycosylation on the stability of α1-antitrypsin toward urea denaturation and thermal deactivation. Biochimica et Biophysica Acta (BBA) - General Subjects 1997;1335(3):265–72.

[18] Powell LM, Pain RH. Effects of glycosylation on the folding and stability of human, recombinant and cleaved α1-antitrypsin. Journal of Molecular Biology 1992;224(1):241–52.
[19] Sarkar A, Wintrode PL. Effects of glycosylation on the stability and flexibility of a metastable protein: the human serpin α(1)-antitrypsin. International journal of mass spectrometry 2011;302(1-3):69–75.
[20] Chung H-S, Kim J-S, Lee SM, Park SJ. Additional N-glycosylation in the N-terminal region of recombinant human alpha-1 antitrypsin enhances the circulatory half-life in Sprague-Dawley rats. Glycoconjugate journal 2016;33(2):201–8.
[21] Lechowicz U, Rudzinski S, Jezela-Stanek A, Janciauskiene S, Chorostowska-Wynimko J. Post-Translational Modifications of Circulating Alpha-1-Antitrypsin Protein. International journal of molecular sciences 2020;21(23).
[22] Martin SL, Downey D, Bilton D, Keogan MT, Edgar J, Elborn JS. Safety and efficacy of recombinant alpha(1)-antitrypsin therapy in cystic fibrosis. Pediatr. Pulmonol. 2006;41(2):177–83.
[23] McElvaney NG, Hubbard RC, Birrer P, et al. Aerosol α1 -antitrypsin treatment for cystic fibrosis. The Lancet 1991;337(8738):392–4.
[24] Griese M, Latzin P, Kappler M, et al. alpha1-Antitrypsin inhalation reduces airway inflammation in cystic fibrosis patients. The European respiratory journal 2007;29(2):240–50.
[25] Andersen OJ, Risør MW, Poulsen EC, et al. Reactive Center Loop Insertion in α-1-Antitrypsin Captured by Accelerated Molecular Dynamics Simulation. Biochemistry 2017;56(4):634–46.
[26] Khan MS, Singh P, Azhar A, et al. Serpin Inhibition Mechanism: A Delicate Balance between Native Metastable State and Polymerization. Journal of amino acids 2011;2011:606797.
[27] Dementiev A, Simonovic M, Volz K, Gettins PGW. Canonical inhibitor-like interactions explain reactivity of alpha1-proteinase inhibitor Pittsburgh and antithrombin with proteinases. The Journal of biological chemistry 2003;278(39):37881–7.
[28] Perlmutter DH, Joslin G, Nelson P, Schasteen C, Adams SP, Fallon RJ. Endocytosis and degradation of alpha 1-antitrypsin-protease complexes is mediated by the serpin-enzyme complex (SEC) receptor. The Journal of biological chemistry 1990;265(28):16713–6.
[29] Dau T, Sarker RSJ, Yildirim AO, Eickelberg O, Jenne DE. Autoprocessing of neutrophil elastase near its active site reduces the efficiency of natural and synthetic elastase inhibitors. Nature communications 2015;6:6722.
[30] Silberstein DZ, Karuppanan K, Aung HH, Chen C-H, Cross CE, McDonald KA. An oxidation-resistant, recombinant alpha-1 antitrypsin produced in Nicotiana benthamiana. Free radical biology & medicine 2018;120:303–10.
[31] Taggart C, Cervantes-Laurean D, Kim G, et al. Oxidation of either methionine 351 or methionine 358 in alpha 1-antitrypsin causes loss of anti-neutrophil elastase activity. The Journal of biological chemistry 2000;275(35):27258–65.
[32] Gaggar A, Chen J, Chmiel JF, et al. Inhaled alpha1-proteinase inhibitor therapy in patients with cystic fibrosis. Journal of cystic fibrosis official journal of the European Cystic Fibrosis Society 2016;15(2):227–33.
[33] Cochrane CG, Spragg R, Revak SD. Pathogenesis of the adult respiratory distress syndrome. Evidence of oxidant activity in bronchoalveolar lavage fluid. The Journal of clinical investigation 1983;71(3):754–61.
[34] Chalmers JD, Chang AB, Chotirmall SH, Dhar R, McShane PJ. Bronchiectasis. Nat Rev Dis Primers 2018;4(1):45.
[35] Ueda M, Mashiba S, Uchida K. Evaluation of oxidized alpha-1-antitrypsin in blood as an oxidative stress marker using anti-oxidative α1-AT monoclonal antibody. Clinica Chimica Acta 2002;317(1-2):125–31.

[36] Duranton J, Bieth JG. Inhibition of proteinase 3 by alpha1-antitrypsin in vitro predicts very fast inhibition in vivo. American journal of respiratory cell and molecular biology 2003;29(1):57–61.
[37] Petrache I, Fijalkowska I, Medler TR, et al. alpha-1 antitrypsin inhibits caspase-3 activity, preventing lung endothelial cell apoptosis. The American journal of pathology 2006;169(4):1155–66.
[38] Janciauskiene S, Wrenger S, Immenschuh S, et al. The Multifaceted Effects of Alpha1-Antitrypsin on Neutrophil Functions. Frontiers in pharmacology 2018;9:341.
[39] Korkmaz B, Horwitz MS, Jenne DE, Gauthier F. Neutrophil elastase, proteinase 3, and cathepsin G as therapeutic targets in human diseases. Pharmacological reviews 2010;62(4):726–59.
[40] Kalsheker N. Alpha 1-antitrypsin: structure, function and molecular biology of the gene. Bioscience reports 1989;9(2):129–38.
[41] Bai X, an Bai, Honda JR, et al. Alpha-1-Antitrypsin Enhances Primary Human Macrophage Immunity Against Non-tuberculous Mycobacteria. Frontiers in immunology 2019;10:1417.
[42] Hunt JM, Tuder R. Alpha 1 anti-trypsin: one protein, many functions. Current molecular medicine 2012;12(7):827–35.
[43] Lee S, Lee Y, Hong K, et al. Effect of recombinant α1-antitrypsin Fc-fused (AAT-Fc)protein on the inhibition of inflammatory cytokine production and streptozotocin-induced diabetes. Mol Med 2013;19(1):65–71.
[44] Wang X, Gong J, Zhu J, Jin Z, Gao W. Alpha 1-antitrypsin for treating ventilator-associated lung injury in acute respiratory distress syndrome rats. Experimental lung research 2019;45(7):209–19.
[45] Toldo S, Seropian IM, Mezzaroma E, et al. Alpha-1 antitrypsin inhibits caspase-1 and protects from acute myocardial ischemia-reperfusion injury. Journal of Molecular and Cellular Cardiology 2011;51(2):244–51.
[46] Jonigk D, Al-Omari M, Maegel L, et al. Anti-inflammatory and immunomodulatory properties of α1-antitrypsin without inhibition of elastase. Proceedings of the National Academy of Sciences of the United States of America 2013;110(37):15007–12.
[47] Reeves EP, Dunlea DM, McQuillan K, et al. Circulating Truncated Alpha-1 Antitrypsin Glycoprotein in Patient Plasma Retains Anti-Inflammatory Capacity. Journal of immunology (Baltimore, Md. 1950) 2019;202(8):2240–53.
[48] Marciniak SJ, Ordóñez A, Dickens JA, et al. New Concepts in Alpha-1 Antitrypsin Deficiency Disease Mechanisms. Annals of the American Thoracic Society 2016;13 Suppl 4:S289-96.
[49] Pott GB, Chan ED, Dinarello CA, Shapiro L. Alpha-1-antitrypsin is an endogenous inhibitor of proinflammatory cytokine production in whole blood. Journal of Leukocyte Biology 2009;85(5):886–95.
[50] Fleixo-Lima G, Ventura H, Medini M, Bar L, Strauss P, Lewis EC. Mechanistic evidence in support of alpha1-antitrypsin as a therapeutic approach for type 1 diabetes. Journal of Diabetes Science and Technology 2014;8(6):1193–203.
[51] Lior Y, Shtriker E, Kahremany S, Lewis EC, Gruzman A. Development of anti-inflammatory peptidomimetics based on the structure of human alpha1-antitrypsin. European Journal of Medicinal Chemistry 2022;228:113969.
[52] Wettstein L, Conzelmann C, Müller JA, et al. Alpha-1 antitrypsin inhibits SARS-CoV-2 infection. bioRxiv 2020:2020.07.02.183764.
[53] Victoria Callahan, Ivan V Akhrymuk, Katarina Elez, et al. Alpha 1 Antitrypsin is an Inhibitor of the SARS-CoV2-Priming Protease TMPRSS2, 2020.
[54] Loyola MB de, Dos Reis TTA, Oliveira GXLM de, da Fonseca Palmeira J, Argañaraz GA, Argañaraz ER. Alpha-1-antitrypsin: A possible host protective factor against Covid-19. Reviews in medical virology 2021;31(2):e2157.

[55] Marzouk S, Attia N, Mashal M. Insights into the potential role of alpha1-antitrypsin in COVID-19 patients: Mechanisms, current update, and future perspectives. The clinical respiratory journal 2021;15(9):1019–24.
[56] Hashemi M, Naderi M, Rashidi H, Ghavami S. Impaired activity of serum alpha-1-antitrypsin in diabetes mellitus. Diabetes research and clinical practice 2007;75(2):246–8.
[57] Wang J, Sun Z, Gou W, et al. α-1 Antitrypsin Enhances Islet Engraftment by Suppression of Instant Blood-Mediated Inflammatory Reaction. Diabetes 2017;66(4):970–80.
[58] Kalis M, Kumar R, Janciauskiene S, Salehi A, Cilio CM. α 1-antitrypsin enhances insulin secretion and prevents cytokine-mediated apoptosis in pancreatic β-cells. Islets 2010;2(3):185–9.
[59] Park SS, Rodriguez Ortega R, Agudelo CW, et al. Therapeutic Potential of Alpha-1 Antitrypsin in Type 1 and Type 2 Diabetes Mellitus. Medicina (Kaunas, Lithuania) 2021;57(4).
[60] Wang Q, Du J, Yu P, et al. Hepatic steatosis depresses alpha-1-antitrypsin levels in human and rat acute pancreatitis. Scientific reports 2015;5:17833.
[61] Lebenthal Y, Brener A, Hershkovitz E, et al. A Phase II, Double-Blind, Randomized, Placebo-Controlled, Multicenter Study Evaluating the Efficacy and Safety of Alpha-1 Antitrypsin (AAT) (Glassia®) in the Treatment of Recent-Onset Type 1 Diabetes. International journal of molecular sciences 2019;20(23).
[62] Janciauskiene SM, Bals R, Koczulla R, Vogelmeier C, Köhnlein T, Welte T. The discovery of α1-antitrypsin and its role in health and disease. Respiratory medicine 2011;105(8):1129–39.
[63] Fregonese L, Stolk J. Hereditary alpha-1-antitrypsin deficiency and its clinical consequences. Orphanet journal of rare diseases 2008;3:16.
[64] Alper CA. Deficiency of alpha-1 antitrypsin. Annals of internal medicine 1973;78(2):298–9.
[65] Fairbanks KD, Tavill AS. Liver Disease in Alpha 1-Antitrypsin Deficiency: A Review. Official journal of the American College of Gastroenterology | ACG 2008;103(8):2136.
[66] Allen RC, Harley RA, Talamo RC. A new method for determination of alpha-1-antitrypsin phenotypes using isoelectric focusing on polyacrylamide gel slabs. American journal of clinical pathology 1974;62(6):732–9.
[67] Nukiwa T, Brantly ML, Ogushi F, Fells GA, Crystal RG. Characterization of the gene and protein of the common alpha 1-antitrypsin normal M2 allele. American Journal of Human Genetics 1988;43(3):322–30.
[68] Alpha-1 Antitrypsin Deficiency: Humana Press, New York, NY, 2017.
[69] Wewers MD, Crystal RG. Alpha-1 antitrypsin augmentation therapy. COPD 2013;10 Suppl 1:64–7.
[70] Jardim JR, Casas-Maldonado F, Fernandes FLA, Castellano MVCdO, Torres-Durán M, Miravitlles M. Update on and future perspectives for the diagnosis of alpha-1 antitrypsin deficiency in Brazil. Jornal brasileiro de pneumologia publicacao oficial da Sociedade Brasileira de Pneumologia e Tisilogia 2021;47(3):e20200380.
[71] Pérez-Holanda S, Blanco I, Menéndez M, Rodrigo L. Serum concentration of alpha-1 antitrypsin is significantly higher in colorectal cancer patients than in healthy controls. BMC cancer 2014;14:355.
[72] Serres FJ de, Blanco I, Fernández-Bustillo E. Estimated numbers and prevalence of PI*S and PI*Z deficiency alleles of alpha1-antitrypsin deficiency in Asia. The European respiratory journal 2006;28(6):1091–9.
[73] Belmonte I, Barrecheguren M, López-Martínez RM, et al. Application of a diagnostic algorithm for the rare deficient variant Mmalton of alpha-1-antitrypsin deficiency: a new approach. International journal of chronic obstructive pulmonary disease 2016;11:2535–41.
[74] Carroll TP, O'Connor CA, Floyd O, et al. The prevalence of alpha-1 antitrypsin deficiency in Ireland. Respiratory research 2011;12:91.

[75] Blanco I, Bueno P, Diego I, et al. Alpha-1 antitrypsin Pi*Z gene frequency and Pi*ZZ genotype numbers worldwide: an update. International journal of chronic obstructive pulmonary disease 2017;12:561–9.
[76] Serres FJ de. Alpha-1 antitrypsin deficiency is not a rare disease but a disease that is rarely diagnosed. Environmental health perspectives 2003;111(16):1851–4.
[77] Denden S, Chibani JB, Khelil AH. Origins and spreads of Alpha 1 antitrypsin variants in world human populations: a synthetic review. Int.J.Mod.Anthrop 2012;1(5).
[78] Forsyth S, Horvath A, Coughlin P. A review and comparison of the murine α1-antitrypsin and α1-antichymotrypsin multigene clusters with the human clade A serpins. Genomics 2003;81(3):336–45.
[79] Heit C, Jackson BC, McAndrews M, et al. Update of the human and mouse SERPIN gene superfamily. Human genomics 2013;7:22.
[80] Hill RE, Shaw PH, Boyd PA, Baumann H, Hastie ND. Plasma protease inhibitors in mouse and man: divergence within the reactive centre regions. Nature 1984;311(5982):175–7.
[81] Sifers RN, Ledley FD, Reed-Fourquet L, Ledbetter DH, Ledbetter SA, Woo SL. Complete cDNA sequence and chromosomal localization of mouse α1-antitrypsin. Genomics 1990;6(1):100–4.
[82] Dewilde M, van de Craen B, Compernolle G, et al. Subtle structural differences between human and mouse PAI-1 reveal the basis for biochemical differences. Journal of structural biology 2010;171(1):95–101.
[83] Wiesner O, Litwiller RD, Hummel AM, et al. Differences between human proteinase 3 and neutrophil elastase and their murine homologues are relevant for murine model experiments. FEBS letters 2005;579(24):5305–12.
[84] Strnad P, McElvaney NG, Lomas DA. Alpha1-Antitrypsin Deficiency. The New England journal of medicine 2020;382(15):1443–55.
[85] Callea F, Giovannoni I, Francalanci P, et al. Mineralization of alpha-1-antitrypsin inclusion bodies in Mmalton alpha-1-antitrypsin deficiency. Orphanet journal of rare diseases 2018;13(1):79.
[86] Patel D, Teckman JH. Alpha-1-Antitrypsin Deficiency Liver Disease. Clinics in Liver Disease 2018;22(4):643–55.
[87] Tejwani V, Stoller JK. The spectrum of clinical sequelae associated with alpha-1 antitrypsin deficiency. Therapeutic advances in chronic disease 2021;12_suppl:2040622321995691.
[88] Chukowry PS, Edgar RG, Turner AM. Alpha 1 antitrypsin deficiency: a rare multisystem disease, predominantly affecting the lung. Expert Opinion on Orphan Drugs 2019;7(7-8):315–26.
[89] Miravitlles M, Herr C, Ferrarotti I, et al. Laboratory testing of individuals with severe alpha1-antitrypsin deficiency in three European centres. European Respiratory Journal 2010;35(5):960–8.
[90] Teckman JH, Blomenkamp KS. Pathophysiology of Alpha-1 Antitrypsin Deficiency Liver Disease. In: Alpha-1 Antitrypsin Deficiency: Humana Press, New York, NY, 2017:1–8.
[91] Bals R, Koczulla R, Kotke V, Andress J, Blackert K, Vogelmeier C. Identification of individuals with alpha-1-antitrypsin deficiency by a targeted screening program. Respiratory medicine 2007;101(8):1708–14.
[92] Sørheim I-C, Bakke P, Gulsvik A, et al. α1-Antitrypsin protease inhibitor MZ heterozygosity is associated with airflow obstruction in two large cohorts. Chest 2010;138(5):1125–32.
[93] Senn O, Russi EW, Imboden M, Probst-Hensch NM. alpha1-Antitrypsin deficiency and lung disease: risk modification by occupational and environmental inhalants. The European respiratory journal 2005;26(5):909–17.
[94] Eden E, Mitchell D, Mehlman B, et al. Atopy, asthma, and emphysema in patients with severe alpha-1-antitrypysin deficiency. American journal of respiratory and critical care medicine 1997;156(1):68–74.

[95] Bailey KL. The importance of the assessment of pulmonary function in COPD. The Medical clinics of North America 2012;96(4):745–52.
[96] Huang Y-CT, Wencker M, Driehuys B. Imaging in alpha-1 antitrypsin deficiency: a window into the disease. Therapeutic advances in chronic disease 2021;12_suppl:20406223211024523.
[97] Chalmers JD, Chang AB, Chotirmall SH, Dhar R, McShane PJ. Bronchiectasis. Nat Rev Dis Primers 2018;4(1):45.
[98] Longstreth GF, Weitzman SA, Browning RJ, Lieberman J. Bronchiectasis and homozygous alpha1-antitrypsin deficiency. Chest 1975;67(2):233–5.
[99] Parr DG, Guest PG, Reynolds JH, Dowson LJ, Stockley RA. Prevalence and impact of bronchiectasis in alpha1-antitrypsin deficiency. American journal of respiratory and critical care medicine 2007;176(12):1215–21.
[100] Veith M, Tüffers J, Peychev E, et al. The Distribution of Alpha-1 Antitrypsin Genotypes Between Patients with COPD/Emphysema, Asthma and Bronchiectasis. International journal of chronic obstructive pulmonary disease 2020;15:2827–36.
[101] Siri D, Farah H, Hogarth DK. Distinguishing alpha1-antitrypsin deficiency from asthma. Annals of allergy, asthma & immunology official publication of the American College of Allergy, Asthma, & Immunology 2013;111(6):458–64.
[102] Pini L, Paoletti G, Heffler E, Tantucci C, Puggioni F. Alpha1-antitrypsin deficiency and asthma. Current opinion in allergy and clinical immunology 2021;21(1):46–51.
[103] Brand P, Schulte M, Wencker M, et al. Lung deposition of inhaled alpha1-proteinase inhibitor in cystic fibrosis and alpha1-antitrypsin deficiency. European Respiratory Journal 2009;34(2):354–60.
[104] Dowsett J, Tully O. Cystic Fibrosis. In: Encyclopedia of Human Nutrition: Elsevier, 2012:416–22.
[105] Egan ME. Genetics of Cystic Fibrosis: Clinical Implications. Clinics in chest medicine 2016;37(1):9–16.
[106] Cantin AM, Hartl D, Konstan MW, Chmiel JF. Inflammation in cystic fibrosis lung disease: Pathogenesis and therapy. Journal of cystic fibrosis official journal of the European Cystic Fibrosis Society 2015;14(4):419–30.
[107] Vidal R, Blanco I, Casas F, Jardí R, Miravitlles M. Guidelines for the Diagnosis and Management of α1-Antitrypsin Deficiency. Archivos de Bronconeumología ((English Edition)) 2006;42(12):645–59.
[108] Soy D, La Roza C de, Lara B, Esquinas C, Torres A, Miravitlles M. Alpha-1-antitrypsin deficiency: optimal therapeutic regimen based on population pharmacokinetics. Thorax 2006;61(12):1059–64.
[109] Herth FJF, Sandhaus RA, Turner AM, Sucena M, Welte T, Greulich T. Alpha 1 Antitrypsin Therapy in Patients with Alpha 1 Antitrypsin Deficiency: Perspectives from a Registry Study and Practical Considerations for Self-Administration During the COVID-19 Pandemic. International journal of chronic obstructive pulmonary disease 2021;16:2983–96.
[110] Greulich T, Vogelmeier CF. Alpha-1-antitrypsin deficiency: increasing awareness and improving diagnosis. Therapeutic advances in respiratory disease 2016;10(1):72–84.
[111] Sieluk J, Slejko JF, Silverman H, Perfetto E, Mullins CD. Medical costs of Alpha-1 antitrypsin deficiency-associated COPD in the United States. Orphanet journal of rare diseases 2020;15(1):260.
[112] López-Campos JL, Carrasco Hernandez L, Caballero Eraso C. Implications of a Change of Paradigm in Alpha1 Antitrypsin Deficiency Augmentation Therapy: From Biochemical to Clinical Efficacy. Journal of clinical medicine 2020;9(8).
[113] Barjaktarevic I, Miravitlles M. Alpha-1 antitrypsin (AAT) augmentation therapy in individuals with the PI*MZ genotype: a pro/con debate on a working hypothesis. BMC pulmonary medicine 2021;21(1):99.

[114] McElvaney GN, Sandhaus RA, Miravitlles M, et al. Clinical considerations in individuals with α1-antitrypsin PI*SZ genotype. European Respiratory Journal 2020;55(6).
[115] Usmani OS. Feasibility of Aerosolized Alpha-1 Antitrypsin as a Therapeutic Option. Chronic obstructive pulmonary diseases (Miami, Fla.) 2020;7(3):272–9.
[116] Hubbard RC, Brantly ML, Sellers SE, Mitchell ME, Crystal RG. Anti-neutrophil-elastase defenses of the lower respiratory tract in alpha 1-antitrypsin deficiency directly augmented with an aerosol of alpha 1-antitrypsin. Annals of internal medicine 1989;111(3):206–12.
[117] Stolk J, Tov N, Chapman KR, et al. Efficacy and safety of inhaled α1-antitrypsin in patients with severe α1-antitrypsin deficiency and frequent exacerbations of COPD. European Respiratory Journal 2019;54(5).
[118] Bafadhel M, McKenna S, Terry S, et al. Acute exacerbations of chronic obstructive pulmonary disease: identification of biologic clusters and their biomarkers. American journal of respiratory and critical care medicine 2011;184(6):662–71.
[119] Vogelmeier CF, Chapman KR, Miravitlles M, et al. Exacerbation heterogeneity in COPD: subgroup analyses from the FLAME study. International journal of chronic obstructive pulmonary disease 2018;13:1125–34.
[120] Sala V, Murabito A, Ghigo A. Inhaled Biologicals for the Treatment of Cystic Fibrosis. Recent patents on inflammation & allergy drug discovery 2019;13(1):19–26.
[121] Conese M, Copreni E, Di Gioia S, Rinaldis P de, Fumarulo R. Neutrophil recruitment and airway epithelial cell involvement in chronic cystic fibrosis lung disease. Journal of Cystic Fibrosis 2003;2(3):129–35.
[122] Fazleen A, Wilkinson T. The emerging role of proteases in α1-antitrypsin deficiency and beyond. ERJ open research 2021;7(4).
[123] Melvin Berger, Michael W Konstan, Jay B Hilliard. Late-breaking science abstracts: Ninth annual North American cystic fibrosis (CF) conference. Pediatr. Pulmonol. 1995;20(6):418–26.
[124] Brand P, Beckmann H, Maas Enriquez M, et al. Peripheral deposition of alpha1-protease inhibitor using commercial inhalation devices. The European respiratory journal 2003;22(2):263–7.
[125] Viglio S, Bak EG, Schouten IGM, Iadarola P, Stolk J. Protease-Specific Biomarkers to Analyse Protease Inhibitors for Emphysema Associated with Alpha 1-Antitrypsin Deficiency. An Overview of Current Approaches. International journal of molecular sciences 2021;22(3).
[126] Remih K, Amzou S, Strnad P. Alpha1-antitrypsin deficiency: New therapies on the horizon. Current opinion in pharmacology 2021;59:149–56.
[127] Lomas DA. New Therapeutic Targets for Alpha-1 Antitrypsin Deficiency. Chronic obstructive pulmonary diseases (Miami, Fla.) 2018;5(4):233–43.
[128] Mukherjee A, Hidvegi T, Araya P, Ewing M, Stolz DB, Perlmutter DH. NFκB mitigates the pathological effects of misfolded α1-antitrypsin by activating autophagy and an integrated program of proteostasis mechanisms. Cell death and differentiation 2019;26(3):455–69.
[129] Wu S-S, Li Q-C, Yin C-Q, Xue W, Song C-Q. Advances in CRISPR/Cas-based Gene Therapy in Human Genetic Diseases. Theranostics 2020;10(10):4374–82.
[130] Song C-Q, Wang D, Jiang T, et al. In Vivo Genome Editing Partially Restores Alpha1-Antitrypsin in a Murine Model of AAT Deficiency. Human gene therapy 2018;29(8):853–60.
[131] Bjursell M, Porritt MJ, Ericson E, et al. Therapeutic Genome Editing With CRISPR/Cas9 in a Humanized Mouse Model Ameliorates α1-antitrypsin Deficiency Phenotype. EBioMedicine 2018;29:104–11.
[132] Shen S, Sanchez ME, Blomenkamp K, et al. Amelioration of Alpha-1 Antitrypsin Deficiency Diseases with Genome Editing in Transgenic Mice. Human gene therapy 2018;29(8):861–73.
[133] Parr DG, Lara B. Clinical utility of alpha-1 proteinase inhibitor in the management of adult patients with severe alpha-1 antitrypsin deficiency: a review of the current literature. Drug design, development and therapy 2017;11:2149–62.

[134] Rahaghi FF. Alpha-1 antitrypsin deficiency research and emerging treatment strategies: what's down the road? Therapeutic advances in chronic disease 2021;12_suppl:20406223211014025.
[135] Seersholm N, Wencker M, Banik N, et al. Does alpha1-antitrypsin augmentation therapy slow the annual decline in FEV1 in patients with severe hereditary alpha1-antitrypsin deficiency? Wissenschaftliche Arbeitsgemeinschaft zur Therapie von Lungenerkrankungen (WATL) alpha1-AT study group. The European respiratory journal 1997;10(10):2260–3.
[136] Survival and FEV1 decline in individuals with severe deficiency of alpha1-antitrypsin. The Alpha-1-Antitrypsin Deficiency Registry Study Group. American journal of respiratory and critical care medicine 1998;158(1):49–59.
[137] Dirksen A, Dijkman JH, Madsen F, et al. A randomized clinical trial of alpha(1)-antitrypsin augmentation therapy. American journal of respiratory and critical care medicine 1999;160(5 Pt 1):1468–72.
[138] Lieberman J. Augmentation therapy reduces frequency of lung infections in antitrypsin deficiency: a new hypothesis with supporting data. Chest 2000;118(5):1480–5.
[139] Wencker M, Fuhrmann B, Banik N, Konietzko N. Longitudinal follow-up of patients with alpha(1)-protease inhibitor deficiency before and during therapy with IV alpha(1)-protease inhibitor. Chest 2001;119(3):737–44.
[140] Stockley RA, Bayley DL, Unsal I, Dowson LJ. The effect of augmentation therapy on bronchial inflammation in alpha1-antitrypsin deficiency. American journal of respiratory and critical care medicine 2002;165(11):1494–8.
[141] Tonelli AR, Rouhani F, Li N, Schreck P, Brantly ML. Alpha-1-antitrypsin augmentation therapy in deficient individuals enrolled in the Alpha-1 Foundation DNA and Tissue Bank. International journal of chronic obstructive pulmonary disease 2009;4:443–52.
[142] Dirksen A, Piitulainen E, Parr DG, et al. Exploring the role of CT densitometry: a randomised study of augmentation therapy in alpha1-antitrypsin deficiency. European Respiratory Journal 2009;33(6):1345–53.
[143] Chapman KR, Stockley RA, Dawkins C, Wilkes MM, Navickis RJ. Augmentation therapy for alpha1 antitrypsin deficiency: a meta-analysis. COPD 2009;6(3):177–84.
[144] Gøtzsche PC, Johansen HK. Intravenous alpha-1 antitrypsin augmentation therapy for treating patients with alpha-1 antitrypsin deficiency and lung disease. The Cochrane database of systematic reviews 2010(7):CD007851.
[145] Stockley RA, Parr DG, Piitulainen E, Stolk J, Stoel BC, Dirksen A. Therapeutic efficacy of α-1 antitrypsin augmentation therapy on the loss of lung tissue: an integrated analysis of 2 randomised clinical trials using computed tomography densitometry. Respiratory research 2010;11:136.
[146] Barros-Tizón JC, Torres ML, Blanco I, Martínez MT. Reduction of severe exacerbations and hospitalization-derived costs in alpha-1-antitrypsin-deficient patients treated with alpha-1-antitrypsin augmentation therapy. Therapeutic advances in respiratory disease 2012;6(2):67–78.
[147] Ma S, Lin YY, He J, Rouhani FN, Brantly M, Turino GM. Alpha-1 antitrypsin augmentation therapy and biomarkers of elastin degradation. COPD 2013;10(4):473–81.
[148] Chapman KR, Burdon JGW, Piitulainen E, et al. Intravenous augmentation treatment and lung density in severe α1 antitrypsin deficiency (RAPID): a randomised, double-blind, placebo-controlled trial. The Lancet 2015;386(9991):360–8.
[149] McElvaney NG, Burdon J, Holmes M, et al. Long-term efficacy and safety of α1 proteinase inhibitor treatment for emphysema caused by severe α1 antitrypsin deficiency: an open-label extension trial (RAPID-OLE). The Lancet Respiratory Medicine 2017;5(1):51–60.
[150] Gupta V, Bhavanasi S, Quadir M, et al. Protein PEGylation for cancer therapy: bench to bedside. Journal of cell communication and signaling 2019;13(3):319–30.

[151] Turecek PL, Bossard MJ, Schoetens F, Ivens IA. PEGylation of Biopharmaceuticals: A Review of Chemistry and Nonclinical Safety Information of Approved Drugs. Journal of pharmaceutical sciences 2016;105(2):460–75.
[152] Stidl R, Denne M, Goldstine J, Kadish B, Korakas KI, Turecek PL. Polyethylene Glycol Exposure with Antihemophilic Factor (Recombinant), PEGylated (rurioctocog alfa pegol) and Other Therapies Indicated for the Pediatric Population: History and Safety. Pharmaceuticals (Basel, Switzerland) 2018;11(3).
[153] Belén LH, Rangel-Yagui CdO, Beltrán Lissabet JF, et al. From Synthesis to Characterization of Site-Selective PEGylated Proteins. Frontiers in pharmacology 2019;10:1450.
[154] Banerjee SS, Aher N, Patil R, Khandare J. Poly(ethylene glycol)-Prodrug Conjugates: Concept, Design, and Applications. Journal of drug delivery 2012;2012:103973.
[155] Hoffman AS. The early days of PEG and PEGylation (1970s-1990s). Acta Biomaterialia 2016;40:1–5.
[156] Turecek PL, Bossard MJ, Schoetens F, Ivens IA. PEGylation of Biopharmaceuticals: A Review of Chemistry and Nonclinical Safety Information of Approved Drugs. Journal of pharmaceutical sciences 2016;105(2):460–75.
[157] Dozier JK, Distefano MD. Site-Specific PEGylation of Therapeutic Proteins. International journal of molecular sciences 2015;16(10):25831–64.
[158] Santos JHPM, Torres-Obreque KM, Meneguetti GP, Amaro BP, Rangel-Yagui CO. Protein PEGylation for the design of biobetters: from reaction to purification processes. Braz. J. Pharm. Sci. 2018;54(spe).
[159] Roberts MJ, Bentley MD, Harris JM. Chemistry for peptide and protein PEGylation. Advanced Drug Delivery Reviews 2002;54(4):459–76.
[160] Nischan N, Hackenberger CPR. Site-specific PEGylation of proteins: recent developments. The Journal of organic chemistry 2014;79(22):10727–33.
[161] Swierczewska M, Lee KC, Lee S. What is the future of PEGylated therapies? Expert opinion on emerging drugs 2015;20(4):531–6.
[162] Quality by design approach to protein PEGylation: a review. J App Biol Biotech 2017.
[163] Saha-Shah A, Sun S, Kong J, Zhong W, Mann BF. Design and Study of PEG Linkers That Enable Robust Characterization of PEGylated Proteins. ACS pharmacology & translational science 2021;4(4):1280–6.
[164] Cohan RA, Madadkar-Sobhani A, Khanahmad H, et al. Design, modeling, expression, and chemoselective PEGylation of a new nanosize cysteine analog of erythropoietin. International journal of nanomedicine 2011;6:1217–27.
[165] Maiser B, Dismer F, Hubbuch J. Optimization of random PEGylation reactions by means of high throughput screening. Biotechnology and bioengineering 2014;111(1):104–14.
[166] Pasut G, Morpurgo M, Veronese FM. Basic Strategies for PEGylation of Peptide and Protein Drugs. In: Torchilin VP, editor. Delivery of protein and peptide drugs in cancer. London: Imperial College, 2006:53–84.
[167] Carter MC, Meyerhoff ME. Instability of succinyl ester linkages in O2'-monosuccinyl cyclic AMP-protein conjugates at neutral pH. Journal of Immunological Methods 1985;81(2):245–57.
[168] Molineux G. The design and development of pegfilgrastim (PEG-rmetHuG-CSF, Neulasta). Current pharmaceutical design 2004;10(11):1235–44.
[169] Zhang W, Jiang Z, Wang L, Li C, Xia J. An open-label, randomized, multicenter dose-finding study of once-per-cycle pegfilgrastim versus daily filgrastim in Chinese breast cancer patients receiving TAC chemotherapy. Medical oncology (Northwood, London, England) 2015;32(5):147.
[170] Pasut G, Veronese FM. State of the art in PEGylation: the great versatility achieved after forty years of research. Journal of controlled release official journal of the Controlled Release Society 2012;161(2):461–72.

[171] Awoonor-Williams E, Rowley CN. Evaluation of Methods for the Calculation of the pKa of Cysteine Residues in Proteins. Journal of chemical theory and computation 2016;12(9):4662–73.
[172] Schoffelen S, van Eldijk MB, Rooijakkers B, Raijmakers R, Heck AJR, van Hest JCM. Metal-free and pH-controlled introduction of azides in proteins. Chem. Sci. 2011;2(4):701.
[173] Chan AO-Y, Ho C-M, Chong H-C, et al. Modification of N-terminal α-amino groups of peptides and proteins using ketenes. Journal of the American Chemical Society 2012;134(5):2589–98.
[174] Obermeyer AC, Jarman JB, Francis MB. N-terminal modification of proteins with o-aminophenols. Journal of the American Chemical Society 2014;136(27):9572–9.
[175] Song IT, Lee M, Lee H, et al. PEGylation and HAylation via catechol: α-Amine-specific reaction at N-terminus of peptides and proteins. Acta Biomaterialia 2016;43:50–60.
[176] Rosen CB, Francis MB. Targeting the N terminus for site-selective protein modification. Nature chemical biology 2017;13(7):697–705.
[177] Pfister D, Morbidelli M. Process for protein PEGylation. Journal of controlled release official journal of the Controlled Release Society 2014;180:134–49.
[178] Renault K, Fredy JW, Renard P-Y, Sabot C. Covalent Modification of Biomolecules through Maleimide-Based Labeling Strategies. Bioconjugate chemistry 2018;29(8):2497–513.
[179] Brocchini S, Godwin A, Balan S, Choi J, Zloh M, Shaunak S. Disulfide bridge based PEGylation of proteins. Advanced Drug Delivery Reviews 2008;60(1):3–12.
[180] Gunnoo SB, Madder A. Chemical Protein Modification through Cysteine. Chembiochem a European journal of chemical biology 2016;17(7):529–53.
[181] Uprety R, Luo J, Liu J, Naro Y, Samanta S, Deiters A. Genetic encoding of caged cysteine and caged homocysteine in bacterial and mammalian cells. Chembiochem a European journal of chemical biology 2014;15(12):1793–9.
[182] Mulligan C, Mindell JA. Pinning Down the Mechanism of Transport: Probing the Structure and Function of Transporters Using Cysteine Cross-Linking and Site-Specific Labeling. Methods in enzymology 2017;594:165–202.
[183] Gong Y, Leroux J-C, Gauthier MA. Releasable Conjugation of Polymers to Proteins. Bioconjugate chemistry 2015;26(7):1172–81.
[184] Gong Y, Andina D, Nahar S, Leroux J-C, Gauthier MA. Releasable and traceless PEGylation of arginine-rich antimicrobial peptides. Chem. Sci. 2017;8(5):4082–6.
[185] Nollmann FI, Goldbach T, Berthold N, Hoffmann R. Controlled systemic release of therapeutic peptides from PEGylated prodrugs by serum proteases. Angewandte Chemie (International ed. in English) 2013;52(29):7597–9.
[186] Filpula D, Zhao H. Releasable PEGylation of proteins with customized linkers. Advanced Drug Delivery Reviews 2008;60(1):29–49.
[187] Sousa SF, Peres J, Coelho M, Vieira TF. Analyzing PEGylation through Molecular Dynamics Simulations. ChemistrySelect 2018;3(29):8415–27.
[188] Ramezanghorbani F, Lin P, Colina CM. Optimizing Protein-Polymer Interactions in a Poly(ethylene glycol) Coarse-Grained Model. The journal of physical chemistry. B 2018;122(33):7997–8005.
[189] Lin P, Colina CM. Molecular simulation of protein–polymer conjugates. Current Opinion in Chemical Engineering 2019;23:44–50.
[190] Abuchowski A, van Es T, Palczuk NC, Davis FF. Alteration of immunological properties of bovine serum albumin by covalent attachment of polyethylene glycol. The Journal of biological chemistry 1977;252(11):3578–81.
[191] Fishburn CS. The pharmacology of PEGylation: balancing PD with PK to generate novel therapeutics. Journal of pharmaceutical sciences 2008;97(10):4167–83.
[192] Jevsevar S, Kunstelj M, Porekar VG. PEGylation of therapeutic proteins. Biotechnology journal 2010;5(1):113–28.

[193] Lawrence PB, Price JL. How PEGylation influences protein conformational stability. Current opinion in chemical biology 2016;34:88–94.
[194] Arvedson T, O'Kelly J, Yang B-B. Design Rationale and Development Approach for Pegfilgrastim as a Long-Acting Granulocyte Colony-Stimulating Factor. BioDrugs clinical immunotherapeutics, biopharmaceuticals and gene therapy 2015;29(3):185–98.
[195] Luxon BA, Grace M, Brassard D, Bordens R. Pegylated interferons for the treatment of chronic hepatitis C infection. Clinical Therapeutics 2002;24(9):1363–83.
[196] Monkarsh SP, Ma Y, Aglione A, et al. Positional isomers of monopegylated interferon alpha-2a: isolation, characterization, and biological activity. Analytical biochemistry 1997;247(2):434–40.
[197] Freches D, Patil HP, Machado Franco M, Uyttenhove C, Heywood S, Vanbever R. PEGylation prolongs the pulmonary retention of an anti-IL-17A Fab' antibody fragment after pulmonary delivery in three different species. International journal of pharmaceutics 2017;521(1-2):120–9.
[198] Guichard M-J, Wilms T, Mahri S, et al. PEGylation of Recombinant Human Deoxyribonuclease I Provides a Long-Acting Version of the Mucolytic for Patients with Cystic Fibrosis. Adv. Therap. 2021;4(2):2000146.
[199] Zhang X, Wang H, Ma Z, Wu B. Effects of pharmaceutical PEGylation on drug metabolism and its clinical concerns. Expert opinion on drug metabolism & toxicology 2014;10(12):1691–702.
[200] Caliceti P. Pharmacokinetic and biodistribution properties of poly(ethylene glycol)–protein conjugates. Advanced Drug Delivery Reviews 2003;55(10):1261–77.
[201] Su C, Liu Y, Li R, Wu W, Fawcett JP, Gu J. Absorption, distribution, metabolism and excretion of the biomaterials used in Nanocarrier drug delivery systems. Advanced Drug Delivery Reviews 2019;143:97–114.
[202] Webster R, Elliott V, Park BK, Walker D, Hankin M, Taupin P. PEG and PEG conjugates toxicity: towards an understanding of the toxicity of PEG and its relevance to PEGylated biologicals. In: Veronese FM, editor. PEGylated Protein Drugs: Basic Science and Clinical Applications. Basel: Birkhäuser Basel, 2009:127–46.
[203] Garay RP, El-Gewely R, Armstrong JK, Garratty G, Richette P. Antibodies against polyethylene glycol in healthy subjects and in patients treated with PEG-conjugated agents. Expert opinion on drug delivery 2012;9(11):1319–23.
[204] Ivens IA, Achanzar W, Baumann A, et al. PEGylated Biopharmaceuticals: Current Experience and Considerations for Nonclinical Development. Toxicologic pathology 2015;43(7):959–83.
[205] Schellekens H, Hennink WE, Brinks V. The immunogenicity of polyethylene glycol: facts and fiction. Pharmaceutical research 2013;30(7):1729–34.
[206] Yadav D, Dewangan HK. PEGYLATION: an important approach for novel drug delivery system. Journal of biomaterials science. Polymer edition 2021;32(2):266–80.
[207] Shiraishi K, Yokoyama M. Toxicity and immunogenicity concerns related to PEGylated-micelle carrier systems: a review. Science and technology of advanced materials 2019;20(1):324–36.
[208] Bendele A, Seely J, Richey C, Sennello G, Shopp G. Short communication: renal tubular vacuolation in animals treated with polyethylene-glycol-conjugated proteins. Toxicological sciences an official journal of the Society of Toxicology 1998;42(2):152–7.
[209] Fletcher AM, Tellier P, Douville J, et al. Adverse vacuolation in multiple tissues in cynomolgus monkeys following repeat-dose administration of a PEGylated protein. Toxicology letters 2019;317:120–9.
[210] Ivens IA, Banczyk D, Gutberlet K, Jackman S, Vauléon S, Frisk A-L. Nonclinical Safety Assessment of a Long-Acting Recombinant PEGylated Factor Eight (BAY 94-9027) With a 60 kDa PEG. Toxicologic pathology 2019;47(5):585–97.

[211] Rudmann DG, Alston JT, Hanson JC, Heidel S. High molecular weight polyethylene glycol cellular distribution and PEG-associated cytoplasmic vacuolation is molecular weight dependent and does not require conjugation to proteins. Toxicologic pathology 2013;41(7):970–83.
[212] Rondon A, Mahri S, Morales-Yanez F, Dumoulin M, Vanbever R. Protein Engineering Strategies for Improved Pharmacokinetics. Adv. Funct. Mater. 2021;31(44):2101633.
[213] Kozma GT, Shimizu T, Ishida T, Szebeni J. Anti-PEG antibodies: Properties, formation, testing and role in adverse immune reactions to PEGylated nano-biopharmaceuticals. Advanced Drug Delivery Reviews 2020;154-155:163–75.
[214] Zhang P, Sun F, Liu S, Jiang S. Anti-PEG antibodies in the clinic: Current issues and beyond PEGylation. Journal of controlled release official journal of the Controlled Release Society 2016;244(Pt B):184–93.
[215] Richter AW, Akerblom E. Antibodies against polyethylene glycol produced in animals by immunization with monomethoxy polyethylene glycol modified proteins. International archives of allergy and applied immunology 1983;70(2):124–31.
[216] Richter AW, Akerblom E. Polyethylene glycol reactive antibodies in man: titer distribution in allergic patients treated with monomethoxy polyethylene glycol modified allergens or placebo, and in healthy blood donors. International archives of allergy and applied immunology 1984;74(1):36–9.
[217] Awwad S, Ginn C, Brocchini S. The case for protein PEGylation. In: Engineering of Biomaterials for Drug Delivery Systems: Elsevier, 2018:27–49.
[218] Duncan R. Polymer therapeutics: Top 10 selling pharmaceuticals - what next? Journal of controlled release official journal of the Controlled Release Society 2014;190:371–80.
[219] Matsuda F, Torii Y, Enomoto H, et al. Anti-interferon-α neutralizing antibody is associated with nonresponse to pegylated interferon-α plus ribavirin in chronic hepatitis C. Journal of viral hepatitis 2012;19(10):694–703.
[220] Webster R, Didier E, Harris P, et al. PEGylated proteins: evaluation of their safety in the absence of definitive metabolism studies. Drug metabolism and disposition: the biological fate of chemicals 2007;35(1):9–16.
[221] Lubich C, Allacher P, La Rosa M de, et al. The Mystery of Antibodies Against Polyethylene Glycol (PEG) - What do we Know? Pharmaceutical research 2016;33(9):2239–49.
[222] Zhu W, Li L, Deng M, et al. Oxidation-resistant and thermostable forms of alpha-1 antitrypsin from Escherichia coli inclusion bodies. FEBS open bio 2018;8(10):1711–21.
[223] Krishnan B, Gierasch LM. Dynamic local unfolding in the serpin α-1 antitrypsin provides a mechanism for loop insertion and polymerization. Nature structural & molecular biology 2011;18(2):222–6.

CHAPTER II

PRODUCTION AND CHARACTERIZATION OF MONO-PEGYLATED ALPHA-1 ANTITRYPSIN FOR AUGMENTATION THERAPY

Adapted from

Liu X, Vanvarenberg K, Guy Wilfried Kouassi K, Mahri S, Vanbever R. Production and characterization of mono-PEGylated alpha-1 antitrypsin for augmentation therapy. International journal of pharmaceutics 2021:121355.

ABSTRACT

Alpha-1 antitrypsin (AAT) is an endogenous inhibitor of serine proteases which, in physiological conditions, neutralizes the excess of neutrophil elastase and other serine proteases in tissues and especially the lungs. Weekly intravenous infusion of plasma-purified human AAT is used to treat AAT deficiency-associated lung disease. However, only 2 % of the AAT dose reaches the lungs after intravenous infusion. Inhalation of AAT might offer an alternative route of administration. Yet, the rapid clearance of AAT from the respiratory tract results in high and frequent dosing by inhalation and limited efficacy. In the present study, we produced and characterized in vitro a PEGylated version of AAT which could offer a prolonged body residence time and thereby be useful for augmentation therapy by the intravenous and inhalation routes. Two PEGylation reactions – N-terminal and thiol PEGylation – and three polyethylene glycol (PEG) chains – linear 30kDa, linear 40kDa and 2-armed 40kDa – were used. The yields of mono-PEGylated AAT following purification by anion exchange chromatography were 40 – 50 % for N-terminal PEGylation and 60 – 70 % for thiol PEGylation. The PEG-AAT conjugates preserved the ability to form a protease-inhibitor complex with neutrophil elastase and proteinase 3 as well as the full inhibitory capacity to neutralize neutrophil elastase activity. These results open interesting prospects for PEGylated AAT to achieve a prolonged half-life and an improved therapeutic efficacy in vivo.

KEYWORDS

Alpha-1 antitrypsin, chronic obstructive pulmonary disease, PEGylation, neutrophil elastase

Graphic Abstract

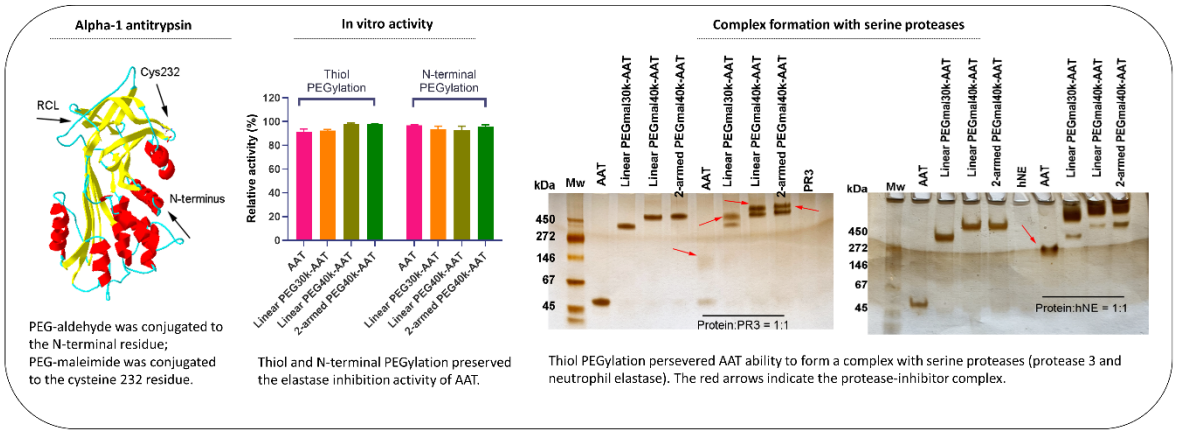

TABLE OF CONTENTS

I. INTRODUCTION

Alpha-1 antitrypsin (AAT) is a 52-kDa serine protease inhibitor primarily produced in the liver. Alpha-1 antitrypsin provides essential protection to the lung tissue against the action of proteolytic enzymes such as neutrophil elastase, proteinase 3 (PR-3) and cathepsin G. Alpha-1 antitrypsin deficiency is characterized by low AAT serum levels (< 11 μM) [1, 2]. AAT deficiency is a hereditary condition caused by a mutation in the SERPINA1 gene [3]. The retention of misfolded and polymerized Z type AAT mutant within hepatocytes causes hepatic damages and cirrhosis [4]. The imbalance between proteases and protease inhibitors in the lungs may lead to premature emphysema and chronic obstructive pulmonary disease (COPD) [5].

Current approved therapies for patients with AAT deficiency and respiratory disease is intravenous augmentation therapy [1]. Although intravenous infusion of highly purified human AAT is safe, high doses of AAT are required (60 mg/kg weekly) due to the low fraction of the dose (2 %) reaching the lung epithelial lining fluid [6]. Moreover, the benefits of augmentation therapy on pulmonary exacerbation or progression of emphysema have not been conclusively demonstrated in randomized controlled clinical trials. An additional drawback of augmentation therapy is its high annual costs with an average of 100,000 dollars per patient [7]. Almost a third of known qualified subjects with AAT deficiency do not receive the therapy due to financial constraints [1].

Inhaled AAT has been developed as an alternative administration route for augmentation therapy in AAT deficiency [8, 9]. The potential advantages of inhaled over intravenous AAT include the noninvasive administration, high lung concentrations, lower doses, lower costs, and improved convenience for the patients. However, these advantages are counterbalanced by the large amount of inhaled AAT required (in total about 200 mg daily) [5, 9]. In a phase II/III clinical trial, patients with emphysema due to AAT deficiency received a twice-daily inhalation of 80 mg AAT [10]. After 50 weeks of treatment, inhaled AAT did not prolong the time to first exacerbation. However, the first exacerbation involved fewer symptoms. The severity of the exacerbation, including the dyspnea degree, the sputum volume and sputum purulence [11], lessened with AAT treatment, indicating AAT possible role in reducing the incidence or severity of dyspnea [10]. The limited efficacy of inhaled AAT might result from the rapid clearance of AAT from the lungs. Proteolytic breakdown within or outside the reactive center loop of AAT [12], oxidation of methionine 351 or 358 [13] and phagocytes uptake might be the causes of the short residence time of AAT in the lungs. Therefore, to improve the therapeutic efficacy of inhaled AAT, it might be beneficial to prolong its residence time in the lungs.

PEGylation is a common process used to improve the therapeutic value of a protein by prolonging

its serum half-life [14]. Several PEGylated proteins have been approved by the FDA and EMA for clinical use by injection [15]. In a few preclinical studies, conjugation of PEG to proteins also showed the potential to improve their local residence time in the lungs after pulmonary delivery. Cantin et al. reported that the conjugation of recombinant non-glycosylated human AAT (rhAAT) to 20 kDa PEG resulted in the retention of the conjugate in the bronchoalveolar lavage after intranasal instillation in mice for at least 48 h whereas the unmodified rhAAT was cleared within 24 h [16]. Similarly, Zhu et al conjugated a 20 kDa PEG to a more thermal stable recombinant AAT expressed in E. coli [17]. The PEGylated version showed the same activity as the unconjugated AAT. Koussoroplis et al. conjugated anti-IL17A F(ab')2 to a 2-armed 40 kDa PEG and demonstrated that the PEGylated antibody fragment presented increased pulmonary residence time and improved anti-inflammatory effect [18]. Guichard et al. showed that the conjugation of linear 30 kDa PEG or 2-armed 40 kDa PEG to recombinant human deoxyribonulease I (rhDNase) sustained its presence in murine lungs for 15 days and a single dose of PEGylated rhDNase provided similar therapeutic efficacy to reduce DNA content in the lungs of $\boldsymbol{\beta}$-ENaC mice, a model of the cystic fibrosis lung disease, as 5 consecutive daily doses of unconjugated rhDNase [19].

Larger PEG (≥30 kDa) chains have been shown more effective to increase protein residence time in the lungs than smaller PEG chains (≤20 kDa) [19]. However, they have not been investigated for pulmonary AAT delivery yet. In addition, rhAAT is unstable *in vivo* (cleared within 4 h in the circulation) and PEG-rhAAT only showed similar serum half-life as plasma-purified glycosylated AAT [17]. Thus, it might be more promising to PEGylate glycosylated AAT rather than rhAAT and to use large PEG chains (≥30 kDa) to increase AAT stability and to sustain its body residence time.

In this study, PEGylated versions of glycosylated AAT were produced and characterized in vitro. Plasma-purified glycosylated AAT was mono-PEGylated selectively on i) its N-terminal residue by reductive alkylation at acidic pH, or ii) its cysteine 232 residue by thiol PEGylation (Figure 1). The size and composition of PEG used included linear 30 kDa PEG, linear 40 kDa PEG and 2-armed 40 kDa PEG. The mono-PEGylated products were purified and characterized for their PEGylation degree, size, protease neutralization capacity and formation of the inhibitor-protease complex.

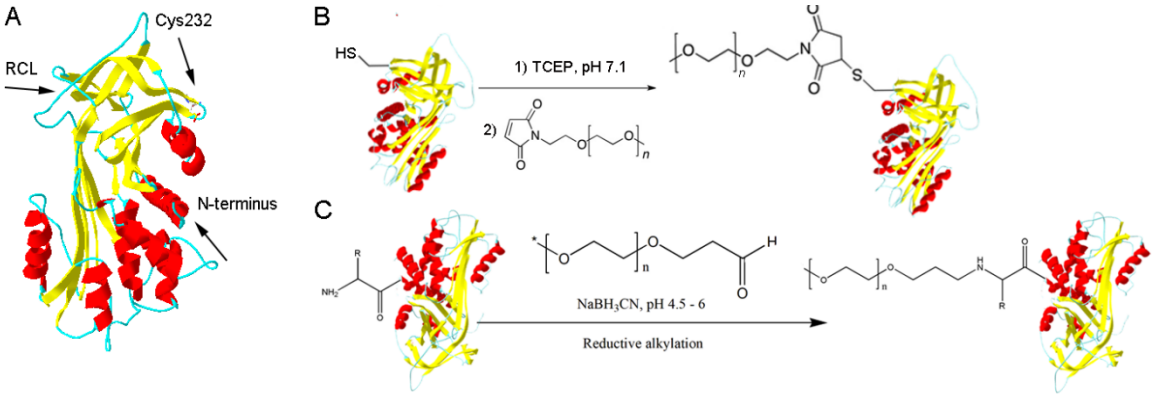

Figure 1. A) 3D structure of AAT (PDB: 2qug), generated by the SWISS-MODEL. The arrows show the reactive center loop (RCL) and the two PEGylation sites. B) Thiol PEGylation on the Cys232. C) N-terminal PEGylation.

II. MATERIALS AND METHODS

II.1. MATERIALS

AAT was purified from Pulmolast® (Lamepro, Breda, The Netherlands) by size exclusion chromatography (SEC; ÄKTA™ purifier 10 system, GE Healthcare Bio-Sciences AB, Uppsala, Sweden) using a HiLoad 16/600 Superdex 200 pg (GE Healthcare Europe GmbH, Diegem, Belgium) and 10 mM NaH_2PO_4 and 110 mM NaCl, pH 7.1, as eluent. This saline solution is the saline composition of Pulmolast® and it was also used for AAT storage at 4°C in our studies. The chromatograms were analyzed by UNICORN software (GE Healthcare Bio-Sciences AB, Uppsala, Sweden). Through SEC purification, we were able to remove impurities which represented 23 ± 3 % of the Pulmolast® product (Supplementary Figure S1). Linear 30 kDa, 40 kDa and 2-armed 40 kDa methoxy-PEG-maleimide and linear 30 kDa, 40 kDa and 2-armed 40 kDa methoxy-PEG-aldehyde were purchased from NOF Europe GmbH (Frankfurt, Germany). Human neutrophil elastase (hNE) and its substrate N-Succinyl-Ala-Ala-Ala-p-nitroanilide were purchased from Elastin Products Company, Inc (Owensville, USA). All other reagents, unless otherwise mentioned, were obtained from Sigma-Aldrich, Inc (Overijse, Belgium).

II.2. PRODUCTION OF PEGYLATED AAT

AAT concentration was determined by the absorbance at 280 nm using Beer-Lambert Law with an extinction coefficient of 4.33 $(g/100\ mL)^{-1}\ cm^{-1}$ (A280, 1 %, 1 cm) [20]. Prior to thiol PEGylation, AAT (5, 10 or 20 mg/ml) was reduced by tris(2-carboxyethyl) phosphine (TCEP) at a molar ratio of TCEP:AAT 4:1 in 10 mM NaH_2PO_4 and 110 mM NaCl, pH 7.1, at room temperature with mild agitation for 1 hour. PEG-maleimide was added to the reduced AAT at a PEG:protein molar ratio of 2:1 or 4:1. The TCEP was kept in the reaction mixture as it does not react with PEG-maleimide. The PEGylation was carried out under mild agitation for 1, 4 or 8 hours and stopped by adding 4-fold molar excess (comparing to the PEG reagent) of cysteine. The PEGylation yield was determined by anion exchange chromatography (AEC) at the different time points.

For the N-terminal PEGylation, AAT (5 or 10 mg/ml) and 2, 4 or 8-fold molar excess of PEG-aldehyde were incubated in 20 mM succinate buffer, pH 6, in the presence of 120-fold molar excess (11.5 μM) of sodium cyanoborohydride ($NaCNBH_3$). The reaction proceeded under mild agitation for 24, 48 or 72 hours.

The yields of mono-PEGylated AAT under different reaction conditions were compared and the condition presenting the highest yield of mono-PEGylated AAT, the lowest yield of side products,

and the shortest reaction time was chosen. In plasma-purified glycosylated AAT, a free cysteine is conjugated to the cysteine 232 residue and is described as a "cysteine cap" [21]. This additional cysteine residue provides an additional N-terminal amino acid residue with an alpha-amino group, which could react with the PEG-aldehyde in addition to the main polypeptide chain N terminal amino acid residue. To investigate the influence of the cysteine cap on N-terminal selectivity, the N-terminal PEGylation was carried out with or without a prior TCEP reduction step.

II.3. PURIFICATION OF MONO-PEGYLATED AAT

Mono-PEGylated AAT was purified by anion-exchange chromatography (AEC). The reaction mixtures were dialyzed against the starting buffer for FPLC (20 mM $N(CH_2CH_2OH)_3$, 5 mM NaCl, pH 7.5) for at least 6 hours (Spectra/Pro molecular porous membrane tubing MWCO 6-8 kDa, Spectrum, Belgium). The samples were filtered through a 0.22 μm polyvinylidene fluoride (PVDF) syringe-tip before loading to the FPLC column.

To optimize the reaction conditions, an anion exchange Resource Q1 column (GE Healthcare Bio-Science AB, Uppsala, Sweden) was used to purify the reaction mixture. A salt gradient elution was performed using the starting buffer 20 mM $N(CH_2CH_2OH)_3$, 5 mM NaCl, pH 7.5 and the elution buffer 20 mM $N(CH_2CH_2OH)_3$, 250 mM NaCl, pH 7.5. Absorbance at 280 nm was recorded during the purification. Chromatograms were recorded by UNICORN 5.2 software and the yield of PEGylated AAT was calculated based on the relative area under the peaks.

An anion exchange Mono Q 4.6/100 PE column (GE Healthcare Bio-Sciences AB, Uppsala, Sweden) was used to purify the PEGylated AAT produced with the optimized conditions, using the same gradient elution as above. The collected fractions containing the mono-PEGylated AAT were pooled and concentrated using Vivaspin 15R sample concentrator (10,000 molecular weight cut-off, Sartorius, Stonehouse, Gloucestershire, UK) and stored in 10 mM NaH_2PO_4, 110 mM NaCl, pH 7.1 at 4 °C.

II.4. SDS-PAGE AND NATIVE PAGE

The purity of the purified AAT and PEGylated AAT was evaluated by SDS-PAGE using a gradient 4-20 % Mini-PROTEAN®TGX™ precast gel (Bio-Rad, Hercules, CA, USA). Samples were diluted with non-reducing or TCEP reducing 4X Laemmli Sample buffer (Bio-Rad, Hercules, CA, USA) and 3 μg of protein was loaded on each well. The Native PAGE was performed as described above but at 4°C instead of room temperature and without the presence of sodium dodecyl sulfate (SDS) in the electrophoresis buffer. The electrophoresis was performed for 1-2 h longer than usual

to ensure a better separation for heavier protein components (PEG-AAT or the protease-inhibitor complex). The native page molecular markers were from SERVA Electrophoresis GmBH. The gels were stained by GelCode® Blue Stain Reagent (Thermo Fisher, Gent, Belgium) according to the manufactory instructions. PEG was stained using the barium iodide staining method based on Kurfürst's method [22].

II.5. DYNAMIC LIGHT SCATTERING (DLS)

The hydrodynamic diameter of AAT and PEGylated AAT was measured by DLS on a Zetasizer Ultra system (Malvern Panalytical Ltd, Malvern, UK). The PEG-maleimide, PEG-aldehyde and protein samples at 1 mg/ml in 10 mM NaH_2PO_4, 110 mM NaCl, pH 7.1 were filtered through a 0.22 μm PVDF syringe-tip prior to the DLS measurements. Observations were made at multiple angles. The scattering intensity data were transformed to volume distribution data and analyzed by Zetasizer Ultra software.

II.6. ELECTROSPRAY-IONIZATION QUADRUPOLE TIME-OF-FLIGHT MASS SPECTROMETRY (ESI-Q-TOF)

The mass spectrometry analysis was performed according to Kolarich et al [21]. The detailed methods are available in the supplementary document.

II.7. ELASTASE INHIBITION ASSAY

The biological activity of AAT and PEGylated AAT was evaluated by a modified elastase inhibition assay according to Bieth [23]. Briefly, at 37 °C, 0.034 μM hNE was pre-incubated with 0.3 mM substrate N-Succinyl-Ala-Ala-Ala-pNitroanilide (Tris-NaCl buffer, pH 7.5) in a 96-well plate for 20 min. Afterwards, AAT or PEG-AAT was added to the mixture at a protein:hNE molar ratio of 0.3:1, 0.6:1, 1:1, 1.3:1, 1.6:1 and 2:1 and incubated for 40 min. During the incubation, the absorbance at 410 nm of each sample was recorded every 1 min. The absorbance at 410 nm increases linearly with incubation time. The increment of the absorbance at 410 nm of each sample (ΔODsp) after adding the unconjugated or PEGylated AAT was used to calculate the relative hNE activity. The ΔOD410 of the sample in absence of AAT (ΔODctr) represented the full activity of hNE. The relative hNE activity was calculated as follows: relative hNE activity (%) = ΔODsp / ΔODctr × 100.

II.8. INHIBITOR-PROTEASE COMPLEX FORMATION

Unconjugated AAT and PEG-AAT were incubated with hNE (on ice) in NaOAc-NaCl, pH 5, or with PR3 (at room temperature) in HEPES buffer, pH 7.4 for 5 min. The molar ratio of AAT or PEG-AAT to the protease was 1:1. The final concentration of AAT and protease in the mixture was 0.32 mMol. The mixture was then subjected to native PAGE and SDS-PAGE, followed by a silver stain using Pierce™ Silver Stain Kit (Thermo Fisher, Gent, Belgium) to visualize the protein and protein-protease complex.

To identify the protein-protease complex in SDS-PAGE, a Western Blot method was performed. Following the separation by SDS-PAGE, the proteins were electroblotted onto a nitrocellulose membrane (Bio-Rad, Hercules, CA, USA). In this step, AAT and PEG-AAT showed different migration rate from the gel to the membrane. To ensure the successful transfer of PEG-AAT, the electroblotting conditions were optimized for PEG-AAT according to the manufacturer instructions. After blocking in 5 % non-fat milk at room temperature for 1 hour, the membrane was incubated in a 1:5,000 dilution rabbit anti-hNE conjugated to HRP (ABIN2753573, CUSABIO, Kampenhout, Belgium) at 4 °C overnight. The membrane was washed with phosphate-buffered saline containing 0.1 % Tween™ 20 (PBST) for three times, the bound antibody was detected by chemiluminescence using Pierce™ ECL Western Blotting Substrate (Thermofisher, Gent, Belgium) according to the manufacturer manual.

II.9. STABILITY OF AAT AND PEG-AAT DURING LONG-TERM STORAGE

The purified unconjugated AAT and PEGylated AAT were stored in 10 mM NaH_2PO_4, 110 mM NaCl, pH 7.1 at 4 °C for 24 weeks. Protein samples were prepared in separate Eppendorf tubes and sealed by PARAFILM® M (Sigma-Aldrich, Overijse, Belgium). The content of monomers, aggregates and fragments of the protein samples were analyzed by UV absorbance and SEC, using a Superose 6 increase 5/150 GL column (GE Healthcare Europe GmbH, Diegem, Belgium) after 2, 4, 8, 12, 16, 20, 24 weeks of storage. The monomer content of each sample was monitored by SEC and calculated using the area under the curve of peaks in SEC chromatograms. The activity of AAT and PEG-AAT was evaluated by the elastase inhibition assay as described in 2.7.

II.10. CYTOTOXICITY OF AAT AND PEG-AAT

Murine alveolar macrophages MHS (ATCC® CRL-2019 TM) were cultured at 37 ◦C and 5 % CO_2 in RPMI-1640 medium (Thermofisher, Gent, Belgium). The medium was supplemented with 10 % Foetal Bovine Serum (FBS, Thermofisher, Gent, Belgium) and 2-mercaptoethanol (2-ME,

Thermofisher, Gent, Belgium) at a final concentration of 0.05 mM. Cells were sub-cultured twice a week and maintained within the passage number between 10 – 20. MHS cells were seeded in 96-well plates (Thermofisher, Gent, Belgium) at a cell density of 2.5×10^4 cells/well and cultured for 24 h before the exposure to the tested proteins. AAT or PEG-AAT were incubated with MHS at a final concentration of 0.02 – 2 μg/ml, the control cells were incubated with complete RPMI medium with the addition of the same volume of AAT storage buffer without the protein. After 48 hour-exposure to AAT or PEG-AAT, the culture medium was replaced with complete RPMI medium with 0.5 mg/ml 3-(4,5-dimethylthiazol-2-yl)-2,5-diphenyltetrazolium bromide (MTT). After 3 hours incubation, 100 μl of lysis buffer (10 % SDS, 0.01 N HCl) were added to each well. The plates were slowly shaked for 4 hours. The absorbance of each well at 560 nm was measured by SpectraMax i3 (Molecular Devices, CA, USA). The cell viability was calculated by the following equation: %cell viability = ODsp/ODctr × 100 %.

II.11. STATISTICS

GraphPad Prism (GraphPad Software, USA) was used to infer statistical differences. In elastase inhibition assays, the values were compared by unpaired multiple T test followed by Holm-Sidak method. In MTT assays, the results were compared by One-Way ANOVA using Dunnett comparison test (* $p<0.05$).

III. RESULTS

III.1. PRODUCTION AND PURIFICATION OF PEG-AAT

Thiol PEGylation was conducted using linear PEG-maleimide (PEGmal) of 30 kDa or 40 kDa and 2-armed PEGmal of 40 kDa (Figure 1). Anion exchange chromatography (AEC) was used to purify PEGylated AAT. As shown in Figure 2, the first eluted peak corresponds to the PEGylated AAT and the second peak to unmodified AAT. An SDS-PAGE of the fractions confirmed the PEGylation degree of PEGylated AAT and no multi-PEGylated products were found (Supplementary Figure S2). The TCEP-reduction step is essential for thiol PEGylation. Omitting the reduction step resulted in a low yield of PEGylated AAT (Figure 2 A).

The molar ratio of PEG to AAT and the AAT concentration were varied to improve the yield of mono-PEGylated AAT using 2-armed 40 kDa PEG-maleimide. At the same AAT concentration (10 mg/ml), doubling the PEG:AAT molar ratio (from 2:1 to 4:1) increased the yield of mono-PEGylated AAT by 1.5-fold (Figure 2 B, bottom and middle curves). At the same PEG:AAT molar ratio of 4:1, doubling the concentration of AAT (from 10 mg/ml to 20 mg/ml) resulted in a 1.6-fold improvement of mono-PEGylated AAT (Figure 2 B, middle and upper curves). Increasing the reaction time from 1 h to 8 h did not result in higher yield (Supplementary Figure S3), indicating that at 1 h, the reaction already reached completion. The conditions showing the highest yield of mono-PEGylated AAT (20 mg/ml AAT, PEG:AAT 4:1, 1 h reaction time) were selected to produce PEG-AAT by thiol PEGylation.

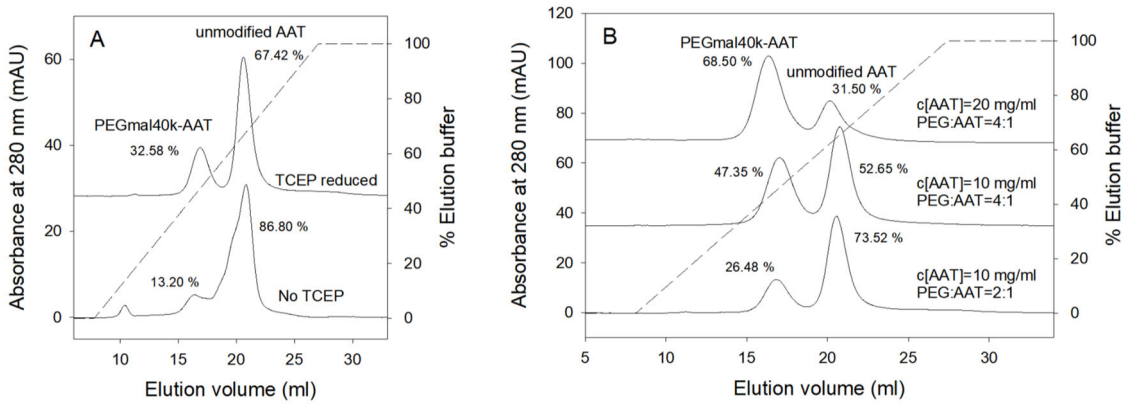

Figure 2. Optimization of thiol PEGylation. Two-armed 40 kDa PEG-maleimide was used. The reaction was at room temperature, pH 7.1, for 24 h, with different concentrations of AAT or PEG. A) Anion exchange chromatograms of non-reduced and TCEP-reduced thiol PEGylation. The concentration of AAT was 5 mg/ml, the molar ratio PEG:AAT 2:1. In TCEP-reduced PEGylation, the AAT was reduced by 4-fold molar excess of TCEP for 1 h prior to the PEGylation reaction for 1 h. Without the prior TCEP reduction, the yield of thiol PEGylation was low. B) Impact of PEG:AAT molar ratio and protein concentration on thiol PEGylation. The AAT was reduced by 4-fold molar excess of TCEP prior to the reaction for 1 h. Increasing PEG:AAT molar ratio or AAT concentration both resulted in higher PEGylation yield.

N-terminal PEGylation was performed using linear PEG-aldehyde (PEGald) of 30 kDa or 40 kDa and 2-armed PEGald of 40 kDa. The full UV spectrum of AAT shifted to higher absorbance values when decreasing the buffer pH. A significant absorbance at the wavelength of 300 – 350 nm (Figure 3 A) where proteins do not absorb indicates the formation of protein aggregates. Due to the instability of AAT in the pH range of 4 to 5.5, pH 6.0 was chosen to perform the N-terminal PEGylation. In the chromatograms of N-terminal PEGylation, three peaks were observed and identified by SDS-PAGE (Supplementary Figure S4) as di-PEGylated, mono-PEGylated and unmodified AAT (Figure 3 B, C). The peak of di-PEGylated AAT showed considerable overlap with the mono-PEGylated product.

The effect of protein concentration and PEG:AAT molar ratio on the degree of PEGylation and yield were investigated. As shown in Figure 3B, at the same PEG:AAT molar ratio (2:1), doubling the protein concentration from 5 mg/ml to 10 mg/ml increased the yield of mono-PEGylated AAT (by 1.8-fold) but also di-PEGylated AAT (by 2.2-fold). At 5 mg/ml, PEG:AAT molar ratios of 2:1, 4:1 and 8:1 were tested for 24-hour reaction time. As shown in Figure 3C, increasing the PEG amount led to an increased yield of mono- and di-PEGylated AAT. The yield of mono-PEGylation increased slightly when increasing the PEG:AAT molar ratio from 4:1 to 8:1, while the di-PEGylation increased tremendously. Interestingly, the yield of mono-PEGylated AAT was similar between PEG:AAT 4 :1, AAT 5mg/ml and PEG;AAT 2:1, AAT 10mg/ml, where the PEG concentration was the same. Increasing the reaction time from 24 h to 72 h did not result in higher mono-PEGylation. However, it slightly increased the di-PEGylation yield (Supplementary Figure S3). The experimental condition of 10 mg/ml AAT, PEG:AAT 2:1, reaction time 24 h were kept to produce the mono-PEGylated AAT as it presented decent yield of mono-PEGylated AAT and lower yield of side products.

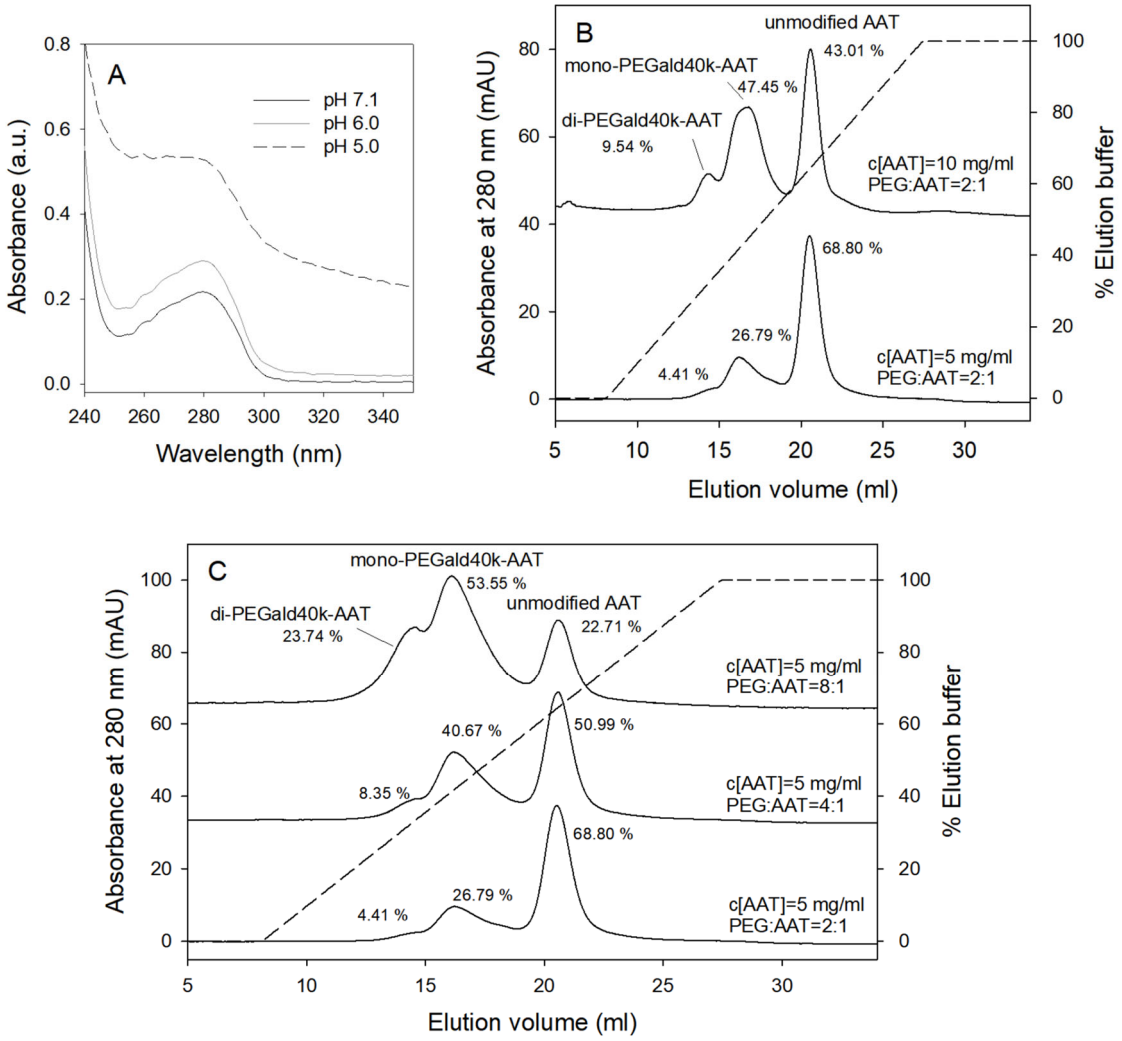

Figure 3. Optimization of N-terminal PEGylation. A) UV spectrum of AAT at different pH. At pH 5, the absorbance of AAT at 310 nm significantly increased, indicating the formation of insoluble aggregates. pH 6 was chosen for N-terminal PEGylation. B) Anion exchange chromatograms showing the effect of protein concentration on N-terminal PEGylation and C) the effect of PEG:AAT molar ratio on N-terminal PEGylation. Reactions were performed at pH 6.0 for 24 h at room temperature. Increasing PEG:AAT molar ratio or AAT concentration both led to higher PEGylation yield. However, when increasing the PEG:AAT molar ratio from 4:1 to 8:1, the mono-PEGylation yield increased slightly while the di-PEGylation yield increased tremendously.

To have a better separation/resolution, a Mono Q 4.6/100 PE column was used to purify the mono-PEGylated AAT as it has smaller particle size (10 μm) than Resource Q1 column (15 μm). Figure 4 shows the chromatograms of thiol and N-terminal PEGylation reaction mixtures, which both show better resolution than in the Resource Q1 column. The overlap between the peaks of di- and mono-PEGylated AAT was reduced for N-terminal PEGylation. Interestingly, in N-terminal PEGylation, the major peak of mono-PEGylated AAT showed a split peak. This might indicate a heterogeneity of the mono-PEGylated product. The yield of each PEGylation reaction is listed in Table 1.

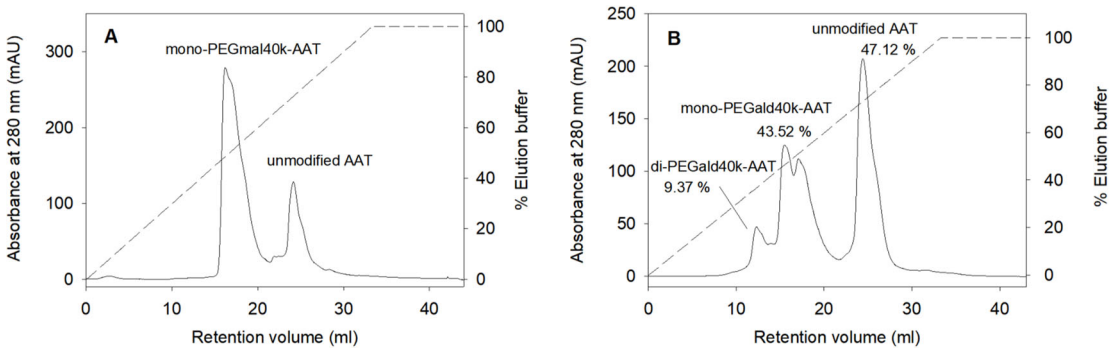

Figure 4. Anion exchange chromatograms of the PEGylation reaction mixtures using Mono Q 4.6/100 PE column. A) Thiol PEGylation; B) N-terminal PEGylation. Mono Q 4.6/100 PE column shows better resolution than the Resource Q1 column.

Table 1. PEGylation conditions and mono-PEGylation yield.

PEGylation	PEG	pH	AAT	Reducing agent	Molar ratio [PEG:AAT]	Reaction time	mono-PEGylation Yield (%)[a]
Thiol	Linear, 30 kDa	7.1	20 mg/ml	1.8 mM TCEP	4:1	1 h	63
	Linear, 40 kDa						66
	2-armed, 40 kDa						64
N-terminal	Linear, 30 kDa	6	10 mg/ml	23 μM $NaBH_3CN$	2:1	24 h	44
	Linear, 40 kDa						40
	2-armed, 40 kDa						44

[a]The yield of mono-PEGylated AAT was calculated by measuring the relative area under the peak corresponding to mono-PEGylated AAT in anion exchange chromatograms to the total surface areas of all peaks. Each reaction was performed at least twice, and the average yield is presented in the table.

The purified mono-PEGylated AAT compounds were visualized on the gel (Figure 5). The unmodified AAT (52 kDa) migrated to ~50 kDa while the PEGylated AAT showed higher apparent molecular weight (MW) compared with the theoretical MW. Linear PEGmal30k-AAT and linear PEGmal40k-AAT migrated to a MW of ~130 and ~150 kDa, respectively. 2-armed PEGmal40k-AAT migrated to even higher MW – approximately 200 kDa. The bands of linear PEGald30k-AAT and linear PEGald40k-AAT split into two separated bands (Figure 5B), which indicates an heterogeneity of these two products. This result is in line with the chromatogram of the reaction mixture of N-terminal PEGylation (Figure 4 B). We suspected that the two separated bands on the gel resulted from PEG conjugation to the alpha-amino groups of the N-terminal glutamate residue and the additional cysteine conjugated to the cysteine 232 residue. To test our hypothesis, we performed the N-terminal PEGylation using linear 30 kDa PEG-aldehyde with a prior TCEP-reduction step to remove the additional cysteine cap on the cysteine 232 residue. The mono-PEGylated products from both reactions (with or without a prior TCEP-reduction) were visualized on the gel. As shown in Figure 5C and D, without the prior TCEP-reduction, the produced mono-PEGylated AAT was degraded, and free AAT and free PEG were released upon incubation with TCEP. While with a TCEP-reduction before PEGylation, the mono-PEGylated product was stable to further reduction.

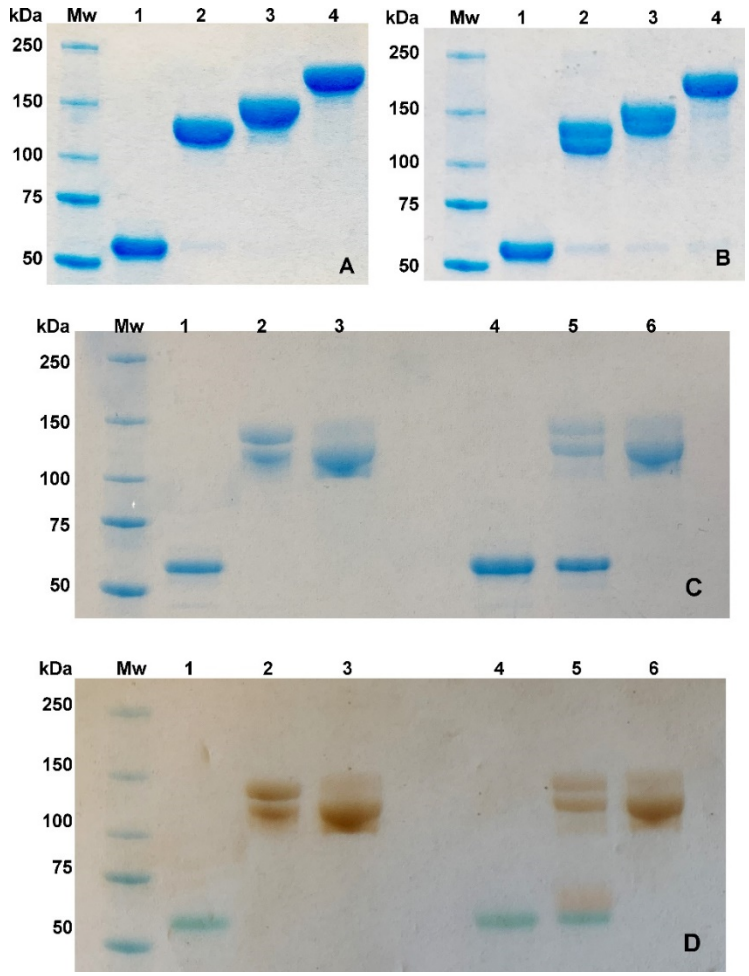

Figure 5. SDS-PAGE of AAT and PEGylated AAT stained by Coomassie blue. A) Thiol PEGylation; B) N-terminal PEGylation. Lane 1: unconjugated AAT; lane 2-4: linear PEG30k-AAT, linear PEG40k-AAT and 2-armed PEG40k-AAT. C) SDS-PAGE of purified AAT and linear PEGald30k-AAT synthesized without or with a prior TCEP-reduction, stained by Coomassie blue. Lane 1-3: purified AAT; linear PEGald30k-AAT; linear PEGald30k-AAT, TCEP-reduced before PEGylation; Lane 4-6: the same as lane 1-3 but after incubation with TCEP before loading on the gel. D) the same gel as in C but stained by barium iodine (PEG staining). With prior TCEP reduction, the mono-PEGylated AAT was stable to further reduction. Without the prior TCEP reduction, the mono-PEGylated AAT was degraded when exposed to reducing agent and released the free PEG and AAT.

III.2. PHYSICO-CHEMICAL CHARACTERIZATION OF PEG-AAT

The hydrodynamic size of PEG-maleimide, PEG-aldehyde and PEGylated AAT was analyzed by dynamic light scattering (DLS). As shown in Supplementary Table S1, PEG chains with the same molecular weight shared the same hydrodynamic diameter independently of PEG architecture. The size of unmodified AAT was 6.2 ± 0.1 nm. Upon PEGylation with linear PEG30k, the hydrodynamic size increased to 10.8 ± 0.4 nm (thiol PEGylation) and 9.6 ± 0.1nm (N-terminal PEGylation). Linear PEGmal40k-AAT and 2-armed PEGmal40k-AAT shared a similar size.

Table 2. Hydrodynamic diameter of unmodified AAT and PEGylated AAT measured by DLS

Macromolecules	Averaged size (nm)	% Volume of the main peak	PDI
AAT	6.2 ± 0.1	100	0.07 ± 0.01
Linear PEGmal30k-AAT	10.8 ± 0.4	100	0.20 ± 0.03
Linear PEGmal40k-AAT	12.9 ± 0.2	99.99	0.20 ± 0.02
2-armed PEGmal40k-AAT	12.5 ± 0.7	100	0.10 ± 0.02
Linear PEGald30k-AAT	9.6 ± 0.1	99.99	0.20 ± 0.01
Linear PEGald40k-AAT	11.9 ± 0.3	100	0.10 ± 0.01
2-armed PEGald40k-AAT	13.0 ± 0.2	100	0.20 ± 0.03

An intact protein mass spectrometry analysis was performed to determine the molecular weight of AAT and PEG-AAT. However, for both AAT and PEG-AAT, we failed to obtain reproducible results with high resolution. This might be due to the three glycosylation sites on the native protein, leading to a highly complex m/z charge distribution. Digested protein samples were analyzed by LC-MS-MSMS and a local database containing the full sequence of AAT was used for peptide matching. The peptide coverage of unconjugated AAT, thiol PEGylated AAT (linear PEGmal30k-AAT) and N-terminal PEGylated AAT (linear PEGald30k-AAT) was 71 %, 40 % and 31 %, respectively (Supplementary Table S2). The peptide sequence containing the cysteine 232 (residue 224 – 244) was found in unconjugated AAT and linear PEGald30k-AAT but not in linear PEGmal30k-AAT, indicating that the linear 30 kDa PEG-maleimide was conjugated to this site. In unconjugated AAT, the N-terminal sequence was weakly detected. This sequence was not found in linear PEGald30k-AAT (Supplementary Table S3).

III.3. BIOLOGICAL ACTIVITY, STABILITY AND BIOCOMPATIBILITY OF PEG-AAT

The elastase inhibitory activity of thiol PEGylated or N-terminal PEGylated AAT was measured and compared to unconjugated AAT (Figure 6). The PEGylated AAT fully preserved the *in vitro* anti-protease activity of the unmodified protein. A complete inhibition of elastase activity was achieved with an inhibitor:hNE molar ratio of 1:1 in both PEGylation chemistries.

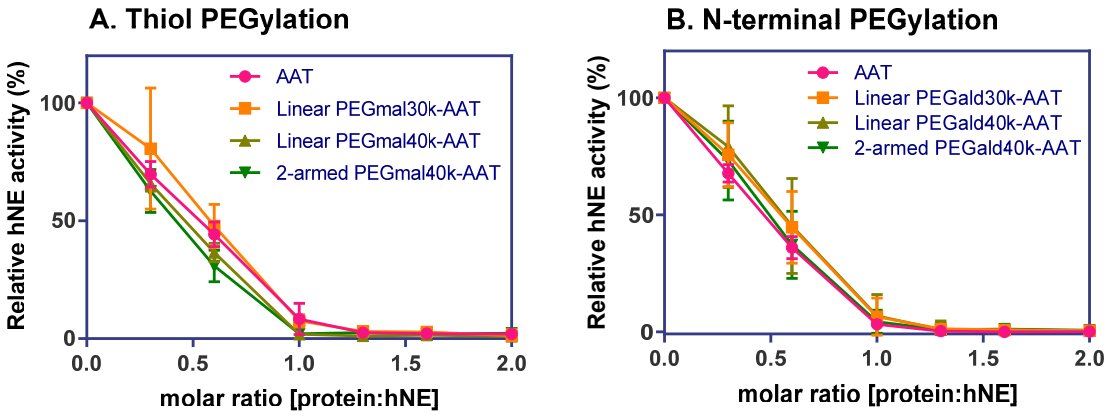

Figure 6. The elastase inhibition activity of unmodified AAT and PEGylated AAT. PEG-AAT showed the same activity as unmodified AAT. A) Thiol PEGylation; B) N-terminal PEGylation. Multiple T test and Holm-Sidak method were performed, and no statistical difference was found ($p>0.05$).

Native AAT neutralizes proteases by forming a covalent acyl AAT-protease complex [24, 25]. The complex AAT formed with hNE and PR3 was separated by native PAGE and SDS-PAGE and visualized by silver staining. Silver binds to the N-terminal or side chain amino groups. The presence of basic amino acids in proteins is essential for the success of silver staining. Unfortunately, hNE comprises no lysine [26]. Therefore, elastase is difficult to visualize by silver staining. As shown in Figure 7A and B, bands at MW higher than the free AAT compounds were observed on the gel separated by native PAGE in both unmodified AAT and thiol PEGylated AAT incubated with PR3 or hNE. This indicates that PEG-AAT preserved the ability to form the protease-inhibitor complex with PR3 and hNE. Interestingly, with SDS-PAGE, bands appeared at higher MW than the unmodified AAT but at lower MW than the PEGylated AAT following incubation with PR3 and hNE (Figure 7C, D). An hNE-specific western blot was performed to identify the AAT-hNE and PEG-AAT-hNE complexes in the SDS-PAGE. As shown in Figure 7 D and E, the faint band above the band of the unmodified AAT and the bands with lower MW than the PEG-AAT contained hNE. This suggests that the PEG-AAT-hNE complex migrated faster in the gel matrix than PEG-AAT. PEG-AAT and the PEG-AAT-hNE complexes are more difficult to transfer to the nitrocellulose membrane than hNE, AAT and AAT-hNE. When an appropriate amount of PEG-AAT and PEG-AAT-hNE complex were electroblotted to the membrane, hNE, AAT and hNE-AAT already penetrated the membrane. This is the reason why we did not detect hNE in WB and the WB band of AAT-hNE was faint.

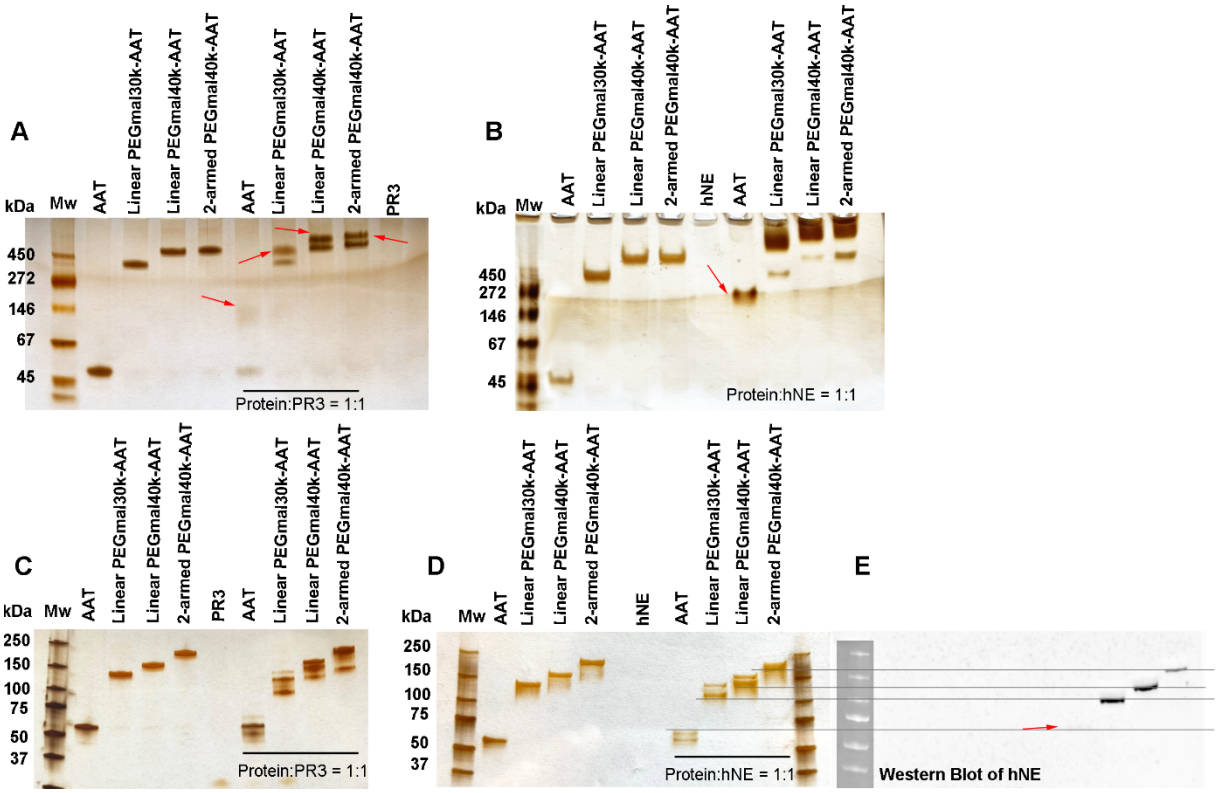

Figure 7. A) Native PAGE of purified and thiol PEGylated AAT incubated with PR3, molar ratio [protein:PR3] = 1:1. The red arrows on the gel indicate the AAT-PR3 complex; B) Native PAGE of purified and thiol PEGylated AAT incubated with hNE at a 1:1 protein:hNE molar ratio; AAT and PEG-AAT were able to form the protease-inhibitor complex with PR3 or hNE. C) SDS-PAGE of purified AAT and thiol PEGylated AAT incubated with PR3 at a 1:1 protein:PR3 molar ratio. D) SDS-PAGE of purified AAT and thiol PEGylated AAT incubated with hNE at a 1:1 protein:hNE molar ratio; E) Western Blot of hNE in AAT-hNE or PEG-AAT-hNE complexes. The original SDS-PAGE gel of E) was to the same as the gel shown in D). The bands with lower molecular weight than PEG-AAT contained hNE, indicating that the hNE-PEG-AAT complex migrates faster than PEG-AAT in SDS-PAGE.

Although PEG-AAT presents the same biological activity as AAT, we were concerned about the long-term stability of the conjugates. Therefore, the activity of AAT and PEGmal-AAT stored in solution at 4°C was monitored over a period of 24 weeks. The possible aggregation was determined by UV absorbance and SEC. During the 24 weeks of storage, the UV spectrum of AAT or PEG-AAT showed no significant change (Figure S6), indicating that there was no formation of insoluble aggregates. The monomer content of each sample monitored by SEC remained stable during 24 weeks of storage (Figure 8A). The monomer content of all protein samples on the last day of storage was not statistically different from the one on the first day of storage ($p>0.05$). Figure 8B illustrates the hNE inhibition capacity of AAT and PEG-AAT at a protein:hNE molar ratio 1:1. The elastase inhibitory activities of AAT and 2-armed PEGmal40k-AAT showed no significant changes after 24 weeks of storage, while the activity of linear PEGmal-AAT decreased ($p<0.01$). These results indicate that AAT and 2-armed PEGmal40k-AAT are stable during 24 weeks of storage, while linear PEGmal-AAT might lose some biological activity.

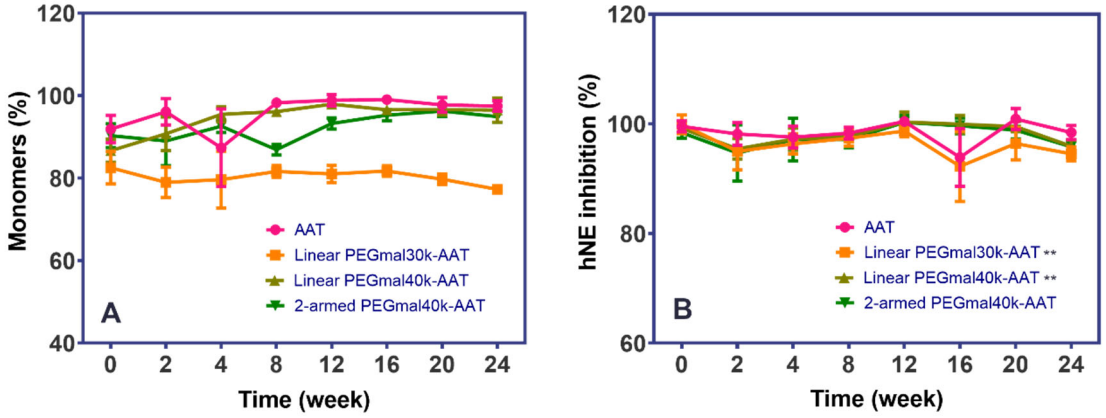

Figure 8. A) The protein monomer content of AAT and PEGmal-AAT during storage. The percentage of monomer was calculated by the area under the curve of SEC chromatograms. No significant difference was found between the results of the last day and the first day of storage. B) The hNE inhibition capacity of AAT and PEG-AAT (protein:hNE molar ratio was 1:1) during storage. The inhibitory activities of linear PEGmal30k-AAT and liner PEGmal40k-AAT on the last day of storage were significantly different from those on the first day of storage. Statistical difference was determined by one-way ANOVA using Dunnett comparison test (n=3, ** $p<0.01$).

The cytotoxicity of AAT and PEG-AAT was determined by the MTT assay. MHS cells were incubated with different concentrations of AAT or PEG-AAT for 48 hours. As shown in Figure S7, AAT and PEG-AAT did not show cytotoxicity in MHS cells. After 48 hours exposure to 2 μg/ml AAT, 2-armed PEGmal40k-AAT or 2-armed PEGald40k-AAT, the cell viability was 101 ± 5 %, 100 ± 3 % and 101 ± 7 %, respectively.

IV. DISCUSSION

In this article, we successfully PEGylated AAT at two different sites: the N-terminus and the cysteine 232. In both PEGylation chemistries, a prior reduction step was required and the AAT concentration and PEG:AAT molar ratio influenced the yield of mono-PEGylated AAT. An acidic reaction pH was essential for N-terminal selectivity in N-terminal PEGylation but the pH could not be chosen too acidic because of AAT instability. PEGylation preserved AAT biological activity and its capacity to form an inhibitor-protease complex.

The results of the hNE inhibition assay confirmed the full preservation of the biological activity of AAT upon PEGylation on either the N-terminus or the cysteine 232, which is consistent with the capacity of the PEGylated protein to form a protease complex with both PR3 and hNE. This result is in line with Cantin et al [16], who demonstrated that thiol PEGylation (using 20 and 40 kDa PEG) of rhAAT did not affect its *in vitro* elastase inhibition activity. However, protein PEGylation can actually result in a significant loss of biological activity of therapeutic proteins. Granulocyte colony-stimulating factor (G-CSF), a 19 kDa glycoprotein, showed reduced *in vitro* biological activity by 3 - to 50-fold after PEGylation, depending upon the number and sizes of the attached PEG molecules [27, 28]. However, G-CSF conjugated to 20 kDa PEG was later developed as Neulasta®, a marketed medicine to treat neutropenia, as it provides prolonged half-life, which offsets the loss of activity and leads to an overall better therapeutic value. Similarly, Pegasys®, a PEGylated interferon-α-2a, preserved only 7 % of the *in vitro* activity of the unconjugated cytokine but showed an excellent *in vivo* efficacy [29]. Therefore, the full preservation of the biological activity of AAT after PEGylation *in vitro* is promising and PEGylation might improve its *in vivo* activity even more.

Interestingly, we have noticed that the PEG-AAT-hNE complex migrated more slowly in native PAGE but faster in SDS-PAGE compared to the free PEG-AAT. Taking linear PEGmal30k-AAT as an example, the protein part of the conjugate is 52kDa, which comprises 63 % of the total MW of 82kDa. While after forming a complex with hNE, the molecular weight of the protein part in the complex (AAT+ hNE) is 81.5 kDa which accounts for 73 % of the total MW of 111.5kDa of the complex. The increase in the protein proportion in the complex appears to counterbalance the slowdown due to PEG in the electrophoretic migration rate in SDS-PAGE, probably because the negativey-charged SDS binds the protein rather than the PEG moiety.

Thiol PEGylation is commonly performed at slightly acidic or neutral pH [30] while N-terminal PEGlyation is widely performed at pH 4.5 – 6 for better selectivity [31–33]. The selectivity of N-terminal PEGylation is achieved by taking advantages of the different pKa values of the ε-amino

residue (9.3 – 9.5) of lysines and the α-amino residue (7.6 – 8.0) of the N-terminal residue [14]. At acidic pH, conjugation by nucleophilic attack favors the α-amino groups, which are less protonated compared with the ε-amino groups in the lysines. A reduction step was necessary before thiol PEGylation as the cysteine 232 in AAT is linked to another cysteine via a disulfide bond [21], making the -SH group inaccessible. Omitting the prior reduction step resulted in a low yield (14 %) for thiol PEGylation when conjugating PEG-maleimide directly to native AAT. Surprisingly, in the previous work of Cantin et al, the prior reduction step was not mentioned in the thiol PEGylation of AAT. Yet, Cantin did not report the yield of PEGylated AAT. The additional cysteine cap on the cysteine 232 residue provides another free N-terminal residue for N-terminal PEGylation. With no prior reduction, PEG-aldehyde reacted with both the amino groups on the cysteine cap and the N-terminal amine and this heterogeneous product was unstable in reducing conditions and partly degraded into free AAT and free PEG. In both PEGylation chemistries, increasing the AAT concentration or the PEG:AAT molar ratio increased the yield of mono-PEGylation. In both cases as well, prolonging the reaction time beyond a threshold did not increase the yield of mono-PEGylation as the yield of mono-PEGylation reached a plateau at 1 h (thiol PEGylation) and 24 h (N-terminal PEGylation). Between the two PEGylation chemistries, we favor thiol PEGylation for its shorter reaction time, milder reaction conditions, easier purification (no di-PEGylated products) and higher yield. Based on Guichard et al [19], we expect that the conjugation to the largest PEG already used clinically (2-armed 40kDa PEG) will best lead to prolonged AAT half-life and improved AAT therapeutic efficacy in vivo.

The PEGylation degree was mainly characterized by SDS-PAGE and DLS and confirmed the mono-PEGylation of the products. The intact protein MS analysis of AAT was unsuccessful due to its heterogeneous glycosylation profile [20, 34]. In peptide mapping, the N-terminal sequence was weakly detected in unconjugated AAT while completely absent in N-terminal PEGylated AAT. Mills et al separated 6 subspecies of AAT by isoelectric focusing and two-dimension SDS-PAGE and showed that two lacked the five N-terminal amino acid (EDPQG) [35]. In addition, the N-terminal sequence showed a weak signal and sometimes was undetectable, especially in di-glycosylated AAT [36]. These results highlight the difficulties to detect the N-terminal sequence of AAT in MS analysis. Therefore, due to the low peptide coverage as well as the technical difficulty in detecting the N-terminus of AAT, it is not fully proven that the PEG-aldehyde was indeed conjugated to the N-terminus. On the other hand, the sequence containing the cysteine 232 residue was detected in both native AAT and N-terminal PEGylated AAT, but not in thiol PEGylated AAT, which confirms that PEG-maleimide was successfully conjugated to Cys232 in thiol PEGylation and the TCEP reduction step prior to the N-terminal PEGylation prevented the conjugation to the free cysteine cap.

We produced mono-PEGylated AAT with preserved biological activity with the goal to increase the half-life of AAT following systemic or pulmonary administration. Besides the potential benefits from PEGylation, limitations of PEGylation have also been reported [15]. Anti-PEG antibodies have been detected in patients receiving PEGylated therapeutics and some of the patients displayed accelerated blood clearance or allergic reactions. Severe immunological response induced by PEGylated proteins in patients has been strongly associated with the immunogenecity of the carrier protein [37]. PEGylated non-human enzymes such as uricase (porcine enzyme) and asparaginase (*E coli* enzyme), generated severe issues because of anti-PEG antibodies, while some other PEGylated proteins were safe. In our case, we PEGylated human plasma-purified glycosylated AAT, which in theory would not exhibit high immunogenecity in patients. However, the safety of PEGylated AAT should still be fully studied. It has been reported that anti-PEG antibodies might cause rapid clearance of the PEGylated protein [15]. However, the clinical outcome of these effects is difficult to predict as it will depend on the levels of antibodies generated. To conclude, PEGylated AAT needs to be thoroughly characterized for its immunogenicity, safety, and biodistribution before considering it for clinical use.

V. CONCLUSION

PEGylation of AAT with linear 30 kDa, 40 kDa and 2-armed 40 kDa PEG was achieved by N-terminal and thiol PEGylation with satisfactory yields of mono-PEGylated products. The mono-PEG-AAT preserved the capacity to form an inhibitor-protease complex and the full biological activity of unconjugated AAT. These results support further research on PEG-AAT and in particular pharmacokinetic and therapeutic efficacy studies in preclinical in vivo models following both inhalation and intravenous injection.

VI. REFERENCES

[1] Tonelli AR, Brantly ML. Augmentation therapy in alpha-1 antitrypsin deficiency: advances and controversies. Therapeutic advances in respiratory disease 2010;4(5):289–312.

[2] Chotirmall SH, Al-Alawi M, McEnery T, McElvaney NG. Alpha-1 proteinase inhibitors for the treatment of alpha-1 antitrypsin deficiency: safety, tolerability, and patient outcomes. Therapeutics and clinical risk management 2015;11:143–51.

[3] Chapman KR, Chorostowska-Wynimko J, Koczulla AR, Ferrarotti I, McElvaney NG. Alpha 1 antitrypsin to treat lung disease in alpha 1 antitrypsin deficiency: recent developments and clinical implications. International journal of chronic obstructive pulmonary disease 2018;13:419–32.

[4] Blanco I. Alpha-1 Antitrypsin Deficiency: Liver Pathophysiology. In: Blanco's Overview of Alpha-1 Antitrypsin Deficiency: Elsevier, 2017:51–65.

[5] Brebner JA, Stockley RA. Recent advances in α-1-antitrypsin deficiency-related lung disease. Expert review of respiratory medicine 2013;7(3):213-29; quiz 230.

[6] Griese M, Scheuch G. Delivery of Alpha-1 Antitrypsin to Airways. Annals of the American Thoracic Society 2016;13 Suppl 4:S346-51.

[7] Lomas DA, Hurst JR, Gooptu B. Update on alpha-1 antitrypsin deficiency: New therapies. Journal of hepatology 2016;65(2):413–24.

[8] Brand P, Schulte M, Wencker M, et al. Lung deposition of inhaled alpha1-proteinase inhibitor in cystic fibrosis and alpha1-antitrypsin deficiency. The European respiratory journal 2009;34(2):354–60.

[9] Franciosi AN, McCarthy C, McElvaney NG. The efficacy and safety of inhaled human α-1 antitrypsin in people with α-1 antitrypsin deficiency-related emphysema. Expert review of respiratory medicine 2015;9(2):143–51.

[10] Stolk J, Tov N, Chapman KR, et al. Efficacy and safety of inhaled α1-antitrypsin in patients with severe α1-antitrypsin deficiency and frequent exacerbations of COPD. The European respiratory journal 2019;54(5).

[11] Pauwels R, Calverley P, Buist AS, et al. COPD exacerbations: the importance of a standard definition. Respiratory medicine 2004;98(2):99–107.

[12] Goldklang MP, Stearns KN, Anguiano V, Reed RM, Elkington PT, D'Armiento JM. Alpha-1 Antitryspin Inhibition of MMP-13: Implications in Acute Exacerbations of COPD. In: B61. COPD: BASIC DISCOVERY 2019:A3773-A3773.

[13] Li Z, Alam S, Wang J, Sandstrom CS, Janciauskiene S, Mahadeva R. Oxidized {alpha}1-antitrypsin stimulates the release of monocyte chemotactic protein-1 from lung epithelial cells: potential role in emphysema. American journal of physiology. Lung cellular and molecular physiology 2009;297(2):L388-400.

[14] Pasut G, Veronese FM. State of the art in PEGylation: the great versatility achieved after forty years of research. Journal of controlled release official journal of the Controlled Release Society 2012;161(2):461–72.

[15] Rondon A, Mahri S, Morales-Yanez F, Dumoulin M, Vanbever R. Protein Engineering Strategies for Improved Pharmacokinetics. Adv. Funct. Mater. 2021:2101633.

[16] Cantin AM, Woods DE, Cloutier D, Dufour EK, Leduc R. Polyethylene glycol conjugation at Cys232 prolongs the half-life of alpha1 proteinase inhibitor. American journal of respiratory cell and molecular biology 2002;27(6):659–65.

[17] Zhu W, Li L, Deng M, et al. Oxidation-resistant and thermostable forms of alpha-1 antitrypsin from Escherichia coli inclusion bodies. FEBS Open Bio 2018;8(10):1711–21.

[18] Koussoroplis SJ, Paulissen G, Tyteca D, et al. PEGylation of antibody fragments greatly increases their local residence time following delivery to the respiratory tract. Journal of controlled release official journal of the Controlled Release Society 2014;187:91–100.

[19] Guichard M-J, Wilms T, Mahri S, et al. PEGylation of Recombinant Human Deoxyribonuclease I Provides a Long-Acting Version of the Mucolytic for Patients with Cystic Fibrosis. Adv. Therap. 2021;4(2):2000146.

[20] Chen Y, Snyder MR, Zhu Y, et al. Simultaneous phenotyping and quantification of α-1-antitrypsin by liquid chromatography-tandem mass spectrometry. Clinical chemistry 2011;57(8):1161–8.

[21] Kolarich D, Turecek PL, Weber A, et al. Biochemical, molecular characterization, and glycoproteomic analyses of alpha(1)-proteinase inhibitor products used for replacement therapy. Transfusion 2006;46(11):1959–77.

[22] Kurfürst MM. Detection and molecular weight determination of polyethylene glycol-modified hirudin by staining after sodium dodecyl sulfate-polyacrylamide gel electrophoresis. Analytical Biochemistry 1992;200(2):244–8.

[23] Lestienne P, Bieth JG. The inhibition of human leukocyte elastase by basic pancreatic trypsin inhibitor. Archives of Biochemistry and Biophysics 1978;190(1):358–60.

[24] Duranton J, Bieth JG. Inhibition of proteinase 3 by alpha1-antitrypsin in vitro predicts very fast inhibition in vivo. American journal of respiratory cell and molecular biology 2003;29(1):57–61.

[25] James HL, Cohen AB. Mechanism of inhibition of porcine elastase by human alpha-1-antitrypsin. The Journal of clinical investigation 1978;62(6):1344–53.

[26] Heck LW, Darby WL, Hunter FA, Bhown A, Miller EJ, Bennett J. Isolation, characterization, and amino-terminal amino acid sequence analysis of human neutrophil elastase from normal donors. Analytical Biochemistry 1985;149(1):153–62.

[27] Kumari M, Sahni G, Datta S. Development of Site-Specific PEGylated Granulocyte Colony Stimulating Factor With Prolonged Biological Activity. Front. Bioeng. Biotechnol. 2020;8:572077.

[28] Rosendahl MS, Doherty DH, Smith DJ, Bendele AM, Cox GN. Site-Specific Protein PEGylation: Application to Cysteine Analogs of Recombinant Human Granulocyte Colony-Stimulating Factor. BioProcess international 2005;3(4):52–60.

[29] Veronese FM, Mero A. The impact of PEGylation on biological therapies. BioDrugs clinical immunotherapeutics, biopharmaceuticals and gene therapy 2008;22(5):315–29.

[30] Dozier JK, Distefano MD. Site-Specific PEGylation of Therapeutic Proteins. International journal of molecular sciences 2015;16(10):25831–64.

[31] Hu J, Sebald W. N-terminal specificity of PEGylation of human bone morphogenetic protein-2 at acidic pH. International journal of pharmaceutics 2011;413(1-2):140–6.

[32] Wu L, Ho SV, Wang W, et al. N-terminal mono-PEGylation of growth hormone antagonist: correlation of PEG size and pharmacodynamic behavior. International journal of pharmaceutics 2013;453(2):533–40.

[33] Zhao T, Yang Y, Zong A, et al. N-terminal PEGylation of human serum albumin and investigation of its pharmacokinetics and pulmonary microvascular retention. Bioscience trends 2012;6(2):81–8.

[34] Bengtson P, Valtonen-André C, Jonsson M. Phenotyping of α-1-Antitrypsin by liquid chromatography–high resolution mass spectrometry. Clinical Mass Spectrometry 2016;2:34–40.

[35] Mills K, Mills PB, Clayton PT, Johnson AW, Whitehouse DB, Winchester BG. Identification of alpha(1)-antitrypsin variants in plasma with the use of proteomic technology. Clinical chemistry 2001;47(11):2012–22.

[36] Mills K, Mills PB, Clayton PT, Mian N, Johnson AW, Winchester BG. The underglycosylation of plasma alpha 1-antitrypsin in congenital disorders of glycosylation type I is not random. Glycobiology 2003;13(2):73–85.

[37] Zhang P, Sun F, Liu S, Jiang S. Anti-PEG antibodies in the clinic: Current issues and beyond PEGylation. Journal of controlled release official journal of the Controlled Release Society 2016;244(Pt B):184–93.

VII. SUPPLEMENTARY MATERIALS

VII.1. ELECTROSPRAY-IONIZATION QUADRUPOLE TIME-OF-FLIGHT MASS SPECTROMETRY (ESI-Q-TOF)

We used the intact protein analysis to verify the PEGylation degree and the peptide mapping was performed to determine the PEGylation site.

VII.1.1. Intact proteins

For intact protein analysis, samples were diluted 2 to 10 times in 50% (v/v) acetonitrile, 0.1% formic acid depending on the quality and the intensity of the signal. To concentrate samples and to intensify the signal, samples were acidified with 1% (v/v) TFA, desalted and concentrated with C4 ZipTip® (Millipore) according to the protocol manufacturer. The fast liquid chromatography quadrupole time-of-flight mass spectrometry (LC-QTOF-MS) was performed on a SYNAPT G2-Si high definition mass spectrometer (Waters) equipped with a NanoLockSpray dual electrospray ion source (Waters). Coated fused silica PicoTip™ Econo12 Emitters for nanoelectrospray, outer diameter 1 µm Tip (New Objective, USA) were filled with 5 µl of samples and placed on the Universal NanoFlow™ Sprayer (Waters). The eluent was sprayed at a spray voltage of 2.8 k. The source temperature was set to 100 °C. The cone gas flow was 20 liters/h with a nanoflow gas pressure of 0.3 bar. MS spectra were acquired and processed with MassLynx software (Waters).

VII.1.2. Peptide mapping

VII.1.2.1. Preparation of samples

Ten µg of each protein sample was transferred to 0.5 mL polypropylene Protein LoBind Eppendorf tubes and precipitated with the chloroform-methanol method (Wessel and Flügge, 1984). Fifty µl of 100 mM triethylammonium bicarbonate (TEAB) pH 8.5 were added to the pellets for solubilisation on vortex for 30 min and by sonication at 45 kHz at room temperature with an Emmi-H40 ultrasonic bath (EMAG, Germany) for 15 min. The samples were incubated with 2500 U of N-glycosidase F (PNGase F, Biolabs, England) at 37°C overnight. Samples were dried under vacuum with a savant Speed Vac Concentrator. Fifty µl of 100 mM triethylammonium bicarbonate (TEAB), pH 8.5 was added to the pellets again followed by vortex and sonication as described above. The samples were then incubated with 0.75 mM iodoacetamide in the dark at room temperature for 30 min. With the presence of 2 M urea, 5 µg of sequencing grade trypsin (Promega, USA) was incubated with the samples at 37°C overnight. Each sample was dried under vacuum

with Savant Speed Vac Concentrator.

VII.1.2.2.Peptide separation using nanoUPLC

Before peptide separation, the samples were dissolved in 20 µl of 0.1 % (v/v) formic acid and 2% (v/v) acetonitrile (ACN). Peptide mixture was separated by reverse phase chromatography on a NanoACQUITY UPLC MClass system (Waters) working with MassLynx V4.1 (Waters) software. Two hundred nanograms of digested proteins were desalted on a trap C18, 100Å 5 µm, 180 µm x 20 mm column (Waters) and eluted using isocratic conditions with a flow rate of 15 µl/min, using a 99 % formic acid and 1% (v/v) ACN buffer for 3 min. The desalted peptide mixture was then separated by reverse phase chromatography on a C18, 100Å 1.8 µm, 75 µm x 150 mm column (Waters) PepMap at 35°C for 35 min with a flow rate of 300 nl/min, using a two-part linear gradient from 1% (v/v) ACN, 0.1 % formic acid to 35 % (v/v) ACN, 0.1 % formic acid and from 35% (v/v) ACN, 0.1 % formic acid to 85 % (v/v) ACN, 0.1 % formic acid. The column was re-equilibrated at initial conditions after washing 10 min at 85% (v/v) ACN, 0.1 % formic acid with a flow rate of 300 nL/min. For online LC-MS analysis, the nanoUPLC was coupled to the mass spectrometer through a nano-electrospray ionization (nanoESI) source emitter.

VII.1.2.3. LC-QTOF-MS/MS Analysis

Data Dependent Analysis (DDA) was performed on an SYNAPT G2-Si high-definition mass spectrometer (Waters) equipped with a NanoLockSpray dual electrospray ion source (Waters). Precut fused silica PicoTip^{R} Emitters for nanoelectrospray (outer diameters: 360 µm; inner diameter: 20 µm; 10 µm tip); 2.5" length (Waters) was used for samples and Precut fused silica TicoTip^{R} Emitters for nanoelectrospray (outer diameters: 360 µm; inner diameter: 20 µm; 2.5" length, Waters) were used for the lock mass solution. The eluent was sprayed at a spray voltage of 2.8 kV with a sampling cone voltage of 25 V and a source offset of 30 V. The source temperature was set to 80 °C. The cone gas flow was 20 liters/h with a nanoflow gas pressure of 0.4 bar and the purge gas was turned off. The SYNAPT G2Si instrument was operated in DDA, automatically switching between the first spectrometer (MS) and the second spectrometer (MS2). Full scan MS and MS2 spectra (m/z 400 - 2000) were acquired from 2 min to 30 min after injection in resolution mode (20,000 resolution FWHM at m/z 400) with a scan time of 0.1 sec. Tandem mass spectra of up to 10 precursors were generated in the trapping region of the ion mobility cell by using a collision energy ramp from 17/19 V (low mass, start/end) to up to 65/75 V (high mass, start/end). Charged ions (+2, +3, +4) were selected to be submitted to the MSMS fragmentation over the m/z range from 50 to 2000 with a scan time of 0.25 sec. For the post-acquisition lock mass correction of the data in the MS method, the doubly charged monoisotopic ion of [Glu^{1}]-fibrinopeptide B was used

at 100 fmol/µl using the reference sprayer of the nanoESI source with a frequency of 30 s at 0.5 µl/min into the mass spectrometer.

VII.1.2.4.ESI-QTOF data processing

Data were processed with Progenesis QI (Nonlinear DYNAMICS, Waters) and with an in-house MASCOT software server (Matrix Science, USA) using a local protein database containing sequences of interest. Propionamide as the fixed cysteine modification, oxidation as the variable methionine modification, trypsin as the digestion enzyme were selected and one miss cleavage allowed. Tolerances of 10 ppm on precursors and 0.1 Da on fragments were applied.

VII.2. FIGURES AND TABLES

Table S1. Hydrodynamic diameter of PEG molecules.

Macromolecules	Averaged size (nm)	% Volume of the main peak	PDI
Linear PEGmal30k	9.4 ± 0.1	100	0.20 ± 0.03
Linear PEGmal40k	11.5 ± 0.1	100	0.10 ± 0.02
2-armed PEGmal40k	11.5 ± 0.3	100	0.08 ± 0.01
Linear PEGald30k	9.5 ± 0.3	100	0.20 ± 0.01
Linear PEGald40k	11.0 ± 0.3	100	0.10 ± 0.03
2-armed PEGald40k	11.0 ± 0.1	100	0.10 ± 0.01

Table S2. Protein sequence coverage of peptide mapping analysis for AAT and PEGmal-AAT.

Number	Amino acid Sequence				
1-50	EDPQGDAAQK	TDTSHHDQDH	PTFNKITPNL	AEFAFSLYRQ	LAHQSNSTNI
51-100	FFSPVSIAAA	FAMLSLGAKG	DTHDEILEGL	NFNLTEIPEA	QIHEGFQELL
101-150	RTLNQPDSQL	QLTTGNGLFL	SEGLKLVDKF	LEDVKKLYHS	EAFTVNFGDT
151-200	EEAKKQINDY	VEKGTQGKIV	DLVKELDRDT	VFALVNYIFF	KGKWERPFEV
201-250	KDTEEEDFHV	DQVTTVKVPM	MKRLGMFNIQ	HCKKLSSWVL	LMKYLGNATA
251-300	IFFLPDEGKL	QHLENELTHD	IITKFLENED	RRSASLHLPK	LSITGTYDLK
301-350	SVLGQLGITK	VFSNGADLSG	VTEEAPLKLS	KAVHKAVLTI	DEKGTEAAGA
351-394	MFLEAIPMSI	PPEVKFNKPF	VFLMIEQNTK	SPLFMGKVVN	PTQK

The sequence coverage of unconjugated AAT and linear PEGmal30k-AAT was 70 % and 40 %, respectively. The peptides found in both AAT and linear PEGmal30k-AAT are marked green, while the peptides found only in unconjugated AAT are marked blue. The thiol PEGylation site (the single cysteine 232) is in bold red and underlined. The peptide sequence containing the cysteine 232 was found in unconjugated AAT but not in linear PEGmal30k-AAT, indicating that the 2-armed 40 kDa PEG-maleimide was conjugated at this site.

Table S3. Protein sequence coverage of peptide mapping analysis for AAT and PEGald-AAT.

Number	Amino acid Sequence				
1-50	EDPQGDAAQK	TDTSHHDQDH	PTFNKITPNL	AEFAFSLYRQ	LAHQSNSTNI
51-100	FFSPVSIAAA	FAMLSLGAKG	DTHDEILEGL	NFNLTEIPEA	QIHEGFQELL
101-150	RTLNQPDSQL	QLTTGNGLFL	SEGLKLVDKF	LEDVKKLYHS	EAFTVNFGDT
151-200	EEAKKQINDY	VEKGTQGKIV	DLVKELDRDT	VFALVNYIFF	KGKWERPFEV
201-250	KDTEEEDFHV	DQVTTVKVPM	MKRLGMFNIQ	HCKKLSSWVL	LMKYLGNATA
251-300	IFFLPDEGKL	QHLENELTHD	ITKFLENED	RRSASLHLPK	LSITGTYDLK
301-350	SVLGQLGITK	VFSNGADLSG	VTEEAPLKLS	KAVHKAVLTI	DEKGTEAAGA
351-394	MFLEAIPMSI	PPEVKFNKPF	VFLMIEQNTK	SPLFMGKVVN	PTQK

The sequence coverage of unconjugated AAT and linear PEGald30k-AAT was 70 % and 31 %, respectively. The peptides found in both AAT and linear PEGald30k-AAT are marked green, while the peptides found only in unconjugated AAT are marked blue. The single cysteine 232 is in bold red and underlined. In linear PEGald30k-AAT, the N-terminal sequence was not found.

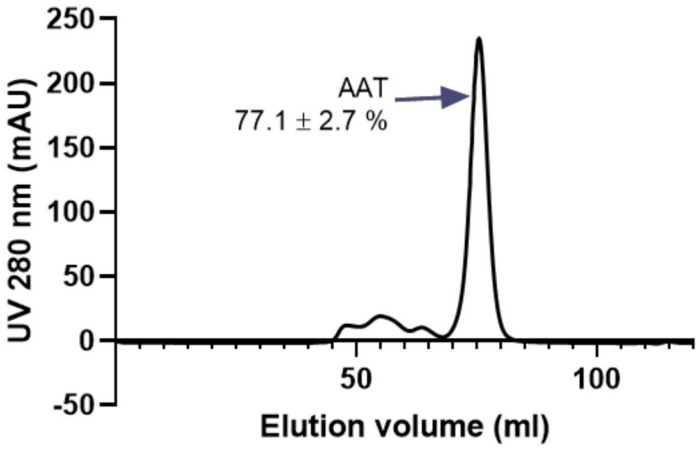

Figure S1. Size exclusion chromatogram of Pulmolast® purification. The area under the peak of AAT comprised 77.1 ± 2.7 % of the total areas under the peaks.

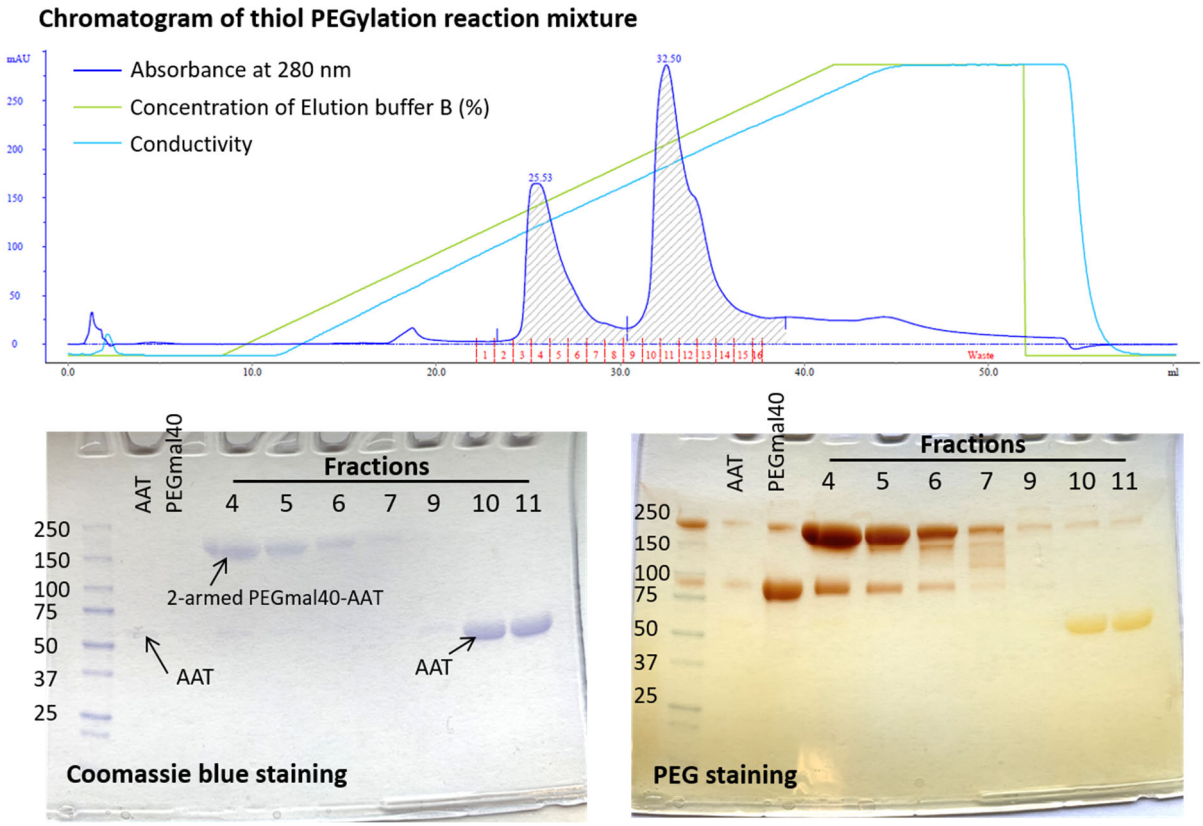

Figure S2. SDS-PAGE of AEC purification fractions of thiol PEGylation reaction mixture, followed by iodine (PEG) staining and Coomassie blue (protein) staining. The first peak (fractions 3 – 8) corresponds to 2-armed PEGmal40-AAT and the second peak (fractions 10 – 14) corresponds to unmodified AAT. The reaction conditions were: AAT 10 mg/ml, PEG:AAT molar ratio 4:1, in 10 mM NaH_2PO_4 and 110 mM NaCl, pH 7.1, at room temperature with mild agitation for 1 hour. Prior to PEGylation, AAT was reduced by tris(2-carboxyethyl) phosphine (TCEP) at a molar ratio of TCEP:AAT 4:1 in the same buffer.

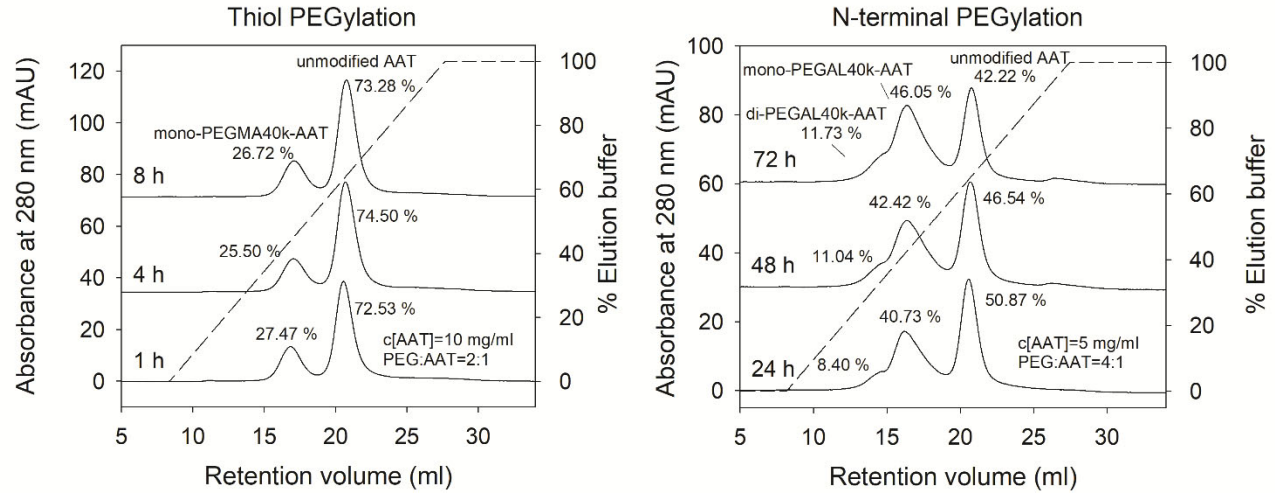

Figure S3. The effect of reaction time on thiol and N-terminal PEGylation. The reaction conditions not mentioned in the figure were pH 7.1 for thiol PEGylation and pH 6.0 for N-terminal PEGylation, both at room temperature. In thiol PEGylation, the AAT was reduced by 4-fold molar excess of TCEP prior the reaction for 1 h. The column used in AEC was Resource Q1.

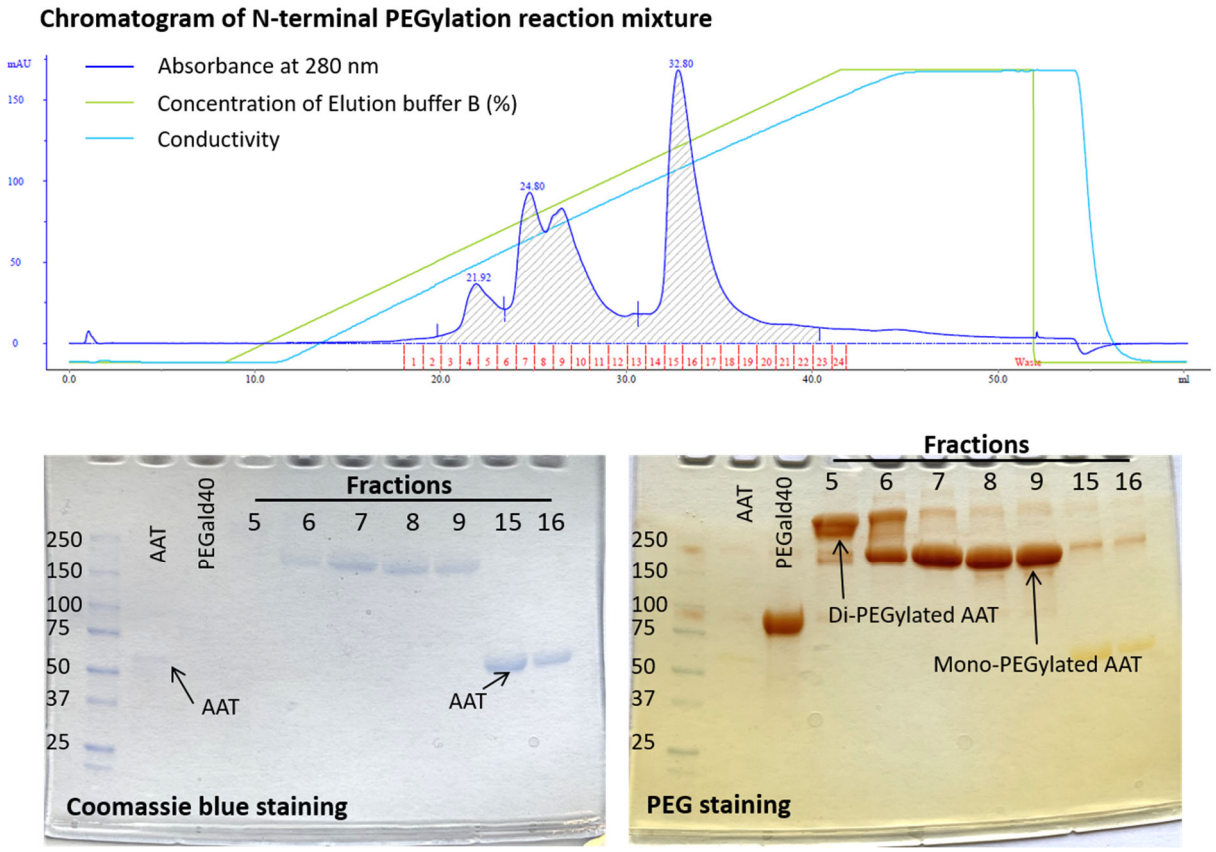

Figure S4. SDS-PAGE of AEC purification fractions of N-terminal PEGylation reaction mixture, followed by iodine (PEG) staining and Coomassie blue (protein) staining. The first peak (fractions 3 – 6) corresponds to di-PEGylated AAT, the second peak (fractions 7 – 11) corresponds to mono-PEGylated AAT and the third peak (fractions 15 – 18) corresponds to unmodified AAT. The reaction conditions were: AAT 5 mg/ml, PEG:AAT molar ratio 4:1, in 20 mM succinate buffer, pH 6, in presence of 120-fold molar excess (11.5 μM) of sodium cyanoborohydride ($NaCNBH_3$) with mild agitation for 24 hours.

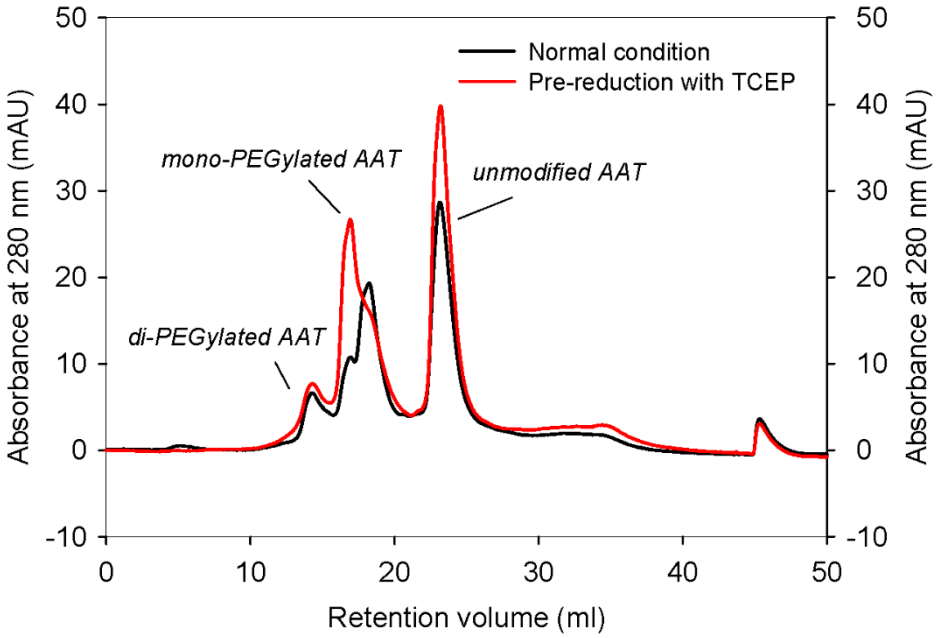

Figure S5. The influence of a pre-TCEP-reduction on N-terminal PEGylation. The reactions were carried out with linear PEGald 30kDa. The reaction conditions were: AAT 10 mg/ml, PEG:AAT molar ratio 2:1, in 20 mM succinate buffer, pH 6, in presence of 120-fold molar excess (11.5 μM) of sodium cyanoborohydride (NaCNBH3) with mild agitation for 24 hours. The pre-reduction condition was: tris(2-carboxyethyl) phosphine (TCEP) at a molar ratio of TCEP:AAT 4:1 in 10 mM NaH2PO4 and 110 mM NaCl, pH 7.1, at room temperature with mild agitation for 1 hour. The column used for AEC was Mono Q 4.6/100 PE column.

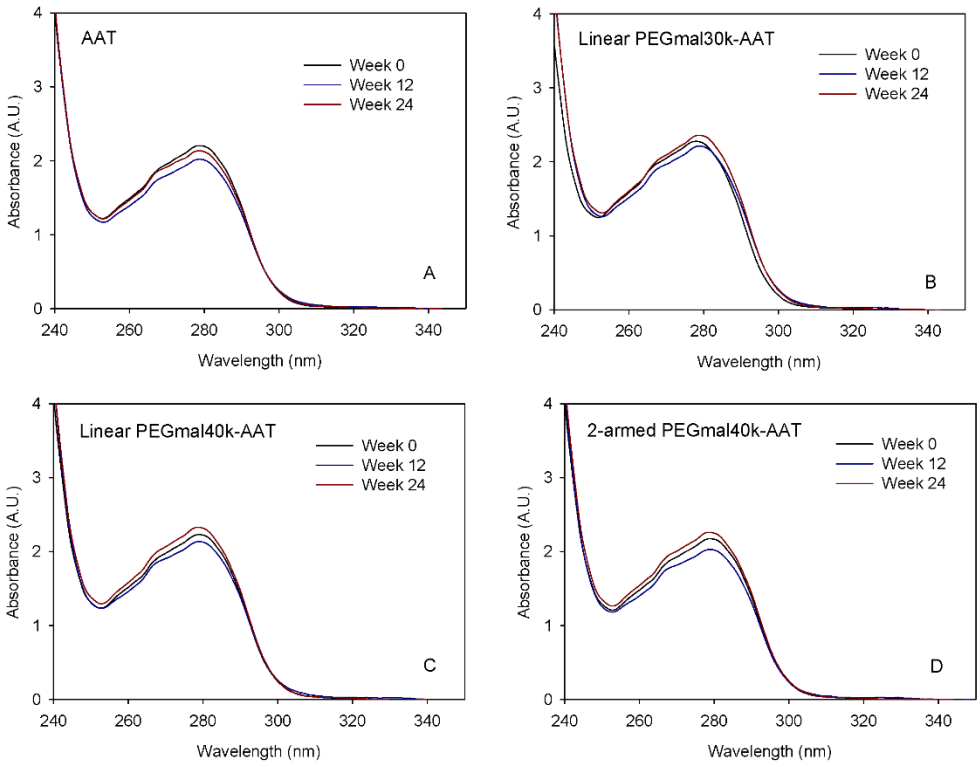

Figure S6. The UV spectrum of AAT and PEG-AAT during storage. The spectrum of each sample after 12- and 24-week of storage showed no significant changes, indicating that there was no significant formation of insoluble aggregates.

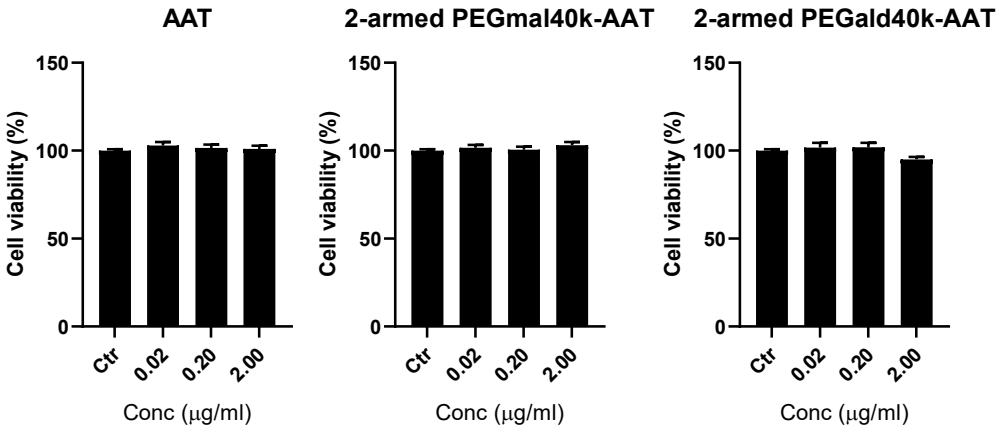

Figure S7. Cytotoxicity of AAT, thiol PEGylated AAT and N-terminal PEGylated AAT in MHS cells. No significant difference was found between control and treated cells, indicating that AAT and PEG-AAT did not induce toxicity in MHS cells at concentrations up to 2 g/ml. Statistical analysis was performed by two-way ANOVA with Dunnett comparison post-test.

VII.3. REFERENCES

Wessel, D., Flügge, U.I., 1984. A method for the quantitative recovery of protein in dilute solution in the presence of detergents and lipids. Analytical Biochemistry 138 (1), 141–143.

CHAPTER III

IMPACT OF THE PEG LENGTH AND PEGYLATION SITE ON THE STRUCTURAL, THERMODYNAMIC AND THERMAL STABILITY OF MONO-PEGYLATED ALPHA-1 ANTITRYPSIN

Adapted from

Liu X, Guy Wilfried Kouassi K, Vanbever R, Dumoulin M. Impact of the PEG length and PEGylation site on the structural, thermodynamic and thermal stability of mono-PEGylated alpha-1 antitrypsin. Submitted to Prot Sc.

ABSTRACT

Conjugation to polyethylene glycol (PEG) is a widely used approach to improve the therapeutic value of proteins essentially by prolonging their body residence time. PEGylation may however induce changes in the structure and/or the stability of proteins and thus on their function(s). The effects of PEGylation on the thermodynamic stability can either be positive (stabilization), negative (destabilization) or neutral (no effect). Moreover, various factors such as PEG length and PEGylation sites can influence the consequences of PEGylation on the structure and stability of proteins. The mechanism underlying the effects of PEGylation on protein structure and stability remains however unclear. In this study, the effects of PEGylation on the structure, stability and polymerization of alpha1-antitrypsin (AAT) were investigated, using PEGs with different lengths, different structures (2-armed or not) and different linking chemistries (via amine or thiol) at two distinct positions of the sequence. The results obtained show that whatever the size, position, and structure of PEG chains, PEGylation (i) does not induce significant changes in the AAT structure (either at the secondary or tertiary level); and (ii) does not alter the stability of the native protein upon both chemical- and heat-induced denaturation. The propensity of AAT to aggregate upon heat treatment was however significantly decreased by PEGylation, although it does not prevent the irreversible inactivation of the enzyme. Specifically, conjugation of a 2-armed 40 kDa PEG to the cysteine232 residue resulted in a better resistance to heat-induced polymerization. This systematic study highlights the importance of PEG size, structure and PEGylation site on the properties of proteins.

KEYWORDS

PEGylation, alpha-1 antitrypsin (AAT), thermodynamic stability, heat-induced aggregation, inhibition of aggregation, proteolysis

TABLE OF CONTENTS

I. INTRODUCTION

Alpha-1 antitrypsin (AAT) is a serine protease inhibitor, which is predominantly expressed by hepatocytes and then diffuses into the circulation [1]. Its primary site of action is the lung, where it provides a protection against serine proteases such as neutrophil elastase (NE) [2], proteinase-3 (PR-3) [3]and cathepsin G [4]. Moreover, deficiency in AAT, which is associated with mutations in the *SERPINA1* gene, can result in various diseases including hepatic disease, emphysema and chronic obstructive pulmonary disease (COPD) [1]. The major approach to treat pulmonary disease associated with AAT deficiency is the weekly intravenous infusion of human AAT. However, a high dose (60 mg/kg/week) is mandatory to maintain the efficacious serum level of AAT (>11 μM) , which results in high expenses [5]. Moreover, in a phase II/III clinical trial involving AAT deficiency patients with severe COPD and frequent exacerbations, a twice-daily inhalation of 80 mg of AAT for 50 weeks did not prolong the time to exacerbation, but it significantly reduced symptomatic Anthonisen type I exacerbations [6]. Our hypothesis to explain this limited efficacy of inhaled AAT, is its rapid clearance caused by a combination of a proteolytic breakdown, the oxidation of methionine358 belonging to the reactive center loop (RCL) and a phagocyte uptake [6]. Hence, it is necessary to develop AAT derivatives presenting longer residency time following both intravenous and pulmonary administration, as it will improve the efficacy of therapy, reduce the administration frequency, and increase the patience compliance.

Polyethylene glycol (PEG) is one of the most popular polymers for protein conjugation [7]. Several PEGylated proteins have been approved by FDA and EMA in the pharmaceutical market [8]. The conjugation of PEG chains to proteins can prolong their serum half-life by decreasing the kidney clearance, it can also reduce the immunogenic response of the target proteins and protect them from the action of proteases [9]. Despite the advantages of PEGylation on therapeutic proteins, one concern is the reduction in their biological activity and/or stability upon PEGylation. Although the reduced activity could be compensated by the prolonged serum half-life in some cases [10, 11], it is still of great interest for researchers to maintain the activity of the therapeutic protein after PEGylation.

Various factors such as the PEG length, and the PEGylation site can influence the effects of PEGylation on the stability and biological activity of a protein, which might result from conformational changes at the level of tertiary and secondary structures and/or from the steric hindrance of the conjugated PEG [12]. Thermodynamically destabilized proteins tend to more easily populate unfolded states which are generally devoid of activity and prone to aggregation [13]. Therefore, a preserved or improved thermodynamic stability is preferred after PEGylation. So far,

the impact of PEGylation on thermodynamic stability of a protein is not yet thoroughly investigated. PEGylation can either stabilize or destabilize a protein, or sometimes have no effect [14–19]. Some researchers predicted the impact of PEGylation site on the conformational stability of the protein using molecular dynamic (MD) simulations [20, 21]. However, predictions were only verified on small peptides conjugated to short PEG chains.

The molecular mechanism of the effects from PEG addition to the protein properties remains unclear. The different impacts of PEGylation on protein structure and/or stability may result, at least in part, from the strategy used to carry out the PEGylation. Indeed, the size of PEG chains, the site of PEGylation and the linking chemistry may contribute to the consequences of PEG addition on the structure and/or stability of the protein. Therefore, the aims of this study were to compare the overall structure, thermodynamic stability, and aggregation propensity of PEGylated AAT using PEGs with different lengths and different linking chemistries at two separated sites, on the properties of the protein. The results obtained indicated that whatever the size of the PEG and the site of conjugation, PEGylation had no effect on the structure and stability of the protein. On the other hand, the PEG size and PEGylation site, had a significant effect on the protection conferred to the protein against heat-induced aggregation. Conjugation of a 2-armed 40 kDa PEG to the cysteine232 residue resulted in the best resistance to heat-induced polymerization.

II. MATERIAL AND METHODS

II.1. MATERIAL

The wild type AAT was purified by size exclusion chromatography (SEC) from a commercial human AAT product – Pulmolast®. The linear 30 kDa, 40 kDa and 2-armed 40 kDa PEG-maleimide and linear 30 kDa, 40 kDa and 2-armed 40 kDa PEG-aldehyde were purchased from NOF Europe GmbH. Guanidinium chloride (GdmCl) (>99 %) and 8-anilino-1-naphtalene-sulfonic acid (ANS) were purchased from Sigma Chemical Co. The human sputum elastase (hNE) and the substrate N-Succinyl-Ala-Ala-Ala-pNitroanilide were purchased from Elastin Products Company, Inc. The other reagents, if not mentioned specifically, were from Sigma-Aldrich, Inc.

II.2. PRODUCTION AND PURIFICATION OF MONO-PEGYLATED AAT

The synthesis of mono-PEGylated AAT was performed as described previously [22]. Unlike in thiol PEGylation, the prior reduction step was not included in N-terminal PEGylation. Briefly, a 2-armed PEG-aldehyde (2-armed PEGAL40k) was used in N-terminal PEGylation which was carried out in 20 mM succinate buffer, pH 6, in the presence of 11.5 μM of sodium cyanoborohydride ($NaCNBH_3$). The concentration of AAT in the reaction mixture was 10 mg/ml and the molar ratio of PEGAL to AAT was 2:1. The reaction was carried out overnight with mild agitation at room temperature. Linear or 2-armed PEG-maleimide of 30 kDa or 40 kDa (linear PEGMA30k, PEGMA40k and 2-armed PEGMA40k) was used for thiol PEGylation on the unique cysteine residue (Cys232), the purified AAT was first reduced by 1.5 μM tris(2-carboxyethyl) phosphine (TCEP) and then incubated with PEGMA for 1 hour with mild agitation in 10 mM NaH_2PO_4, 110 mM NaCl, pH 7.1; both steps were carried out at room temperature. The PEGylation sites of both reactions are shown in Fig 1.

The mono-PEGylated AAT was purified by anion exchange chromatography (AEC) using a Mono Q 4.6/100 PE column (GE Healthcare Bio-Sciences AB, Uppsala, Sweden). With the start buffer 20 mM $N(CH_2CH_2OH)_3$, 5 mM NaCl, pH 7.5 and the elution buffer 20 mM $N(CH_2CH_2OH)_3$, 250 mM NaCl, pH 7.5, a salt gradient elution was performed. The collected fractions were analyzed by SDS-PAGE followed by silver staining, and the fractions containing the mono-PEGylated AAT were pooled and concentrated using VIVASPIN 15R sample concentrator (10,000 molecular weight cut-off, Sartorius).

II.3. CHEMICAL-INDUCED UNFOLDING

II.3.1. Preparation of samples

The protein concentration was determined by the absorbance at 280 nm where PEG has no signal contribution, using Beer-Lambert Law with the extinction coefficient of 19940 $M^{-1}cm^{-1}$ [23]. Samples containing 0.15 mg/ml AAT or PEGylated AAT in DPBS buffer were incubated overnight at 25 °C in the presence of various concentrations of GdmCl; the GdmCl concentration of each sample was determined by a R5000 refractometer from Atago (Japan) using a refractive index measurement [24]. The same samples were used for intrinsic fluorescence and circular dichroism (CD) measurements. Afterwards, aliquots of the same samples were incubated with 20-folds molar excess of ANS for ANS-bound fluorescence measurements.

II.3.2. Intrinsic fluorescence measurements

The intrinsic fluorescence spectra were recorded at 25 °C using a Cary Eclipse fluorescence spectrophotometer equipped with a Peltier cell holder (Varian, Palo Alto, CA, USA), using a 0.4*1cm pathlength quartz micro-cuvette. The excitation and emission slit widths were both 5 nm and a low scan speed (120 nm/min) was used. The high voltage on the photomultiplicator (PMT) was 870 V. The excitation wavelength was 280 nm, and the emission spectra were recorded between 300-460 nm.

The unfolding kinetics study of AAT was carried out as follows: twenty microliters of 1 mg/ml AAT solution was placed in a 0.4*1cm pathlength quartz micro-cuvette; 180 µl DPBS or DPBS solution containing 1, 2, 3, 4 and 5 M of GdmCl were added to the cuvette; immediately after mixing the solution, the fluorescence intensity at 350 nm was recorded every 0.1 min for 30 min following excitation at 280 nm; the excitation and emission slit widths were 5 nm, the high voltage on the PMT was 870 V.

II.3.3. Far UV-CD measurements

CD signals were recorded with a J-810 spectropolarimeter equipped with a Peltier cell holder (Jasco International Co., Ltd, Tokyo, Japan) using a 1-mm pathlength quartz cuvette. The spectra were recorded at 25 °C from 190 nm to 250 nm, with a scan speed of 50 $nm \cdot min^{-1}$, 1-nm bandwidth and a 2-s integration time. Five spectra were recorded, averaged and corrected from the contribution of the buffer alone. For GdmCl-induced unfolding, the CD signal at 222 nm was recorded for every 5 s for 5 min at 25 °C, with a 1-nm bandwidth and a 4-s integration time. The thirty-six values obtained were averaged and corrected from the contribution of the buffer recorded under the same

conditions.

II.3.4. ANS-bound fluorescence measurements

The ANS-bound fluorescence spectra were recorded using the same conditions as above for intrinsic fluorescence except that the excitation wavelength was 350 nm, and the emission spectra were recorded between 400 - 660 nm. The fluorescence intensity at 480 nm (corrected from the contribution of the buffer and GdmCl) was used to monitor the transitions.

II.3.5. Analysis of the data

The chemically induced unfolding curves were monitored by the fluorescence intensity at 330, 336 and 360 nm, as well as the wavelength of the maximum fluorescence (λ_{max}), determined from fitting each spectrum with a Weibull five parameters equation model from SigmaPlot 12 (SPSS Inc.) and CD signal at 222 nm at 25 °C corrected form the contribution of the buffer alone.

The thermodynamic parameters were computed on the assumption of a three-state model for the unfolding reaction (N ⇋I⇋U). The transition curves were analyzed according to the following equation [25]:

$$F = \frac{(F_{N_0}+p[D])+(F_{I_0})\times e^{-\alpha}+(F_{U_0}+q[D])\times e^{-\alpha}e^{-\beta}}{1+e^{-\alpha}+e^{-\alpha}e^{-\beta}} \quad (1)$$

Where $\alpha = \frac{\Delta G^{\circ}_{NI(H2O)}-m_{NI}[D]}{RT}$, $\beta = \frac{\Delta G^{\circ}_{IU(H2O)}-m_{IU}[D]}{RT}$,

and where F is the measured parameter (i.e., fluorescence intensity or far UV-CD signal) at a given GdmCl concentration. F_{N_0}, F_{I_0} and F_{U_0} represent the values of this parameter for the native (N), intermediate (I) and unfolded (U) states, in the absence of denaturant, respectively. $\Delta G^{\circ}_{NI(H2O)}$ and $\Delta G^{\circ}_{IU(H2O)}$ are the difference in free energy between N and I, I and U states, respectively. And m_{NI} and m_{IU} are the measures of the dependence of the free energy on the denaturant concentration. [D] is the denaturant concentration. And p, and q are the slopes of the pre-transition, and post-transition baselines, respectively. R is the gas constant, and T is the absolute temperature. Cm_{NI} and Cm_{IU}, the denaturant concentration at the midpoint of each transition and are defined as $\Delta^{\circ}G_{NI\ (H2O)}/m_{NI}$ and $\Delta^{\circ}G_{IU\ (H2O)}/m_{IU,}$ respectively. GraFit 3.09 (Erithacus software Ltd.) and Sigmaplot 12.0 (SPSS Inc.) were used to perform the non-linear fit of the data.

II.4. HEAT-INDUCED UNFOLDING

II.4.1. Fluorescence measurements

For intrinsic fluorescence measurements, samples containing 0.15 mg·ml^{-1} AAT or PEGylated AAT were prepared in DPBS buffer at 25 °C. A 1-cm pathlength quartz cuvette was used and mineral oil was added on top of the protein solution surface in order to prevent evaporation. The temperature was linearly increased from 25 °C to 95 °C at 0.5 °C·min^{-1}. The excitation wavelength was 280 nm and the fluorescence intensity at 324 nm was recorded every 0.5 °C. The excitation and emission slit widths were 5 nm. The high voltage on the PMT was 870 V. The actual temperature inside the sample was recorded using a thermo-couple (PT200 differential thermometer, IMPO Electronics). For ANS-bound fluorescence, the measurement parameters were the same as the ones for intrinsic fluorescence except that the excitation wavelength was 350 nm and the monitored emission wavelength was 480 nm.

II.4.2. Size exclusion chromatography (SEC)

Samples containing 0.15 mg·ml^{-1} AAT or PEGylated AAT in DPBS buffer were incubated at 70 °C for 1 hour and then cooled down to room temperature. The heating temperature was selected based on the following observations made by Lomas et al [26] : (i) AAT in sodium citrate only partially losses its activity when incubated at temperature below 70 °C for 24 h; (ii) AAT tends to remain monomeric until 70 °C. Prior to the SEC analysis, to remove the large aggregates, the samples were filtered through a 0.22 μm membrane. Samples were analyzed on a Superose 6 Increase 10/300 column (GE Healthcare Bio-Sciences AB, Uppsala, Sweden). The relative content of the monomeric protein was calculated from the peak integration from the chromatograms. The chromatograms of the control samples were indicated in dark blue while the heated samples were indicated in red.

II.4.3. Dynamic Light Scattering measurements (DLS)

Samples containing 1 mg·ml^{-1} AAT or PEGylated AAT in DPBS buffer at 25 °C were analyzed in a 1 cm square glass cuvette by Malvern Zetasizer Ultra (Sysmex Belgium) and mineral oil was added on top of the protein solution to prevent evaporation. The temperature was linearly increased from 25 °C to 95 °C at 0.5 °C/min. The hydrodynamic diameters were measured three times every 3 degrees.

II.4.4. Data analysis

The thermal unfolding curves monitored by the intrinsic fluorescence and ANS-bond fluorescence, were analyzed on the assumption of a two-state transition model using the following equation [27]:

$$F = \frac{(F_N + p[T]) + (F_U + q[T]) \times e^a}{1 + e^a} \quad (2)$$

Where $a = \frac{-\Delta H_m (1 - \frac{[T]}{T_m})}{RT}$,

And where F is the measured variable parameter, F_N and F_U represent the values of this parameter for the native (N) and unfolded (U) states at 273 K. [T] is the measured temperature in Kelvin. p and q are the slopes of the pre-transition and post-transition baselines. R is the gas constant and T is the absolute temperature. T_m is the temperature of mid-transition and ΔH_m is the enthalpy value at T_m. The fluorescence data above 70 degrees were excluded due to the presence of aggregates in the samples. Since the transitions were not reversible, only the apparent T_m was considered for the analysis. GraphPad Prism 8 (GraphPad Software, USA) were used to perform the non-linear fit of the data.

II.5. HUMAN ELASTASE INHIBITION ASSAY

The activity of native, refolded or denatured AAT and PEGylated AAT were determined by monitoring their ability to inhibit the activity of human elastase purified from sputum (hNE).

The refolded proteins were prepared as follows: AAT or PEGylated AAT were incubated with 6.9 M GdmCl for at least 2 h to assure the full unfolding of the proteins. Afterwards, a microdialysis [28] in DPBS was performed to remove >99.9 % of the GdmCl. The fluorescence spectrum of the refolded samples was recorded to confirm the refolded state of the proteins.

The activity of hNE was measured according to Bieth [29]. Briefly, 0.17 µM hNE was incubated with 1.51 mM substrate N-Succinyl-Ala-Ala-Ala-pNitroanilide (Tris-NaCl buffer, pH 7.5) in a 96-well plate for 20 min at 37 °C. Afterwards, 0.17 µM of refolded or heated AAT or PEGylated AAT samples were added to the mixture and incubated for 40 min. During the incubation, the optical density at 410 nm (OD410) of each sample was recorded every 1 min. The changes in OD410 after adding AAT or PEGylated AAT were used to quantify the hNE activity and the relative hNE activity was calculated using the changes in OD410 for hNE alone as control.

III. RESULTS

III.1. CHEMICAL INDUCED UNFOLDING TRANSITIONS OF AAT

According to the unfolding kinetic studies of AAT denaturation at different concentrations of GdmCl, the equilibrium is reached within 10 min. To ensure that the equilibrium is reached at all concentrations, all the GdmCl-induced unfolding samples were incubated overnight at 25°C before being analyzed.

The fluorescence spectrum of native AAT shows a wavelength of maximum fluorescence (λ_{max}) at around 330 nm (Fig 2A insert), indicating that the two tryptophan residues (Trp194 and Trp238) (or at least the one with the highest contribution) are relatively embedded within the core of the protein. Trp194 is at the top of β-sheet A and Trp238 on β-sheet B [30], which is shown in Fig 1. With the increase of GdmCl concentration, the fluorescence intensity first increases and reaches its maximum at 1 M GdmCl; then it gradually decreases as the GdmCl concentration increases up to 6 M. As shown in Supplement Fig 1, the thermodynamic stability of the protein cannot be computed based on the unfolding curves monitored by the fluorescence intensity at single wavelength (i.e. either at 330, 336 or 360 nm). The changes in wavelength at the maximum fluorescence (λ_{max}), exhibite, on the other hand, a clear double-sigmoid profile (Fig 2A) suggesting that the tertiary structure is denatured according to a three-state model (N ↔ I ↔ U). The first transition occurs between 0.7 and 1 M GdmCl, where the protein unfolds cooperatively into an intermediate state, followed by the second transition (from 1 to 4 M GdmCl) to the unfolded state. At 4 - 6 M GdmCl, the λ_{max} reaches a plateau, indicating that the protein is fully unfolded. The values of the thermodynamic parameters are calculated assuming a three-state unfolding model and the Equation 1 (Figure 2A and Table 1). AAT shows a $\Delta G°_{NI(H2O)}$ of 13.7 ± 2.3 kJ·mol^{-1} and $\Delta G°_{IU(H2O)}$ of 14.2 ± 0.7 kJ·mol^{-1}, and mid-transition denaturant concentration of each transition is 0.79 M and 2.41 M, respectively.

Figure 2B insert shows the far UV-CD spectrum of AAT in the presence of different concentrations of GdmCl. The spectrum of native AAT shows negative maximum at 208 nm and 222 nm, indicating that AAT is an alpha helix-dominated protein, which is in agreement with the secondary content determined from X-ray crystallographic data: 33 % in alpha-helices (9 alpha-helices), 28 % in beta-sheet (3beta-strands) and 39 % in loops/unstructured [31]. The CD signal decreases following a bimodal sigmoid. In 6 M GdmCl, the CD signal is near to 0, indicating the full denaturation of the secondary structures. The unfolded transition monitored at 222 nm, exhibits a double-sigmoid profile (Fig 2B) suggesting that the secondary structure is also denatured

according to a three-state model. Thus, the characteristic thermodynamic parameters are computed with the help of Equation 1, assuming a three-state unfolding model (Figure 2B and Table 1). The $\Delta G°_{NI(H2O)}$ is 16.3 ± 2.3 kJ·mol^{-1} and $\Delta G°_{IU(H2O)}$ is 13.1 ± 0.8 kJ·mol^{-1}; these values are similar to those derived from fluorescent measurements within the error limit. The Cm value of both transitions (0.8 ± 0.2 M and 2.4 ± 0.1 M) are also similar to the one obtained from fluorescence measurements.

The ANS-bound fluorescence increases when it binds to the exposed hydrophobic clusters, which makes it a commonly used tool to detect the intermediate species exposing such clusters upon the unfolding of a protein [32]. Figure 2C shows the ANS-bound spectrum of AAT in presence of various concentrations of GdmCl. ANS binds to AAT in its native state, suggesting the presence of hydrophobic clusters on the protein surface; this is confirmed by the X-ray structure of the protein (Figure 1). Elliott et al [33]also observed ANS-binding to native ATT. With the increase in GdmCl concentration, the ANS-bound fluorescence intensity at 480 nm first increased (from 0 and 1 M in GmdCl) then it decreases to near zero. These results suggest that the intermediate formed in the presence of 1M GdmCl is associated with the exposure of a hydrophobic cluster.

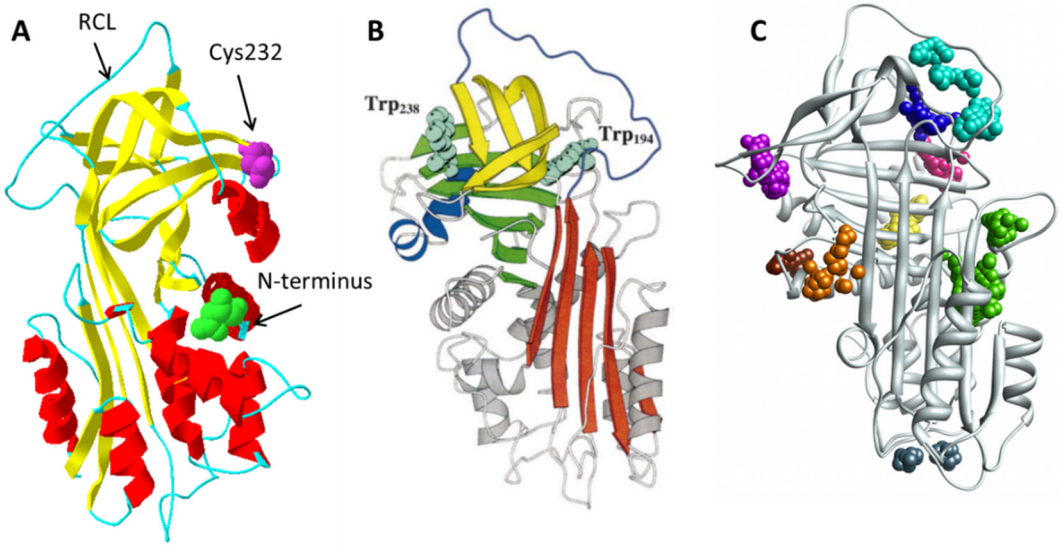

Figure 1. A) 3D structure of AAT (PDB: 2qug), generated by SWISS-MODEL [34]. The arrows indicate the reactive center loop and the two PEGylation sites. B) 3D structure of AAT with the two tryptophan residues highlighted. The A β-sheet is highlighted in red, the B β-sheet in green and the C β-sheet in yellow. The reactive center loop is in purple. C) The nine top-ranking surface pockets identified by SiteMap on AAT. The green and the yellow ones are relatively hydrophobic. This figure is adapted from Liu et al, Tew et al [35] and Patschull et al [36].

Figure 2D shows the normalized transitions monitored by intrinsic fluorescence, far UV-CD and ANS-bound fluorescence. The normalized unfolding transition obtained by far UV-CD and intrinsic fluorescence are virtually superimposed, indicating that the secondary and the tertiary

structures of the protein unfold cooperatively. This observation suggests that two structural domains of the protein unfold cooperatively and independently from each other. The increase of the ANS fluorescence during the first transition, suggests however that a small amount of intermediate state exposing some hydrophobic surface is formed, perhaps at the interface between the unfolded and the native domains. These results are in full agreements with those previously published [35, 37]. Tew et al [35] investigated the chemical denaturation of AAT with single tryptophan mutants. Their data suggests that A β-sheet undergoes a conformational change resulting in the increased exposure of Trp194 to solvent in 3.5 M urea, while no change in the B β-sheet (where Trp238 is located) is observed. Similarly, Krishnan et al [37] demonstrate that the chemical unfolding intermediate of AAT contains an intact B β-sheet.

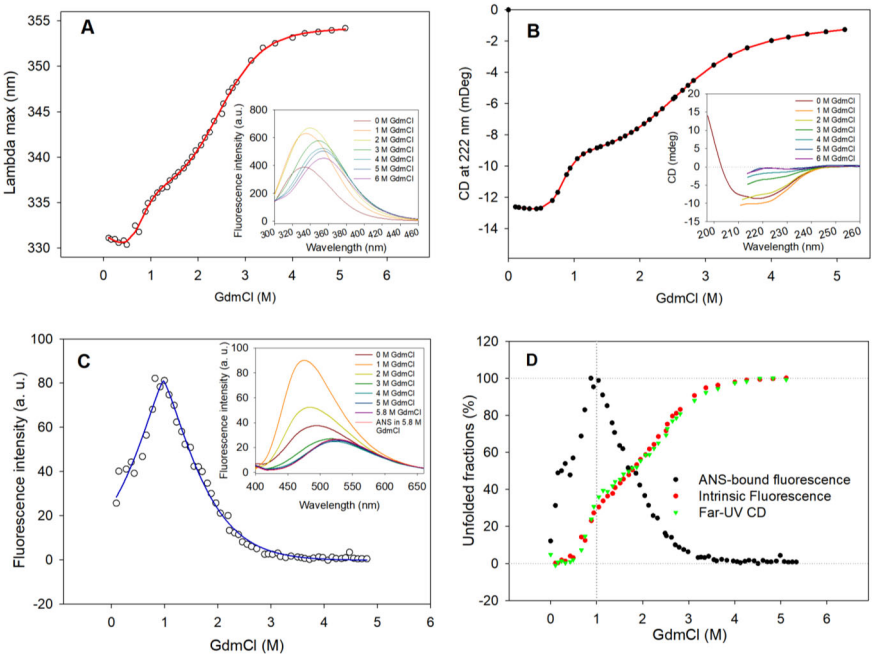

Figure 2. A) GdmCl-induced unfolding transition of AAT monitored by intrinsic fluorescence. The insert shows the intrinsic fluorescence spectra of AAT in the presence of various concentrations of GdmCl. With the increase of GdmCl concentration, the fluorescence intensity first increased (0 – 2 M GdmCl) and then decreased (2 – 6 M GdmCl). A red shift (from approximately 330 nm to 355 nm) of the wavelength of maximum fluorescence is observed. B) GdmCl unfolding transition of AAT monitored by far UV-CD. The insert shows the CD spectra of AAT in the presence of various concentrations of GdmCl. The CD signal decreased following a bimodal sigmoid. In 6 M GdmCl, the CD signal is near to 0, indicating the full denaturation of the secondary structures. C) GdmCl unfolding transition monitored by ANS-bound fluorescence. The insert shows the ANS-bound fluorescence spectra of AAT in the presence of various concentrations of GdmCl. The red line shows the fluorescence spectrum of free ANS in 5.8 M GdmCl. ANS binds to AAT at native state, indicating the presence of hydrophobic clusters on the protein surface. With the increase of GdmCl concentration, the ANS-bound fluorescence intensity at 480 nm first increases then decreases, indicating the denaturation of hydrophobic patches of AAT. In the presence of >4 M GdmCl, the spectrum was superimposed with that of free ANS, indicating that the hydrophobic patches were fully unfolded. D) The unfolded fractions of AAT in GdmCl-induced transition curves monitored by intrinsic fluorescence (solid dots), far UV-CD (blank squares) and ANS-bound fluorescence (blank triangles).

III.2. EFFECT OF PEGYLATION ON STRUCTURE AND STABILITY OF AAT

III.2.1. Secondary and tertiary structures

Figure 3A shows the fluorescence spectra of AAT and PEGylated AAT in the native and unfolded states (i.e., in 6.9 M GdmCl). The spectra of the different PEGylated AAT exhibit the same λ_{max} as AAT but show significantly higher fluorescence intensity in their native state. This suggests that there are no changes in the exposure of the tryptophan residues to the solvent and thus, no major conformational changes due to PEGylation. The increase in fluorescence intensity is observed whether the PEG moiety is attached via the W128-closed-by cysteine 232 or via the farer N-terminus; moreover, there is no obvious correlation between the amplitude of the increase in fluorescence intensity and the length of the PEG. The molecular reason of the fluorescence increase is therefore not straightforward. In the presence of 6.9 M GdmCl, the spectra of PEGylated AAT are similar to that AAT, which indicates the full denaturation of the tertiary structures of PEGylated proteins.

Figure 4B shows the far-UV CD spectra of the unmodified and PEGylated AAT. The spectra of PEGylated AAT show the same signal and shape, which confirms that after PEGylation, there is no significant changes in the secondary structure whatever the position and the length of the PEG. In the presence of 6.9 M GdmCl, the CD signals of all the proteins is near zero, indicating that all the proteins are fully unfolded.

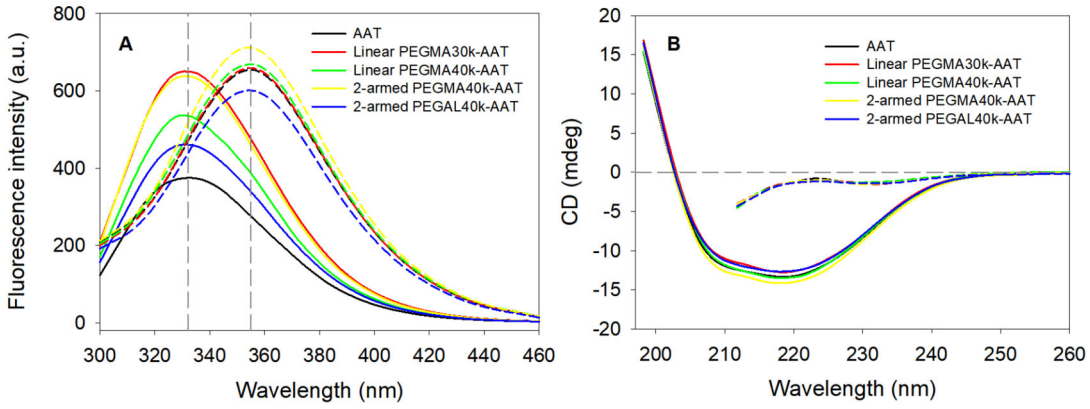

Figure 3. Fluorescence and far UV-CD spectrum of AAT and PEGylated AAT in the absence of GdmCl (solid lines) and in the presence of 6.9 M GdmCl (dashed lines). A) Intrinsic fluorescence spectra. The wavelength of maximum fluorescence of PEGylated AAT in native state is ~ 330 nm, while at denatured state (in presence of 6.9 M GdmCl) is ~ 355 nm, indicating the full denaturation of tertiary structures. B) Far UV-CD spectrum. AAT and PEG-AAT shared the identical CD spectrum, indicating that the secondary structure was non modified upon PEGylation.

III.2.2. Thermodynamic stability

Figure 4A shows the normalized GdmCl unfolding transition of AAT and the PEGylated protein monitored by intrinsic fluorescence. Whatever the length and the position of the PEG chain, PEGylated AAT unfold according to a three-state transition. The unfolding curves of PEGylated AAT are superimposed with that of AAT, indicating that the PEGylation does not significantly affect the thermodynamic stability of the protein. A non-linear fit is performed using Equation 1 to all the non-normalized transition data, which results in similar thermodynamic parameters within experimental errors for unmodified and PEGylated proteins (Table 2).

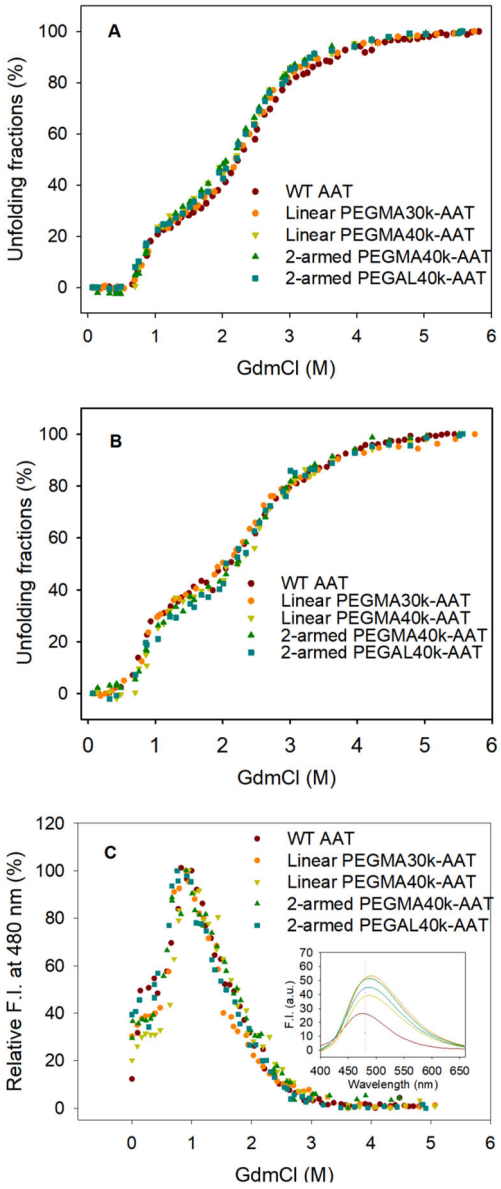

Figure 4. Normalized GdmCl-induced transitions monitored by the wavelength of maximum intrinsic fluorescence intensity (A), far UV-CD signal at 222 nm (B) and ANS-bound fluorescence intensity at 480 nm (C). The insert in C shows the ANS-bound fluorescence spectra of AAT and PEG-AAT in the absence of GdmCl. The colors of the spectra are the same as in C. AAT and PEG-AAT unfold in a three-state transition. The unfolding curves of PEG-AAT are superimposed with that of AAT, indicating that the PEGylation does not affect the stability of AAT.

Table 1. Thermodynamic parameters derived from the GdmCl-induced unfolding transition of AAT and PEG-AAT, based on intrinsic fluorescence measurement (of the changes in wavelength at the maximum fluorescence) and far UV-CD (at 222 nm). The transitions were analyzed assuming a three-state unfolding model.

Protein	$\Delta G°_{NI(H2O)}$ ($kJ \cdot mol^{-1}$)	m_{NI} ($kJ \cdot mol^{-1} \cdot M^{-1}$)	Cm_{NI} (M)	$\Delta G°_{IU(H2O)}$ ($kJ \cdot mol^{-1}$)	m_{IU} ($kJ \cdot mol^{-1} \cdot M^{-1}$)	Cm_{IU} (M)
Intrinsic fluorescence						
WT AAT	13.7 ± 2.3	17.4 ± 2.4	0.8 ± 0.2	14.2 ± 0.7	5.9 ± 0.3	2.4 ± 0.1
Linear PEGMA30k-AAT	13.5 ± 2.9	16.7 ± 3.0	0.8 ± 0.3	14.2 ± 0.9	6.0 ± 0.4	2.4 ± 0.1
Linear PEGMA40k-AAT	15.6 ± 2.6	19.7 ± 2.9	0.8 ± 0.2	14.3 ± 0.8	6.2 ± 0.3	2.3 ± 0.1
2-armed PEGMA40k-AAT	11.9 ± 3.1	15.5 ± 3.1	0.8 ± 0.3	13.7 ± 1.4	5.8 ± 0.6	2.4 ± 0.2
2-armed PEGAL40k-AAT	13.0 ± 3.0	17.5 ± 3.3	0.7 ± 0.3	13.3 ± 0.8	5.6 ± 0.4	2.4 ± 0.1
Far UV-CD						
WT AAT	16.3 ± 2.3	20.4 ± 2.3	0.8 ± 0.2	13.1 ± 0.8	5.5 ± 0.5	2.4 ± 0.1
Linear PEGMA30k-AAT	13.1 ± 2.5	15.5 ± 2.7	0.8 ± 0.3	14.4 ± 0.9	5.4 ± 0.6	2.7 ± 0.1
Linear PEGMA40k-AAT	15.6 ± 1.9	17.9 ± 1.9	0.9 ± 0.2	13.2 ± 1.8	5.4 ± 0.6	2.5 ± 0.2
2-armed PEGMA40k-AAT	14.5 ± 3.7	15.9 ± 3.2	0.9 ± 0.3	14.9 ± 0.9	6.0 ± 0.3	2.5 ± 0.2
2-armed PEGAL40k-AAT	13.0 ± 2.7	16.0 ± 3.2	0.8 ± 0.3	13.0 ± 0.9	5.6 ± 0.4	2.3 ± 0.1

As monitored by intrinsic fluorescence, AAT has a $\Delta G°(H_2O)$ value of 13.7 ± 2.3 and 14.2 ± 0.7 $kJ \cdot mol^{-1}$, and the C_m value of 0.8 ± 0.2 and 2.4 ± 0.1 M for the first and second transition, respectively. As shown in Table 2, PEGylation did not change the thermodynamic parameters of AAT significantly.

The unfolding transitions were also monitored by the CD signal at 222 nm. Figure 4B displays the normalized unfolding transitions. The transition curves of PEGylated AAT are superimposed with that of AAT, suggesting that the PEGylation does not affect the unfolding of the secondary structure of AAT. A satisfactory fit was obtained using Equation 1 to each transition curve before normalization. The analysis gives a similar $\Delta G°(H_2O)$ value of AAT of 16.3 ± 2.3 and 13.1 ± 0.8 $kJ \cdot mole^{-1}$ (Table 1) and the C_m value of 0.8 ± 0.2 and 2.4 ± 0.1 M for the first and second transition. PEG-AAT showed similar thermodynamic parameters monitored by far UV-CD (Table 1), indicating that PEGylation did not drastically altered the stability of AAT towards GdmCl-induced unfolding.

As shown in the insert of Figure 4C, the transitions of PEGylated proteins are superimposed with

that of AAT, with the same maxima at 1 M and decreasing signal from 1 to 3 M GdmCl, supporting the results from intrinsic fluorescence and far-UV CD measurements that PEGylation did not influence the stability of AAT to GdmCl-induced unfolding.

The activity of the samples refolded from GdmCl-induced unfolded protein (6M) were determined by measuring their ability to inhibit hNE activity (Supplement figure 3). The refolded samples showed similar hNE inhibition capacity as the native proteins. This indicates that the GdmCl-induced unfolding of AAT is largely reversible and that the PEGylation does not interfere with the refolding process.

III.3. HEAT-INDUCED UNFOLDING TRANSITIONS

III.3.1. Intrinsic fluorescence and far UV-CD spectra of AAT

To determine the appropriate wavelength to monitor thermal-induced denaturation of AAT and PEGylated AAT, the fluorescence and far-UV CD spectrum of AAT at different temperatures was recorded (Fig 5). The insert shows the fluorescence spectrum of AAT at 25 (solid line), 65 (dotted line) and 95 °C (dashed line). At 65 °C, the fluorescence maximum (λ_{max}) shifted to higher wavelength (i.e. 340 nm), with a slight decrease in fluorescence intensity. At 95 °C, the fluorescence intensity dropped drastically; the λ_{max}, however, barely changed. The most significant difference in the fluorescence intensity occurs at around 324 nm, therefore this wavelength was chosen to monitor the thermal unfolding of the proteins. In the far-UV CD spectra, the CD signal decreased with the increasing temperature, especially for the negative minimum at 222 nm. However, at 95 °C, the spectrum suggests that a significant amount of secondary structure is still present. When AAT is fully denatured, the λ_{max} in fluorescence will shift to approximately 355 nm and the CD signal will be nearly zero, which is neither the case with AAT at high temperature. This suggests that at high temperature, AAT is not completely denatured; this is however not likely the case since the apparent T_m observed was around 57°C (see below). Therefore, it is more likely that the unfolded protein has significantly aggregated. The heated AAT shows no elastase inhibition activity (Supplement Fig 3), which supports that the thermal denaturation of AAT is not reversible most likely due to the aggregation of the protein. These observations are in agreement with those of Lomas [26]. Thus, transition monitored by intrinsic fluorescence will only allow grossly evaluate if the PEGylation has an effect on the thermostability.

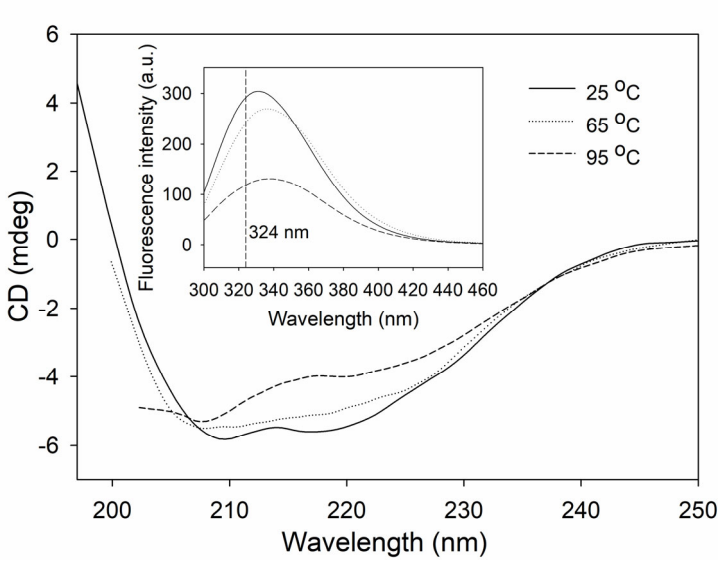

Figure 5. Far UV-CD spectrum of AAT at different temperatures. The insert shows the intrinsic fluorescence spectrum of WT AAT at different temperatures.

III.3.2. Effect of PEGylation on thermal stability of AAT

Figures 6A and B show the thermal transitions of the unmodified and PEGylated AAT monitored by intrinsic fluorescence at 324 nm. All the transitions show a steady decrease in fluorescence intensity from 25 to 50 °C, which corresponds to the pre-transition baseline. With the continuous increase of the temperature, the fluorescence intensity increased and peaked at around 60 °C. From 60 to 70 °C, the fluorescence intensity kept decreasing, corresponding to the post-transition baseline. The transitions probed by ANS-bound fluorescence (Fig 6C, D) are similar to thermal-induced denaturation monitored by intrinsic fluorescence, which decreases first, followed by an increase to its maxima at around 60 °C. This suggests that a possible intermediate populated at T_m. The transition curves monitored by intrinsic fluorescence and ANS-bound fluorescence were fitted using the Equation 2. As shown in Table 3, AAT and PEG-AAT showed the similar mid-transition temperature (T_m) around 57 – 59 °C.

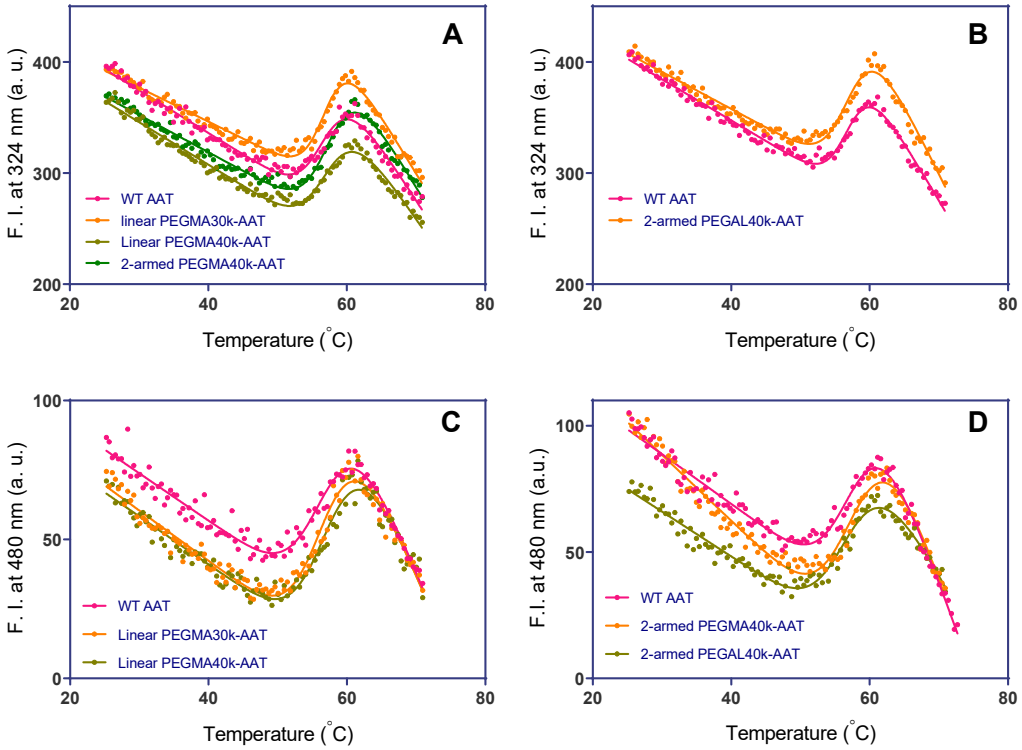

Figure 6. Thermal-induced transitions of AAT and PEG-AAT, followed by the changes of intrinsic fluorescence at 324 nm (A and B), or by ANS-bound fluorescence at 480 nm (C and D). All the transitions showed a pre-transition zone from 25 to 50 °C, followed by a transition of 50 – 60 °C.

Table 2. Thermal induced unfolding of AAT and PEGylated AAT followed by intrinsic fluorescence at 324 nm and ANS-bound fluorescence at 480 nm. The transition curves were fitted using Equation 2 by GraphPad Prism 7. T_m is the mid-transition temperature.

Tm (°C)	Intrinsic fluorescence (°C)	ANS-bound fluorescence (°C)
AAT	57.2 ± 0.3	57.9 ± 0.5
Linear PEGMA30k-AAT	57.3 ± 0.2	57.7 ± 0.4
Linear PEGMA40k-AAT	57.8 ± 0.3	58.4 ± 0.5
2-armed PEGMA40k-AAT	58.1 ± 0.2	59.3 ± 0.6
2-armed PEGAL40k-AAT	57.8 ± 0.3	58.0 ± 0.5

Figure 7 shows the changes of the averaged hydrodynamic size of unmodified and PEGylated AAT with the increase in temperature. The hydrodynamic diameter of AAT and PEGylated AAT at different temperatures were measured by Malvern Zetasizer Ultra. AAT has a size of 6.2 ± 0.1 nm at 25 °C, which was unchanged until 55 °C. The size of heated protein increased gradually and

reached 16.1 ± 0.9 nm from 55 to 97 °C, indicating either the unfolding of the protein, or the formation of aggregates, or the combination of both. The size change occurred at around 55 °C, which corresponds to the T_m derived from the thermal unfolding experiments monitored by intrinsic fluorescence and ANS-bound fluorescence. This observation further supports that the irreversibility of the heat-induced denaturation is due to aggregation of (partially) unfolded protein. The normalized data show that the relative size of AAT significantly increased starting from 55 °C while for PEG-AAT from the increase starts at around 60 °C. Since the Tm measured by far UV-CD is similar weather the protein is PEGylated or not, these results suggest that the PEG moiety act by decreasing the intermolecular interactions between unfolded molecules. In addition, at 95 °C, the size of PEG-AAT was approximately 1.6 folds larger than the native monomers. While for AAT, the size almost tripled at 95 °C. The inhibition of the aggregation is similar whatever the PEGylation site and length.

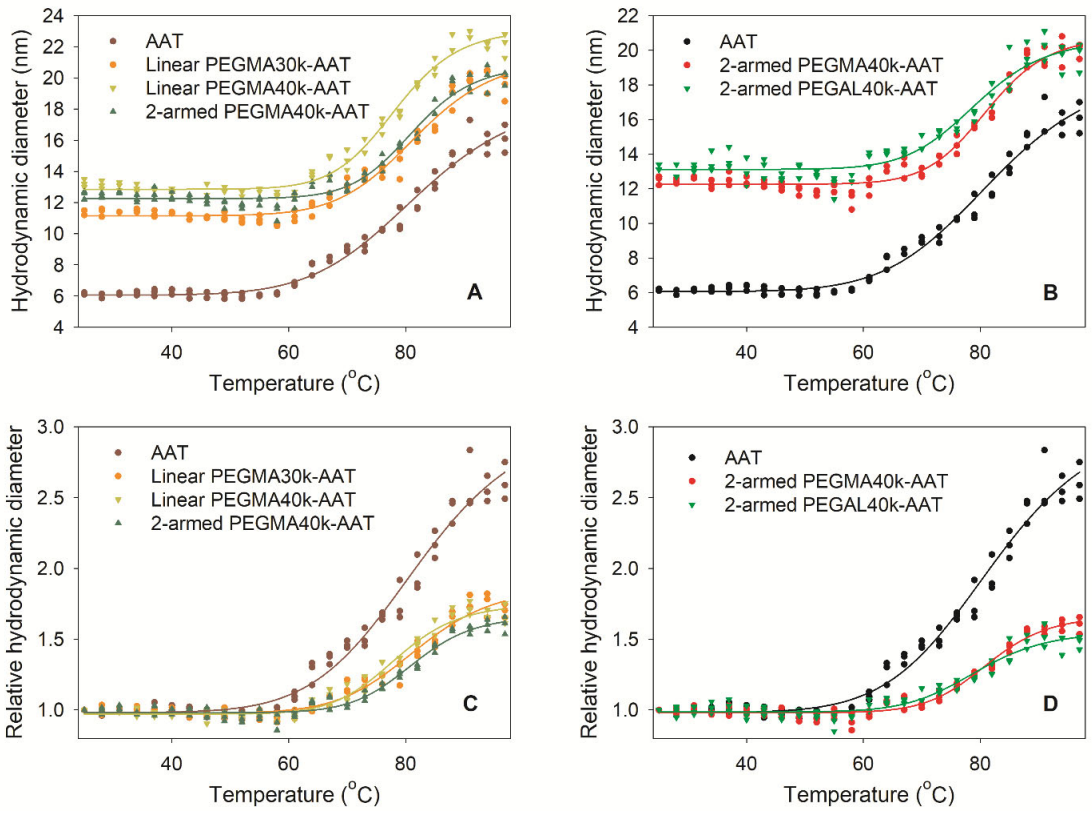

Figure 7. Thermal-induced aggregates of AAT and PEG-AAT monitored by DLS. A) AAT and thiol PEGylated AAT. B) AAT, 2-armed PEGMA40k-AAT and 2-armed PEGAL40k-AAT. C and D show the normalized data from A and B. PEGylated AAT has larger hydrodynamic diameter than AAT. With the increase of the temperature, the size of AAT and PEG-AAT stayed unchanged until 55 °C, followed by a gradual increase. The aggregation in PEG-AAT involved less molecules than AAT.

The effect of PEGylation on the irreversible aggregation of AAT was also monitored by SEC following treatment at 70°C for 1h. The samples were let to return to RT before analysis. Insoluble aggregates in thermally denatured samples were first removed by filtering through a 0.22 µm cut-off membrane. The soluble aggregates were quantified by size exclusion chromatography. As shown in Fig 8 and Supplement Fig 2, the content of AAT and PEG-AAT remaining in solution was determined by analyzing the peak area percentage of the chromatograms. Both AAT and PEG-AAT, show an increase of aggregation after thermal denaturation. The chromatogram of AAT after denaturation shows 32.7 % of the native monomers (the peak at 16 ml), which decreased by 60 % compared to the control sample. Besides the monomers, there are several peaks eluting earlier than the monomers, which correspond to aggregated species (54.7 %). Worth mentioning, the aggregates measured by DLS shows the largest entities of 23 nm, which would remain in the solution after filtration through 0.22 µm membrane. The non-filtered heated samples show increased optical density at 310 nm, indicating the presence of insoluble aggregates, which should be removed by filtration. Following N-terminal PEGylation with 2-armed 40 kDa PEG-AL, the aggregation content was significantly decreased (only 25.7 %). Following thiol PEGylation, the linear PEG-MA modified AAT showed a lower content of aggregates. Two-armed PEGMA40k-AAT showed a better resistance to polymerization, as there was only 13.5 % of the aggregates. The remaining activity of the heated samples was determined by elastase inhibition assay. As shown in Supplement Fig 3, the hNE activity was completely inhibited by native unmodified or PEGylated AAT at a HNE:AAT molar ratio 1:1, while it was not inhibited at all by heated AAT. The heated PEGylated AAT did not, therefore present any hNE inhibition capacity despite the fact that heat-induced aggregation was reduced. This demonstrated that the activity of unmodified and PEGylated AAT was fully and irreversibly lost after heating.

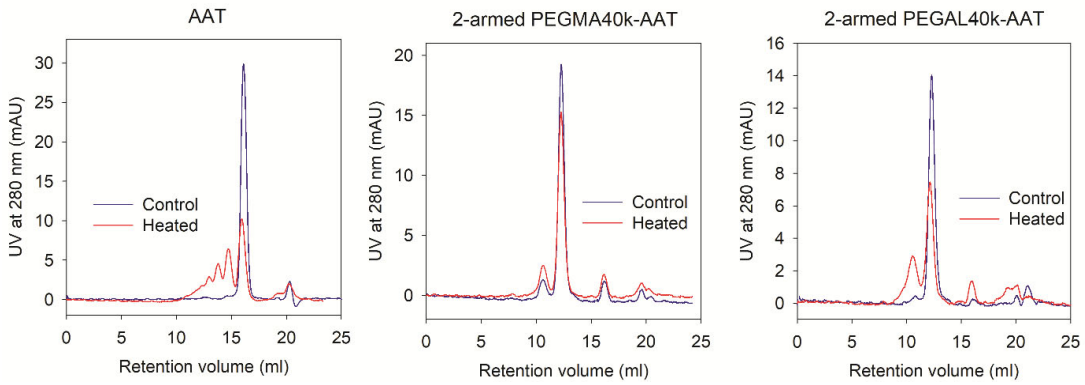

Figure 8. Size exclusion chromatogram of AAT and PEG-AAT after heat treatment (70 °C, 1 h). The control samples of the same concentration were kept at room temperature for 1 h. The large insoluble aggregates were priorly removed via filtration through 0.22 µm membrane. PEG-AAT showed less content of aggregates after heating. And thiol PEGylated AAT has better resistance to heat induced aggregates.

IV. DISCUSSION

IV.1. EFFECTS OF PEGYLATION ON THE SECONDARY AND TERTIARY STRUCTURES OF AAT

The far-UV CD spectrum of unmodified and PEGylated AAT shows that the secondary structure of AAT is not significantly affected upon both thiol and N-terminal PEGylation. Among numerous studies concerning PEGylation of a protein, an alteration of protein secondary structure was seen only in the cases where a large PEG was used, which often combined with some loss of activity. For instance, Chiu *et al.* found that the conjugation of a 20 kDa PEG to trypsin caused a significant loss in its secondary structure, especially α-helices, and in its biological activity [38]. In this case, however, there were multiple PEGylation sites, and the reaction was not site selective. In the cases of mono-PEGylation to a selective PEGylation site, PEGylation usually does alter the protein secondary structure [16, 39–41]. As for the tertiary structure, the PEGylated AAT showed the same λ_{max} as that of AAT, suggesting that there were no significant structural changes in the environment of the tryptophan residues, and thus of the tertiary structure of the protein upon PEGylation. In addition, the ability of AAT to inhibit human neutrophil elastase was fully preserved after PEGylation as previously described [22]. An increase in intrinsic fluorescence intensity is however observed for the PEGylated AAT compared to AAT. With thiol PEGylation, the linear PEGMA30k-AAT and 2-armed PEGMA40k-AAT showed higher fluorescence intensity than the linear PEGMA40k-AAT. In the native state, the fluorescence of tryptophan residues may be quenched by the disulfide bond between Cys232 and the cysteine cap. When conjugating a PEG-maleimide to Cys232, the disulfide bond between Cys232 to the additional cysteine cap no longer exists, thus its quenching should not be present anymore, causing the increase of the intrinsic fluorescence intensity. PEGylation often decreases the protein intrinsic fluorescence [42] or has no effect [43–45]. The decrease of intrinsic fluorescence in β-lactoglobulin (β-LG) after PEGylation was explained as a combined action of the shielding effect of PEG chain and the exposure of Trp residues to the solvent upon PEGylation [42]. In the case of granulocyte colony stimulating factor (G-CSF) [43], PEGylation at two different sites (Lys41 and Gln135) resulted in unchanged or increased intrinsic fluorescence intensity, respectively.

PEGylated AAT displays the same biological activity as AAT [22], indicating that PEGylation does not affect the structure of the most important part of this protein, the reaction center loop (RCL). These results are in line with Zhu et al [46] and Cantin et al [47]. It is reported from several studies that the PEGylation does not alter the tertiary structure of a protein substantially. Bitten [41] reported the PEGylation of bovine serum albumin (BSA) and recombinant human factor VIIa respectively, whose results showed identical near UV-CD spectra of unmodified and PEGylated

proteins. Rodriguez-Martinez [16] reported that no major spectral changes were observed as a result of PEGylation of α-chymotrypsin. Guichard [39] demonstrated that mono-PEGylated recombinant human deoxyribonuclease I (rhDNase) shared the same intrinsic tryptophan fluorescence spectrum as the unmodified rhDNase, in whose case the PEGylation site is at N-terminal residue, which is distant from all four tryptophan residues.

IV.2. EFFECTS OF PEGYLATION ON THE THERMODYNAMIC STABILITY OF AAT

The thermodynamic stability of AAT and PEGylated AAT were determined by intrinsic fluorescence, far-UV CD and ANS-bound fluorescence measurements in the presence of increasing concentrations in GdmCl. The reversibility of GdmCl-induced unfolding of AAT and PEGylated AAT was established by hNE inhibition assay of refolded AAT samples. After refolding, the hNE inhibition capacity of AAT and PEGylated AAT were fully regained. Both fluorescence and far-UV CD data show that AAT and PEGylated AAT unfold via a three-state transition (N ⇋ I ⇋ U, where N represents the native state, I the intermediate state and U unfolded state), with the C_m value around 0.8 M and 2.4 M, respectively, which is in good agreement with previous reports [35, 37, 48, 49]. However, the ΔG values from different studies vary. Krishnan reported both $\Delta G°_{NI(H2O)}$ and $\Delta G°_{IU(H2O)}$ as 16.7 kJ·mol^{-1} [37], while in the study of Tew et al, $\Delta G°_{NI(H2O)}$ was 19.7 kJ·mol^{-1} and $\Delta G°_{IU(H2O)}$ was 25.5 kJ·mol^{-1} [35]. In both studies above, the unfolding curves were monitored by far-UV CD. Our data ($\Delta G°_{NI(H2O)}$ as 16.2 ± 3.2 kJ·mol^{-1} and $\Delta G°_{IU(H2O)}$ as 14.0 ± 0.9 kJ·mol^{-1}) were in better agreement with Krishnan. The superimposition of transitions monitored by fluorescence and far-UV CD indicates the simultaneous denaturation of the secondary and tertiary structures for unmodified and PEGylated AAT. This denaturation profile suggests that the protein behaves as two structurally domains that cooperatively unfold independently. It was reported that the intermediate of AAT in chemical unfolding involves only the A and C β-sheet, while the B β-sheet was intact, which corresponds to our proposition that the protein unfolds as two domains independently. Tsutsui et al, using H/D exchange experiments suggested however, that the unfolding of α1-AT involves a cooperative transition to a molten globule form, followed by a non-cooperative transition to a random-coil form as more guanidine is added. Thus, the entire α1-AT molecule consists of one cooperative structural unit rather than multiple structural domains with different stabilities [48]. The intermediate species we have observed at 1 M GdmCl were described previously. However, the concentration of GdmCl where this intermediate is formed varies from 1 – 1.5 M [37, 50].

For all proteins investigated in the present study, the transition curves monitored by ANS-bound fluorescence show an increase in fluorescence intensity up to around 1 M GdmCl, followed by a

decrease in intensity at higher GdmCl concentrations. The increase of ANS-bound fluorescence upon the first transition might be due to the exposure of a hydrophobic cluster at the interface of the two domains. The cluster is likely to be denatured at higher denaturant concentrations.

The free energy of each protein was obtained by adjusting the experimental data by the Equation 1 (Table 2). All the proteins share the similar $\Delta G°(H_2O)$ value (25 – 30 kJ·mol^{-1}). The $\Delta G°(H_2O)$ and Cm value for the first and second transitions of AAT did not change drastically after PEGylation. These results highlight that the conformational stability of AAT towards chemical denaturant is not significantly altered upon PEGylation.

García-Arellano [17] and coworkers reported that the thermodynamic stability of Cytochrome C (12.4 kDa) decreased after conjugating a 5000 Da PEG – the $\Delta G°(H_2O)$ of PEGylated Cyt was 5.7 kJ·mol^{-1}, while that in unmodified protein was 30.4 kcal/mol. Similarly, Sorret [51] demonstrated that the $\Delta G°(H_2O)$ of recombinant human interleukin-1 receptor antagonist (rhIL-1ra) , a 17 kDa cytokine inhibitor, decreased by 22.6 kJ·mol^{-1} upon conjugation of a 20 kDa PEG chain, suggesting that PEGylation decreased the conformational stability of rhIL-1ra.

Interestingly, as shown in Figure 3, ANS binds to AAT and PEGylated AAT in the native state. The native state of AAT is meta-stable, which does not correspond to the most stable conformation that its sequence can adopt [52, 53]. Indeed, upon binding to its cognate protease, AAT undergoes a massive conformational change, in which the reactive center loop (RCL) inserts into β-sheet A, becoming a sixth strand. The resulting conformation is more stable than the initial native structure [54, 55]. Inspecting the crystal structure of AAT, a hydrophobic pocket that is lined by two of A β-sheets and α-helices D and E (Figure 1, purple area on the right) is observed [56], which plays a crucial role in the polymerization of misfolded AAT [57, 58]. Another hydrophobic surface was detected as shown in Fig 1 (purple area on the left), where locates one of the tryptophan residues (Trp194). These hydrophobic areas could be the binding region for ANS.

IV.3. EFFECT OF PEGYLATION ON THERMAL STABILITY

The apparent mid-transition temperatures of AAT and PEG-AAT monitored by intrinsic fluorescence intensity at 324 nm and ANS-bound fluorescence intensity at 480 nm were similar (~ 56 °C). ATT and PEGylated AAT did not recover any activity after heat treatment. The SEC analysis of the denatured samples proved that the thermal denaturation of unmodified and PEGylated AAT is associated with significant aggregation. Previous studies have shown that heat-induced denaturation of AAT is a concentration-dependent aggregation process [59, 60]. Kwon et al [59] deactivated AAT at 58 °C for 70 min while Jha et al used 54 °C for 120 min. The

concentration used by the two research teams (5 μg/ml) is significantly lower than ours. Both teams reported the loss of activity after the heat treatment. However, whether the activity loss was due to the denaturation, or the aggregation of AAT remains unclear.

The results of size distribution data illustrate that the size enlargement started from around 50 – 55 °C for AAT and 60 – 65 °C for PEG-AAT. This could result from the unfolding of the protein, followed by the aggregation of AAT during the heat denaturation. However, we were not able to determine the exact temperature where aggregation occurred. Although Tew et al [35] and Krishnan et al [37] have demonstrated that the chemical-induced unfolding intermediate of AAT involves an intact B β-sheet and expanded A and C β-sheet, it is slightly different in heat-induced unfolding. According to Haq, the heat-induced AAT intermediate has a more compact state than that observed in 1 M GdmCl [61]. The PEG-AAT has a lower tendency to aggregate indicating that PEGylation prevents intermolecular interactions as previously reported Roque *et al.* demonstrated that the conjugation of two 30 kDa PEG-maleimide to a monoclonal antibody antigen-binding fragment (Fab') protected the Fab' against formation of heat-induced large aggregates and precipitation, possibly by sterically hindering intermolecular association between partially unfolded Fab's [62]. N-terminal PEGylation of granulocyte colony stimulating factor (GCSF) with a 20 kDa PEG prevents protein precipitation, and slows aggregation rate [63]. However, PEG-maleimide conjugation to the Cys17 of GCSF, enhanced the tendency of GCSF to aggregate [64]. These results suggest that the PEGylation site has a strong influence on protein aggregation. Unfortunately, the activity of the aggregated proteins was not demonstrated in the above studies.

The results of the SEC analysis also support that the effects of PEGylation on the properties of the protein is site-specific. AAT shows weak resistance to thermal-induced aggregation. Among all the PEGylated protein, 2-armed PEGMA40k-AAT presents the highest number of monomers after thermal denaturation, with a loss of only 15 % of monomeric proteins. Although at least 30 % of the proteins remained monomeric after thermal denaturation, the hNE inhibition assay showed the complete loss of activity in all samples. This indicates that after heating, either polymerized or monomeric AAT are inactive, which is in agreement with the findings from Persson [65]. Lomas [26] reported that when heating at high temperature, the uncleaved reactive center loop can be stably incorporated into the A β-sheet, which is characterized as latent AAT. Latent AAT is inactive [37] but more resistant to heat-induced polymerization [26, 66]. Therefore, it is likely that the monomeric species present in the heat-treated sample are latent AAT. In our case, thiol PEGylated AAT showed better resistance to heat-induced polymerization than N-terminal PEGylated AAT.

In the case of GCSF, N-terminal PEGylated GCSF is more stable than thiol PEGylated one [63, 64]. This indicates that the influence of PEGylation site on protein thermal stability differ between proteins.

IV.4. EFFECT OF PEGYLATION ON THE STABILITY TOWARDS PROTEOLYSIS

PEGylation is often used to increase the stability of a therapeutic protein in biological media. Zhang et al demonstrated that the conjugation of 2 – 10 kDa PEG on lysine residue of fibronectin (FN) enhanced its resistance to proteolysis [67]. Similar effect was reported with FN PEGylated on cysteine residue by thiol PEGylation [68]. Danial et al showed that conjugating a 2 kDa PEG to the peptides derived from the HR1 or HR2 regions of the HIV-1 envelope glycoprotein gp41 resulted in an increase of 3.4-fold in degradation half-life against trypsin [69]. However, the mechanism behind this is not yet thoroughly investigated. The prominent explanation of the proteolytic protection of PEG is the steric shielding effect, which impedes the access of proteases towards the protein [9]. Nevertheless, this shielding effect can sometimes result in the loss of binding affinity or activity of a protein. Growth hormone antagonist (GHA), a 22 kDa protein, lost its binding affinity after conjugating to a 40 kDa PEG at the N-terminus [10]. Pegaptanib®, the PEGylated aptamer against vascular endothelial growth factor (VEGF) using 2-armed 40 kDa PEG, preserves only 25 % of the *in vitro* binding affinity comparing to its unconjugated counterpart [11]. Nonetheless, the tremendous increase in half-life (9 d for Pegaptanib® while 30 min for unconjugated anti-VEGF) offsets the loss of activity, leading to an overall better therapeutic value. Similarly, Pegasys®, a PEGylated interferon-α-2a, preserved only 7 % of the *in vitro* activity but showed an excellent *in vivo* efficacy [11].Our results showed that two-armed PEGMA40k-AAT has the most enhanced resistance to proteolysis. Moreover, the reduction of proteolysis was achieved without compromising the biological activity.

V. CONCLUSIONS

Alpha-1 antitrypsin was mono-PEGylated at the single cysteine with 3 different PEG polymers (30 kDa and 40 kDa linear PEG-maleimide and 40 kDa 2-armed PEG-maleimide), and at the N-terminal residue with 40 kDa 2-armed PEG-aldehyde. The far-UV CD and intrinsic fluorescence spectra suggest that the secondary and tertiary structures of AAT are not altered upon PEGylation. The GdmCl-induced transitions monitored by intrinsic fluorescence, far-UV CD and ANS-bound fluorescence indicate that the thermodynamic stability of AAT to chemical denaturant is not affected upon PEGylation. Thiol PEGylated AAT shows high stability to thermal-induced aggregation although PEG does not prevent the irreversible inactivation of the enzyme upon heat treatment.

VI. REFERENCES

[1] Chapman KR, Chorostowska-Wynimko J, Koczulla AR, Ferrarotti I, McElvaney NG. Alpha 1 antitrypsin to treat lung disease in alpha 1 antitrypsin deficiency: recent developments and clinical implications. International journal of chronic obstructive pulmonary disease 2018;13:419–32.

[2] Duranton J, Bieth JG. Inhibition of proteinase 3 by alpha1-antitrypsin in vitro predicts very fast inhibition in vivo. American journal of respiratory cell and molecular biology 2003;29(1):57–61.

[3] Korkmaz B, Attucci S, Jourdan M-L, Juliano L, Gauthier F. Inhibition of neutrophil elastase by alpha1-protease inhibitor at the surface of human polymorphonuclear neutrophils. Journal of immunology (Baltimore, Md. 1950) 2005;175(5):3329–38.

[4] Marc Padrines, Martine Schneider-Pozzer, and Joseph G. Bieth. Inhibition of Neutrophil Elastase by Alpha-1-Proteinase Inhibitor Oxidized by Activated Neutrophils.

[5] Tonelli AR, Brantly ML. Augmentation therapy in alpha-1 antitrypsin deficiency: advances and controversies. Therapeutic advances in respiratory disease 2010;4(5):289–312.

[6] Stolk J, Tov N, Chapman KR, et al. Efficacy and safety of inhaled α1-antitrypsin in patients with severe α1-antitrypsin deficiency and frequent exacerbations of COPD. The European respiratory journal 2019;54(5).

[7] Pasut G, Veronese FM. State of the art in PEGylation: the great versatility achieved after forty years of research. Journal of controlled release official journal of the Controlled Release Society 2012;161(2):461–72.

[8] Turecek PL, Bossard MJ, Schoetens F, Ivens IA. PEGylation of Biopharmaceuticals: A Review of Chemistry and Nonclinical Safety Information of Approved Drugs. Journal of pharmaceutical sciences 2016;105(2):460–75.

[9] Veronese FM, Pasut G. PEGylation, successful approach to drug delivery. Drug Discovery Today 2005;10(21):1451–8.

[10] Wu L, Ho SV, Wang W, et al. N-terminal mono-PEGylation of growth hormone antagonist: correlation of PEG size and pharmacodynamic behavior. International journal of pharmaceutics 2013;453(2):533–40.

[11] Veronese FM, Mero A. The impact of PEGylation on biological therapies. BioDrugs clinical immunotherapeutics, biopharmaceuticals and gene therapy 2008;22(5):315–29.

[12] Lawrence PB, Price JL. How PEGylation influences protein conformational stability. Current opinion in chemical biology 2016;34:88–94.

[13] Frokjaer S, Otzen DE. Protein drug stability: a formulation challenge. Nature reviews. Drug discovery 2005;4(4):298–306.

[14] Jain A, Ashbaugh HS. Helix stabilization of poly(ethylene glycol)-peptide conjugates. Biomacromolecules 2011;12(7):2729–34.

[15] Price JL, Powers ET, Kelly JW. N-PEGylation of a reverse turn is stabilizing in multiple sequence contexts, unlike N-GlcNAcylation. ACS chemical biology 2011;6(11):1188–92.

[16] Rodríguez-Martínez JA, Solá RJ, Castillo B, et al. Stabilization of alpha-chymotrypsin upon PEGylation correlates with reduced structural dynamics. Biotechnology and bioengineering 2008;101(6):1142–9.

[17] García-Arellano H, Valderrama B, Saab-Rincón G, Vazquez-Duhalt R. High Temperature

Biocatalysis by Chemically Modified Cytochrome c. Bioconjugate Chem. 2002;13(6):1336–44.

[18] Plesner B, Fee CJ, Westh P, Nielsen AD. Effects of PEG size on structure, function and stability of PEGylated BSA. European journal of pharmaceutics and biopharmaceutics official journal of Arbeitsgemeinschaft fur Pharmazeutische Verfahrenstechnik e.V 2011;79(2):399–405.

[19] Rodríguez-Martínez JA, Rivera-Rivera I, Griebenow K. Prevention of benzyl alcohol-induced aggregation of chymotrypsinogen by PEGylation. The Journal of pharmacy and pharmacology 2011;63(6):800–5.

[20] Shu JY, Tan C, DeGrado WF, Xu T. New design of helix bundle peptide-polymer conjugates. Biomacromolecules 2008:2111–7.

[21] Lawrence PB, Gavrilov Y, Matthews SS, et al. Criteria for selecting PEGylation sites on proteins for higher thermodynamic and proteolytic stability. Journal of the American Chemical Society 2014:17547–60.

[22] Liu X, Vanvarenberg K, Guy Wilfried Kouassi K, Mahri S, Vanbever R. Production and characterization of mono-PEGylated alpha-1 antitrypsin for augmentation therapy. International journal of pharmaceutics 2021:121355.

[23] Chen Y, Snyder MR, Zhu Y, et al. Simultaneous phenotyping and quantification of α-1-antitrypsin by liquid chromatography-tandem mass spectrometry. Clinical chemistry 2011;57(8):1161–8.

[24] Pace CN. Determination and analysis of urea and guanidine hydrochloride denaturation curves. In: Enzyme Structure Part L: Elsevier, 1986:266–80.

[25] Vandenameele J, Lejeune A, Di Paolo A, et al. Folding of class A beta-lactamases is rate-limited by peptide bond isomerization and occurs via parallel pathways. Biochemistry 2010;49(19):4264–75.

[26] Lomas DA, Elliott PR, Chang WS, Wardell MR, Carrell RW. Preparation and characterization of latent alpha 1-antitrypsin. The Journal of biological chemistry 1995;270(10):5282–8.

[27] El Hajjaji H, Dumoulin M, Matagne A, et al. The zinc center influences the redox and thermodynamic properties of Escherichia coli thioredoxin 2. Journal of molecular biology 2009;386(1):60–71.

[28] Christopher M. A microtechnique for dialysis of small volume solutions with quantitative recoveries. Analytical Biochemistry 1987;165(1):208–14.

[29] Lestienne P, Bieth JG. The inhibition of human leukocyte elastase by basic pancreatic trypsin inhibitor. Archives of Biochemistry and Biophysics 1978;190(1):358–60.

[30] Knaupp AS, Bottomley SP. Structural change in β-sheet A of Z α(1)-antitrypsin is responsible for accelerated polymerization and disease. Journal of molecular biology 2011;413(4):888–98.

[31] Dasi Sangachini E, Hasannia S, Taghdir M, Pirooznia N, Khalili Ghadicholaei K. Construction of an engineered alpha 1-antitrypsin with inhibitory activity based on theoretical studies. Electro Journal of Biotech 2012;15(2).

[32] Gasymov OK, Glasgow BJ. ANS fluorescence: potential to augment the identification of the external binding sites of proteins. Biochimica et biophysica acta 2007;1774(3):403–11.

[33] Elliott PR, Abrahams JP, Lomas DA. Wild-type alpha 1-antitrypsin is in the canonical inhibitory conformation. Journal of molecular biology 1998;275(3):419–25.

[34] Guex N, Peitsch MC, Schwede T. Automated comparative protein structure modeling with SWISS-MODEL and Swiss-PdbViewer: a historical perspective. Electrophoresis 2009;30 Suppl 1:S162-73.

[35] Tew DJ, Bottomley SP. Probing the equilibrium denaturation of the serpin alpha(1)-antitrypsin with single tryptophan mutants; evidence for structure in the urea unfolded state. Journal of molecular biology 2001;313(5):1161–9.

[36] Patschull AOM, Gooptu B, Ashford P, Daviter T, Nobeli I. In silico assessment of potential druggable pockets on the surface of α1-antitrypsin conformers. PLOS ONE 2012;7(5):e36612.

[37] Krishnan B, Gierasch LM. Dynamic local unfolding in the serpin α-1 antitrypsin provides a mechanism for loop insertion and polymerization. Nature structural & molecular biology 2011;18(2):222–6.

[38] Chiu K, Agoubi LL, Lee I, Limpar MT, Lowe JW, Goh SL. Effects of polymer molecular weight on the size, activity, and stability of PEG-functionalized trypsin. Biomacromolecules 2010;11(12):3688–92.

[39] Guichard M-J, Patil HP, Koussoroplis SJ, Wattiez R, Leal T, Vanbever R. Production and characterization of a PEGylated derivative of recombinant human deoxyribonuclease I for cystic fibrosis therapy. International journal of pharmaceutics 2017;524(1-2):159–67.

[40] Plesner B, Fee CJ, Westh P, Nielsen AD. Effects of PEG size on structure, function and stability of PEGylated BSA. European journal of pharmaceutics and biopharmaceutics official journal of Arbeitsgemeinschaft fur Pharmazeutische Verfahrenstechnik e.V 2011;79(2):399–405.

[41] Plesner B, Westh P, Nielsen AD. Biophysical characterisation of GlycoPEGylated recombinant human factor VIIa. International journal of pharmaceutics 2011;406(1-2):62–8.

[42] Luo S, Lu X, Liu C, Zhong J, Zhou L, Chen T. Site specific PEGylation of β-lactoglobulin at glutamine residues and its influence on conformation and antigenicity. Food research international (Ottawa, Ont.) 2019;123:623–30.

[43] Mero A, Grigoletto A, Maso K, Yoshioka H, Rosato A, Pasut G. Site-selective enzymatic chemistry for polymer conjugation to protein lysine residues: PEGylation of G-CSF at lysine-41. Polym. Chem. 2016;7(42):6545–53.

[44] Wang J, Hu T, Liu Y, Zhang G, Ma G, Su Z. Kinetic and stoichiometric analysis of the modification process for N-terminal PEGylation of staphylokinase. Analytical Biochemistry 2011;412(1):114–6.

[45] Suo X, Lu X, Hu T, Ma G, Su Z. A solid-phase adsorption method for PEGylation of human serum albumin and staphylokinase: preparation, purification and biochemical characterization. Biotechnology letters 2009;31(8):1191–6.

[46] Zhu W, Li L, Deng M, et al. Oxidation-resistant and thermostable forms of alpha-1 antitrypsin from Escherichia coli inclusion bodies. FEBS open bio 2018;8(10):1711–21.

[47] Cantin AM, Woods DE, Cloutier D, Dufour EK, Leduc R. Polyethylene glycol conjugation at Cys232 prolongs the half-life of alpha1 proteinase inhibitor. American journal of respiratory cell and molecular biology 2002;27(6):659–65.

[48] Tsutsui Y, Wintrode PL. Cooperative unfolding of a metastable serpin to a molten globule suggests a link between functional and folding energy landscapes. Journal of molecular biology 2007;371(1):245–55.

[49] Knaupp AS, Levina V, Robertson AL, Pearce MC, Bottomley SP. Kinetic instability of the serpin Z alpha1-antitrypsin promotes aggregation. Journal of molecular biology 2010;396(2):375–83.

[50] Tran ST, Shrake A. The folding of alpha-1-proteinase inhibitor: kinetic vs equilibrium control. Archives of Biochemistry and Biophysics 2001;385(2):322–31.

[51] Sorret LL, Monticello CR, DeWinter MA, Schwartz DK, Randolph TW. Steric Repulsion Forces Contributed by PEGylation of Interleukin-1 Receptor Antagonist Reduce Gelation and Aggregation at the Silicone Oil-Water Interface. Journal of pharmaceutical sciences 2019;108(1):162–72.

[52] Bottomley SP. The folding pathway of alpha1-antitrypsin: avoiding the unavoidable. Proceedings of the American Thoracic Society 2010;7(6):404–7.

[53] Tsutsui Y, Dela Cruz R, Wintrode PL. Folding mechanism of the metastable serpin α1-antitrypsin. Proceedings of the National Academy of Sciences of the United States of America 2012;109(12):4467–72.

[54] Dobó J, Gettins PGW. alpha1-Proteinase inhibitor forms initial non-covalent and final covalent complexes with elastase analogously to other serpin-proteinase pairs, suggesting a common mechanism of inhibition. The Journal of biological chemistry 2004;279(10):9264–9.

[55] Kang U-B, Baek J-H, Ryu S-H, Kim J, Yu M-H, Lee C. Kinetic mechanism of protease inhibition by alpha1-antitrypsin. Biochemical and biophysical research communications 2004;323(2):409–15.

[56] Ali MF, Kaushik A, Kapil C, Gupta D, Jairajpuri MA. A hydrophobic patch surrounding Trp154 in human neuroserpin controls the helix F dynamics with implications in inhibition and aggregation. Scientific Reports;7:42987.

[57] Mallya M, Phillips RL, Saldanha SA, et al. Small molecules block the polymerization of Z alpha1-antitrypsin and increase the clearance of intracellular aggregates. Journal of medicinal chemistry 2007;50(22):5357–63.

[58] Chang Y-P, Mahadeva R, Chang W-SW, Lin S-C, Chu Y-H. Small-molecule peptides inhibit Z alpha1-antitrypsin polymerization. Journal of cellular and molecular medicine 2009;13(8B):2304–16.

[59] Kwon K-S, Yu M-H. Effect of glycosylation on the stability of α1-antitrypsin toward urea denaturation and thermal deactivation. Biochimica et Biophysica Acta (BBA) - General Subjects 1997;1335(3):265–72.

[60] Lomas DA, Evans DL, Stone SR, Chang WS, Carrell RW. Effect of the Z mutation on the physical and inhibitory properties of alpha 1-antitrypsin. Biochemistry 1993;32(2):500–8.

[61] Haq I, Irving JA, Saleh AD, et al. Deficiency Mutations of Alpha-1 Antitrypsin. Effects on Folding, Function, and Polymerization. American journal of respiratory cell and molecular biology 2016;54(1):71–80.

[62] Roque C, Sheung A, Rahman N, Ausar SF. Effect of polyethylene glycol conjugation on conformational and colloidal stability of a monoclonal antibody antigen-binding fragment (Fab'). Molecular pharmaceutics 2015;12(2):562–75.

[63] Rajan RS, Li T, Aras M, et al. Modulation of protein aggregation by polyethylene glycol conjugation: GCSF as a case study. Protein science a publication of the Protein Society 2006;15(5):1063–75.

[64] Veronese FM, Mero A, Caboi F, Sergi M, Marongiu C, Pasut G. Site-specific pegylation of G-CSF by reversible denaturation. Bioconjugate Chem. 2007;18(6):1824–30.

[65] Persson C, Subramaniyam D, Stevens T, Janciauskiene S. Do native and polymeric alpha1-antitrypsin activate human neutrophils in vitro? Chest 2006;129(6):1683–92.

[66] Janciauskiene S, Dominaitiene R, Sternby NH, Piitulainen E, Eriksson S. Detection of circulating and endothelial cell polymers of Z and wild type alpha 1-antitrypsin by a monoclonal antibody. The Journal of biological chemistry 2002;277(29):26540–6.

[67] Zhang C, Desai R, Perez-Luna V, Karuri N. PEGylation of lysine residues improves the proteolytic stability of fibronectin while retaining biological activity. Biotechnology journal 2014;9(8):1033–43.

[68] Zhang C, Hekmatfar S, Ramanathan A, Karuri NW. PEGylated human plasma fibronectin is proteolytically stable, supports cell adhesion, cell migration, focal adhesion assembly, and fibronectin fibrillogenesis. Biotechnology progress 2013;29(2):493–504.

[69] Danial M, van Dulmen THH, Aleksandrowicz J, Pötgens AJG, Klok H-A. Site-specific PEGylation of HR2 peptides: effects of PEG conjugation position and chain length on HIV-1 membrane fusion inhibition and proteolytic degradation. *Bioconjugate Chem.* 2012;23(8):1648–60.

VII. SUPPLEMENTARY MATERIALS

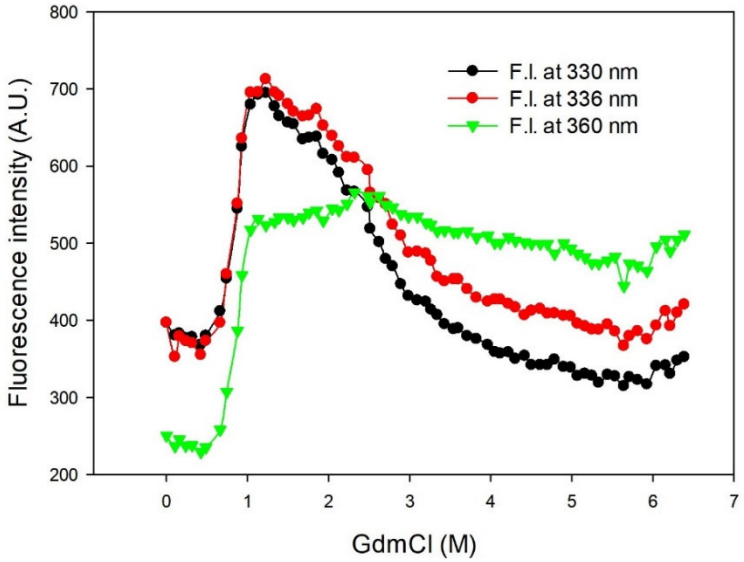

Supplement figure 1. GdmCl-unfolding curve monitored by fluorescence intensity at 330, 336 and 360 nm. The curves do not show a clear two- or three-state unfolding transition, which prevent the determination of the thermodynamic parameters associated with the unfolding transition.

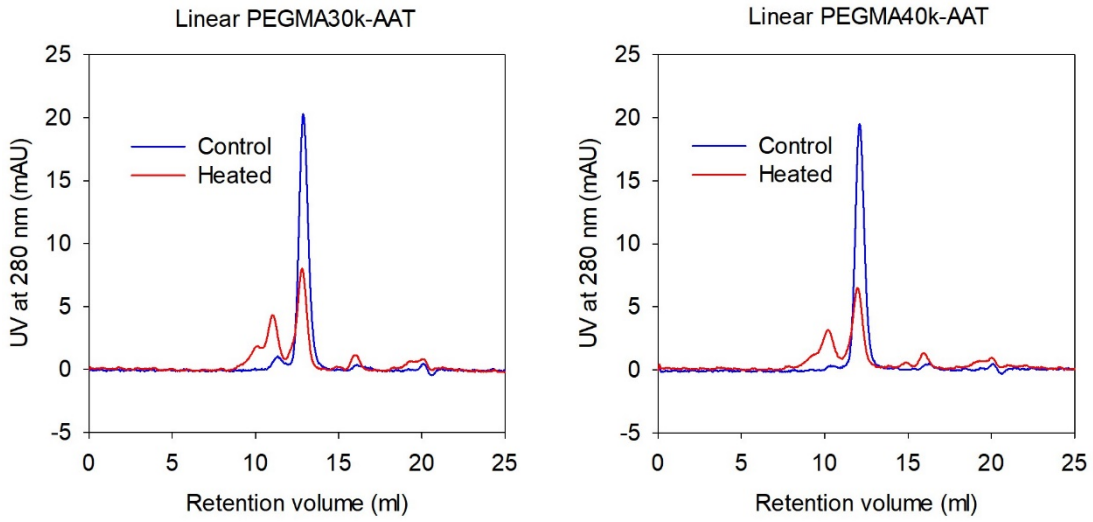

Supplement figure 2. Size exclusion chromatogram of linear PEGMA30k-AAT and linear PEGMA40k-AAT after heat treatment (70 °C, 1 h). PEG-AAT showed less content of aggregates after heating comparing to the unconjugated AAT.

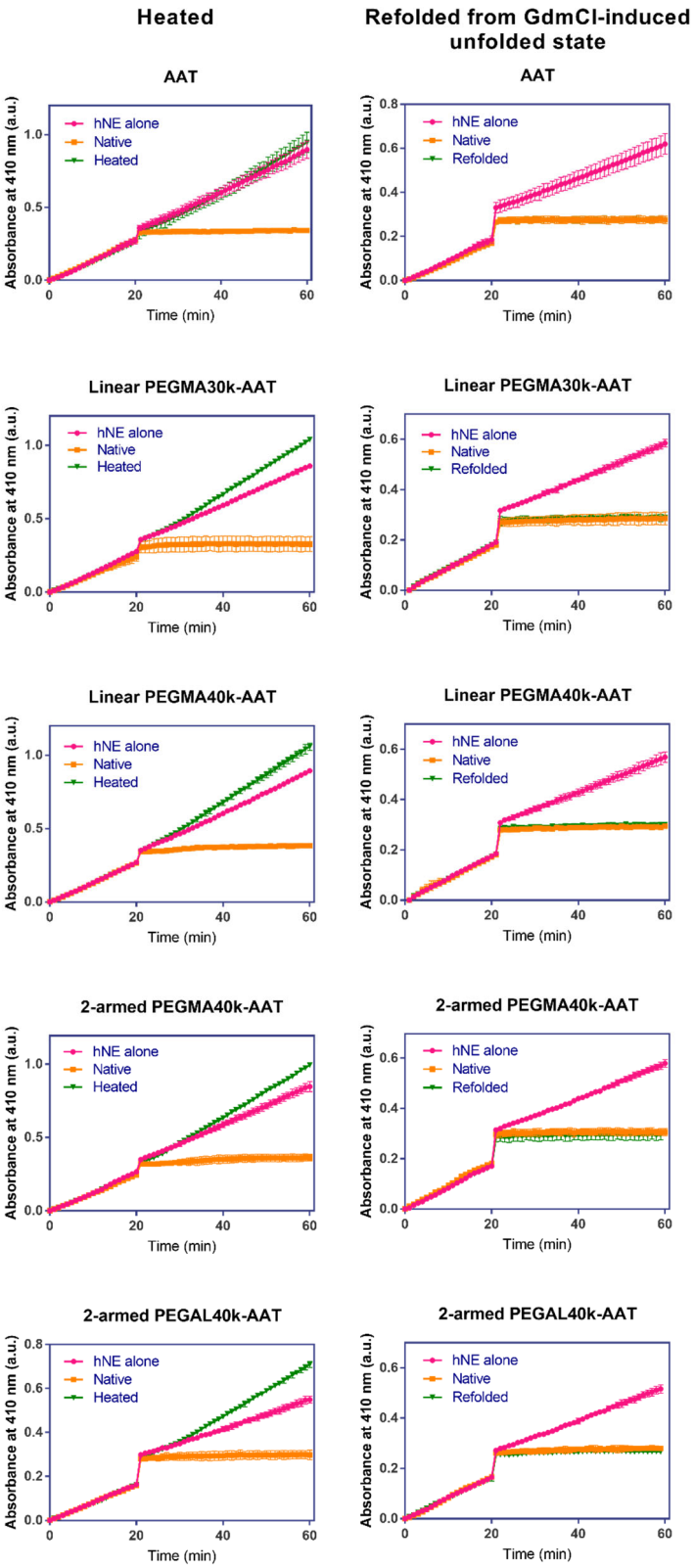

Supplement figure 3. hNE inhibitive capacity of AAT and PEGylated AAT at native state and refolded state from thermal and GdmCl-induced denaturation. The molar ratio of AAT or PEG-AAT to hNE was 1:1. After thermal denaturation, AAT and PEG-AAT were brought back to 25 °C and showed no inhibition to hNE, indicating that the thermal denaturation was not reversible. While after refolding from GdmCl-induced denaturation, the hNE inhibition activity was regained for AAT and PEG-AAT, indicating that the GdmCl-induced denaturation was reversible. In Chapter IV, this assay was optimized by adding 0.1 % BSA in the incubation buffer to reduce the protein binding of the 96-well plate.

CHAPTER IV

PEGYLATION OF ALPHA1-ANTITRYPSIN EXTENTS ITS CIRCULATION TIME AND PULMONARY RETENTION AND IMPROVES ITS THERAPEUTIC VALUE IN VIVO

Adapted from

Liu X, Ucakar B, Vanvarenberg K, Guy Wilfried Kouassi K, Marbaix E, Vanbever R. PEGylation of alpha1-antitrypsin extents its circulation time and pulmonary retention and improves its therapeutic value in vivo. In preparation.

ABSTRACT

Patients suffering from respiratory diseases associated with alpha-1 antitrypsin (AAT) deficiency can benefit from inhalation of AAT as an alternative to a weekly intravenous infusion. As a result of the rapid clearance of AAT from the respiratory tract, the rate of inhalation dosage is high and frequent, and the benefit of the treatment is limited. Because of the poor distribution in the lung after intravenous infusion, there is a high dose and, as a consequence, a high cost for augmentation therapy. Here, we present a PEGylated version of AAT that provides a prolonged body residence time following both administration routes. Specifically, conjugation of a 2-armed 40 kDa PEG increased eight-fold the serum half-life of AAT after intravenous injection and two-fold the half-life of AAT in the lung following intratracheal instillation. In a murine model of chronic obstructive pulmonary disease (COPD) induced by endotoxin and porcine elastase (PPE), AAT was able to decrease lung injury and the number of inflammatory cells in the lung. Conjugation of a 2-armed 40 kDa PEG to AAT offered similar efficacy as AAT conjugated to a linear 20 kDa PEG via intravenous route. Through an IV route, AAT was most effective in reducing inflammation and injury in the lung. Conjugation of a 2-armed PEG to AAT improved its efficacy via the IN route. In the course of establishing the COPD model and undergoing AAT or PEG-AAT treatment, anti-AAT, anti-PPE and anti-PEG antibodies developed. In spite of this, the generation of these antibodies did not cause any pathological changes in the lung tissue. PEGylated AAT exhibited the same stability to jet nebulization as AAT. The AAT derivative presented in our study provides sustained body residency. With an IN route, a 2-armed 40 kDa PEG was successful in improving the therapeutic efficacy in a murine model of COPD with a significantly lower dose compared to an IV route. Our study has provided promising data regarding the use of PEGylated AAT in the augmentation therapy for patients with AAT deficiency.

KEYWORDS

Alpha-1 antitrypsin, chronic obstructive pulmonary disease, PEGylation, neutrophil elastase

TABLE OF CONTENTS

I. INTRODUCTION

Alpha-1 antitrypsin (AAT) deficiency is a genetic autosomal disease, characterized by low serum level (<11 μM) of alpha-1 antitrypsin (AAT) [1]. AAT is a 52-kDa glycoprotein produced primarily by hepatocytes [2]. It is an abundant circulating serine protease inhibitor with anti-inflammation and immune-regulatory capacities [3]. Insufficient levels of AAT within the lung results in premature emphysema and chronic obstructive pulmonary disease (COPD) [4]. Intravenous augmentation of plasma-purified human AAT is the only approved therapy for patients who develop respiratory disease. Despite the long half-life (4-5 days), only 2 % of the delivered AAT can reach the lung epithelial lining fluid following administration [5, 6]. Thus, a very high dose of AAT (60 mg/kg) is necessary in this therapy, resulting in high costs (over 100,000 dollars per patient). Financial constraints prevent approximately one third of those known to be AAT deficient from receiving the therapy [7].

To overcome the low penetration rate in the lung following intravenous injection, inhaled AAT has been developed as an alternative route of administration, providing easier and more effective delivery of AAT directly to the lung. In a phase II/III clinical trial in patients with AAT deficiency (dose of AAT: 80 mg twice daily per patient), inhaled AAT did not prolong the time to first exacerbation. However, the severity of the disease exacerbation, including the degree of dyspnea, the sputum volume, and the sputum purulence [8], decreased with AAT treatment, suggesting that it is capable of reducing the incidence or severity of dyspnea [9]. The limited efficacy of inhaled AAT may result from the rapid clearance from the lung caused by proteolytic breakdown [10], oxidation [11, 12] and phagocytes uptake. Therefore, it may be beneficial to prolong the residence of AAT within the lungs in order to improve the therapeutic efficacy of inhaled AAT.

PEGylation is commonly used to improve the therapeutic value of a protein by prolonging its body residence time and there are several PEGylated proteins approved by the FDA and EMA for clinical use [13–15]. PEGylation increases the serum half-life of a protein by reducing renal clearance, enhancing proteolytic resistance and reducing recognition by specific antibodies [16]. PEGylation can also reduce the recognition and uptake by macrophages thus prolonging the protein half-life [17]. PEGylation has been demonstrated to improve the residency in the lung of proteins after pulmonary delivery [18–21]. Accordingly, PEGylation could extend the local residency of AAT. However, PEGylation was reported to have different effects on different proteins, making it difficult to predict its influence on AAT. In addition, PEGylation may affect a protein's structure, stability [22] and most importantly, activity [23]. It is therefore important to determine the physicochemical and biological properties of PEGylated derivatives to identify the most suitable candidate.

Cantin et al. reported that recombinant non-glycosylated human AAT (rhAAT) conjugated to 20 kDa PEG was persistent in bronchoalveolar lavage (BAL) in mice for at least 48 hours following intranasal administration, in contrast to unmodified rhAAT which was cleared within 24 hours [18]. In addition, the PEGylated rhAAT provided longer lung protection against human elastase in a murine model of acute lung injury than the unconjugated protein. However, the therapeutic efficacy of the PEGylated rhAAT in a comprehensive or long-term murine model was not investigated, nor did the authors investigated the immunogenicity of PEGylated rhAAT and the unconjugated rhAAT. In our previous studies, we synthesized PEG-AAT conjugates using linear 30 kDa PEG, linear 40 kDa PEG and 2-armed 40 kDa PEG by two different PEGylation reactions, using plasma-derived AAT, which presents longer half-life compared to rhAAT. The mono-PEGylated AAT showed full biological activity and the same stability to chemical denaturant as the unconjugated AAT[24]. In addition, PEGylation increased AAT resistance to high temperature (Chapter III).

The present study examines the stability of AAT and PEG-AAT to proteolysis. The in vivo study was conducted on a PEG-AAT conjugate that exhibited the best proteolysis resistance. The in vivo pharmacokinetics of the selected PEG-AAT was investigated. Based on the promising finding that PEGylation prolongs the residence time of AAT following intravenous injection and inhalation, we investigated the therapeutic efficacy of AAT and PEG-AAT in an in vivo long-term COPD murine model following both routes of administration. The model was established by the IN instillation of 1.2 U PPE on day 1 of each week and 7 μg LPS on day 4 of each week for 4 consecutive weeks [25]. The results showed that intranasal delivery of AAT conjugated to a 2-armed 40 kDa PEG resulted in greater reductions in pulmonary injury and inflammation. A major cause of protein instability is unfolding and aggregation at the air-liquid interface [26], which is a particular challenge for the aerosolization of a protein. Mesh nebulization was used in the clinical trial of inhaled AAT [9]. Therefore, the stability of PEG-AAT to aerosolization was also determined.

II. MATERIALS AND METHODS

II.1. MATERIALS

Alpha-1 antitrypsin was purified from a commercial human AAT product – Pulmolast® (Lamepro; Breda, The Netherlands) by size exclusion chromatography (SEC) using an HiLoad 16/600 Superdex 200 pg (GE Healthcare Europe GmbH, Diegem, Belgium). The linear 30 kDa, 40 kDa and branched 40 kDa PEG-maleimide (PEGmal) were purchased from NOF Europe GmbH. The human sputum elastase (hNE), porcine pancreatic elastase (PPE) and the substrate N-Succinyl-Ala-Ala-Ala-pNitroanilide were purchased from Elastin Products Company, Inc (Owensville, USA). PEGylated recombinant human deoxyribonuclease I (PEG-rhDNase, PEG-dornase alfa) was provided by Williams et al previously. Unless otherwise mentioned, other reagents and chemicals were from Sigma-Aldrich, Inc (Overijse, Belgium).

II.2. PRODUCTION AND PURIFICATION OF MONO-PEGYLATED ALPHA1-ANTITRYPSIN

The mono-PEGylated AAT was synthesized by thiol PEGylation and N-terminal PEGylation as previously described[24]. Briefly, for thiol PEGylation, AAT (20 mg/ml) was reduced by tris(2-carboxyethyl) phosphine (TCEP) at a molar ratio of TCEP:AAT 4:1 in 10 mM NaH_2PO_4 and 110 mM NaCl, pH 7.1, at room temperature with mild agitation for 1 hour. PEG-maleimide (linear 30 kDa, 40 kDa and 2-armed 40 kDa) was then added to the reduced AAT at a PEG:protein molar ratio of 4:1. The PEGylation was carried out under mild agitation for 1 hour and ceased by adding 4-fold molar excess (comparing to the PEG reagent) of cysteine. For N-terminal PEGylation, a two-armed PEG-aldehyde (2-armed PEGald40k) was used. The reaction was carried out in 20 mM succinate buffer, pH 6, in the presence of 11.5 μM of sodium cyanoborohydride ($NaCNBH_3$). The concentration of AAT in the reaction mixture was 10 mg/ml and the molar ratio of PEGald to AAT was 2:1. The reaction was carried out overnight with mild agitation at room temperature. The mono-PEGylated AAT was purified by anion exchange chromatography. The fractions containing the mono-PEGylated AAT were pooled and concentrated using Vivaspin 15R sample concentrator (10,000 molecular weight cut-off, Sartorius, Stonehouse, Gloucestershire, UK) and stored in 10 mM NaH_2PO_4, 110 mM NaCl, pH 7.1 at 4 °C.

II.3. ELASTASE INHIBITION ASSAY

A modified elastase inhibition assay was used to evaluate the biological activity of AAT and PEG-AAT according to Bieth [27]. Briefly, at 37 °C, 0.034 μM hNE was pre-incubated with 0.3 mM

substrate N-Succinyl-Ala-Ala-Ala-pNitroanilide (Tris-NaCl buffer, pH 7.5) in a 96-well plate, with the presence of 0.1 % BSA, for 20 min. Afterwards, AAT or PEG-AAT was added to the mixture at a protein:hNE molar ratio of 0.5:1, 1:1, 1.5:1 and incubated for 40 min. During the incubation, the absorbance at 410 nm of each sample was recorded every 1 min. If the absorbance at 410 nm increases linearly in accordance with the incubation time, the increment of the absorbance at 410 nm of each sample (ΔODsp) after adding the unconjugated or PEGylated AAT was used to calculate the relative hNE activity. The ΔOD410 of the sample in absence of AAT or PEG-AAT (ΔODctr) represented the full activity of hNE. The relative hNE activity was calculated as follows: relative hNE activity (%) = ΔODsp / ΔODctr × 100 %.

II.4. STABILITY TO PROTEOLYSIS

Unconjugated AAT and thiol PEGylated AAT were incubated with matrix metalloproteinase-13 (MMP-13) with a protein:MMP-13 molar ratio of 30:1, in 50 mM Tris-HCl, 250 mM NaCl, 5 mM $CaCl_2$, pH 7, at 37 °C. MMP-13 was chosen as it does not form a protease-inhibitor covalent complex with AAT. After 3, 5 and 27 hours, the remaining activity of AAT or PEG-AAT were evaluated by elastase inhibition assay as described in section 2.3 with the protein:hNE molar ratio of 1:1. In parallel, protein samples were incubated in the absence of MMP-13 under the same conditions and was used as positive controls. The remaining elastase activity in control sample (RA_{ctr}) and proteolyzed sample (RA_{pro}) was calculated as described in 2.3. The relative elastase inhibition activity of AAT or PEG-AAT was calculated as follows: relative elastase inhibition activity (%) = $(1 - RA_{pro}) / (1 - RA_{ctr}) \times 100$ %.

II.5. KINETICS OF *IN VIVO* DISPOSITION FOLLOWING INTRAVENOUS INJECTION AND INTRATRACHEAL INSTILLATION

Experimental protocols were approved by the Institutional Animal Care and Use Committee of the Université Catholique de Louvain (2019/UCL/MD043). Female Swiss mice (6- to 8-week-old, Janvier Labs, France) were used. All experiments were conducted with an aim to minimize the discomfort of animals.

II.5.1. Administration

Unconjugated AAT and PEG-AAT were administrated by intravenous injection (60 mg/kg) or by the intratracheal route (1.35 mg/kg). The protein solution in 10 mM NaH_2PO_4, 110 mM NaCl, pH 7.1 was injected intravenously (100 µl), or instilled by intratracheal instillation (25 µl). For intratracheal instillation, the mice were anesthetized by ketamine/xylazine (90/10 mg/kg)

intraperitoneal injection prior to the instillation and were positioned with a 45 ◦ angle of tilt. A laryngoscope (Penn-Century Inc., Philadelphia, USA) was used to correctly place a 20G catheter (VWR International BVBA, Leuven, Belgium) into the trachea through the arytenoid cartilages. A precision syringe (100 µl, Model 710, Hamilton, Bonaduz, Switzerland) was used to deliver 25 µl of protein solution or storage buffer into the lung, followed by an air bolus of 200 µl (1 ml syringe, HSW SOFT-JECT®, VWR International BVBA, Leuven, Belgium). Another five mice did not receive any instillation, which served as negative controls.

II.5.2. Sample collection

Hank's balanced salt solution (HBSS, Thermo Fisher Scientific, Gent, Belgium) containing 0.1 % SDS and protease inhibitors was prepared using Pierce Protease inhibitor tablets (Thermo Fisher Scientific, Gent, Belgium) according to the manufacturer's instruction. The addition of SDS aimed to improve the recovery of PEG-AAT constructs. At pre-determined time points (immediately after administration, 4 h, 1, 3, 7 d after intravenous or intratracheal administration), the mice were sacrificed by cervical dislocation and the blood was collected intracardially. Five mice which did not receive any instillation were sacrificed as negative controls. Bronchoalveolar lavages (BAL) were performed by injecting 1 ml of Hank's balanced salt solution (HBSS, Thermo Fisher) containing protease inhibitors into the trachea followed by the withdrawal and re-injection of half of the fluid. The procedure was repeated 4 times. The lungs were harvested and grounded in 3 ml of HBSS containing protease inhibitors using a tissue grinder (Potter, Merck Eurolab, Belgium). The blood samples were centrifuged at 4,500 rpm at 4 °C for 10 min. The lung homogenate samples were centrifuged at 9,000 g at 4 °C for 10 min. The supernatant of BAL and lung homogenate was stored at -80 °C until they were analyzed for AAT and PEG-AAT content. The BAL samples were centrifuged at 300 g for 5 min. The supernatant was stored at -80 °C before further analysis while the cell pellets were suspended in 1 ml HBSS for the total cell counts. Afterwards, the cells were collected, and the cell lysis was performed using M-PER™ Mammalian Protein Extraction Reagent (Thermo Fisher Scientific, Gent, Belgium) and stored at -80 °C before further analysis.

II.5.3. Quantification of PEG, AAT and PEG-AAT in biological samples

The PEG content in biological samples were quantified by ELISA using a PEGylated protein ELISA kit (Enzo Life Science; Farmingdale, NY, USA). The AAT or PEG-AAT content were quantified using a Human Serpin A1 DuoSet ELISA kit (R&D system, Abingdon, UK) according to the manufacturer's protocols. The assay exhibits no cross-reactivity or interference with murine AAT. The concentration of AAT or PEG-AAT was plotted against the time after administration.

The half-life in plasma or in BAL were calculated by fitting the data with a one phase decay model in GraphPad Prism 9 (GraphPad Software, USA).

II.5.4. Quantification of total protein and cytokine content in BAL

The total protein content in BAL (at the time point of 4 h and 1 day) was quantified by bicinchoninic acid (BCA) assay using Pierce BCA Protein Assay Kit (Thermo Fisher Scientific, Gent, Belgium). The TNF-α content in BAL (at the time point of 4 h) was quantified by Mouse TNF-alpha DuoSet ELISA (R&D system, Abingdon, UK) according to the manufacturer's protocol.

II.6. THERAPEUTIC EFFICACY OF AAT AND PEG-AAT ON COPD MICE

Experimental protocols were approved by the Institutional Animal Care and Use Committee of the Université Catholique de Louvain (2020/UCL/MD/030). Female C57BL/6 (6- to 8-week-old, Janvier Labs, Laval, France) were used. All experiments were conducted with an aim to minimize the discomfort of animals.

II.6.1. COPD model and administration

The murine COPD model was established according to Sajjan and Singanayagam [25, 28]. In the AAT protocol, fifty-five C57BL/6 mice were divided randomly into 5 groups: saline, LPS/PPE, 12 μg, 40 μg and 120 μg AAT treatment group. Mice were anesthetized with ketamine/xylazine (72/8 mg/kg) and then challenged by intranasal (IN) instillation of 1.2 U porcine pancreatic elastase (1.2 U PPE/50 μl) on day 1 of each week and 7 μg (~ 70 U) of lipopolysaccharide (7 μg LPS/50 μl) on day 4 of each week for 4 consecutive weeks. Mice in the saline group received the same volume of saline solution (phosphate buffered saline, PBS) intranasally instead of PPE and LPS. Unconjugated AAT (doses: 12 μg, 40 μg, 120 μg in 50 μl/mouse) were administrated intranasally 2 hours before each administration of PPE or LPS. Each intranasal administration involved the delivery of a total volume of 50 μl: 25 μl deposited in each nostril. Mice in the LPS/PPE group were challenged with PPE and LPS but received the same volume of AAT storage buffer (10mM NaH_2PO_4, 110mM NaCl, pH 7.1, LPS-free) without AAT. Seven days after the last administration, the mice were sacrificed by cervical dislocation.

In the PEG-AAT protocol, a dose of AAT (12 μg per mouse) presenting a sub-optimal efficacy in the AAT protocol was used. In the PK study, the dose of injected AAT reaching the lung was 2.65 %. The IV dose of AAT and PEG-AAT was determined by taking into account of AAT penetration in the lung following IV, which was 454 μg per mouse to enable that ~12 μg protein

will penetrate in the lung. PEG was not counted in the mass of PEG-AAT. Eighty-eight mice were divided randomly into 8 groups: saline, two LPS/PPE groups (as controls for either IV or IN treatment, IV LPS/PPE and IN LPS/PPE), IV AAT, IV 2-armed PEG40k-AAT (IV PEG40), IV linear PEG20k-AAT (IV PEG20), IN AAT, IN 2-armed PEG40k-AAT (IN PEG40) treatment group. The model establishment was performed as described in the AAT protocol.

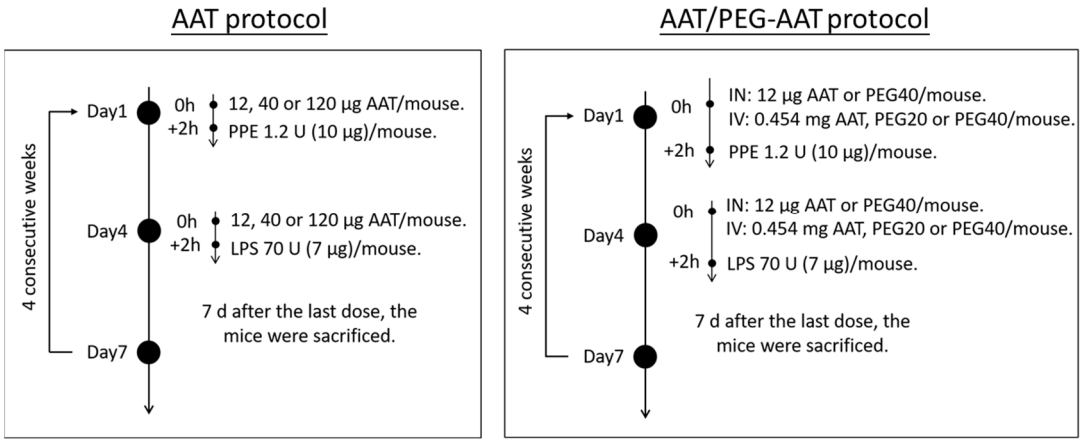

Figure 1. Timeline of the long-term in vivo efficacy study in C57BL/6 mice. The COPD murine model was established by the IN instillation of 1.2 U PPE on day 1 of each week and 7 µg LPS on day 4 of each week for 4 consecutive weeks. The treatment groups received AAT or PEG-AAT 2 h prior to the PPE or LPS challenge. The control groups received the corresponding buffer (for AAT, PEG-AAT, LPS and PPE) instead. PEG was not counted in the mass of PEG-AAT delivered.

II.6.2. Sample collection

In both experiments, blood samples were collected from all the mice in each group. For 6 mice in each group, a nasal lavage (NAL) was performed by cannulating the trachea toward the nasal cavity and instilling 1 ml HBSS. BALs, cell pellet and lung tissue homogenates were collected as described above using HBSS. The lungs from the other 5 mice were primarily used for histological analysis. The NAL and BAL were not performed on those mice to prevent the damage to the lung air spaces.

II.6.3. Sample analysis

On the day of sacrifice, collected BAL samples were analyzed for lactate dehydrogenase (LDH) activity according to the manufactory instructions (Sigma-Aldrich, Inc; Overijse, Belgium). Further, the total protein content in BAL was quantified by bicinchoninic acid (BCA) assay using Pierce BCA Protein Assay Kit. The mouse albumin content in BAL was quantified by Mouse Albumin AssayMax™ ELISA Kit (ImTec Diagnostics NV, Antwerp, Belgium). Cytokine and chemokine levels (Interleukin 1 beta, IL-1β; Interleukin 6, IL-6; Tumor necrosis factor alpha, TNF-α; Macrophage inflammatory protein 2, MIP-2) were quantified using U-PLEX Biomarker Assay. The

assay kit was purchased from Meso Scale Discovery (Maryland, USA). The level of AAT and PEG-AAT in biological samples were measured using commercial Human SerpinA1 DuoSet ELISA kits according to the manufacturer's instructions. To assess the immunological response caused by PPE, AAT or PEG in the COPD mice, anti-PPE, anti-AAT or anti-PEG antibodies in the plasma was determined by an in-house ELISA using PPE-, AAT- or PEG-rhDNase coated plates and a polyclonal donkey anti-mouse IgG conjugated to HRP (R&D Systems, Abingdon, UK) as detection antibody. The plasma samples were serially diluted 3- or 5-fold and then tested on the ELISA. The level of anti-AAT or anti-PPE was expressed by ELISA titer which was the dilution that presented an optical density of 0.3 at 450 nm. The ELISA titer was calculated by linear fitting the Log (dilution factor) versus optical density at 410 nm in GraphPad Prism 9 (GraphPad Software, USA).

After collecting the cell pellet from the BAL, the total cell count was performed by mixing 10 µl of cell suspension with 10 µl trypan blue and counting by a TC20™ automated cell counter (Bio-Rad, Hercules, CA, USA). Afterwards, a cytospin™ (Thermo Fisher Scientific, Rockford, IL, USA) was performed to get 30,000 cells on Superfrost plus® microscope slides (Thermo Fisher Scientific, Rockford, IL, USA). Fixation of cells was carried using staining set Diff-Quik® (Medion Diagnostics, Düdingen, Switzerland). Macrophages, neutrophils, lymphocytes and eosinophils were counted using Axioskop 40 microscope (Carl Zeiss, Oberkochen, Germany).

For 3 - 5 mice in each group, the lung tissue was removed and inflated with 4 % formaldehyde. The lung tissues were fixed in 50 ml 4 % formaldehyde for 24 h. Fixed lung samples were embedded in paraffin wax and 5-μm-thick histological sections were cut and stained with hematoxylin and eosin (H&E). The analysis of histological sections was performed in collaboration with Prof. Etienne Marbaix, in Institut de Duve, Université Catholique de Louvain. The sections were scanned by a Hamamatsu NanoZoomer 2.0 RS (Hamamatsu, Japan) at original magnification 40X.

To systematically evaluate the efficacy of AAT and PEG-AAT, we generated a score system where if a readout was decreased by less than 50%, the treatment scored 1 point, if decreased more than 50% but not significantly, the treatment scored 2 points, if the decrease was significant, the treatment scored 3 points. The treatment which scored the highest points exhibited better therapeutic efficacy.

II.7. STABILITY TO AEROSOLIZATION

Unconjugated AAT and PEG-AAT (2 ml, 0.4 mg/ml) were nebulized by a jet nebulizer compressor system (Lot. IIA924, Philips, The Netherlands) for 10 min. The droplets were collected from the nebulizer using a homemade collection system. The UV spectra of nebulized and control samples were recorded by a NanoDrop 2000/2000c Spectrophotometer (Thermo Fisher Scientific, Gent, Belgium) to identify the insoluble aggregates. The biological activity of each sample was assessed by the elastase inhibition assay. The samples were then filtered through a 0.22 μm polyvinylidene fluoride (PVDF) syringe-tip and subjected to a Superose 6 increase 5/150 GL column (GE Healthcare Europe GmbH, Diegem, Belgium) to analyze soluble aggregates or degradation fragments.

II.8. STATISTICS

All results are presented as mean values ± standard error of the mean (SEM). GraphPad Prism 9 (GraphPad Software, USA) was used to analyze the statistical differences.

III. RESULTS

III.1. STABILITY OF AAT AND PEG-AAT TO PROTEOLYSIS IN VITRO

AAT is a serine protease inhibitor, which can inhibit a wide range of proteases, including the serine proteases family, cysteine proteases family, et cetera. Matrix metalloproteinases (MMPs) were reported to have a proteolytic effect on AAT, without being inhibited by AAT [29]. This family of proteases is produced by inflammatory cells (neutrophils and alveolar macrophages). In patients with COPD, MMP-13 expression is increased in the lungs [30]. It is therefore of interest to investigate the resistance of AAT and PEG-AAT to this protease. According to Figure 2, after exposure to MMP-13 for 3, 5 and 27 hours, AAT and PEG-AAT showed decreased activities as exposure time increased. AAT is susceptible to MMP-13 proteolysis; it actually loses approximately 50% of its ability to inhibit hNE after three hours of exposure to MMP-13 and all of its activity after twenty-seven hours. PEG-AAT showed stronger resistance to MMP-13. All PEG-AAT lost less than 20% of their activity after three hours. The activity loss of AAT conjugated to 2-armed 40 kDa PEG molecules was lower with prolonged exposure compared to those conjugated to linear PEG molecules. Over fifty percent of the activity of two-armed PEG40k-AAT remains after a 27-hour exposure. These results highlight that PEGylation very significantly improves the proteolytic resistance of AAT. Proteolytic resistance can be enhanced by increasing the PEG molecular weight or changing the structure of the PEG; in fact, the 2-armed PEG conferred the best enhancement.

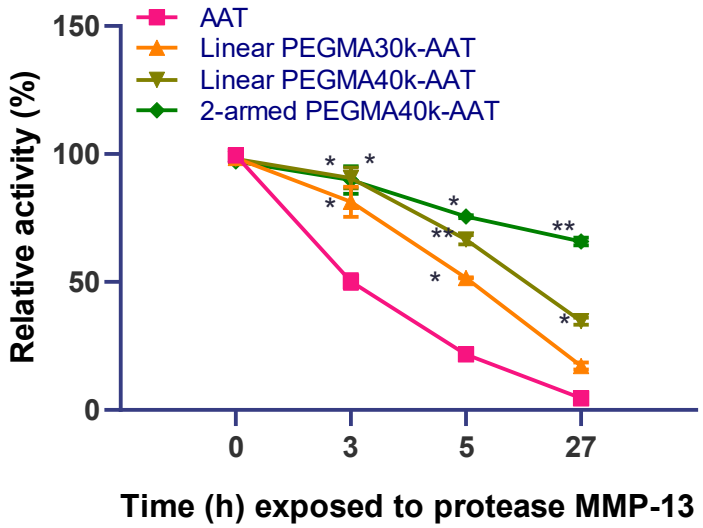

Figure 2. The hNE inhibition activity (AAT or PEG-AAT:hNE molar ratio was 1:1) of AAT and PEG-AAT after the exposure to the protease MMP-13 for 3, 5 and 27 hours. MMP-13 exposure led to the loss of AAT's hNE inhibitory activity more rapidly than PEG-AAT. Two-armed PEGmal40k-AAT maintained >50 % of the activity after 27 h exposure. The statistic difference was analyzed by fitting a mixed model in GraphPad Prism 9. The star marks next to each data point indicate a significant difference (* $p<0.05$, ** $p<0.01$) relative to AAT.

III.2. PHARMACOKINETICS OF AAT AND PEG-AAT *IN VIVO* FOLLOWING INTRAVENOUS OR PULMONARY DELIVERY

To compare the body residence of AAT and PEG-AAT in Swiss mice, unconjugated AAT and PEG-AAT were given intravenously (60 mg/kg) or intratracheally (1.35 mg/kg). The IV dose was selected based on the clinical dose of AAT for intravenous infusion [5]. The IT dose was determined according to the inhaled dose of AAT in clinical trials [9]. At different time points after administration, we measured the protein or PEG content of plasma, BAL, BAL cells lysis, and lung homogenate supernatants by ELISA.

The body residence time of AAT was significantly prolonged upon conjugation of PEG. As shown in Figure 3A, seven days after the IV injection, AAT and PEG40-AAT were both detectable in the plasma, however, the concentration of PEG40-AAT (8.27 ± 1.9 μg/ml) was 132-fold as that of AAT (0.06 ± 0.003 μg/ml). Figure 3B showed that following IT delivery, on day 7, the concentration of PEG40-AAT in BAL (0.23 ± 0.07 μg/ml) was 29-fold that of AAT (0.007 ± 0.002 μg/ml). In addition, PEG40-AAT was detectable in BAL 10 days after IT administration (0.07 ± 0.03 μg/ml) while AAT was fully cleared. Following IV injection, the serum half-life of PEG40-AAT was eight-fold longer than the one of unconjugated AAT (Figure 3A). In addition, PEG40-AAT presented a two-fold longer half-life than AAT following IT (Figure 3B).

In the four hours following the IV dose, AAT content in BAL and cell lysis was significantly higher ($p<0.05$) than that of PEG40-AAT (Figure 3C, E), indicating that AAT diffused more quickly into the alveolar spaces and was also rapidly up taken by alveolar macrophages. AAT levels and PEG40-AAT levels in lung homogenates did not differ significantly (Figure 3D), suggesting that despite PEG40-AAT's prolonged plasma residence, its lung penetration may be limited. Due to its prolonged residence in the lung, PEG40-AAT levels in plasma were significantly higher following IT (Figure 3F). AAT levels in lung homogenates dramatically increased at 4 h (Figure 3G), suggesting that AAT was rapidly absorbed in the lung and PEG40-AAT remained longer in the airways. By comparing the area under the curve (AUC) in BAL, lung homogenate and plasma, we observed that 2.65 % of the IV dose finally reached the lung, which is consistent with the clinical data [5, 6].

The PEG content on day 3 and day 7 following IV or IT was also quantified by ELISA. On day 7, the plasma and lung PEG content decreased compared to day 3, indicating that the PEG was gradually eliminated from the body (Figure 4A, B). Following IV, PEG content in pulmonary cell lysis increased on day 7. This may indicate that PEG accumulates in alveolar macrophages.

AAT and PEG-AAT were measured for their bioavailability in mice by determining the total protein content and total TNF-α concentration in BAL four hours after administration. Figure S1 illustrates how AAT and PEG40-AAT had an increasing tendency on total protein content in BAL following both administration routes. TNF-α levels in BAL of the AAT group were higher than those in the saline group following IT ($p<0.05$). Similar trend was observed following IV route. On the other hand, the TNF-α level in PEG40-AAT group did not show significant difference compared with that of the saline group.

PEG40-AAT had a slower rate of lung penetration and diffusion following IV administration, as revealed in the PK profile. Despite its longer residence in the circulation, PEG40-AAT did not significantly differ from AAT in terms of pulmonary content. Our hypothesis was that the large size of the conjugated PEG hindered the lung penetration of the PEG-AAT conjugate. In order to investigate whether conjugating a smaller PEG would facilitate lung penetration, we measured PEG20-AAT levels in plasma and lung following IV injection. Although PEG20-AAT also showed increased body residence time, the prolongation was not as remarkable as PEG40-AAT (Figure 4C, D). In the plasma on day 3, the content of PEG20-AAT was 2.2-fold that of AAT, whereas that of PEG40-AAT was 5.7-fold that of AAT. Interestingly, on day 1, the level of AAT, PEG20-AAT and PEG40-AAT in the lung were similar. The PEG20-AAT content in the lung was slightly higher on day 3 than that of the PEG40-AAT, although this difference was not significant ($p=0.44$). This suggests that PEG20-AAT presents similar lung penetration as PEG40-AAT.

To understand whether the PEGylation site has an impact on the body residency of PEG-AAT, we delivered N-terminal PEGylated AAT (synthesized using 2-armed 40 kDa PEG-aldehyde, PEGald40-AAT) by IT and compared the content of PEGald40-AAT to PEGmal40-AAT 3 days after the instillation. According to Figure 4E - H, PEG40-AAT and PEGald40-AAT were both retained longer in the lungs than AAT. PEGmal40-AAT, however, remained in the airways for a longer period of time than PEGald40-AAT ($p<0.05$), suggesting that thiol PEGylation might be more effective in improving pulmonary retention of AAT.

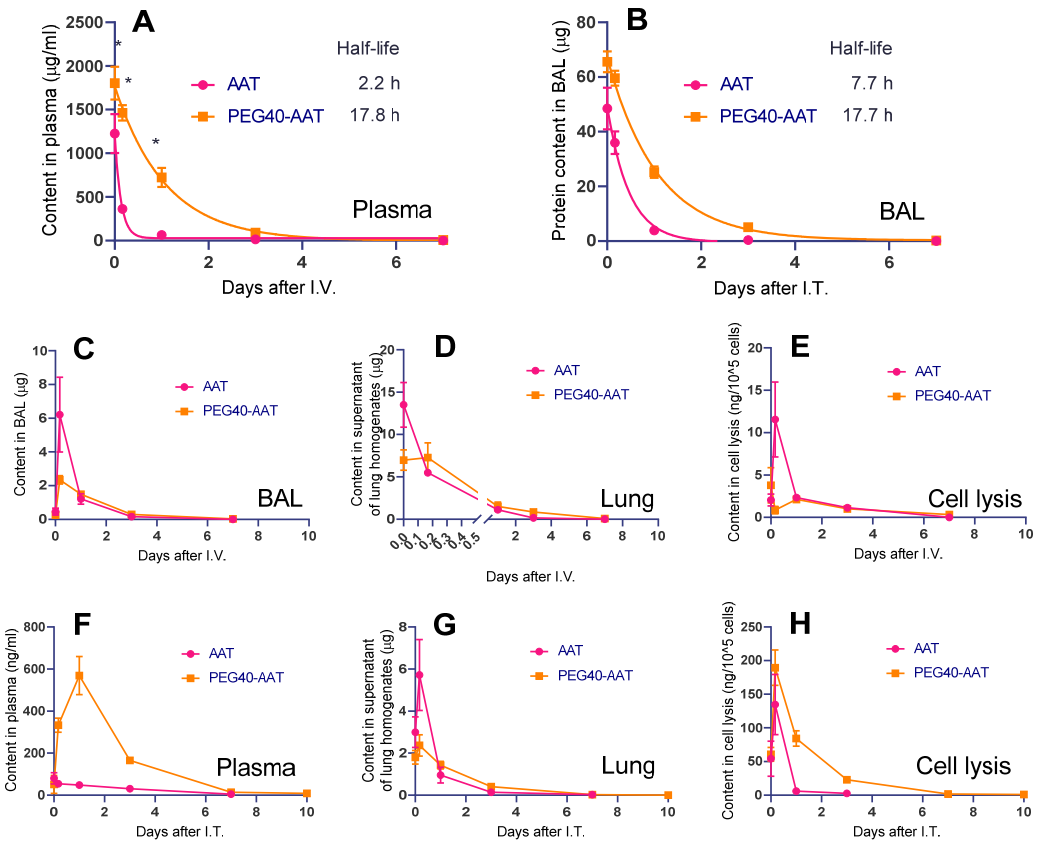

Figure 3. Pharmacokinetics of AAT and PEG-AAT in Swiss mice. The PEG-AAT conjugate were synthesized by thiol PEGylation using 2-armed 40 kDa PEG-maleimide. The amount of AAT and PEG40-AAT was expressed without considering the mass of the PEG. Data are presented as mean ± SEM of 5–6 mice per group. PK profile and half-life of AAT and PEG40-AAT following IV (A) or IT (B). PEGylation increased eight-fold the serum half-life of AAT and increased two-fold the half-life of AAT in the lung. Quantities of AAT or PEG40-AAT recovered from BAL (C), supernatant of lung homogenates (D), and cell lysis (E) at 10 min, 4 h, 1, 3, and 7 d following IV, or from plasma (F), supernatant of lung homogenates (G) and cell lysis (H) at 10 min, 4 h, 1, 3, 7 and 10 d following IT. Via IV route, AAT diffused into airways more rapidly than PEG40-AAT, but was also quickly cleared by macrophage uptake as AAT levels in cell lysis significantly exceeded those of PEG40-AAT at 4 h after IV ($p<0.05$). PEG40-AAT remained longer in the airway spaces following IT, while AAT was absorbed more rapidly into the lung. The level of PEG40-AAT in plasma was significantly higher ($p<0.05$) due to its prolonged residency in the lung. The half-life of AAT and PEG-AAT was calculated by fitting the data to a one phase decay model by GraphPad Prism 9. AAT was compared to PEG40-AAT for each time point by fitting a mixed model using Sidak comparison (* $p<0.05$).

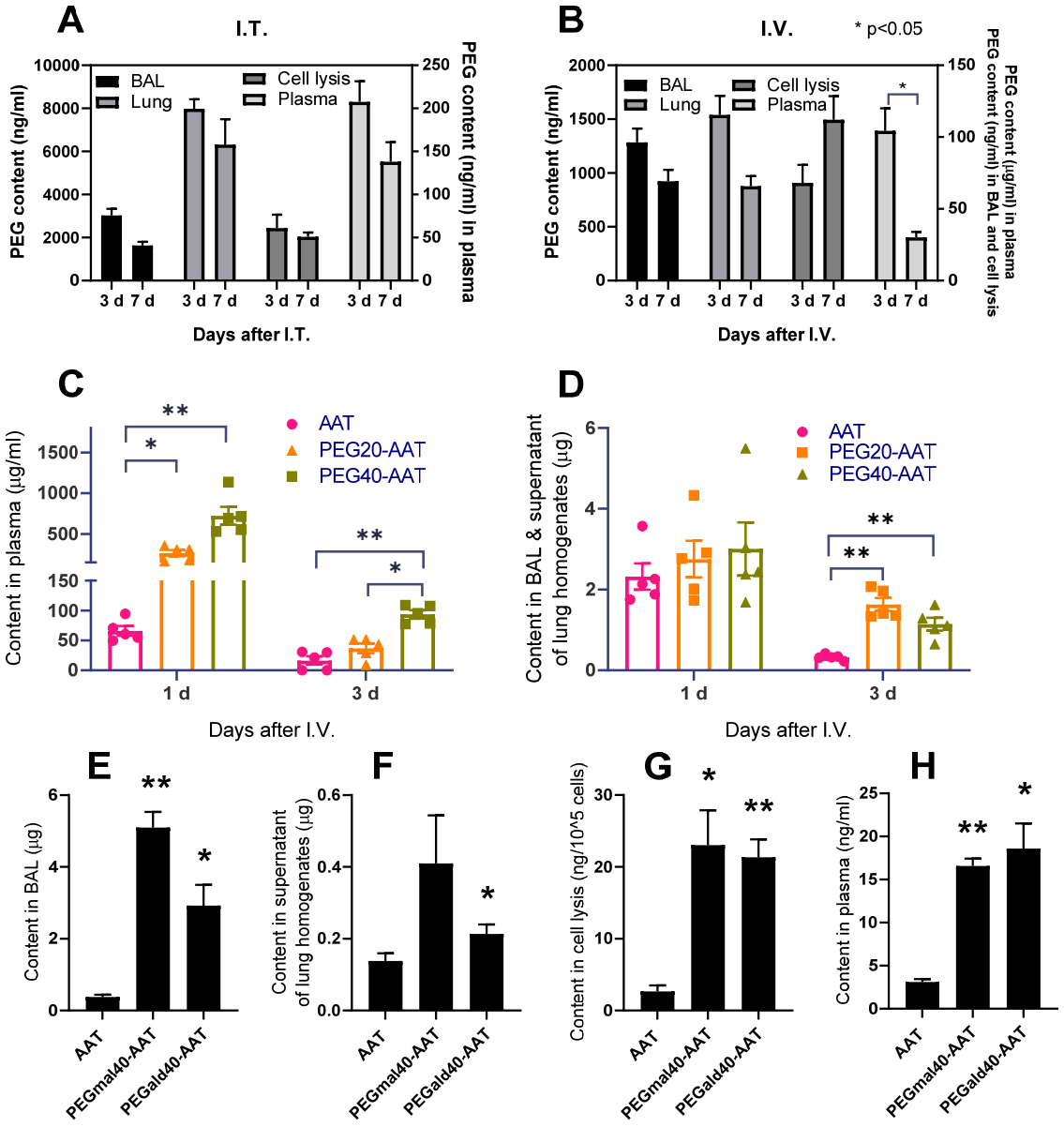

Figure 4. The content of PEG on day 3 and day 7 following IT (A) and IV (B). In the lung and plasma, the content of PEG on day 7 was lower than the one on day 3, indicating that PEG was gradually eliminated. On day 7, however, the amount of PEG in pulmonary cell lysis increased following IV. This may indicate that PEG was cleared by the endocytosis of the alveolar macrophages. The content of AAT, PEG20-AAT and PEG40-AAT in plasma (C) and in the lung (D) 1 and 3 days after IV. At day 1 and 3, both PEG20-AAT and PEG40-AAT showed higher levels in circulation, while on day 3, the levels of PEG40-AAT were twice as high as those of PEG20-AAT, indicating that increasing the PEG size would further prolong AAT's body residency. Neither PEG20-AAT nor PEG40-AAT were significantly different in their lung content, indicating that their lung penetrations were comparable. Quantities of AAT, PEGmal40-AAT and PEGald40-AAT recovered from BAL (E), supernatant of lung homogenates (F), cell lysis (G) and plasma (H) 3 d after IT. As compared to AAT, PEGmal40-AAT and PEGald40-AAT remained longer in the lung. They also showed a high level of plasma and cell lysis. In contrast, PEGmal40-AAT showed longer residency in the airway spaces than PEGald40-AAT ($p<0.05$). The comparison of AAT and PEG-AAT were performed by two-way ANOVA using Turkey comparison (* $p<0.05$, ** $p<0.01$).

III.3. THERAPEUTIC EFFICACY OF AAT AND PEG-AAT IN COPD MICE

We evaluated the therapeutic efficacy of AAT, PEG20-AAT and PEG40-AAT via the IV or IN route to resolve the lung injury and inflammation in COPD mice. Since over 90 % of delivered AAT was cleared within 24 h from the lung after intratracheal instillation, while PEG40-AAT offered a doubled half-life, we planned to administrate AAT and PEG-AAT twice a week, 2 h prior to the PPE or LPS challenge. With the goal to choose an AAT dose which presents a sub-optimal efficacy, we evaluated three different AAT doses (12, 40 and 120 μg per mouse) in the AAT protocol (Figure 1). Three doses represent a third, the same and a threefold molar ratio of AAT compared with the PPE delivered, in which the 40 g per mouse dose was approximately 1.5-fold as the dose of inhaled AAT in clinical trials (1.35 mg/kg).

During the model establishment and IN treatment, the average weight of all mice did not show significant increase (Figure 5A), possibly due to the repeated anesthesia before each IN instillation. There were no weight differences between groups. Total protein, albumin content and LDH activity in BAL were determined to assess the alveolo-capillary barrier integrity, and pulmonary cell injury. According to Figure 5B and C, all groups exhibited similar levels of total protein and albumin. As shown in Figure 5D, the LDH activity in the LPS/PPE group was significantly higher than that in the saline group, suggesting that the COPD modeling resulted in damaged pulmonary cells. Upon increasing the AAT dose, the LDH activity in BAL also decreased, indicating an apparent dose-dependent effect on reduction in pulmonary cell injury and inflammation. This effect was dose dependent. Four inflammation markers were quantified in BAL, in which IL-1β and IL-6 were not detected in any BAL samples. The level of MIP2 and TNF-α in the LPS/PPE group was not higher compared with the saline group (Figure 5E and F). All three doses of AAT successfully decreased the level of MIP2 and TNF-α in BAL. However, the decreases were not dose-dependent.

Differential cell counts were used to evaluate the lung inflammation. Figure 6 showed that the numbers of neutrophils, lymphocytes and eosinophils significantly increased in LPS/PPE group, confirming that the model resulted in pulmonary inflammation. As compared to the LPS/PPE group, AAT significantly reduced the number of neutrophils. However, this effect was not dose dependent. There was an increased number of eosinophils in groups other than the saline group. This might indicate an allergic response in COPD mice as both PPE and AAT are not of murine source.

To confirm the possible immunological response caused by AAT and PPE in COPD mice, we analyzed the level of anti-PPE and anti-AAT in the plasma by an in-house ELISA assay (Figure 7). Anti-AAT antibodies were detected in AAT treatment groups. The level of anti-AAT antibody in AAT 40 μg group was significantly higher than that of AAT 12 μg group. Anti-PPE was not detected in the saline group. The level of anti-PPE antibodies was not significantly different between each group. These results suggest that both PPE and AAT induced an immunological response in COPD mice, possibly associated with increased levels of eosinophils in all groups except the saline group.

Histological examination of the lungs was conducted to detect any possible pathological differences among the groups. As shown in Figure S2, mice in the saline group showed histology with no accumulation of inflammatory cells in the alveolar spaces. In the LPS/PPE group, peribronchial and perivascular inflammation with small accumulations of inflammatory cells were observed. Mice treated with different doses of AAT also showed mild small accumulation of inflammatory cells near blood vessels.

Attempts were made to quantify the possible residual levels of AAT in BAL, lungs and plasma. However, AAT was not detected by ELISA, indicating that AAT was fully cleared 7 days after the IN administration.

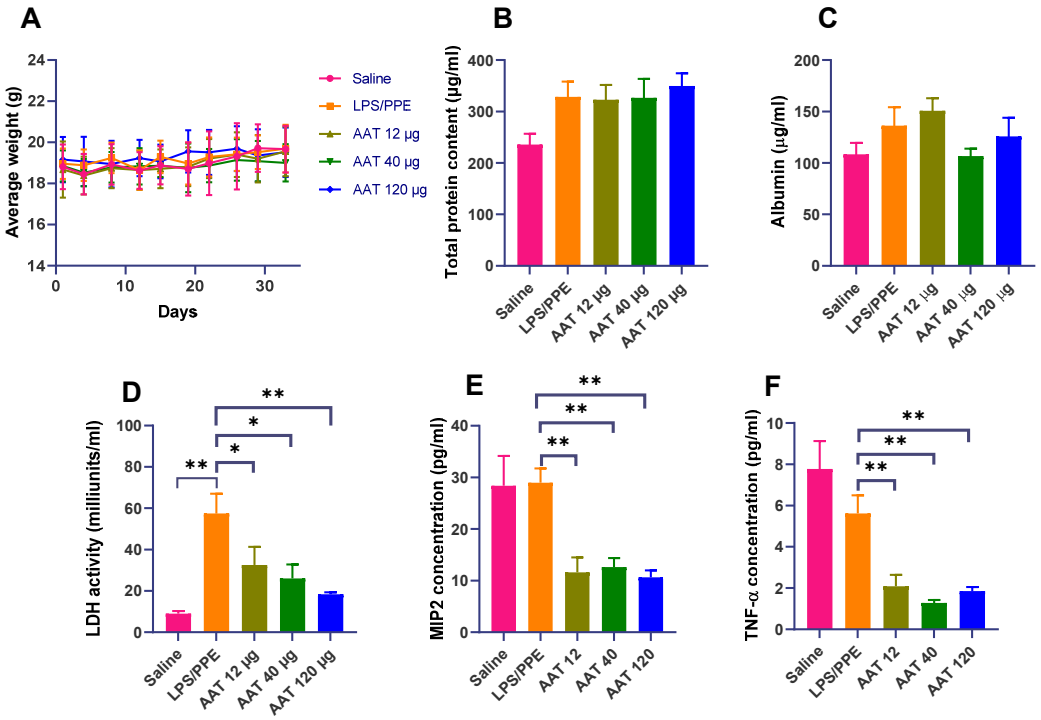

Administration	Groups				
	Saline	LPS/PPE	AAT 12 µg	AAT 40 µg	AAT 120 µg
Saline	+	+	-	-	-
LPS/PPE	-	+	+	+	+
AAT	-	-	12 µg	40 µg	120 µg

Figure 5. In vivo therapeutic efficacy of different doses (12, 40 and 120 µg per mouse by IN) of AAT on murine COPD model, which was established by intranasal instillation of 1.2 U PPE on day 1 and 7 µg of LPS on day 4 of each week for 4 consecutive weeks. Mice in the saline group received the same volume of saline solution intranasal instead of PPE and LPS. AAT treatment was given to each mouse 2 h prior to the PPE or LPS challenge. The mice were sacrificed 7 days after the last administration. Data are presented as mean ± SEM of 5–6 mice per group. A) Body weight change of COPD mice during the model establishment and treatment. Body weight did not significantly increase in either group. No significant difference was found between each group ($p>0.05$). B) Total protein content quantified by BCA assay in BAL, 7 days after the last dose. C) Albumin concentration in BAL. No significant changes in total protein or albumin content were observed ($p>0.05$). D) LDH activity in BAL. The LDH level in the LPS/PPE group was significantly higher than that in the saline group. AAT administered at a higher dose resulted in lower levels of LDH, which indicates that AAT decreased pulmonary cell damage. The concentration of MIP2 (E) and TNF-α (F) in BAL. The cytokine levels were significantly lower in the AAT treatment groups than those in the saline or LPS/PPE groups, which suggests that AAT reduced the inflammatory response in COPD mice. The statistic difference was determined by one-way ANOVA using Bartlett's test. In E and F, the star mark (*) indicates the statistic difference of that group compared to the LPS/PPE group (* $p<0.05$, ** $p<0.01$).

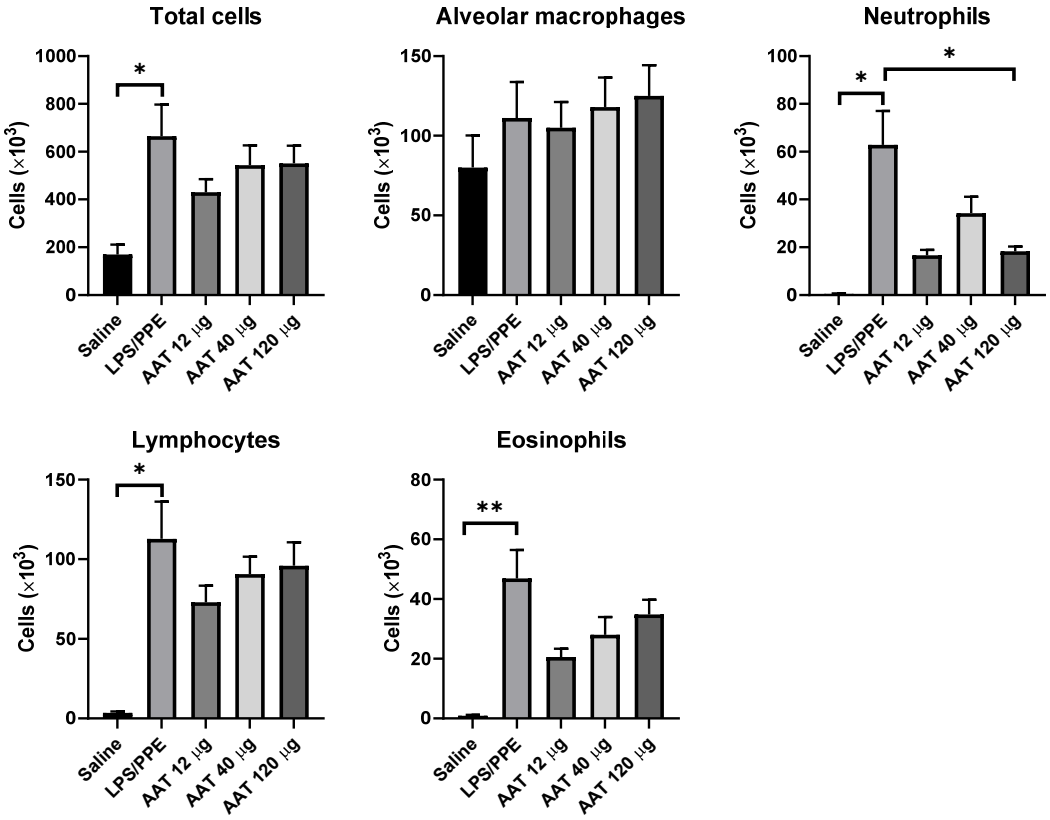

Figure 6. Total and differential cell counts in BAL. Neutrophils were reduced by AAT in comparison to the LPS/PPE group, however, this effect was not dose dependent. In the groups other than the saline group, an increased number of eosinophiles was observed. The statistic difference was determined by a fitting Mixed-effects model (REML) (* $p<0.05$, ** $p<0.01$).

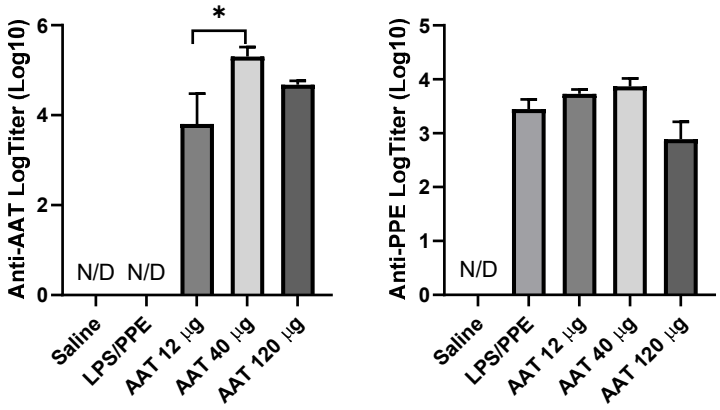

Figure 7. The level of anti-AAT and anti-PPE antibodies in plasma. LogTiter of anti-AAT antibody tended to increase with the higher AAT dose. AAT treatment groups showed significantly higher level of anti-AAT antibodies. Anti-PPE was not detected in the saline group. The highest dose of AAT (excessive AAT) resulted in the lowest anti-PPE EC50 value. However, a lower dose (less AAT than PPE) or medium dose (same molarity of AAT as PPE) did not reduce the allergic reaction caused by PPE. The statistical difference was determined by one-way ANOVA using Bartlett's test (* $p<0.05$).

Based on the findings from the AAT protocol, we concluded that AAT is effective in reducing pulmonary injury and inflammation in the COPD model. Considering that the two doses of 12 and 40 μg per mouse offered similar therapeutic efficacy, 12 μg per mouse was chosen as a sub-optimal dose by the IN route to compare the efficacy of AAT and PEG40-AAT in the second experiment. Similarly, we included PEG20-AAT by IV route, with the aim of determining whether the PEG size conjugated to AAT affects the therapeutic efficacy. The IV dose was determined based on the PK data where 2.65 % of the IV dose reached the lung. We calculated the corresponding IV dose of 450 μg which would enable approximately 12 μg of AAT or PEG-AAT to distribute in the lung. Similar readouts were determined to evaluate the therapeutic efficacy of AAT and PEG-AAT as in the AAT protocol.

An overview of the therapeutic efficacy of intravenous administration will be provided first. During the treatment, the average weight of the mice from the LPS/PPE IV group was significantly lower than that of the saline group (Figure 8A). In terms of protein content in BAL, there was no significant difference between the IV groups (Figure 8B); however, AAT and PEG-AAT appeared to decrease albumin content in BAL following IV treatment (Figure 8C). As shown in Figure 8D, the LPS/PPE IV control group exhibited a higher level of LDH activity in BAL than the saline group, whereas the AAT and PEG-AAT groups displayed a similar level of activity as the saline group, indicating that the IV dose of AAT and PEG-AAT provided adequate protection. In addition, when compared to the LPS/PPE, the LDH activity of the PEG40-AAT group was significantly lower, while the ones in the AAT and PEG20-AAT groups did not reach statistical significance. These data indicate that AAT and PEG-AAT, especially PEG40-AAT, eased the pulmonary inflammation in the murine COPD model. Unfortunately, cytokine levels in BAL do not support this indication as neither AAT nor PEG-AAT reduced the levels of MIP2 and TNF-α (Figure 8 E and F).

On the other hand, the results of differential cell counts indicated that AAT and PEG-AAT reduced inflammation. Figure 9 illustrates how the total number of cells, neutrophils, lymphocytes, and eosinophils were significantly lower in the saline and treatment groups than those in the LPS/PPE IV control group. In addition, AAT and PEG20-AAT drastically decreased the number of neutrophils in BAL.

The residual AAT or PEG-AAT in BAL, lung homogenates and plasma was quantified by ELISA. Following IV, the content of PEG40-AAT and PEG20-AAT in BAL was significantly higher than that of the AAT group (Figure 9). The levels of PEG40-AAT were also significantly higher in the lung and plasma compared with AAT.

According to the histopathological analysis of the lung tissue, however, IV injections of AAT, PEG40-AAT and PEG20-AAT were ineffective in reducing lung inflammation (Figure S3). The saline group showed normal lung tissue. A mild peribronchial and perivascular inflammation was observed in the LPS/PPE IV group. The AAT IV, PEG40-AAT IV and PEG20-AAT IV treatment groups showed varying degrees of inflammation, with AAT-treated mice accumulating more perivascular inflammatory cells.

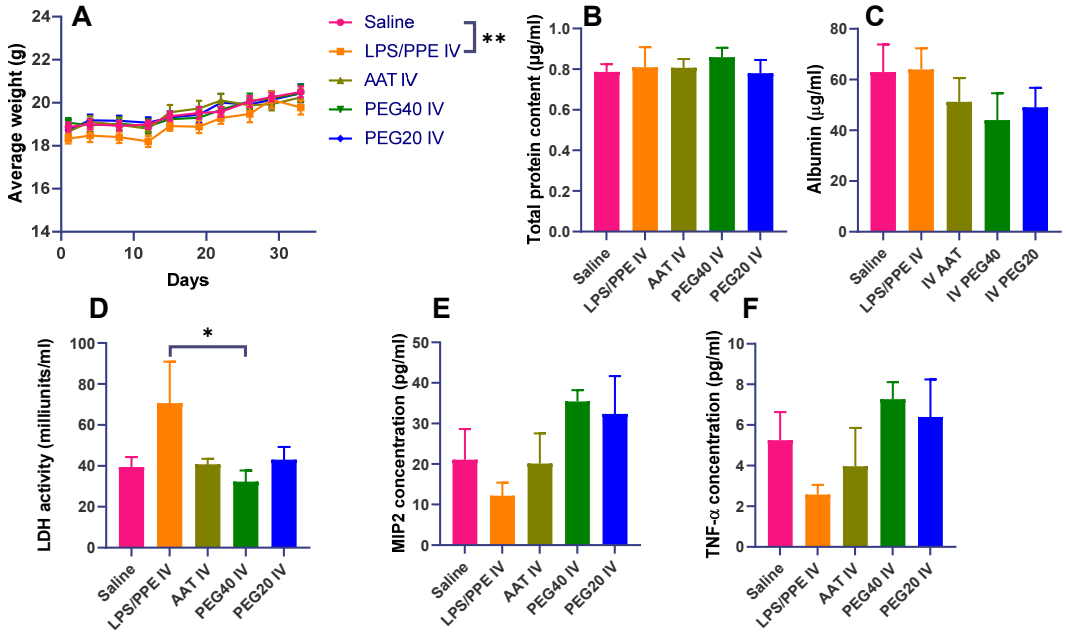

Figure 8. In vivo therapeutic efficacy of AAT, PEG20-AAT and PEG40-AAT on murine COPD model by IV (450 µg per mouse). The model was established as described in Figure 1. In each group n=5-6. A) Body weight change of COPD mice during the model establishment and treatment. The average weight of the LPS/PPE IV group was significantly lower than that of the saline group at the conclusion of the experiment. B) Total protein content in BAL. No significant difference was found between each group. C) Albumin concentration in BAL. The treatment tended to decrease the albumin content. D) LDH activity in BAL. LDH activity of the IV treatment groups was similar to that of the saline group, whereas that of the LPS/PPE IV group was higher. PEG40-AAT group showed a slightly lower LDH activity ($p=0.09$). The concentration of MIP2 (E) and TNF-α (F) in BAL. The LPS/PPE IV group produced lower levels of cytokines than the saline group. AAT or PEG-AAT treatment did not decrease the level of MIP2 and TNF-α, although no significant difference was found. The statistical difference was determined by one-way ANOVA using the Dunnett test (* $p<0.05$, ** $p<0.01$).

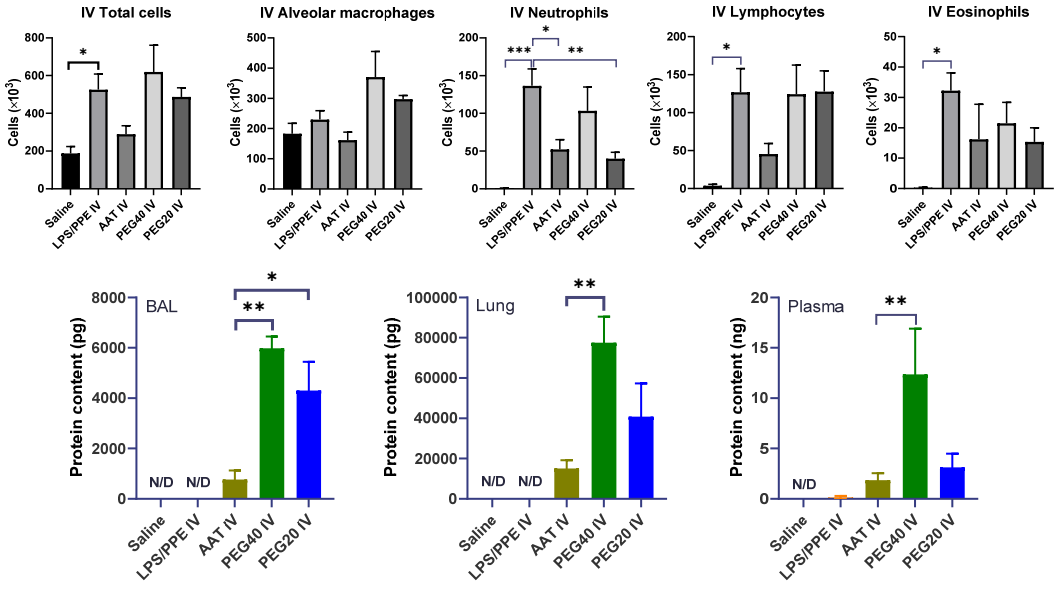

Figure 9. Total and differential cell count and the content of AAT and PEG-AAT in BAL following IV treatment. AAT and PEG-AAT reduced the number of neutrophils in BAL. The number of total cells and lymphocytes decreased more rapidly with AAT. The content of PEG40-AAT and PEG20-AAT in BAL was significantly higher than that of AAT group. In addition, PEG40-AAT displayed significantly higher concentrations in the lung and plasma compared to AAT. PEG was not considered in the mass recovered. The statistical difference was determined by one-way ANOVA using Dunnett test (* $p<0.05$, ** $p<0.01$, *** $p<0.001$). N/D: Not detected.

In the following paragraphs, we will present the therapeutic efficacy of intranasal administration. In the LPS/PPE IN, AAT IN and PEG40-AAT IN groups, no weight loss was observed, and the average weight of the mice from AAT IN and PEG40-AAT IN groups was higher than that of the saline group (Figure 10A). PEG40-AAT had a tendency to decrease the total protein content in BAL, while AAT was not significant in this respect (Figure 10B). The level of albumin in BAL of the PEG40-AAT group was significantly reduced in comparison to the LPS/PPE group (Figure 10C). These results provide evidence that PEG40-AAT offers better protection for the integrity of the alveoli-capillary barrier. Figure 10D showed that AAT did not reduce the LDH activity in BAL. PEG40-AAT exhibited slightly decreased LDH activity; however, this difference was not significant when compared with the LPS/PPE group ($p=0.53$). Furthermore, instilled PEG40-AAT also showed a tendency to reduce MIP2 and TNF-α in BAL (Figure 10E and F).

Figure 11 illustrates the results of differential cell counts and AAT/PEG-AAT content in BAL following IN treatment. Accordingly, the total number of cells, neutrophils, lymphocytes and eosinophils in the saline, AAT IN and PEG40-AAT IN groups were significantly lower than those in the LPS/PPE IN control group. Particularly, PEG40-AAT reduced the number of neutrophils in BAL in comparison to the LPS/PPE IN group ($p<0.05$). This suggested that AAT as well as PEG-AAT could reduce pulmonary inflammatory cells via IN and that PEG40-AAT offered a

better effect on reducing the number of neutrophils.

Following IN, no AAT or PEG40-AAT was detected in the plasma following IN treatment. In contrast, AAT was fully cleared from the airway spaces (BAL) and lung parenchyma, whereas PEG40-AAT could still be detected 7 days after the final dose (Figure 11).

The lung histology highlights the inflammation reduction in the IN treatment group. In Figure 12, the LPS/PPE IN group exhibited peribronchial and perivascular inflammation infiltration and accumulation of inflammatory cells in the airway spaces. In both AAT and PEG40-AAT IN treatment, inflammatory cell aggregates were reduced near bronchi and vessels.

Both methods resulted in increased eosinophils in LPS/PPE and treatment groups (Figures 9 and 11). We analyzed the plasma for the presence of anti-PPE and anti-AAT by means of an in-house ELISA assay, similar to the results in AAT protocol. AAT and PEG-AAT, as illustrated in Figure 13, both induced the production of anti-AAT antibodies. By IV route, there was no statistically significant difference between IV treatment groups in anti-AAT or anti-PPE antibody levels. On the other hand, via the IN route, the PEG40-AAT group showed a higher anti-AAT level than did the AAT group. Anti-PPE antibody levels were similar in all IV or IN treatment groups and did not differ statistically from the LPS/PPE group. The level of anti-PEG IgG was also characterized. The administration of PEG-AAT induced the generation of anti-PEG antibodies. Following IN, PEG20-AAT caused more antibodies production than PEG40-AAT.

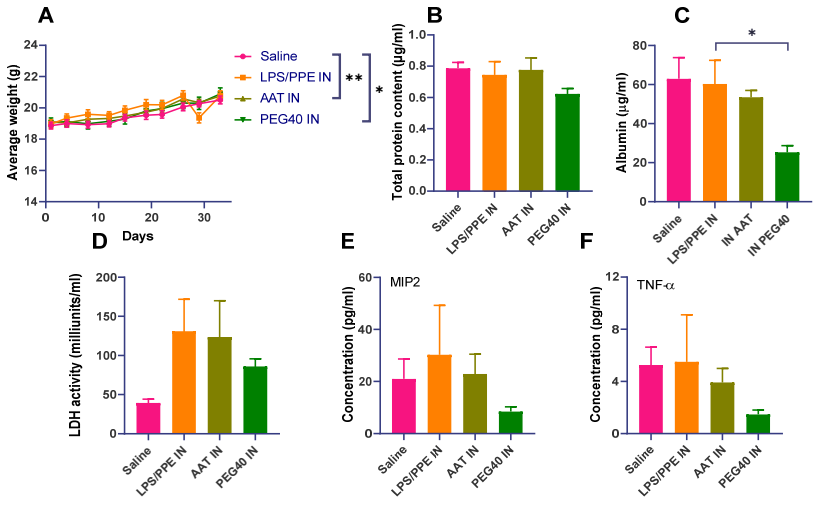

Figure 10. In vivo therapeutic efficacy of AAT and PEG40-AAT on murine COPD model by IV (12 µg per mouse). A) Body weight change of COPD mice during the model establishment and treatment. AAT IN and PEG40-AAT IN groups had higher average weights than the saline group at the end of the experiment. B) Total protein content in BAL. PEG40-AAT tended to decrease the total protein content. C) Albumin concentration in BAL. The treatment of PEG40-AAT decreased the albumin content in BAL. D) LDH activity in BAL. Following IN, AAT did not reduce the LDH activity in BAL while PEG40-AAT group showed a slightly lower LDH activity level. However, no statistical difference was found ($p>0.05$). The concentration of MIP2 (E) and TNF-α (F) in BAL. The PEG40-AAT group showed lower cytokine levels following the IN route. The statistical difference was determined by one-way ANOVA using Dunnett test (* $p<0.05$, ** $p<0.01$).

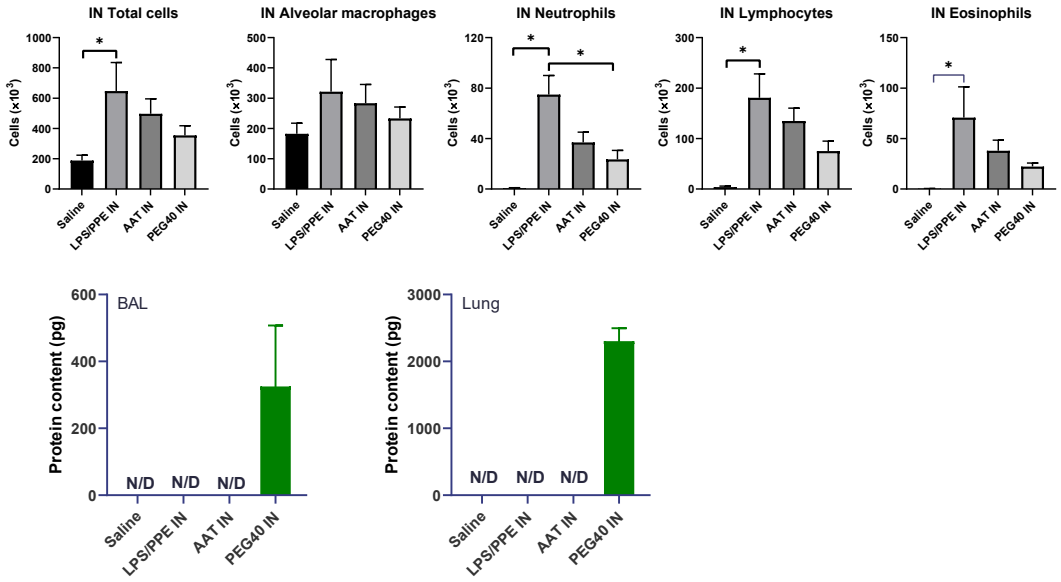

Figure 11. Total and differential cell count and the content of AAT and PEG-AAT in BAL following IN treatment. PEG40-AAT reduced the number of neutrophils in BAL. PEG40-AAT also tended to reduce the total cell number and other inflammatory cell numbers. The statistical difference was determined by one-way ANOVA using Dunnett test (* $p<0.05$, ** $p<0.01$, *** $p<0.001$). No AAT or PEG40-AAT was detected in the plasma following IN treatment. PEG40-AAT remained detectable in the airways spaces (BAL) and lung parenchyma for 7 days following the last dose of AAT. N/D: Not detected.

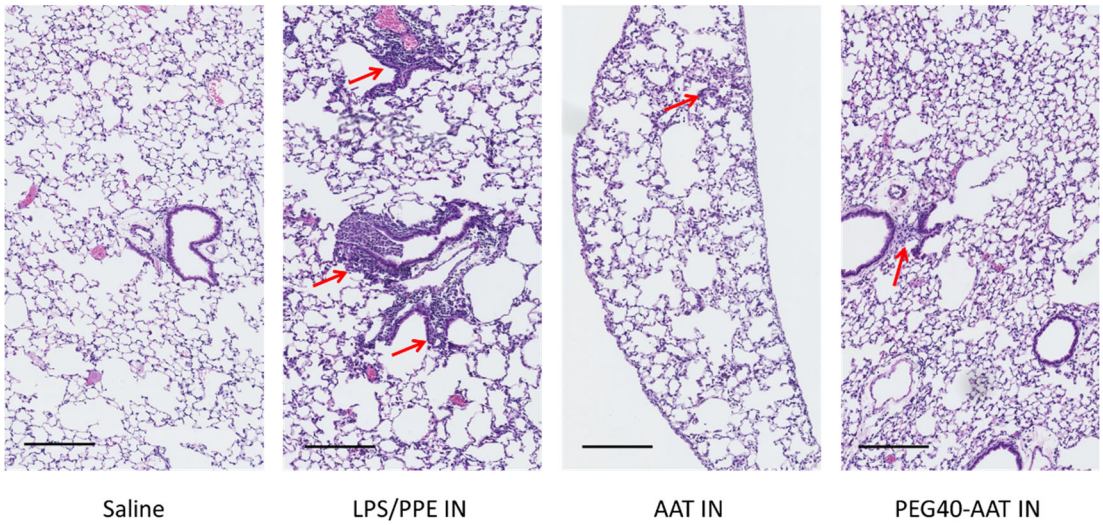

Figure 12. Representative images of lung tissue stained with hematoxylin–eosin. Magnification 400×. Scale bar: 200 μm. The LPS/PPE group showed strong peribronchial and perivascular inflammation infiltration and accumulation of inflammatory cells in airway spaces. IN treatment of AAT and PEG40-AAT both reduced the inflammatory cell aggregates near bronchi and vessels. The red arrows indicate the accumulation of inflammatory cells.

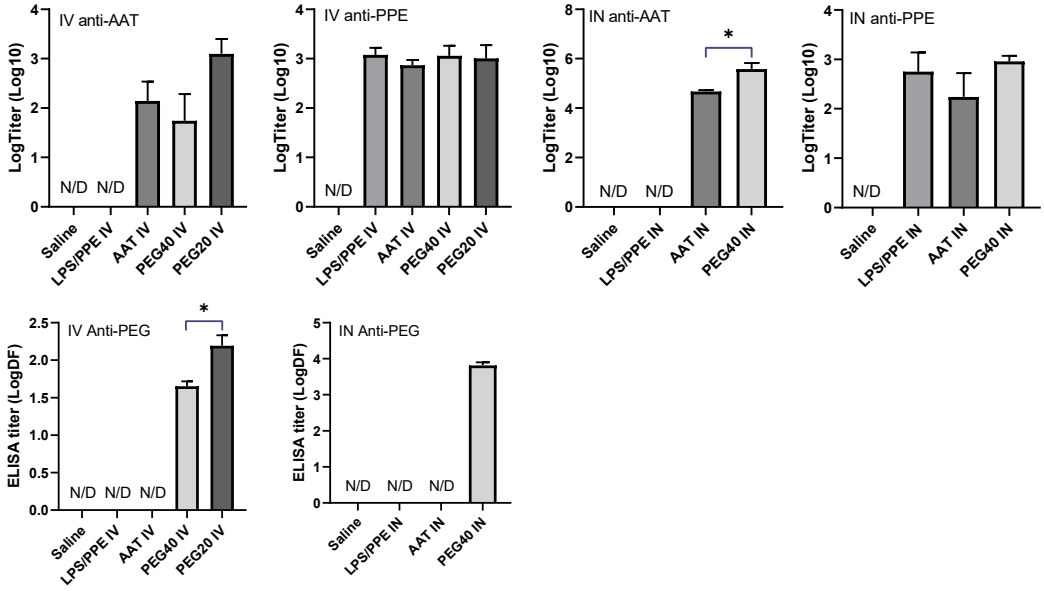

Figure 13. The level of anti-AAT, anti-PPE and anti-PEG antibodies in plasma following IV and IN administration. Both AAT and PEG-AAT induced the generation of anti-AAT antibody. The IN treatment of AAT and PEG-AAT induced more anti-AAT comparing to IV treatment. AAT and PEG-AAT had no significant impact on the anti-PPE antibody. The star marks indicate the statistic difference comparing to the saline. Anti-PEG antibody was not detected in the saline, LPS/PPE groups and AAT treatment groups. PEG40-AAT and PEG20-AAT promoted the anti-PEG antibody production, by both administration routes. The statistical difference was determined by one-way ANOVA using Dunnett test (* $p<0.05$, ** $p<0.01$, *** $p<0.001$).

III.4. STABILITY TO AEROSOLIZATION

As aerosolization is frequently used in pulmonary drug delivery, we investigated the stability of AAT, linear PEGmal30k-AAT, linear PEGmal40k-AAT and 2-armed PEGmal40k-AAT to jet nebulization. AAT and PEG-AAT showed excellent stability to jet nebulization. After 10-min nebulization, the UV spectrum of each sample did not show higher absorbance at the wavelength over 300 nm (Figure 15A, B, S4), indicating that there was no detectable formation of insoluble aggregates. In SEC analysis, we found no evidence of nebulization-induced soluble aggregates (Figure 15C, D, S4). In addition, the elastase inhibition capacity of each protein was preserved after the exposure to nebulization (Figure 15E, F, S4).

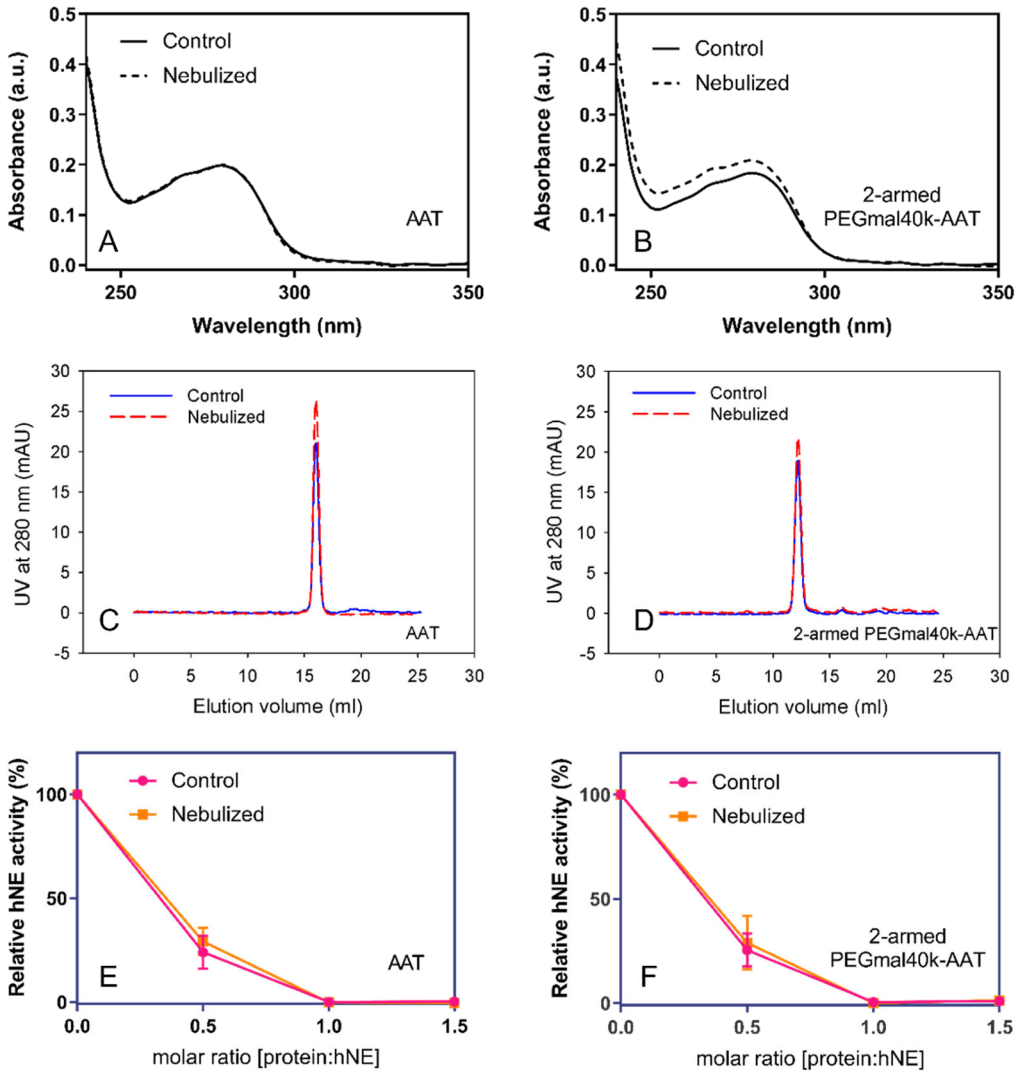

Figure 14. UV spectrum of unconjugated AAT (A) and 2-armed PEGmal40k-AAT (B) after jet nebulization (0.4 mg/ml, 2 ml, 10 min). Following jet nebulization, there were no significant changes in absorbance at 310 nm, indicating the absence of insoluble aggregates. The concentration of PEG-AAT slightly increased after nebulization. The data of linear PEGmal30k-AAT and linear PEGmal40k-AAT were shown in Figure S4. Size exclusion chromatograms of unconjugated AAT (C) and 2-armed PEGmal40k-AAT (D) after jet nebulization. The elution volume of AAT was approximately 16 ml while it was around 12 ml for PEGylated AAT. There was no additional peak appearing after jet nebulization or freeze/thawing, indicating the absence of soluble aggregates or degradation. The data of linear PEGmal30k-AAT and linear PEGmal40k-AAT were shown in Figure S4. Elastase inhibition activity of unconjugated AAT (E) and 2-armed PEGmal40k-AAT (F) after jet nebulization. There was no statistical difference between control and nebulized or freeze/thawed samples, indicating the conservation of biological activity. The statistic difference was determined by two-way ANOVA using Turkey comparison (n=3).

IV. DISCUSSION

Weekly intravenous infusion of AAT is an inconvenient and expensive treatment for patients with AAT deficiency. On the other hand, the daily inhaled AAT shows limited efficacy, possibly due to the rapid clearance of AAT from the lung. Thus, a long-acting version of AAT could be beneficial as i) it could reduce the administration frequency of intravenous AAT, ii) it could offer an improved efficacy following inhalation, iii) it could decrease the frequency of inhalation. In addition, the long-acting version of AAT might improve patient adherence.

Compared with the previous work of Cantin et al [18], we used glycosylated human AAT, which is reported to be more stable in the circulation than the non-glycosylated recombinant AAT. We conjugated a large PEG chain to AAT, which further improved its stability to proteolysis. Our data showed that conjugation of PEG to AAT significantly prolonged its body and pulmonary residency. Moreover, conjugation to 2-armed 40 kDa PEG contributed more to the pulmonary retention than conjugating linear 20 kDa PEG. Our data are in line with that of Koussoroplis et al who demonstrated that conjugation of a 2-armed 40 kDa PEG to anti-IL17A F(ab')2 successfully increased its pulmonary residence time [20]. Similarly, Guichard et al showed that the conjugation of linear 30 kDa PEG or 2-armed 40 kDa PEG to recombinant human deoxyribonulease I (rhDNase) prolonged its pulmonary residency. In addition, in a murine model of cystic fibrosis, a single dose of PEGylated rhDNase provided similar therapeutic efficacy to reduce DNA content in the lung, as 5 consecutive daily doses of unconjugated rhDNase [21].

The retention offered by PEGylation to AAT was assumed to be due to its increased hydrodynamic size, which reduced the renal clearance. Following pulmonary delivery, the transport of AAT across respiratory epithelia to the circulation, and the alveolar macrophages uptake might be restrained due to the conjugated PEG [21]. The improved proteolytic resistance also facilitates the pulmonary retention of PEG-AAT.

Interestingly, our data suggest that the PEGylation site also influenced the prolongation effect within the lung. Both thiol PEGylated and N-terminal PEGylated AAT showed prolonged body residency, however, thiol PEGylated AAT stayed longer in the airway spaces following IT. Our hypothesis is that in N-terminal PEGylation, PEGald might be conjugated to the free N-terminus of AAT, which makes it more difficult to form a steric protection around the protein. While in thiol PEGylation, PEGmal is conjugated to Cys232, which is on the protein surface. This may result in different biological stability of PEGmal-AAT and PEGald-AAT, thus leading to different pulmonary retention.

The COPD model used in the efficacy study was established using two inflammation inducers LPS and PPE according to Singanayagam [25] and Kim [31]. The LPS/PPE group showed increased LDH activity and inflammatory cells in BAL, which was in line with the literature. However, the LPS/PPE groups presented lower level of cytokines than the saline group, which was similar to Singanayagam [25]. The author found that after 4-week model establishment, the level of Interferon gamma-induced protein 10 (IP-10) in the LPS/PPE group did not change, and the level of IL-6 decreased. Nevertheless, all three doses of AAT decreased the lung inflammation markers in the COPD mice, which is consistent with several researchers, who reported that AAT reduced the inflammation induced by LPS in murine models [32, 33] or eased the lung damage induced by elastase in murine models [34, 35]. Our study is the first report to demonstrate the therapeutic efficacy of AAT in a LPS & PPE induced long-term lung injury model. The anti-elastase and anti-inflammation properties of AAT both contributed to the decrease of lung injury and inflammation in this COPD model.

In the second experiment, in the COPD model, we noticed that the LPS/PPE IN group presented stronger lung inflammation than LPS/PPE IV group. It showed higher level of LDH activity, cytokine and inflammatory cell number in BAL, as well as stronger inflammatory infiltrate in the lung histology analysis. Our hypothesis is that the mice in the LPS/PPE IN group received an additional IN instillation, which delivered more volume of solution in the lung, leading to further injury and inflammation. As shown in Table 1, PEG40-AAT via IN offered the most improved therapeutic efficacy, as it not only decreased 58 % of lymphocytes number in BAL and 34 % of the LDH activity, but also significantly decreased the neutrophils number by 69 % and the albumin content by 58 % in BAL. Via the IN route, PEG40-AAT presented better efficacy than AAT. On the other hand, via the IV route, PEG20-AAT and PEG40-AAT did not show an improvement in efficacy. This might be due to the restrained lung penetration and diffusion of PEG-AAT following IV injection. Our PK data suggest that the lung penetration of PEG20- and PEG40-AAT was slower than AAT. Since the COPD model involves direct deposition of PPE in the lung, the pulmonary delivery of AAT or PEG-AAT will neutralize the PPE within a short period of time since it is delivered directly to the site of injury. In contrast, PEG-AAT takes a longer time to diffuse in the lung after IV administration, which makes it inherently less effective than AAT in this model.

To the best of our knowledge, this is the first study to systematically investigate the pharmacokinetics and therapeutic efficacy of PEGylated AAT using large PEG molecules. According to our data, we were able to achieve the highest efficacy using a lower dose (12 ug/mouse, 38-fold lower than the IV dose) via IN using PEG40-AAT.

Table 1. Therapeutic efficacy evaluation of AAT, PEG20-AAT and PEG40-AAT. The star mark indicates the statistic difference comparing to the LPS/PPE group ($p<0.05$).

Readouts	IV			IN	
	AAT	PEG40-AAT	PEG20-AAT	AAT	PEG40-AAT
LDH activity	↓ 42 % (1)	***↓ 54 % (3)**	↓ 45 % (1)	↓ 6 % (1)	↓ 34 % (1)
Albumin content	↓ 19 % (1)	↓ 31 % (1)	↓ 23 % (1)	↓ 11 % (1)	***↓ 58 % (3)**
Neutrophil number in BAL	***↓ 62 % (3)**	↓ 24 % (1)	↓ 71 % (2)	↓ 51 % (2)	***↓ 69 % (3)**
Lymphocyte number in BAL	↓ 64 % (2)	x (0)	x (0)	↓ 25 % (1)	↓ 58 % (2)
Total score	7	5	4	5	9

If a readout was decreased by less than 50%, the treatment scored 1 point, if decreased more than 50% but not significantly, the treatment scored 2 points, if the decrease was significant, the treatment scored 3 points. The individual of each readout is shown in the brackets.

We observed an unexpected increase of eosinophils in BAL of the groups which were received PPE instillation. Despite the fact that AAT and PEG-AAT treatment tended to decrease the number of eosinophils, these groups still presented higher level of eosinophils compared with the saline group. Our hypothesis is that the increase of eosinophils is a consequence caused by i) the inflammation induced by PPE and LPS and ii) the allergies caused by PPE or AAT, as both proteins are endogenous for mice. It has been reported that in murine COPD model induced by PPE, increased number of eosinophils, combined with other types of inflammatory cells, was observed [36, 37]. However, this effect was simply considered as a result of the inflammatory stimuli in general, without relating it to an immunologic response resulting from the administration of proteins from a different species. Our data from the in-house ELISA confirmed the existence of anti-PPE and anti-AAT antibodies in the plasma of the mice. The hypersensitivity induced by PPE and AAT might be a drawback of this COPD model. However, during the experiment, no mouse exhibited allergic symptoms such as shortness of breath or wheezing. The influence of this immunological response reflected mostly in the increased number of eosinophils, which would not affect much on other inflammatory markers, total protein or albumin content in BAL. Therefore, we believe that despite the immunological response caused by AAT and PPE, this COPD model was still representative for AAT-deficiency-related pulmonary disease. However, this model showed limitations in evaluating the efficacy following IV administration. The inducer PPE was directly distributed to the pulmonary tracts, while the injected PEG-AAT would only slowly penetrate the lung.

This inevitably leads to a limited efficacy of PEG-AAT as PPE is not neutralized as quickly as possible (which was the case in the IN treatment).

Despite the fact that the presence of anti-PEG antibody in the plasma of PEG-AAT treatment groups was confirmed, no allergic reaction was observed in the treated mice. Although it has been reported that anti-PEG antibodies were detected in patients receiving PEGylated therapeutics, these anti-PEG antibodies not always result in severe consequences. Allergies or severe immunological response induced by PEGylated therapeutics are strongly associated with the immunogenicity of the carrier protein [38]. When the PEGylated proteins are non-human, e.g., uricase and asparaginase, it generated more severe issues resulting from anti-PEG antibodies. In our case, AAT derived from human plasma, whose PEGylated version in theory would not exhibit high immunogenicity in the patients. Nevertheless, the immunogenicity of PEGylated AAT in patients should still be well characterized.

PEGylation is reported to increase the stability of a therapeutic protein to proteolysis [39–41]. The prominent explanation of the proteolytic protection of PEG is the steric shielding effect, which impedes the access of proteases towards the protein[42]. Nevertheless, this shielding effect can sometimes result in the loss of binding affinity or activity of a protein. For instance, Growth hormone antagonist (GHA), vascular endothelial growth factor (VEGF) and interferon-α-2a lost some in vitro activity after PEGylation [23, 43]. Nonetheless, the tremendous increase in half-life of the mentioned proteins above offsets the loss of activity, leading to an overall better therapeutic value. Our results showed that two-armed PEGmal40k-AAT has the most enhanced resistance to proteolysis. Moreover, the reduction of proteolysis was achieved without compromising the biological activity.

Aerosolization is known to create air-liquid interfaces (especially in jet nebulization), not all proteins can survive this stress [44]. AAT was used in clinical trials via pulmonary route using a mesh nebulizer eFlow® Rapid (PARI Pharma GmbH, Germany)[9], which is milder comparing to jet nebulizer. It has been reported that PEGylation significantly improved the stability of proteins towards aggregation [45, 46], which is possibly due to the steric shielding effect of PEGs. Therefore, we expect PEG-AAT to exhibit better stability than AAT to jet nebulization. To our surprise, AAT and PEG-AAT all presented excellent stability towards jet nebulization. This result is similar to Guichard et al, who demonstrated that PEGylation did not change the stability of rhDNase to jet nebulization [21].

V. CONCLUSION

Our study presented a PEGylated version of AAT that had improved proteolytic resistance, extended body residence time, and improved therapeutic efficacy. Specifically, PEG40-AAT increased eight-fold the serum half-life of AAT following intravenous injection and two-fold the half-life of AAT in the lung following intratracheal instillation. The PEGylation of AAT, however, limited its lung penetration following IV. In a murine COPD model, AAT was found to be more effective than PEG20- and PEG40-AAT following IV administration, while PEG40-AAT was found to be most effective following IN administration. With a low dose (12 μg IN comparing to 454 μg IV), we were able to achieve the highest efficacy in reducing lung injury and inflammation in the murine COPD model. Moreover, conjugation of linear 30 kDa, 40 kDa or 2-armed 40 kDa PEG did not affect the stability of AAT to jet nebulization. To conclude, our data are informative and promising for applying PEGylated AAT in the augmentation therapy for AAT-deficient patients by inhalation.

VI.REFERENCES

[1] Chotirmall SH, Al-Alawi M, McEnery T, McElvaney NG. Alpha-1 proteinase inhibitors for the treatment of alpha-1 antitrypsin deficiency: safety, tolerability, and patient outcomes. Therapeutics and clinical risk management 2015;11:143–51.

[2] Strnad P, McElvaney NG, Lomas DA. Alpha1-Antitrypsin Deficiency. The New England journal of medicine 2020;382(15):1443–55.

[3] Janciauskiene S, Welte T. Well-Known and Less Well-Known Functions of Alpha-1 Antitrypsin. Its Role in Chronic Obstructive Pulmonary Disease and Other Disease Developments. Annals of the American Thoracic Society 2016;13 Suppl 4:S280-8.

[4] Wells AD, Woods A, Hilleman DE, Malesker MA. Alpha-1 Antitrypsin Replacement in Patients With COPD. Pharmacy and Therapeutics 2019;44(7):412–5.

[5] Brantly ML, Lascano JE, Shahmohammadi A. Intravenous Alpha-1 Antitrypsin Therapy for Alpha-1 Antitrypsin Deficiency: The Current State of the Evidence. Chronic obstructive pulmonary diseases (Miami, Fla.) 2018;6(1):100–14.

[6] Chapman KR, Chorostowska-Wynimko J, Koczulla AR, Ferrarotti I, McElvaney NG. Alpha 1 antitrypsin to treat lung disease in alpha 1 antitrypsin deficiency: recent developments and clinical implications. International journal of chronic obstructive pulmonary disease 2018;13:419–32.

[7] Tonelli AR, Brantly ML. Augmentation therapy in alpha-1 antitrypsin deficiency: advances and controversies. Therapeutic advances in respiratory disease 2010;4(5):289–312.

[8] Pauwels R, Calverley P, Buist AS, et al. COPD exacerbations: the importance of a standard definition. Respiratory medicine 2004;98(2):99–107.

[9] Stolk J, Tov N, Chapman KR, et al. Efficacy and safety of inhaled α1-antitrypsin in patients with severe α1-antitrypsin deficiency and frequent exacerbations of COPD. The European respiratory journal 2019;54(5).

[10] Goldklang MP, Stearns KN, Anguiano V, Reed RM, Elkington PT, D'Armiento JM. Alpha-1 Antitryspin Inhibition of MMP-13: Implications in Acute Exacerbations of COPD. In: M. P. Goldklang,K. N. Stearns, editor. Alpha-1 Antitryspin Inhibition of MMP-13: Implications in Acute Exacerbations of COPD: American Thoracic Society, 2019:A3773-A3773.

[11] Li Z, Alam S, Wang J, Sandstrom CS, Janciauskiene S, Mahadeva R. Oxidized {alpha}1-antitrypsin stimulates the release of monocyte chemotactic protein-1 from lung epithelial cells: potential role in emphysema. American journal of physiology. Lung cellular and molecular physiology 2009;297(2):L388-400.

[12] Taggart C, Cervantes-Laurean D, Kim G, et al. Oxidation of either methionine 351 or methionine 358 in alpha 1-antitrypsin causes loss of anti-neutrophil elastase activity. The Journal of biological chemistry 2000;275(35):27258–65.

[13] Turecek PL, Bossard MJ, Schoetens F, Ivens IA. PEGylation of Biopharmaceuticals: A Review of Chemistry and Nonclinical Safety Information of Approved Drugs. Journal of pharmaceutical sciences 2016;105(2):460–75.

[14] Zaman R, Islam RA, Ibnat N, et al. Current strategies in extending half-lives of therapeutic proteins. Journal of controlled release official journal of the Controlled Release Society 2019;301:176–89.

[15] Rondon A, Mahri S, Morales-Yanez F, Dumoulin M, Vanbever R. Protein Engineering Strategies for Improved Pharmacokinetics. Adv. Funct. Mater. 2021;31(44):2101633.
[16] Zheng Z, Okada R, Kobayashi H, et al. Site-Specific PEGylation of Anti-Mesothelin Recombinant Immunotoxins Increases Half-life and Antitumor Activity. Molecular cancer therapeutics 2020;19(3):812–21.
[17] Holm LS, Mcumber A, Rasmussen JE, et al. The effect of protein PEGylation on physical stability in liquid formulation. Journal of pharmaceutical sciences 2014;103(10):3043–54.
[18] Cantin AM, Woods DE, Cloutier D, Dufour EK, Leduc R. Polyethylene glycol conjugation at Cys232 prolongs the half-life of alpha1 proteinase inhibitor. American journal of respiratory cell and molecular biology 2002;27(6):659–65.
[19] Guichard M-J, Kinoo D, Aubriot A-S, et al. Impact of PEGylation on the mucolytic activity of recombinant human deoxyribonuclease I in cystic fibrosis sputum. Clinical science (London, England 1979) 2018;132(13):1439–52.
[20] Koussoroplis SJ, Paulissen G, Tyteca D, et al. PEGylation of antibody fragments greatly increases their local residence time following delivery to the respiratory tract. Journal of controlled release official journal of the Controlled Release Society 2014;187:91–100.
[21] Guichard M-J, Wilms T, Mahri S, et al. PEGylation of Recombinant Human Deoxyribonuclease I Provides a Long-Acting Version of the Mucolytic for Patients with Cystic Fibrosis. Adv. Therap. 2021;4(2):2000146.
[22] Lawrence PB, Price JL. How PEGylation influences protein conformational stability. Current opinion in chemical biology 2016;34:88–94.
[23] Veronese FM, Mero A. The impact of PEGylation on biological therapies. BioDrugs clinical immunotherapeutics, biopharmaceuticals and gene therapy 2008;22(5):315–29.
[24] Liu X, Vanvarenberg K, Guy Wilfried Kouassi K, Mahri S, Vanbever R. Production and characterization of mono-PEGylated alpha-1 antitrypsin for augmentation therapy. International Journal of Pharmaceutics 2021:121355.
[25] Singanayagam A, Glanville N, Walton RP, et al. A short-term mouse model that reproduces the immunopathological features of rhinovirus-induced exacerbation of COPD. Clinical Science 2015;129(3):245–58.
[26] Frokjaer S, Otzen DE. Protein drug stability: a formulation challenge. Nature reviews. Drug discovery 2005;4(4):298–306.
[27] Lestienne P, Bieth JG. The inhibition of human leukocyte elastase by basic pancreatic trypsin inhibitor. Archives of Biochemistry and Biophysics 1978;190(1):358–60.
[28] Sajjan U, Ganesan S, Comstock AT, et al. Elastase- and LPS-exposed mice display altered responses to rhinovirus infection. American journal of physiology. Lung cellular and molecular physiology 2009;297(5):L931-44.
[29] Elkington PTG, Friedland JS. Matrix metalloproteinases in destructive pulmonary pathology. Thorax 2006;61(3):259–66.
[30] Pandey KC, De S, Mishra PK. Role of Proteases in Chronic Obstructive Pulmonary Disease. Frontiers in pharmacology 2017;8:512.
[31] Kim KY, Lee HS, Seol GH. Anti-inflammatory effects of trans-anethole in a mouse model of chronic obstructive pulmonary disease. Biomedicine & pharmacotherapy = Biomedecine & pharmacotherapie 2017;91:925–30.

[32] Jonigk D, Al-Omari M, Maegel L, et al. Anti-inflammatory and immunomodulatory properties of α1-antitrypsin without inhibition of elastase. Proceedings of the National Academy of Sciences of the United States of America 2013;110(37):15007–12.

[33] Subramaniyam D, Steele C, Köhnlein T, et al. Effects of alpha 1-antitrypsin on endotoxin-induced lung inflammation in vivo. Inflammation research official journal of the European Histamine Research Society … [et al.] 2010;59(7):571–8.

[34] Ni K, Serban KA, Batra C, Petrache I. Alpha-1 Antitrypsin Investigations Using Animal Models of Emphysema. Annals of the American Thoracic Society 2016;13 Suppl 4(Supplement_4):S311-6.

[35] Moreno J-A, Ortega-Gomez A, Rubio-Navarro A, et al. High-density lipoproteins potentiate α1-antitrypsin therapy in elastase-induced pulmonary emphysema. American journal of respiratory cell and molecular biology 2014;51(4):536–49.

[36] Inoue K, Koike E, Takano H. Comprehensive analysis of elastase-induced pulmonary emphysema in mice: effects of ambient existing particulate matters. International Immunopharmacology 2010;10(11):1380–9.

[37] Shibata S, Miyake K, Tateishi T, et al. Basophils trigger emphysema development in a murine model of COPD through IL-4-mediated generation of MMP-12-producing macrophages. Proc Natl Acad Sci USA 2018;115(51):13057–62.

[38] Zhang P, Sun F, Liu S, Jiang S. Anti-PEG antibodies in the clinic: Current issues and beyond PEGylation. Journal of controlled release official journal of the Controlled Release Society 2016;244(Pt B):184–93.

[39] Zhang C, Desai R, Perez-Luna V, Karuri N. PEGylation of lysine residues improves the proteolytic stability of fibronectin while retaining biological activity. Biotechnology journal 2014;9(8):1033–43.

[40] Zhang C, Hekmatfar S, Ramanathan A, Karuri NW. PEGylated human plasma fibronectin is proteolytically stable, supports cell adhesion, cell migration, focal adhesion assembly, and fibronectin fibrillogenesis. Biotechnology progress 2013;29(2):493–504.

[41] Danial M, van Dulmen THH, Aleksandrowicz J, Pötgens AJG, Klok H-A. Site-specific PEGylation of HR2 peptides: effects of PEG conjugation position and chain length on HIV-1 membrane fusion inhibition and proteolytic degradation. Bioconjugate Chemistry 2012;23(8):1648–60.

[42] Veronese FM, Pasut G. PEGylation, successful approach to drug delivery. Drug Discovery Today 2005;10(21):1451–8.

[43] Wu L, Ho SV, Wang W, et al. N-terminal mono-PEGylation of growth hormone antagonist: correlation of PEG size and pharmacodynamic behavior. International Journal of Pharmaceutics 2013;453(2):533–40.

[44] Hertel SP, Winter G, Friess W. Protein stability in pulmonary drug delivery via nebulization. Advanced drug delivery reviews 2015;93:79–94.

[45] Rajan RS, Li T, Aras M, et al. Modulation of protein aggregation by polyethylene glycol conjugation: GCSF as a case study. Protein science a publication of the Protein Society 2006;15(5):1063–75.

[46] Sorret LL, Monticello CR, DeWinter MA, Schwartz DK, Randolph TW. Steric Repulsion Forces Contributed by PEGylation of Interleukin-1 Receptor Antagonist Reduce Gelation and Aggregation at the Silicone Oil-Water Interface. *Journal of pharmaceutical sciences* 2019;108(1):162–72.

VII. SUPPLEMENTARY MATERIALS

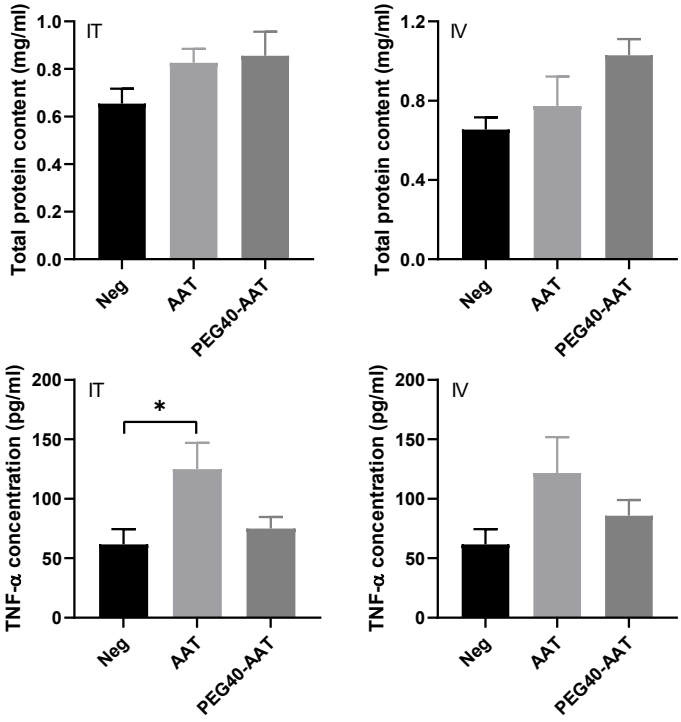

FigureS 1. The total protein and TNF-α content in BAL at 4 h after IT and IV administration. Following both administration routes, AAT and PEG40-AAT tended to increase the total protein content in BAL. AAT increased the level of TNF-α in BAL following IT ($p<0.05$) and IV ($p>0.05$), while PEG40-AAT did not show the same effect.

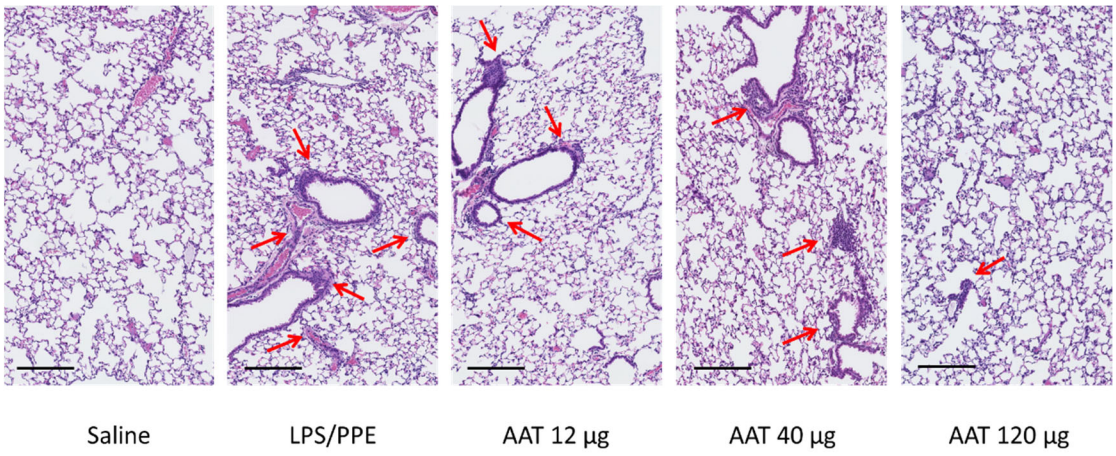

FigureS 2. Representative images of lung tissue stained with hematoxylin–eosin. Magnification 400×. Scale bar: 200 µm. LPS/PPE group showed mild peribronchial and perivascular inflammation with small accumulations of inflammatory cells. Mice treated with different doses of AAT also showed mild small accumulation of inflammatory cells near blood vessels. The statistic difference was determined by one-way ANOVA using Bartlett's test. The red arrows indicate the accumulation of inflammatory cells.

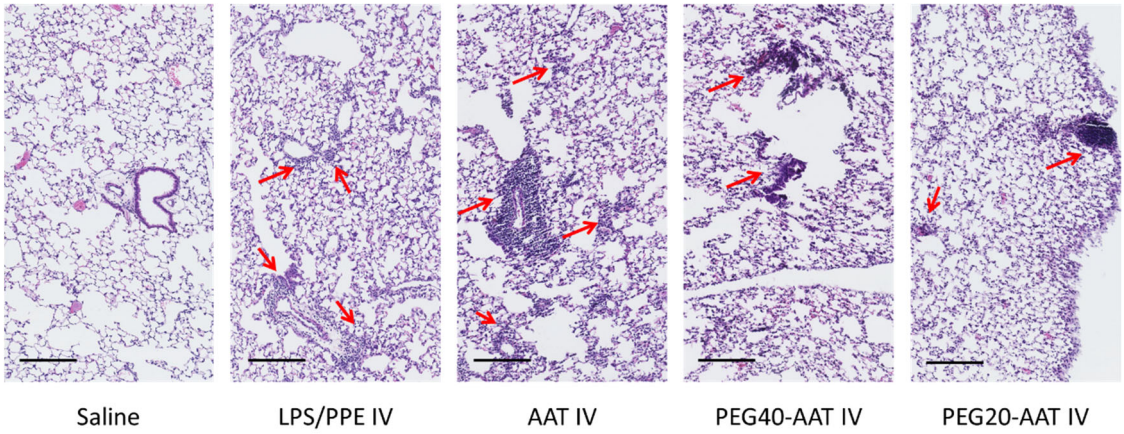

FigureS 3. Representative images of lung tissue stained with hematoxylin–eosin. Magnification 200×. Scale bar: 200 μm. LPS/PPE IV group presented mild peribronchial and perivascular inflammation. The IV treatment of AAT, PEG40-AAT and PEG20-AAT failed to ease the lung inflammation. AAT treated mice showed more pericascular inflammatory cell accumulation. The red arrows indicate the accumulation of inflammatory cells.

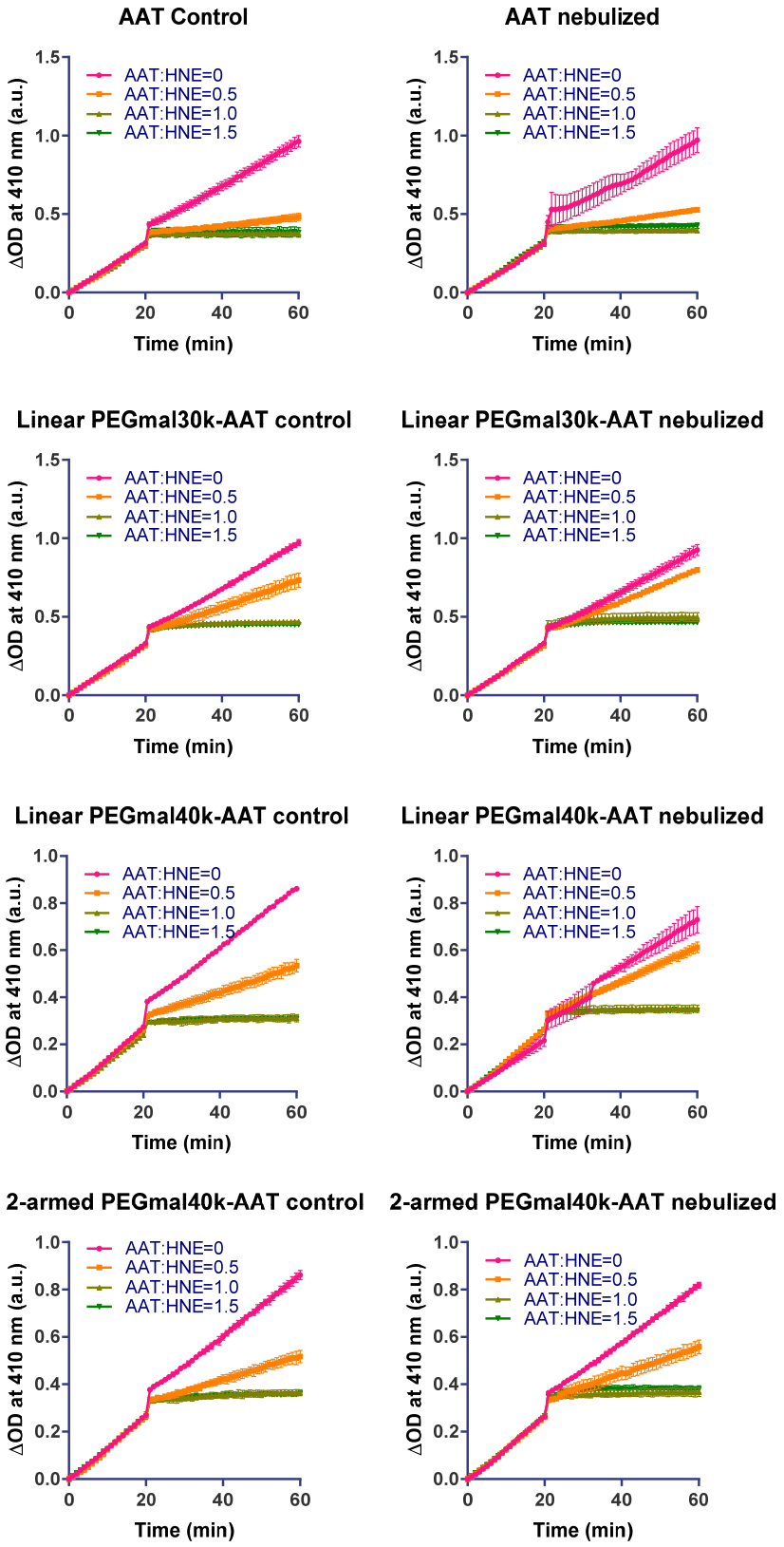

FigureS 4. The kinetics of elastase inhibition assay of nebulized AAT and PEG-AAT. The absorbance at 410 nm of each sample increased linearly in accordance with the incubation time.

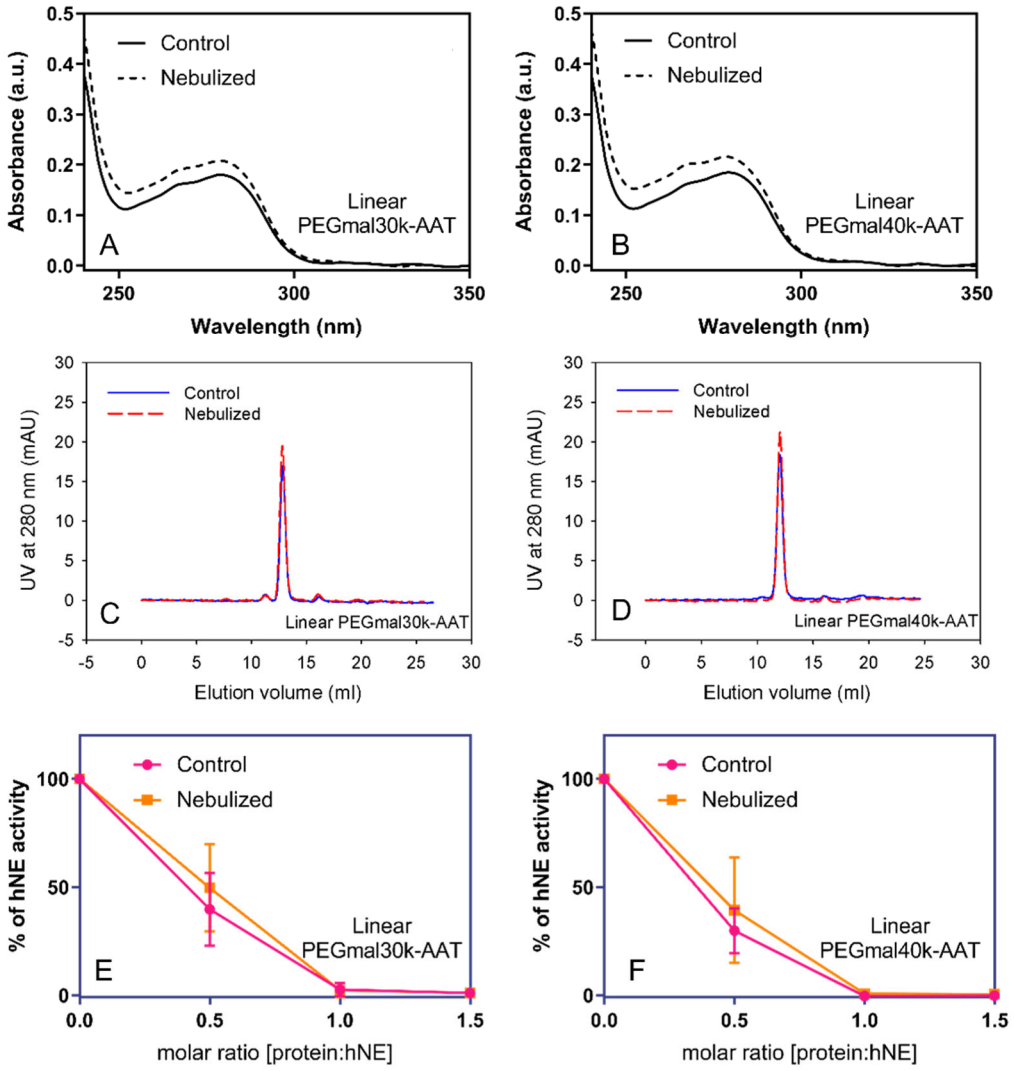

FigureS 5. UV spectrum of linear PEGmal30k-AAT (A) and linear PEGmal40k-AAT (B) after jet nebulization (0.4 mg/ml, 2 ml, 10 min). There was no significant changes of absorbance at 310 nm after jet nebulization, indicating the absence of insoluble aggregates. Size exclusion chromatogram of linear PEGmal30k-AAT (C) and linear PEGmal40k-AAT (D) after jet nebulization. Both PEGylated AAT eluted around 13 ml. No additional peak was observed after nebulization. Elastase inhibition activity of linear PEGmal30k-AAT (E) and linear PEGmal40k-AAT (F) after jet nebulization. There was no statistic difference between control and nebulized or freeze/thawed samples, indicating the conservation of biological activity.

CHAPTER V

DISCUSSION AND PERSPECTIVES

TABLE OF CONTENTS

I. MAJOR FINDINGS

AAT is a serine protease inhibitor which, in physiological conditions, neutralizes the excess of neutrophil elastase and other serine proteases in tissues and especially the lungs [1]. AAT deficiency is a hereditary condition caused by a mutation in the SERPINA1 gene, which is characterized by low AAT serum levels (< 11 μM) [2]. The insufficient level of AAT within the lung leads to premature emphysema and COPD [3].

Weekly intravenous infusion of plasma-purified human AAT is used to treat patients with AAT deficiency associated with respiratory disease [4]. However, only 2 % of the AAT dose reaches the lungs after intravenous infusion [5]. Inhalation of AAT might offer an alternative route of administration. However, the rapid clearance of AAT from the respiratory tract results in high and frequent dosing by inhalation and limited efficacy. PEGylation is a common process used to improve the therapeutic value of a protein by prolonging its serum half-life [6]. We hypothesized that the PEGylation of AAT would prolong its time of residence in intact form within the lungs and thereby greatly increase its local potency.

In this thesis, PEGylated AAT was produced and characterized for its physicochemical properties, activity, stability, in vivo pharmacokinetic profile and therapeutic efficacy. AAT was mono-PEGylated on its N-terminal residue by reductive alkylation at acidic pH, or on its cysteine 232 by thiol PEGylation using PEG molecules of different sizes. PEGylation was shown to increase the hydrodynamic size of AAT. PEGylation on either amino acid did not alter the secondary/tertiary structure, biological activity, the denaturation process to chemical denaturant, the stability to jet nebulization and freeze/thawing, and the long-term storage at 4°C of AAT. Our data showed that PEGylation stabilized AAT to heat-induced polymerization and to proteolysis in vitro.

Two-armed PEGmal40k-AAT presented the highest stability and therefore was selected for in vivo experiments. In vivo pharmacokinetic studies in mice showed that PEGylation increased eight-fold the serum half-life of AAT following IV and two-fold the half-life of AAT in the lungs following IT. However, PEGylation slowed down the lung penetration of AAT following IV. The influence of PEG size and PEGylation site to the prolongation effect was investigated. Following IV injection, increasing the PEG size conjugating to AAT led to longer body residence time. Thiol PEGylated AAT stayed longer in the lung comparing to N-terminal PEGylated AAT.

The therapeutic efficacy of AAT and PEG-AAT was evaluated in a murine model of COPD. PEG40-AAT presented improved efficacy in reducing lung injury and inflammation at a low dose (12 μg/mouse) delivered by IN, over the same dose of unconjugated AAT administrated by IN, or

a high dose (454 μg/mouse) of unconjugated AAT and PEGylated AAT delivered by IV. Our findings support the hypothesis of this thesis and successfully provide a PEGylated version of AAT which presented improved body residency and therapeutic efficacy.

II. DISCUSSION

II.1. SELECTION OF PEGYLATION CHEMISTRY, PEGYLATION SITE AND PEG SIZE

With the goal to develop a PEGylated version of AAT, offering prolonged body residency and improved therapeutic efficacy, we first determined the appropriate PEGylation chemistry for conjugating AAT.

Random PEGylation was not considered as it is often associated with a loss of protein activity or binding affinity [7]. Moreover, the PEGylated product of random PEGylation is heterogeneous, which is not ideal for further purification, characterization and quality control [8]. We favored mono-PEGylation as it overcomes the above drawbacks of random PEGylation. Previous studies in our laboratory have also demonstrated the feasibility of mono-PEGylation in prolonging the residence time of therapeutic proteins in the lung.

The work of Koussoroplis [9], Freches [10] and Patil [11] involved conjugating PEG-maleimide to an antibody fragment by thiol PEGylation. The reaction takes place by forming a thioether bond via Michael's addition between the double bond of the maleimide ring and the thiol group. Generally, this reaction is mild and fast, resulting in a satisfactory conjugation rate when the reaction conditions are optimal.

Thiol PEGylation was utilized by other researchers on AAT. As discussed in Chapter I, Cantin [12] and Zhu [13] both produced thiol PEGylated recombinant AAT with fully preserved biological activity. In addition, Cantin et al also demonstrated the prolonged body residency of PEGylated recombinant AAT in the murine lung, as well as the improved protection to elastase mediated lung hemorrhage. Thus, it could also be promising to PEGylate plasma-derived human AAT, which would result in longer residence times in the body since plasma-derived AAT has a longer half-life than recombinant AAT.

The previous work of Guichard et al produced PEGylated rhDNase by N-terminal PEGylation [14]. The selectivity of N-terminus was achieved by taking advantages of the different pKa values between the alpha- and epsilon-amine. An acidic environment is essential for the N-terminal selectivity [15]. The N-terminal PEGylation of rhDNase preserved the full biological activity of rhDNase, which inspired us to pursue the N-terminal PEGylation of AAT that had never been reported in the past.

Therefore, we planned to perform thiol PEGylation and N-terminal PEGylation of AAT, on Cys232 and N-terminal residue.

Considering that increasing the PEG size can greatly extend the body residence time of a protein, we aimed to use large PEGs to conjugate AAT. Cantin et al conjugated 5, 20 and 40 kDa PEG-maleimide to recombinant AAT and compared their body residency following intravenous injection [12]. The results showed that 20 and 40 kDa PEG conjugation resulted in much higher level in the blood of CD1 mice than that of 5 kDa PEG conjugation. However, no significant difference was found between the PEG20 and PEG40 groups. The authors did not demonstrate the therapeutic efficacy of recombinant AAT conjugated to large PEG molecules (>30 kDa).

In our study, we used linear 20 kDa, 30 kDa, 40 kDa and 2-armed 40 kDa PEG to conjugate AAT. The conjugation of large PEG can sometimes alter the activity of a protein. For instance, growth hormone antagonist (GHA), a ~22 kDa protein, lost its activity when conjugating to a 40 kDa PEG, while it preserved some activity when conjugating to a 20 kDa PEG [16]. In our case, all the PEG-AAT conjugates presented the same biological activity as the unconjugated AAT [17].

Our comparison of the two PEGylation chemistries revealed that thiol PEGylation exhibits milder reaction conditions and shorter reaction times. Moreover, thiol PEGylation did not result in any multi-PEGylated products.

II.2. SELECTION OF PEG-AAT CONJUGATE WITH IMPROVED STABILITY

As PEGylation may improve the physicochemical properties and biological stability of AAT [18], we planned to characterize the synthesized PEG-AAT conjugates, with the objective of selecting a candidate which exhibited the best in vitro properties.

Either thiol or N-terminal PEGylation had no significant influence on the following properties of AAT: its secondary and tertiary structure, its biological activity, its unfolding process induced by chemical denaturant or high temperature, its stability to jet nebulization, freeze/thawing cycles and in long-term storage.

The reports that demonstrate the changes of a protein's secondary or tertiary structure after PEGylation are often referring to random and non-specific PEGylation [19]. Mono-PEGylation generally does not alter a protein's secondary/tertiary structure, unless the PEG size used is much larger than the protein itself [20–22]. The influence of PEGylation on protein's stability was difficult to predict, it can stabilize or destabilize a protein, or sometimes have no effect [22–25]. Thus, it is essential for the PEGylated protein to be characterized in terms of its physicochemical and biological properties.

PEGylation did improve the resistance of AAT to heat induced polymerization and proteolysis as discussed in chapter III and IV. The stability of AAT was enhanced more with larger PEG, which

was in line with numerous reports [26–28]. The proteolytic protection of PEG is possibly due to the steric shielding effect, which impedes the access of proteases towards the protein. Among all the PEG-AAT conjugates, 2-armed PEGmal40k-AAT presented the best stability to polymerization, proteolysis and long-term storage, thus was selected for the further in vivo PK and efficacy study.

II.3. PROLONGED BODY AND PULMONARY RESIDENCY: QUANTIFICATION OF AAT IN THE BAL, AND THE IMPACT OF PEG SIZE AND PEGYLATION SITE

In chapter IV, we performed systematic studies to determine the body and pulmonary residency of AAT and PEG-AAT following IV and IT administration. The preliminary study was performed on Swiss mice to optimize the experimental protocols. We encountered a problem with the low recovery of AAT delivered to the lung after IT, which resulted in only ~12.5% of the administered amount being detected immediately after the procedure. Our hypothesis was that AAT continued to neutralize the proteases in the BAL, or to be degraded by the proteases in the BAL, which made it difficult to be detected by sandwich ELISA. To avoid further degradation of AAT after BAL collection, we included protease inhibitors (PIs), which did not contain any serpin inhibitors, in the lavage fluid. The addition of PIs significantly increased the BAL recovery of AAT while had no impact on the recovery of PEG-AAT. To further improve the extraction of PEG-AAT, we adapted the method from Guichard et al [14], which was to add 0.1 % of SDS in the lavage fluid. In the end, our data showed that 2-armed PEGmal40k-AAT presented greatly prolonged retention in the plasma (via IV, by 8-fold) and the lung (via IT, by 2-fold).

We also demonstrated the influence of PEG size on the body residency. The level of linear PEGmal20k-AAT and 2-armed PEGmal40k-AAT in the plasma was compared on day 1 and day 3 after IV administration. Our results showed that larger PEG conjugation resulted in the more prolonged residence time following IV, which is consistent with the data from Lee [29] and Koumenis [30]. Lee et al examined the influence of PEGylation on Single-Chain Fv Protein using different PEG size and structure. The serum half-life was found to be extended more by increasing the length of polymer rather than increasing the total mass of PEG. Koumenis demonstrated that PEGylation of $F(ab')_2$ form of a humanized anti-interleukin-8 (anti-IL-8) antibody resulted in a significant decrease in the clearance, which has a dependence on the hydrodynamic size.

Although thiol PEGylated and N-terminal PEGylated AAT showed the same biological activity in vitro, they exhibited different pulmonary retention after IT administration - thiol PEGylated AAT stayed longer in the air spaces. This is possibly due to the limited steric protection offered by N-terminal conjugated PEG. It has been reported that the PEGylation site plays a role in protein's

stability, thus influences its behavior in vivo. Pan et al reported the thiol and N-terminal PEGylation (using PEG of 5 kDa) of tumor necrosis factor (TNF)-related apoptosis-inducing ligand (TRAIL), an anti-tumor agent [31]. Thiol PEGylated TRAIL possessed superior in vitro stability and antitumor activity than N-terminal PEGylated TRAIL, it also exhibited more therapeutic potentials in tumor xenograft model. The author found that there was less change of secondary structure occurred during the thiol PEGylation of TRAIL. In addition, the thiol PEGylation site – a mutated cysteine – used to be a asparagine, which was a potential N-linked glycosylation site. PEGylation at a glycosylation position has been proved to be beneficial in preserving the structure, biological activity and stability in the modification of Interleukin-2 [32, 33]. Therefore, the author hypothesized that the superior properties of thiol PEGylated TRAIL might all benefit from its structural stability after PEGylation.

II.4. SELECTION OF THE ANIMAL MODEL FOR AAT DEFICIENCY RELATED RESPIRATORY DISEASE

To evaluate the therapeutic efficacy of AAT and PEG-AAT, it was necessary to select a representative animal model for AAT deficiency related respiratory disease. A COPD model, and especially an emphysema model, was favored, as it is one of most common respiratory manifestations developed in AAT-deficient patients [34].

II.4.1. Elastase emphysema model

As the imbalance of protease and anti-protease in the lung is the major cause of the respiratory manifestations in AAT deficiency, instillation of porcine pancreatic elastase or human neutrophil elastase into the lung of mice was used to induce emphysema. This model allows rapid development of airspace enlargement, however, it is generally used as a model of acute lung injury [35–38]. For instance, Cantin et al compared the lung protection of rhAAT and PEGylated rhAAT against elastase-mediated hemorrhage [12]. Elastase was instilled at different time points after the pre-administration of rhAAT or PEGylated rhAAT, and mice were sacrificed only 1 h after the elastase instillation. Although elastase emphysema model exhibits several advantages such us single dose (economic, easy), rapid onset, dose-dependent severity of the disease, the disadvantages still cannot be omitted. The mechanisms behind elastase emphysema are unclear and consistent results depend highly on the choice of enzyme type/dose and animal species/age [39]. Repeated instillations of elastase can cause emphysema-like changes in the lung, but these modifications usually disappear over time upon cessation of the instillation process. The imbalance of protease and anti-protease in the case of AAT deficiency, however, is continuous and long-term, which raised criticism for lack of physiological relevance in this model.

II.4.2. Cigarette smoke model of COPD

Cigarette smoke (CS) model is widely accepted in modeling COPD as i) it is relevant to the environmental causes of human disease; ii) it produces emphysema, airway remodeling, vascular remodeling or pulmonary hypertension in selected species [40]. However, some concerns about the CS model still exist. For instance, the degree of large airway pathology in CS model is relatively mild, it does not produce the severe pathological changes seen in humans. Moreover, it requires several months (usually > 4 mo) of exposure. Last, in AAT-deficient patients, smoking increases the chances of emphysema or COPD, which once occur, would continue to progress when smoking is ceased [41]. This phenomenon cannot be reproduced in CS model, where lesions do not progress after ceasing the smoke exposure. Nevertheless, AAT was reported to ameliorate CS-induced emphysema in mice. Churg et al showed that the treatment of AAT intraperitoneally for 6 months provided 63 % protection against increased airspaces and abolished smoke-mediated increases in plasma tumor necrosis factor-α [42]. Dhami et al demonstrated that the intraperitoneal injection of AAT 24 hours before the CS exposure completely abolished CS-induced connective tissue breakdown, as well as the increase in lavage polymorphonuclear leukocytes [43]. However, contrary to the long-term exposure, this CS model involved exposure to whole cigarette smoke within a short time and acutely induced connective tissue breakdown in the lung.

II.4.3. LPS-induced models of COPD

Besides CS exposure, LPS is also used to induce lung injuries. LPS can induce both acute and chronic lung injury. In the acute model, LPS induces a mixed inflammatory reaction, which is reflected in the increase of neutrophils, inflammatory markers such us TNF-α and IL-1β, as well as the increase in MMP-9 and MMP-12 [44, 45]. Chronic administration of LPS in mice results in enlarged air spaces, remodeled airways and increased goblet cells [46, 47]. However, the mechanisms of those pathological changes were not well defined. LPS instillation can be used to mimic acute exacerbations [48]. It has been reported that AAT could ease the LPS-induced inflammation in vitro and in vivo [49]. Jonigk et al demonstrated that AAT could reduce the cytokine levels produced by LPS-challenged neutrophils from either mice or healthy humans [50]. Wang et al showed that AAT reduced proinflammatory cytokine levels and inflammatory cell counts in the BAL of LPS-challenged rats [51]. In addition, lung tissue injury and cell apoptosis were mitigated by AAT.

II.4.4. Naturally occurring models of COPD

There are some naturally occurring animal models of COPD such us tight skin mice and pallid mice. The tight skin mouse is a genetically induced animal model of tissue fibrosis caused by a large in-frame mutation in the gene encoding fibrillin-1 (Fbn-1) [52]. This strain spontaneously develops pulmonary emphysema and skin fibrosis early in life [53]. Pallid mice are deficient in serum AAT level, which results in pulmonary emphysema within 8 – 10 months after birth [54]. The pathology progress in Pallid mice is similar to that in AAT deficient patients [55]. However, due to the difficulties to obtain those strains, we did not consider the naturally occurring COPD murine model.

II.4.5. Genetically modified models of COPD

With the development of CRISPR technique, the full knockout of serpina1 paralogs in the murine genome becomes possible. Borel et al demonstrated a Serpina1a–e knockout using CRISPR/Cas9-mediated genome editing [56]. The knockout mouse recapitulates the AAT deficiency null phenotype, which shows absence of hepatic and circulating AAT. The knockout mice develop emphysema spontaneously with age, which could also be induced by LPS challenge in younger mice. Nevertheless, with no prior experience with CRISPR, it was difficult for us to apply this model to our study.

II.4.6. The choice of LPS/PPE combination model of COPD

Considering the accessibility and feasibility of each kind of model in our facility, we eventually could not use the CS model or the genetically modified murine model. Therefore, we decided to select a long-term murine COPD model which was primarily mediated by inducers such as elastase and LPS. Table 1 shows the different COPD animal models in rodents induced by either LPS, elastase or the combination of LPS, elastase and other inducers. The combination of LPS and elastase to induce COPD usually involves instillation of LPS and PPE for 4 consecutive weeks [57, 58]. LPS/PPE treated mice show large aggregates of mononuclear inflammatory cells and neutrophils in both peribronchiolar and perivascular spaces, as well as a further increase in the number of PAS-positive cells in both the large and small airways [57]. The challenge of LPS/PPE also resulted in a higher increase in the inflammatory markers in the lung. However, the increase of the cytokines levels in the lung was not always observed. As AAT presents both anti-protease and anti-inflammation property, which was experimentally proved in single inducer model (either only LPS or PPE) [12, 50, 51], we hypothesized that AAT would also reduce the lung injury and inflammation in this combination inducer COPD model.

Table 1. LPS, elastase and combination inducers mediated COPD animal models in rodents. Adapted from Ghorani et al [46].

Inducer	Animal	Method	Ref.
LPS	Mouse	- IN 0.3 mg/kg of LPS, animals were killed 24 h after the challenge to LPS	[59]
		- IN 7 μg of LPS, 1 day/week, for 4 consecutive weeks	[60]
		- intrapulmonary instillation, 0.5 mg/kg; volume =100 μL of LPS	[61, 62]
	Guinea pig	- IN 200 mL of LPS (5 mg/mL in sterile saline), twice/week, for 12 consecutive weeks	[63]
		- IN 100 μL of LPS (10 mg/ml in sterile saline), twice/week, for 12 consecutive weeks	[60, 64]
	Rat	- aerosolized LPS, 30 min/day	[65]
Elastase	Mouse	- IN 1.2 U of PPE, 1 day/week, for 4 consecutive weeks	[60]
		- IT 2 U of PPE/100 g body wt in 100 μl saline	[66]
	Rat	- IT 28 U of PPE/100 g body wt	[67]
		- IT 55 U of PPE/100 g body wt in 0.5 ml saline	[68]
		- IT 0.55 U of PPE/100 g body wt in 0.7 ml or 0.3 ml of 0.15 M NaCl	[38]
	Hamster	- IT 55 U of PPE/100 g body wt in 0.3 ml saline	[68]
		- IT 0.55 U of PPE/100 g body wt in 0.7 ml or 0.3 ml of 0.15 M NaCl	[38]
Combination Inducers	Mouse	- IN 1.2 U of PPE, on day 1 and IN 7 μg of LPS on day 4, for 4 consecutive weeks	[60]
	Rat	- 2 × 30 min/day exposure to CS, for 2 days and on 3-day exposure to aerosolized LPS for 30 min; 5 h after LPS exposure, exposure to CS for 30 min	[65]

II.5. A COMPARISON OF THE PRESENT STUDY WITH CANTIN'S WORK

As discussed in Chapter I, Cantin's work was significant, but it also revealed some limitations that were subsequently improved in our study.

Cantin et al reported the thiol PEGylation conditions as incubating AAT and PEG in phosphate-buffered saline (pH 7.4) at a molar ratio of PEG:AAT of 5:1 for 2 h at 37°C. The reaction did not contain a pre-reduction step to remove the cysteine cap on Cys232, and the PEGylation yield was not mentioned. The work of Cantin et al did not examine the possibility of other PEGylation strategies on AAT. Neither did Cantin et al compared the conformational and thermodynamic stability of AAT and PEGylated AAT.

Cantin et al used rhAAT, whose body residence time is shorter than human AAT due to lack of

glycosylation. Moreover, rhAAT may induce immunological responses in vivo. Yet, the immunogenicity of rhAAT and PEGylated rhAAT was not investigated. In this thesis, human plasma-derived AAT was used, thus avoiding the possibility of an allergic reaction to exogenous proteins. Measurement of anti-AAT antibody levels in murine plasma was used to assess the immunogenicity of human AAT and PEGylated AAT in mice. Furthermore, the histology analysis revealed no evidence of allergic reactions within the lung.

Cantin et al has not investigated the proteolytic resistance of rhAAT and PEGylated rhAAT. While we have confirmed that PEGylation greatly improved the stability of AAT to proteolysis and larger PEG offered better protection on AAT. The PK profile and efficacy of IV route of rhAAT and PEGylated rhAAT was not studied by Cantin, which was further demonstrated in this thesis. In addition, hemoglobin content in the BAL was the only readout used to evaluate the lung protection of rhAAT and PEGylated rhAAT in Cantin's study, which was performed in an acute lung injury model. On the contrary, this thesis evaluated the efficacy of AAT and PEG-AAT in a long-term COPD model, with several different readouts to assess the lung injury and inflammation.

II.6. LIMITATIONS OF THE STUDY

II.6.1. Confirmation of PEGylation site and PEGylation degree by MS

In chapter II, we planned to confirm the PEGylation site and PEGylation degree by MS analysis, which would include intact protein analysis and peptide mapping. However, the intact protein MS analysis of AAT failed due to its heterogeneous glycosylation profile [69, 70]. AAT has three independent glycosylation sites, leading to a highly complex m/z charge distribution. Therefore, the PEGylation degree was determined by SDS-PAGE and DLS.

The peptide mapping was eventually achieved after adapting the method from Kolarich et al [71]. The glycosylation of AAT significantly influenced the trypsin digestion of AAT, as well as its mass distribution after digestion. This was the major reason that our initial attempt for peptide mapping resulted in very low peptide recovery. The adapted method involved a de-glycosylation step, making the following peptide analysis more feasible. Despite our effort to improve the mythology, the N-terminal sequence was still only weakly detected in AAT, which is consistent with Mills et al [72, 73]. Although the N-terminal sequence was completely absent in N-terminal PEGylated AAT, due to the low peptide coverage (only 31 % for N-terminal PEGylated AAT) as well as the technical difficulty in detecting the N-terminus of AAT, the conjugation site of N-terminal PEGylation was not fully confirmed.

II.6.2. Anti-inflammatory properties of AAT and PEG-AAT in vitro

We attempted to evaluate the anti-inflammatory properties of AAT and PEG-AAT in MHS cells. To select a dose of AAT which exhibits a sub-optimal anti-inflammatory effect on MHS cells, we first incubated the cells with AAT at different concentrations (0.02, 0.2, 2 μg/ml) overnight. The cells were then challenged with LPS of 10, 100 and 1000 ng/ml for 24 hours. The secretion of IL-6 in the culture medium was quantified by ELISA to determine the inflammation status of the cells. LPS challenge to MHS cells led to similar IL-6 secretion, and the three concentrations of pre-incubated AAT decreased the IL-6 secretion induced by LPS (FigureS1). Further, we compared the anti-inflammation effect of AAT, PEGmal-AAT and PEGald-AAT on MHS cell challenged by 10 ng/ml LPS. The results showed that PEGmal-AAT and PEGald-AAT at concentration of 2 μg/ml significantly reduced the IL-6 secretion induced by LPS on MHS cells. FigureS2 showed that PEGmal-AAT and PEGald-AAT at concentration of 2 μg/ml significantly reduced the IL-6 secretion induced by LPS on MHS cells. However, AAT failed to ease the inflammation on MHS cells at both concentrations, which was not consistent with our previous results.

In the end, there was not enough solid proof/data that conclusively demonstrate the anti-inflammatory effect of AAT and PEG-AAT. We stopped pursuing the in vitro study as it might be more representative to evaluate the anti-inflammatory properties of AAT and PEG-AAT in vivo.

The failure to determine the anti-inflammation effect of AAT and PEG-AAT on MHS cells could be due to many reasons. First, the cell model might not be completely suitable for this study. Although Jonigk et al demonstrated the anti-inflammation property of AAT in neutrophils and macrophages, they used primary cells instead of an established cell line [50]. Second, the incubation time of AAT, PEG-AAT, and even LPS, might be too long, which decreased the cell viability. Third, the presence of FBS in the culture medium provides excess of bovine AAT, which might also affect the anti-inflammation effect study.

II.6.3. Toxicity of AAT and PEG-AAT in vitro and in vivo

As discussed in Chapter II, we evaluated the toxicity of AAT and PEGylated AAT on MHS cells (Chapter II, FigureS7). However, we did not obtain solid in vitro toxicity data for PEGylated AAT at higher doses. The in vitro toxicity of AAT and PEG-AAT should also be further investigated on other cell lines (including primary cells).

The in vivo toxicity of AAT and PEG-AAT was evaluated by quantifying the TNF-α and total protein content in the BAL collected at 4 h after IT administration of ~40 μg AAT or PEG-AAT. This dose was adapted from the human dose in clinical trials where approximately 80 mg of AAT

was inhaled by the participants. The results showed that AAT, not PEG-AAT, increased the TNF-α level in the BAL. As discussed in Chapter IV, our hypothesis was that the inflammation observed was partially due to instillation itself or the immunogenicity of human AAT to the mice. Nevertheless, there are some limitations in this study: i) the dose of AAT and PEG-AAT used in mice was known to be tolerant in humans. A larger dose might be applied to evaluate the toxicity of AAT and PEG-AAT; ii) the study only involved determining the acute lung injury and inflammation with a single administration of AAT or PEG-AAT. It can be informative to give multiple doses in a relatively longer treatment period; iii) the study only evaluates the toxicity of AAT and PEG-AAT in the lung, the biodistribution of AAT and PEG-AAT in other organs, especially in the kidney and liver, was not investigated.

II.6.4. The limitation of LPS/PPE induced COPD murine model

Although the LPS/PPE induced COPD murine model was the most relevant and economic model for us, there are some limitations in this model. First, this model involves administrating PPE, a non-murine protein, to the mice, which resulted in immunological response, reflected in the increased number of eosinophils in the BAL. However, except for the total cell and differential cell counts, this effect would not significantly influence other inflammatory markers, total protein or albumin content in the BAL. Second, the lung injury (mostly elastin degradation caused by PPE), occurs when excessive elastase is present in the lung. With the prior IN treatment of AAT and PEG-AAT, the administrated PPE would be directly neutralized by the remaining AAT in the pulmonary tracts, resulting in reduced lung injury and inflammation. However, AAT, and especially PEG-AAT, take longer to distribute in the lung after IV treatment. Therefore, the following administrated PPE could not be neutralized immediately, which leads to the limited efficacy of PEG-AAT via the IV. Therefore, to compare the therapeutic efficacy of AAT and PEG-AAT via IV route, it might be better to use naturally occurring animal model or genetically modified animal model, which present lower level of AAT in the lung.

III. PERSPECTIVES

III.1. TOLERABILITY OF PEG-AAT

As discussed in 2.5, the toxicity and tolerability of AAT and PEG-AAT in vivo was not systematically investigated. Therefore, it is interesting to assess the tolerability of AAT and PEG-AAT, with higher and multiple doses, in mice, and other larger animals than rodents. Although the safety of AAT in humans was already well established, it is still crucial to determine the safety of PEG-AAT. Before considering the clinical trials, the safety profile of PEG-AAT should be established in rodent and non-rodent species.

The pulmonary and intravenous routes could both be considered. A systematic toxicological program should be designed, including acute and chronic toxicity evaluation. Different doses of PEG-AAT should be used in the acute toxicity study and more readouts such as inflammation markers and histology analysis would be used to investigate the safety of PEG-AAT. In the chronic exposure study, different doses should be given repeatedly to determine the maximal tolerable dose of PEG-AAT.

III.2. POTENCY OF PEG-AAT IN COPD SPUTA

Our data has demonstrated the increased in vitro stability, prolonged in vivo body residency and improved therapeutic efficacy of PEG-AAT in murine COPD model. However, in the in vitro proteolysis resistance test, AAT and PEG-AAT were exposed to only one protease. Also, the murine COPD model exhibited some limitations as discussed in 2.5. COPD patients present higher level of proteases and oxidants in the lung. Therefore, it would be interesting to investigate the ex-vivo stability and potency of AAT and PEG-AAT in COPD patient sputa, which would be more relevant as AAT and PEG-AAT would be exposed in the pathological condition. If the improved stability and potency of PEG-AAT will be confirmed, it would be more likely that PEG-AAT would lead to improved therapeutic efficacy in patients with COPD.

The potency of PEG-AAT and AAT should be evaluated ex vivo by measuring sputum elastase neutralization by the AAT compounds. The stability of the PEG-AAT conjugate and unconjugated AAT to sputum proteases would be analyzed by western blot analysis of AAT, hNE and AAT-hNE complex in sputa. Each sputum sample would be analyzed for its pH, total and differential cell counts and basal concentration of AAT and hNE.

III.3. THERAPEUTIC EFFICACY OF PEG-AAT IN OTHER ANIMAL MODELS

As discussed in 2.5, the current LPS/PPE induced murine COPD model exhibits some limitations, especially for evaluating the efficacy via the IV administration. Therefore, it might be interesting to use other animal models to compare the therapeutic efficacy of AAT and PEG-AAT by IV injection.

The CS model, palid mice and genetically modified mice model could be considered. The CS model is time-consuming and expensive; however, it offers clear and relevant mechanisms in COPD progress as that in humans. Palid mice and Serpina1 knockout mice would present naturally low level of AAT in circulation and in the lung, which is primarily the same cause in AAT deficiency related emphysema. Not only could these models be more relevant to the cases in humans, but also could result in better comparison between AAT and PEG-AAT as these models all involve a long-term pathological development. Other animal species could also be considered such as rats, guinea pigs and dogs.

III.4. DEVELOPMENT OF LYOPHILIZED OR SPRAY-DRIED POWER FOR PEG-AAT

The currently available products for augmentation therapy of AAT deficiency includes Prolastin, Prolastin C, Trypsone (all from Grifols), Aralast and Aralast NP (from Baxter), Zemaira and Respreeza (from CSL Behring), Alfalastin (from the Laboratoire français fractionnement et de Biotechnologies), and Glassia (from Kamada), which are mostly in powder form with separate solvent for intravenous infusion except for Glassia and the liquid form of Prolastin C [74]. It is therefore important to investigate the stability of PEG-AAT to lyophilization. Spray drying involves a higher throughput, scalable process that produces powders that can be processed into tablets or capsules without requiring milling or other secondary processing [75]. Spray drying is often specifically sought for inhalants. Determining the stability of PEG-AAT to spray drying could be informative to develop PEG-AAT powder for inhalation.

The effect of PEGylation on the stability of AAT to lyophilization is difficult to predict. It has been reported that PEG crystallization was facilitated in freeze-dried PEGylated recombinant human growth hormone [76]. Heller et al demonstrated that PEGylation of hemoglobin reduced the loss of structure induced by lyophilization in a PEG/dextran system, perhaps due to altered partitioning [77]. While PEGylation of brain-derived neurotrophic factor (BDNF) did not drastically influence the conformational stability during lyophilization. Arora et al demonstrated that liquid AAT and lyophilized AAT have similar profiles in terms of biochemical characteristics, PK and safety [78]. It would be interesting to compare those properties of PEG-AAT in liquid and

lyophilized form as well.

The influence of PEGylation to the stability of spray drying process was investigated on small peptides [79, 80], liposomes [81, 82] and phospholipid particles [83]. The data of the stability of PEGylated proteins to spray drying are lacking. The spray dried AAT was previously developed (EU patent: EP0866726B2) and spray-dried AAT was used in aerosolized augmentation therapy in some AAT-deficient patients in a study conducted by Geraghty et al [84]. The PEGylation of proteins could enhance their resistance to aggregation formation during the spray drying process and facilitate a more uniform size distribution during the dry powder process. Thus, it is interesting to investigate and compare the stability of AAT and PEG-AAT to spray drying.

III.5. MOLECULAR DYNAMICS OF PEG-AAT

Even though PEGylation has been successfully applied to protein- and peptide-based pharmaceuticals, it is important to understand how the surface properties and structural stability of PEGylated proteins can be increased to ensure effective drug delivery [85]. However, the current solution-based experimental techniques such as NMR spectroscopy, analytical ultracentrifugation, circular dichroism, fluorescence spectroscopy, and differential scanning calorimetry, etc., are not sufficient to complete our understanding of PEG–protein conjugates to molecular and atomic level [86–88]. Molecular dynamics (MD) simulations have been performed in support of experimental observations made at the atomic scale. The development of all-atom and coarse-grained (CG) PEG FFs in the 1990's has dominated simulations of short linear PEG chains up until the early 2000's [85]. Advances in computing power and simulation methods have made it possible to model more complex (e.g., branched) PEG chains, PEGylated nanoparticle (or protein)-drug complexes and their interactions with plasma proteins and lipid membranes [89–91]. Simulations have revealed, in particular, that PEGylation influences the conformations and surface properties of drug molecules, and therefore modulates the efficiency of drug delivery and release. This allows us to explain atomic-level phenomena, and is critical in determining the best size, structure, and density of PEG for drug delivery. Therefore, it will be beneficial to model PEGylated AAT in MD, which can give more information about the influence of PEG on certain protein domains of AAT.

IV. REFERENCES

[1] Lewis EC. Expanding the clinical indications for α(1)-antitrypsin therapy. Molecular medicine (Cambridge, Mass.) 2012;18:957–70.

[2] Fregonese L, Stolk J. Hereditary alpha-1-antitrypsin deficiency and its clinical consequences. Orphanet journal of rare diseases 2008;3:16.

[3] Cazzola M, Stolz D, Rogliani P, Matera MG. α1-Antitrypsin deficiency and chronic respiratory disorders. European respiratory review an official journal of the European Respiratory Society 2020;29(155).

[4] Brantly ML, Lascano JE, Shahmohammadi A. Intravenous Alpha-1 Antitrypsin Therapy for Alpha-1 Antitrypsin Deficiency: The Current State of the Evidence. Chronic obstructive pulmonary diseases (Miami, Fla.) 2018;6(1):100–14.

[5] Rahaghi FF. Alpha-1 antitrypsin deficiency research and emerging treatment strategies: what's down the road? Therapeutic advances in chronic disease 2021;12_suppl:20406223211014025.

[6] Ginn C, Khalili H, Lever R, Brocchini S. PEGylation and its impact on the design of new protein-based medicines. Future medicinal chemistry 2014;6(16):1829–46.

[7] Veronese FM, Pasut G. PEGylation, successful approach to drug delivery. Drug Discovery Today 2005;10(21):1451–8.

[8] Maiser B, Dismer F, Hubbuch J. Optimization of random PEGylation reactions by means of high throughput screening. Biotechnology and bioengineering 2014;111(1):104–14.

[9] Koussoroplis S-J, Heywood S, Uyttenhove C, Barilly C, van Snick J, Vanbever R. Production, purification and biological characterization of mono-PEGylated anti-IL-17A antibody fragments. International journal of pharmaceutics 2013;454(1):107–15.

[10] Freches D, Patil HP, Machado Franco M, Uyttenhove C, Heywood S, Vanbever R. PEGylation prolongs the pulmonary retention of an anti-IL-17A Fab' antibody fragment after pulmonary delivery in three different species. International journal of pharmaceutics 2017;521(1-2):120–9.

[11] Patil HP, Freches D, Karmani L, et al. Fate of PEGylated antibody fragments following delivery to the lungs: Influence of delivery site, PEG size and lung inflammation. Journal of controlled release official journal of the Controlled Release Society 2018;272:62–71.

[12] Cantin AM, Woods DE, Cloutier D, Dufour EK, Leduc R. Polyethylene glycol conjugation at Cys232 prolongs the half-life of alpha1 proteinase inhibitor. American journal of respiratory cell and molecular biology 2002;27(6):659–65.

[13] Zhu W, Li L, Deng M, et al. Oxidation-resistant and thermostable forms of alpha-1 antitrypsin from Escherichia coli inclusion bodies. FEBS open bio 2018;8(10):1711–21.

[14] Guichard M-J, Wilms T, Mahri S, et al. PEGylation of Recombinant Human Deoxyribonuclease I Provides a Long-Acting Version of the Mucolytic for Patients with Cystic Fibrosis. Adv. Therap. 2021;4(2):2000146.

[15] Rosen CB, Francis MB. Targeting the N terminus for site-selective protein modification. Nature chemical biology 2017;13(7):697–705.

[16] Wu L, Ho SV, Wang W, et al. N-terminal mono-PEGylation of growth hormone antagonist: correlation of PEG size and pharmacodynamic behavior. International journal of pharmaceutics 2013;453(2):533–40.

[17] Liu X, Vanvarenberg K, Guy Wilfried Kouassi K, Mahri S, Vanbever R. Production and characterization of mono-PEGylated alpha-1 antitrypsin for augmentation therapy. International journal of pharmaceutics 2021:121355.

[18] Veronese FM, Mero A. The impact of PEGylation on biological therapies. BioDrugs clinical immunotherapeutics, biopharmaceuticals and gene therapy 2008;22(5):315–29.

[19] Chiu K, Agoubi LL, Lee I, Limpar MT, Lowe JW, Goh SL. Effects of polymer molecular weight on the size, activity, and stability of PEG-functionalized trypsin. Biomacromolecules 2010;11(12):3688–92.

[20] Plesner B, Fee CJ, Westh P, Nielsen AD. Effects of PEG size on structure, function and stability of PEGylated BSA. European journal of pharmaceutics and biopharmaceutics official journal of Arbeitsgemeinschaft fur Pharmazeutische Verfahrenstechnik e.V 2011;79(2):399–405.

[21] Plesner B, Westh P, Nielsen AD. Biophysical characterisation of GlycoPEGylated recombinant human factor VIIa. International journal of pharmaceutics 2011;406(1-2):62–8.

[22] Rodríguez-Martínez JA, Solá RJ, Castillo B, et al. Stabilization of alpha-chymotrypsin upon PEGylation correlates with reduced structural dynamics. Biotechnology and bioengineering 2008;101(6):1142–9.

[23] Jain A, Ashbaugh HS. Helix stabilization of poly(ethylene glycol)-peptide conjugates. Biomacromolecules 2011;12(7):2729–34.

[24] Price JL, Powers ET, Kelly JW. N-PEGylation of a reverse turn is stabilizing in multiple sequence contexts, unlike N-GlcNAcylation. ACS chemical biology 2011;6(11):1188–92.

[25] García-Arellano H, Valderrama B, Saab-Rincón G, Vazquez-Duhalt R. High temperature biocatalysis by chemically modified cytochrome C. Bioconjugate chemistry 2002;13(6):1336–44.

[26] Danial M, van Dulmen THH, Aleksandrowicz J, Pötgens AJG, Klok H-A. Site-specific PEGylation of HR2 peptides: effects of PEG conjugation position and chain length on HIV-1 membrane fusion inhibition and proteolytic degradation. Bioconjugate chemistry 2012;23(8):1648–60.

[27] Zhang C, Desai R, Perez-Luna V, Karuri N. PEGylation of lysine residues improves the proteolytic stability of fibronectin while retaining biological activity. Biotechnology journal 2014;9(8):1033–43.

[28] Zhang C, Hekmatfar S, Ramanathan A, Karuri NW. PEGylated human plasma fibronectin is proteolytically stable, supports cell adhesion, cell migration, focal adhesion assembly, and fibronectin fibrillogenesis. Biotechnology progress 2013;29(2):493–504.

[29] Lee LS, Conover C, Shi C, Whitlow M, Filpula D. Prolonged Circulating Lives of Single-Chain Fv Proteins Conjugated with Polyethylene Glycol: A Comparison of Conjugation Chemistries and Compounds. Bioconjugate Chem. 1999;10(6):973–81.

[30] Koumenis IL, Shahrokh Z, Leong S, Hsei V, Deforge L, Zapata G. Modulating pharmacokinetics of an anti-interleukin-8 F(ab')2 by amine-specific PEGylation with preserved bioactivity. International journal of pharmaceutics 2000;198(1):83–95.

[31] Pan L-Q, Wang H-B, Lai J, Xu Y-C, Zhang C, Chen S-Q. Site-specific PEGylation of a mutated-cysteine residue and its effect on tumor necrosis factor (TNF)-related apoptosis-inducing ligand (TRAIL). Biomaterials 2013;34(36):9115–23.

[32] Goodson RJ, Katre NV. Site-directed pegylation of recombinant interleukin-2 at its glycosylation site. Bio/technology (Nature Publishing Company) 1990;8(4):343–6.

[33] Dozier JK, Distefano MD. Site-Specific PEGylation of Therapeutic Proteins. International journal of molecular sciences 2015;16(10):25831–64.

[34] Brode SK, Ling SC, Chapman KR. Alpha-1 antitrypsin deficiency: a commonly overlooked cause of lung disease. CMAJ Canadian Medical Association journal = journal de l'Association medicale canadienne 2012;184(12):1365–71.

[35] Delacourt C, Hérigault S, Delclaux C, et al. Protection against acute lung injury by intravenous or intratracheal pretreatment with EPI-HNE-4, a new potent neutrophil elastase inhibitor. American journal of respiratory cell and molecular biology 2002;26(3):290–7.

[36] Rao NV, Kennedy TP, Rao G, Ky N, Hoidal JR. Sulfated polysaccharides prevent human leukocyte elastase-induced acute lung injury and emphysema in hamsters. The American review of respiratory disease 1990;142(2):407–12.

[37] Tremblay GM, Vachon E, Larouche C, Bourbonnais Y. Inhibition of human neutrophil elastase-induced acute lung injury in hamsters by recombinant human pre-elafin (trappin-2). Chest 2002;121(2):582–8.

[38] Vecchiola A, La Llera JF de, Ramírez R, Olmos P, Herrera CI, Borzone G. Differences in acute lung response to elastase instillation in two rodent species may determine differences in severity of emphysema development. American journal of physiology. Regulatory, integrative and comparative physiology 2011;301(1):R148-58.

[39] Wright JL, Cosio M, Churg A. Animal models of chronic obstructive pulmonary disease. American journal of physiology. Lung cellular and molecular physiology 2008;295(1):L1-15.

[40] Eltom S, Stevenson C, Birrell MA. Cigarette smoke exposure as a model of inflammation associated with COPD. Current protocols in pharmacology 2013;Chapter 5:Unit5.64.

[41] Ranes J, Stoller JK. A review of alpha-1 antitrypsin deficiency. Seminars in respiratory and critical care medicine 2005;26(2):154–66.

[42] Churg A, Wang RD, Xie C, Wright JL. alpha-1-Antitrypsin ameliorates cigarette smoke-induced emphysema in the mouse. American journal of respiratory and critical care medicine 2003;168(2):199–207.

[43] Dhami R, Gilks B, Xie C, Zay K, Wright JL, Churg A. Acute cigarette smoke-induced connective tissue breakdown is mediated by neutrophils and prevented by alpha1-antitrypsin. American journal of respiratory cell and molecular biology 2000;22(2):244–52.

[44] Righetti RF, Dos Santos TM, Camargo LdN, et al. Protective Effects of Anti-IL17 on Acute Lung Injury Induced by LPS in Mice. Frontiers in pharmacology 2018;9:1021.

[45] Li Q, Liu L, Sun H, Cao K. Carnosic acid protects against lipopolysaccharide-induced acute lung injury in mice. Experimental and therapeutic medicine 2019;18(5):3707–14.

[46] Ghorani V, Boskabady MH, Khazdair MR, Kianmeher M. Experimental animal models for COPD: a methodological review. Tobacco induced diseases 2017;15:25.

[47] Bruscia EM, Zhang P-X, Barone C, et al. Increased susceptibility of Cftr-/- mice to LPS-induced lung remodeling. American journal of physiology. Lung cellular and molecular physiology 2016;310(8):L711-9.

[48] Oliveira MV de, Rocha NdN, Santos RS, et al. Endotoxin-Induced Emphysema Exacerbation: A Novel Model of Chronic Obstructive Pulmonary Disease Exacerbations Causing Cardiopulmonary Impairment and Diaphragm Dysfunction. Frontiers in physiology 2019;10:664.

[49] Lior Y, Zaretsky M, Ochayon DE, et al. Point Mutation of a Non-Elastase-Binding Site in Human α1-Antitrypsin Alters Its Anti-Inflammatory Properties. Frontiers in immunology 2018;9:759.

[50] Jonigk D, Al-Omari M, Maegel L, et al. Anti-inflammatory and immunomodulatory properties of α1-antitrypsin without inhibition of elastase. Proceedings of the National Academy of Sciences of the United States of America 2013;110(37):15007–12.

[51] Wang X, Gong J, Zhu J, Jin Z, Gao W. Alpha 1-antitrypsin for treating ventilator-associated lung injury in acute respiratory distress syndrome rats. Experimental lung research 2019;45(7):209–19.

[52] Rossi GA, Hunninghake GW, Gadek JE, et al. Hereditary emphysema in the tight-skin mouse. Evaluation of pathogenesis. The American review of respiratory disease 1984;129(5):850–5.

[53] Ito S, Bartolák-Suki E, Shipley JM, Parameswaran H, Majumdar A, Suki B. Early emphysema in the tight skin and pallid mice: roles of microfibril-associated glycoproteins, collagen, and mechanical forces. American journal of respiratory cell and molecular biology 2006;34(6):688–94.

[54] Ni K, Serban KA, Batra C, Petrache I. Alpha-1 Antitrypsin Investigations Using Animal Models of Emphysema. Annals of the American Thoracic Society 2016;13 Suppl 4:S311-6.

[55] Yoshida M, Sakiyama S, Kenzaki K, et al. Functional evaluation of pallid mice with genetic emphysema. Laboratory investigation; a journal of technical methods and pathology 2009;89(7):760–8.

[56] Borel F, Sun H, Zieger M, et al. Editing out five Serpina1 paralogs to create a mouse model of genetic emphysema. Proceedings of the National Academy of Sciences of the United States of America 2018;115(11):2788–93.

[57] Sajjan U, Ganesan S, Comstock AT, et al. Elastase- and LPS-exposed mice display altered responses to rhinovirus infection. American journal of physiology. Lung cellular and molecular physiology 2009;297(5):L931-44.

[58] Singanayagam A, Glanville N, Walton RP, et al. A short-term mouse model that reproduces the immunopathological features of rhinovirus-induced exacerbation of COPD. Clinical science (London, England 1979) 2015;129(3):245–58.

[59] Hardaker L, Bahra P, Billy BC de, et al. The ion channel transient receptor potential melastatin-2 does not play a role in inflammatory mouse models of chronic obstructive pulmonary diseases. Respiratory research 2012;13:30.

[60] Sohn S-H, Jang H, Kim Y, et al. The effects of Gamijinhae-tang on elastase/lipopolysaccharide-induced lung inflammation in an animal model of acute lung injury. BMC complementary and alternative medicine 2013;13:176.

[61] Al Faraj A, Shaik AS, Afzal S, Al Sayed B, Halwani R. MR imaging and targeting of a specific alveolar macrophage subpopulation in LPS-induced COPD animal model using antibody-conjugated magnetic nanoparticles. International journal of nanomedicine 2014;9:1491–503.

[62] Al Faraj A, Sultana Shaik A, Pureza MA, Alnafea M, Halwani R. Preferential macrophage recruitment and polarization in LPS-induced animal model for COPD: noninvasive tracking using MRI. PloS one 2014;9(3):e90829.

[63] Pera T, Zuidhof A, Valadas J, et al. Tiotropium inhibits pulmonary inflammation and remodelling in a guinea pig model of COPD. The European respiratory journal 2011;38(4):789–96.

[64] Baarsma HA, Bos S, Meurs H, et al. Pharmacological inhibition of GSK-3 in a guinea pig model of LPS-induced pulmonary inflammation: I. Effects on lung remodeling and pathology. Respiratory research 2013;14:113.

[65] Hardaker EL, Freeman MS, Dale N, et al. Exposing rodents to a combination of tobacco smoke and lipopolysaccharide results in an exaggerated inflammatory response in the lung. British journal of pharmacology 2010;160(8):1985–96.

[66] Vidal D, Fortunato G, Klein W, et al. Alterations in pulmonary structure by elastase administration in a model of emphysema in mice is associated with functional disturbances. Revista portuguesa de pneumologia 2012;18(3):128–36.

[67] Borzone G, Ramírez B, Reyes T, Moreno R, Lisboa C, González S. Enfisema pulmonar experimental en la rata: fenómenos inflamatorios y progresión del daño pulmonar. Revista medica de Chile 1998;126(10):1153–60.

[68] Borzone G, Liberona L, Olmos P, et al. Rat and hamster species differences in susceptibility to elastase-induced pulmonary emphysema relate to differences in elastase inhibitory capacity. American journal of physiology. Regulatory, integrative and comparative physiology 2007;293(3):R1342-9.

[69] Bengtson P, Valtonen-André C, Jonsson M. Phenotyping of α-1-Antitrypsin by liquid chromatography–high resolution mass spectrometry. Clinical Mass Spectrometry 2016;2:34–40.

[70] Chen Y, Snyder MR, Zhu Y, et al. Simultaneous phenotyping and quantification of α-1-antitrypsin by liquid chromatography-tandem mass spectrometry. Clinical chemistry 2011;57(8):1161–8.

[71] Kolarich D, Turecek PL, Weber A, et al. Biochemical, molecular characterization, and glycoproteomic analyses of alpha(1)-proteinase inhibitor products used for replacement therapy. Transfusion 2006;46(11):1959–77.

[72] Mills K, Mills PB, Clayton PT, Johnson AW, Whitehouse DB, Winchester BG. Identification of alpha(1)-antitrypsin variants in plasma with the use of proteomic technology. Clinical chemistry 2001;47(11):2012–22.

[73] Mills K, Mills PB, Clayton PT, Mian N, Johnson AW, Winchester BG. The underglycosylation of plasma alpha 1-antitrypsin in congenital disorders of glycosylation type I is not random. Glycobiology 2003;13(2):73–85.

[74] Mohanka M, Khemasuwan D, Stoller JK. A review of augmentation therapy for alpha-1 antitrypsin deficiency. Expert opinion on biological therapy 2012;12(6):685–700.

[75] Salama AH. Spray drying as an advantageous strategy for enhancing pharmaceuticals bioavailability. Drug delivery and translational research 2020;10(1):1–12.

[76] Bhatnagar BS, Martin SWH, Hodge TS, et al. Investigation of PEG crystallization in frozen and freeze-dried PEGylated recombinant human growth hormone-sucrose systems: implications on storage stability. Journal of pharmaceutical sciences 2011;100(8):3062–75.

[77] Heller MC, Carpenter JF, Randolph TW. Conformational stability of lyophilized PEGylated proteins in a phase-separating system. Journal of pharmaceutical sciences 1999;88(1):58–64.

[78] Arora V, Cruz M, Lang J, et al. Comparison of the liquid and lyophilized formulations of Prolastin®-C for Alpha1-Antitrypsin deficiency: Biochemical characteristics, pharmacokinetics, safety and neoantigenicity in rabbits. Biologicals journal of the International Association of Biological Standardization 2019;62:77–84.

[79] Qiu Y, Man RCH, Liao Q, Kung KLK, Chow MYT, Lam JKW. Effective mRNA pulmonary delivery by dry powder formulation of PEGylated synthetic KL4 peptide. Journal of controlled release official journal of the Controlled Release Society 2019;314:102–15.

[80] Castelletto V, McKendrick JE, Hamley IW, Olsson U, Cenker C. PEGylated amyloid peptide nanocontainer delivery and release system. Langmuir the ACS journal of surfaces and colloids 2010;26(14):11624–7.

[81] van den Hoven JM, Metselaar JM, Storm G, Beijnen JH, Nuijen B. Cyclodextrin as membrane protectant in spray-drying and freeze-drying of PEGylated liposomes. International journal of pharmaceutics 2012;438(1-2):209–16.

[82] Costa C, Nobre B, Matos AS, et al. Inhalable hydrophilic molecule-loaded liposomal dry powder formulations using supercritical CO2 – assisted spray-drying. Journal of CO2 Utilization 2021;53:101709.

[83] Meenach SA, Anderson KW, Zach Hilt J, McGarry RC, Mansour HM. Characterization and aerosol dispersion performance of advanced spray-dried chemotherapeutic PEGylated phospholipid particles for dry powder inhalation delivery in lung cancer. European journal of pharmaceutical sciences official journal of the European Federation for Pharmaceutical Sciences 2013;49(4):699–711.

[84] Geraghty P, Rogan MP, Greene CM, et al. Alpha-1-antitrypsin aerosolised augmentation abrogates neutrophil elastase-induced expression of cathepsin B and matrix metalloprotease 2 in vivo and in vitro. Thorax 2008;63(7):621–6.

[85] Lee H. Molecular Simulations of PEGylated Biomolecules, Liposomes, and Nanoparticles for Drug Delivery Applications. Pharmaceutics 2020;12(6).

[86] Digilio G, Barbero L, Bracco C, et al. NMR structure of two novel polyethylene glycol conjugates of the human growth hormone-releasing factor, hGRF(1-29)-NH2. Journal of the American Chemical Society 2003;125(12):3458–70.

[87] Dhalluin C, Ross A, Leuthold L-A, et al. Structural and biophysical characterization of the 40 kDa PEG-interferon-alpha2a and its individual positional isomers. Bioconjugate Chem. 2005;16(3):504–17.

[88] Cattani G, Vogeley L, Crowley PB. Structure of a PEGylated protein reveals a highly porous double-helical assembly. Nature Chem 2015;7(10):823–8.

[89] Sousa SF, Peres J, Coelho M, Vieira TF. Analyzing PEGylation through Molecular Dynamics Simulations. ChemistrySelect 2018;3(29):8415–27.

[90] Lee H. Molecular Modeling of PEGylated Peptides, Dendrimers, and Single-Walled Carbon Nanotubes for Biomedical Applications. Polymers 2014;6(3):776–98.

[91] Rossi G, Monticelli L. Modeling the effect of nano-sized polymer particles on the properties of lipid membranes. Journal of physics. Condensed matter an Institute of Physics journal 2014;26(50):503101.

V. SUPPLEMENTARY MATERIALS

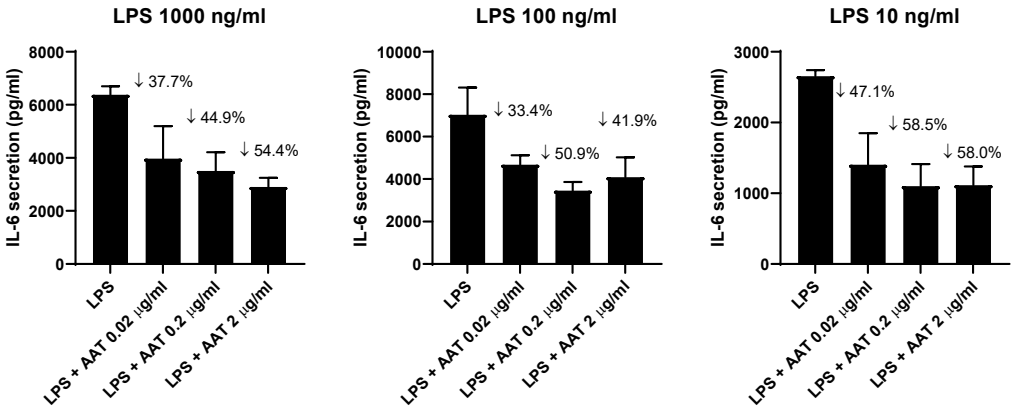

FigureS 1. IL-6 secretion of MHS cell challenged by LPS of different concentrations. The cells were first incubated with AAT (0.02, 0.2, 2 μg/ml) overnight, then challenged with LPS for 24 hours.

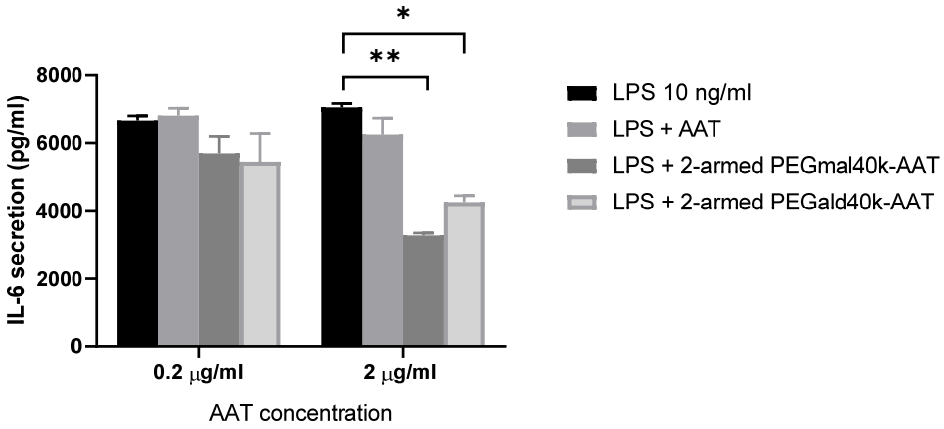

FigureS 2. IL-6 secretion of MHS cells challenged by 10 ng/ml LPS for 24 h. The cells were pre-incubated with AAT, 2-armed PEGmal40-AAT or 2-armed PEGald40k-AAT overnight before the exposure to LPS.